

Multi-bunch longitudinal beam-dynamics code for the DAFNE rings

D. Quartullo

Acknowledgements: *S. Caschera, G. Franzini, A. Gallo, A. Ghigo, M. Migliorati, C. Milardi, D. Pellegrini, M. Zobov*

Introduction (1/2)

- ❑ DAFNE is an electron-positron collider in operation at LNF for physics experiments since 1999.
 - It is composed of two rings, one per type of beam, and operates with (usually) 105 bunches at 510 MeV nominal energy.
- ❑ Due to the high circulating beam-current and the presence of HOMs in the RF accelerating cavity, longitudinal coupled-bunch instabilities can severely limit the performance of the machine.
 - These instabilities grow exponentially with time and can lead to losses of entire bunches in a few thousands of turns.
- ❑ A significant damping of the HOMs was achieved in the 1990s by opening slots onto the cavity-surface and conveying (coupling) the HOMs fields out of the cavity with waveguides terminated onto 50Ω external loads.
 - This solution, although important, couldn't prevent the occurrence of coupled-bunch instabilities at high beam-currents.
- ❑ Therefore a bunch-by-bunch longitudinal feedback was installed in each DAFNE ring and became operational since 1998.
 - The active element of this feedback is a broadband cavity-kicker which provides voltage corrections to the bunches.
 - This feedback system strongly contributed to the achievement of the 1.4 A – 2.4 A beam currents available today.
- ❑ In the 1990s, M. Migliorati developed for his PhD thesis a Fortran code able to simulate the longitudinal beam-dynamics of DAFNE bunches in the presence of synchrotron radiation, HOMs induced-voltage and feedback corrections.
 - Each bunch is represented by just one macroparticle, therefore only oscillations of the bunches centroids can be studied.
 - However this type of oscillations is the main issue as concerns the coupled-bunch instabilities.
 - The code accurately models the HOM induced-voltages, the complete bunch-by-bunch feedback system and even the additional RF feedback able to counteract the beam-loading voltage in the accelerating cavity.

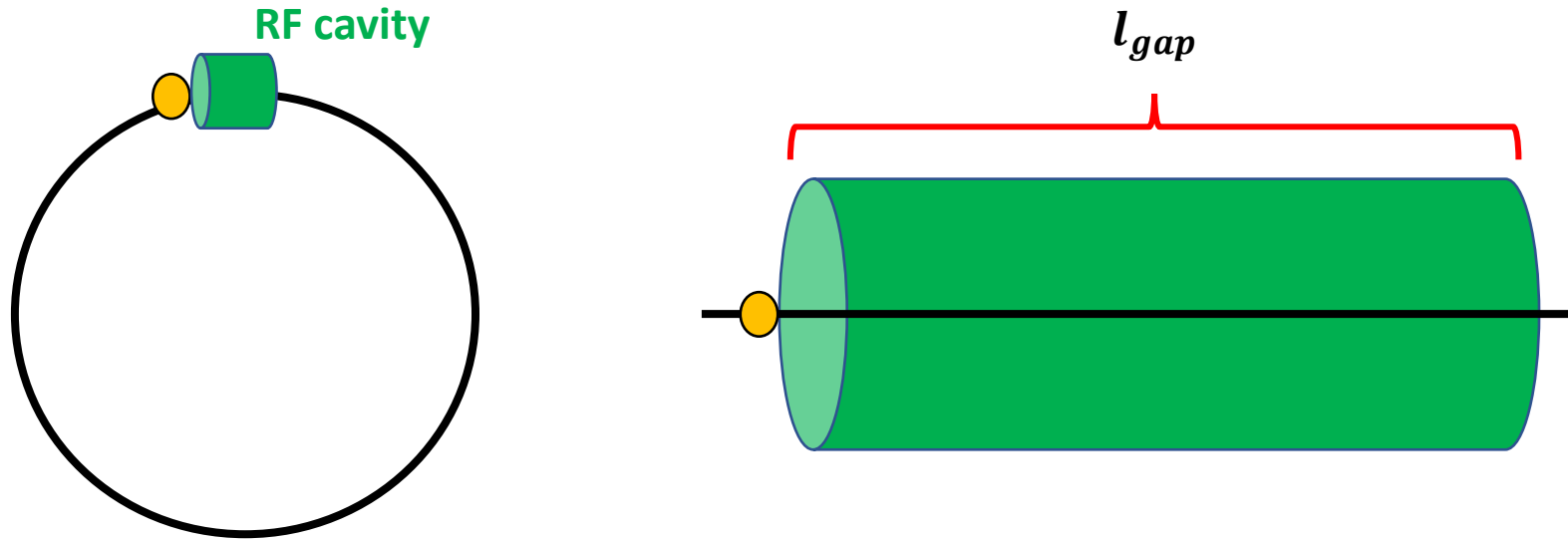
Introduction (2/2)

- ❑ The studies performed with the Fortran code provided useful indications for stable machine operation, such as expected growth rates of coupled-bunch instabilities and optimal feedback parameters to counteract them.
 - The code was rarely used after the 1990s and in particular it was never benchmarked with measurements.
- ❑ The code is relatively fast and easy-to-use. This recently motivated the desire to make it usable again, both for accelerator physicists and operators who can use it in (almost) real time to better understand the beam-dynamics under observation.
 - The code is modular and can be easily customized, therefore it can also be applied to other accelerators.
- ❑ Recently, the Fortran code was rewritten entirely in Python, which is an open-source high-level programming language.
 - Pros of using Python: less lines of code for a given task, better code-readability, easier production of data and plots.
 - Cons of using Python: execution speed. However this can be solved by converting the most time-consuming Python routines into the C++ language and embedding them into the Python code (as done e.g. for the CERN BLoND code).
- ❑ During the code conversion from Fortran to Python, some routines were generalized or improved, some minor bugs were fixed and new functionalities were added.
- ❑ Three types of content are included in this presentation.
 - Essential theoretical concepts, which are needed to understand the principles behind the code, are covered in detail.
 - Complete derivations are presented to make the presentation as self-contained as possible.
 - Several important code-routines are described and explained in depth.
 - The code-capabilities are illustrated by numerous examples.

Contents

- Introduction.
- Single-particle longitudinal beam-dynamics with synchrotron radiation.
 - Equations of motion, synchrotron radiation, small-amplitude synchrotron oscillations, ...
- Longitudinal beam-dynamics with synchrotron radiation and Higher Order Modes (HOMs).
 - HOM induced voltage, synchronous phase shift, HOM initial conditions, coupled-bunch instabilities, ...
- Longitudinal beam-dynamics with synchrotron radiation, HOMs and bunch-by-bunch feedback.
 - Models of the feedback components, growth and damping-rates, cavity-kicker, ideal and real corrections, ...
- Conclusions and suggested next steps.
- Appendices.
 - Execution of the new-Python and old-Fortran codes, structure of the code, exponential fits in Python, ...
- References.

Single particle equations of motion: energy equation (1/5)



- We call l_{gap} the length of the RF cavity.
- We assume that the particle traverses the RF gap along its central axis.
- We assume that the electric field $\vec{\xi}(s)$ seen by the particle in the RF gap is purely longitudinal and given by

$$\vec{\xi}(s) = \hat{\xi} \sin\left(\omega_{rf} \frac{s}{v} + \varphi_{rf}\right) \quad s \in \left[-\frac{l_{gap}}{2}, \frac{l_{gap}}{2}\right]$$

- where $\hat{\xi}$ is the design amplitude of the electric field;
- ω_{rf} and φ_{rf} are respectively the RF angular frequency and phase of $\vec{\xi}$;
- v is the particle speed assumed constant during the passage (in DAFNE $v \approx c$).

Single particle equations of motion: energy equation (2/5)

□ Let's assume that the circulating particle has charge e .

□ The energy gain of the particle after it has crossed the gap one time is

$$\Delta E_{gain} = e \int_{-\frac{l_{gap}}{2}}^{\frac{l_{gap}}{2}} \vec{\xi}(s) \cdot \vec{ds} = e \hat{\xi} \int_{-\frac{l_{gap}}{2}}^{\frac{l_{gap}}{2}} \sin\left(\frac{\omega_{rf}}{c}s + \varphi_{rf}\right) ds = e \hat{\xi} \sin \varphi_{rf} \int_{-\frac{l_{gap}}{2}}^{\frac{l_{gap}}{2}} \cos\left(\frac{\omega_{rf}}{c}s\right) ds = \frac{2e \hat{\xi} c \sin \varphi_{rf}}{\omega_{rf}} \sin\left(\frac{\omega_{rf} l_{gap}}{2c}\right)$$

□ Therefore

$$\Delta E_{gain} = e \hat{V}_{rf} \sin \varphi_{rf}$$

➤ where the peak RF voltage and the transit time factor are given by

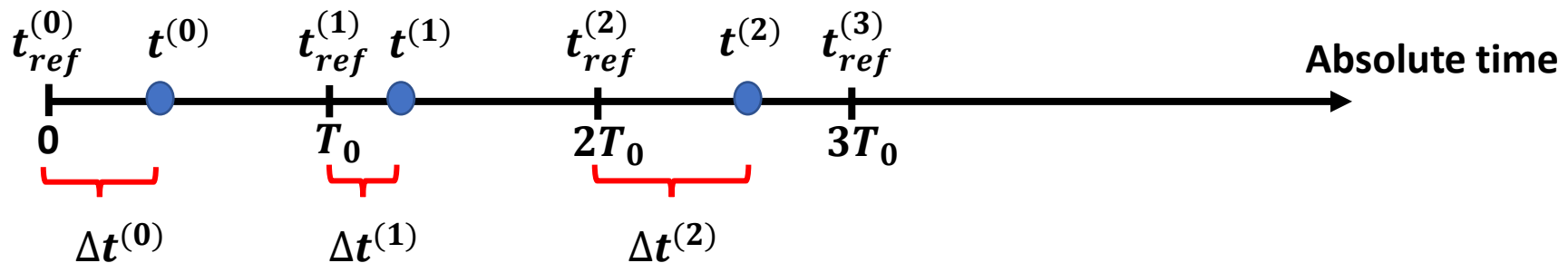
$$\hat{V}_{rf} = \hat{\xi} l_{gap} T_a \quad T_a = \frac{\sin\left(\frac{\omega_{rf} l_{gap}}{2c}\right)}{\frac{\omega_{rf} l_{gap}}{2c}} \quad 0 < T_a < 1$$

Single particle equations of motion: energy equation (3/5)

- We suppose that the nominal energy E_0 is constant, i.e. no acceleration, such as in the DAFNE case ($E_0=510\text{MeV}$).
- From E_0 we compute the reference revolution period T_0 . We use T_0 to define the external clock

$$t_{ref}^{(n)} = nT_0 \quad n = 0, \dots$$

- We call $t^{(n)}$ the n^{th} arrival-time of the particle at the RF cavity (supposed point-like).



- We define the particle arrival time with respect to the reference clock as

$$\Delta t^{(n)} = t^{(n)} - t_{ref}^{(n)} \quad n = 0, \dots$$

Single particle equations of motion: energy equation (4/5)

□ The energy gain of the particle at the crossing time $t^{(n)}$ is

$$(\Delta E_{gain})_n = e\hat{V}_{rf} \sin[\varphi_{rf}(t^{(n)})]$$

➤ where

$$\begin{aligned} \varphi_{rf}(t^{(n)}) &= \int_0^{t^{(n)}} \omega_{rf}(\tau) d\tau + \varphi_{offset} = \int_0^{t_{ref}^{(n)}} \omega_{rf}(\tau) d\tau + \int_{t_{ref}^{(n)}}^{t_{ref}^{(n)} + \Delta t^{(n)}} \omega_{rf}(\tau) d\tau + \varphi_{offset} \\ &= \underbrace{\sum_{i=0}^{n-1} \omega_{rf}^{(i)} T_0}_{\text{multiple of } 2\pi} + \omega_{rf}^{(n)} \Delta t^{(n)} + \varphi_{offset} = \omega_{rf}^{(n)} \Delta t^{(n)} + \varphi_{rf} \end{aligned}$$

- This is multiple of 2π , and therefore irrelevant, only if $\omega_{rf}^{(i)} = 2\pi h f_0$ (h is the harmonic number).
- This condition isn't satisfied e.g. when beam-based LLRF loops, such as phase and radial loops, modify the RF frequency to damp the bunch oscillations.

- It can represent e.g. constant phase offsets or the injection of RF noise in the RF cavity for controlled emittance blow-up.

Single particle equations of motion: energy equation (5/5)

- In DAFNE, supposing $\omega_{rf}^{(i)} = 2\pi h f_0$, we have

$$\varphi_{rf}(t^{(n)}) = \omega_{rf}\Delta t^{(n)} + \varphi_{\text{offset}}$$

- Choosing $\varphi_{\text{offset}} = \pi/2$, we have

$$(\Delta E_{\text{gain}})_n = e\hat{V}_{rf} \cos[\omega_{rf}\Delta t^{(n)}]$$

- After crossing the cavity, the particle energy is

$$E^{(n+1)} = E^{(n)} + e\hat{V}_{rf} \cos[\omega_{rf}\Delta t^{(n)}]$$

- Defining

$$\Delta E^{(n)} = E^{(n)} - E_0$$

- we obtain the energy equation of motion

$$\Delta E^{(n+1)} = \Delta E^{(n)} + e\hat{V}_{rf} \cos[\omega_{rf}\Delta t^{(n)}]$$

Single particle equations of motion: time equation (1/4)

□ Using the definitions given previously we can write

$$\Delta t^{(n+1)} = \Delta t^{(n)} + t^{(n+1)} - t^{(n)} - T_0 = \Delta t^{(n)} + \frac{1}{f^{(n)}} - \frac{1}{f_0} = \Delta t^{(n)} + \frac{1}{f_0} \left(\frac{f_0}{f^{(n)}} - 1 \right) = \Delta t^{(n)} + \frac{1}{f_0} \left(\frac{1}{1 + \frac{f^{(n)} - f_0}{f_0}} - 1 \right)$$

➤ where f_0 is the nominal revolution frequency and $f^{(n)}$ is the particle revolution frequency.

□ It can be proven that

$$\frac{f^{(n)} - f_0}{f_0} = -\eta(\delta^{(n)})$$

➤ where

$$\delta^{(n)} = \frac{\Delta p^{(n)}}{p_0} = \frac{\Delta E^{(n)}}{\beta_0^2 E_0} \approx \frac{\Delta E^{(n)}}{E_0}$$

In DAFNE

$$\beta_0(510 \text{ MeV}) = 0.9999999498 \approx 1$$

- $p_0(E_0)$ and $\beta_0(E_0)$ are respectively the nominal momentum and relativistic beta;
- $\Delta p^{(n)} = p^{(n)} - p_0$, $\Delta E^{(n)} = E^{(n)} - E_0$;
- $p^{(n)}$ and $E^{(n)}$ are respectively the momentum and energy of the circulating particle.

Single particle equations of motion: time equation (2/4)

□ From the previous slide

$$\eta(\delta) = (\eta_0 + \eta_1\delta + \eta_2\delta^2 + \dots)\delta$$

➤ where the η_i are called the slippage factors.

□ The slippage factors are defined through the momentum compaction factors α_i , which are constant numbers for a given machine and depend on the optics.

➤ For instance

$$\eta_0 = \alpha_0 - \frac{1}{\gamma_0^2}$$

➤ where γ_0 is the nominal relativistic gamma.

□ The γ_0 such that $\eta_0 = 0$ is called transition gamma

$$\gamma_{tr} = \frac{1}{\sqrt{\alpha_0}}$$

□ In DAFNE $\alpha_0 = 0.018$, $\gamma_0 = 998$ and $\gamma_{tr} = 7.45$. Since $\gamma_0 > \gamma_{tr}$ the beam is 'above transition energy'.

Single particle equations of motion: time equation (3/4)

□ When $\gamma_0 \gg \gamma_{tr}$, one can take just the first term of the $\eta(\delta)$ expansion, i.e.

$$\eta(\delta) = (\eta_0 + \eta_1\delta + \eta_2\delta^2 + \dots)\delta \approx \eta_0\delta$$

➤ In DAFNE, since $\gamma_0 \gg \gamma_{tr}$,

$$\eta_0 = \alpha_0 - \frac{1}{\gamma_0^2} = 0.018 - 10^{-6} \approx \alpha_0$$

➤ Therefore

$$\frac{f^{(n)} - f_0}{f_0} = -\alpha_0\delta^{(n)}$$

- A particle with $E > E_0$ has $f < f_0$. Indeed above transition energy the particle speed is essentially equal to the light speed and more energy corresponds to more mass and inertia, forcing the particle to travel on a longer orbit.

□ Therefore

$$\Delta t^{(n+1)} = \Delta t^{(n)} + \frac{1}{f_0} \left(\frac{1}{1 + \frac{f^{(n)} - f_0}{f_0}} - 1 \right) \approx \Delta t^{(n)} + \frac{1}{f_0} \left(\frac{1}{1 - \alpha_0\delta^{(n)}} - 1 \right)$$

Single particle equations of motion: time equation (4/4)

□ Since $|\alpha_0 \delta^{(n)}| \ll 1$ then

$$\Delta t^{(n+1)} \approx \Delta t^{(n)} + \frac{1}{f_0} \left(\frac{1}{1 - \alpha_0 \delta^{(n)}} - 1 \right) \approx \Delta t^{(n)} + T_0 \alpha_0 \delta^{(n)}$$

□ Therefore the time equation of motion is

$$\Delta t^{(n+1)} = \Delta t^{(n)} + T_0 \alpha_0 \delta^{(n)}$$

□ To summarize, the two equations of motion are

$$\Delta t^{(n+1)} = \Delta t^{(n)} + \frac{T_0 \alpha_0}{E_0} \Delta E^{(n)}$$



Particle-drift along the ring

$$\Delta E^{(n+1)} = \Delta E^{(n)} + e \hat{V}_{rf} \cos[\omega_{rf} \Delta t^{(n+1)}]$$



RF voltage-kick to particle

- The particle-tracking starts at the exit of the accelerating cavity.
 - The particle drifts along the ring, then it receives an energy-kick by the cavity, then it drifts along the ring with the new energy, etc.

Equations of motion in the code (only RF)

- Using the coordinates

$$\Delta\varphi^{(n)} = \omega_{rf}\Delta t^{(n)} \quad \delta^{(n)} = \frac{\Delta E^{(n)}}{E_0}$$

- the equations of motion become

$$\begin{aligned} \Delta\varphi^{(n+1)} &= \Delta\varphi^{(n)} + 2\pi h\alpha_0\delta^{(n)} \\ \delta^{(n+1)} &= \delta^{(n)} + \frac{e\hat{V}_{rf}\cos[\Delta\varphi^{(n+1)}]}{E_0} \end{aligned}$$

- In the code each bunch is described by only one macroparticle.

- The above equations imply that the evolution of each bunch is independent from the evolutions of the other bunches.
 - As shown later, each bunch is tracked in the code with a more complicated version of these equations.

- These equations of motion can be seen as a map M between coordinates at consecutive turns.

$$\begin{pmatrix} \Delta\varphi^{(n)} \\ \delta^{(n)} \end{pmatrix} \xrightarrow{M} \begin{pmatrix} \Delta\varphi^{(n+1)} \\ \delta^{(n+1)} \end{pmatrix}$$

- It can be easily verified that the Jacobian of M is one, i.e.

$$J(M) = \begin{vmatrix} \frac{\partial(\Delta\varphi^{(n+1)})}{\partial(\Delta\varphi^{(n)})} & \frac{\partial(\Delta\varphi^{(n+1)})}{\partial(\delta^{(n)})} \\ \frac{\partial(\delta^{(n+1)})}{\partial(\Delta\varphi^{(n)})} & \frac{\partial(\delta^{(n+1)})}{\partial(\delta^{(n)})} \end{vmatrix} = 1$$

- This implies that the phase-space area enclosed by the bunch (particle) trajectory is preserved over time.

Synchrotron radiation (1/6)

- Let's assume that a particle with charge e and relativistic factor γ follows a curved trajectory with bending radius $\rho(s)$.
 - It can be proven that the power lost by synchrotron radiation (SR) is given by

$$P(s) = \frac{2}{3} \frac{e^2 c}{4\pi\epsilon_0} \frac{\gamma^4}{\rho^2(s)}$$

- where ϵ_0 is the free-space permittivity.

- If the particle is on the nominal orbit then

$$P_0(s) = \frac{2}{3} \frac{e^2 c}{4\pi\epsilon_0} \frac{\gamma_0^4}{\rho_0^2(s)}$$

- where ρ_0 is the bending radius corresponding to the nominal orbit.

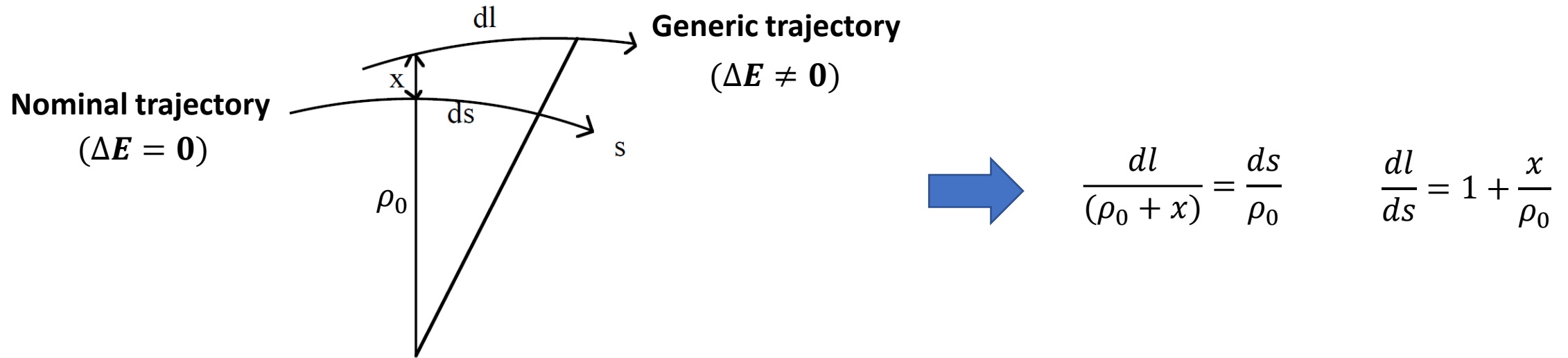
- If the lattice is isomagnetic, i.e. if $\rho_0(s) \equiv \rho_0$, the SR energy-loss per turn for a particle on the nominal orbit is

$$U_0 = \oint P_0(t) dt = \frac{2}{3} \frac{e^2 c}{4\pi\epsilon_0} \frac{\gamma_0^4}{\rho_0^2} \frac{2\pi\rho_0}{c} = \frac{e^2}{3\epsilon_0} \frac{\gamma_0^4}{\rho_0} = \frac{e^2}{3\epsilon_0 m_e^4 c^8} \frac{E_0^4}{\rho_0}$$

- What is the SR energy-loss U for a particle with energy different from E_0 ?

Synchrotron radiation (2/6)

- From the following drawing, we can derive the relations



- We know from transverse beam-dynamics that the horizontal displacement of an off-energy particle can be written as

$$x(s) = D_x(s) \frac{\Delta E}{E_0}$$

- where $D_x(s)$ is the dispersion function of the lattice.

- Therefore

$$\frac{dl}{ds} = 1 + \frac{D_x \Delta E}{\rho_0 E_0}$$

Synchrotron radiation (3/6)

- The energy-loss per turn for the off-energy particle is the integral of the radiated power around the off-energy orbit

$$U(\Delta E) = \oint P(t)dt = \frac{1}{c} \oint P(l)dl = \frac{1}{c} \oint P(s) \left(1 + \frac{D_x}{\rho_0} \frac{\Delta E}{E_0} \right) ds$$

- Equating the magnetic Lorentz-force acting on the particle with the centripetal force we derive the magnetic rigidity formula

$$evB = \frac{mv^2}{\rho} \quad \longrightarrow \quad B(s)\rho(s) = \frac{p}{e}$$

- where B is the dipolar magnetic field bending the particle.

- The following proportionality relations can be deduced

$$P(s) \propto \frac{\gamma^4}{\rho^2(s)} \propto \frac{E^4}{\rho^2(s)} \propto \frac{E^2 p^2}{\rho^2(s)} \propto E^2 B^2(s)$$

- Therefore $P(s)$ can be written as a function of energy and transverse displacements

$$P(\Delta E, x)(s) \propto (E_0 + \Delta E)^2 B^2(x)(s) \qquad P(0,0)(s) = P_0(s) \propto E_0^2 B_0^2(s)$$

- $P_0(s)$ is the power radiated at the position s of the design orbit, where the dipolar field is $B_0(s)$.

Synchrotron radiation (4/6)

□ Expanding $P(\Delta E, x)$ linearly we have

$$P(\Delta E, x) = P(0,0) + \frac{\partial P}{\partial \Delta E}(0,0)\Delta E + \frac{\partial P}{\partial x}(0,0)x = P_0 + \frac{2P_0}{E_0}\Delta E + \frac{2P_0}{B_0} \frac{dB}{dx}(0) x$$

□ Therefore, keeping only the linear terms in ΔE ,

$$U(\Delta E) = \frac{1}{c} \oint P(s) \left(1 + \frac{D_x \Delta E}{\rho_0 E_0} \right) ds = \frac{1}{c} \oint \left(P_0 + \frac{2P_0}{E_0}\Delta E + \frac{2P_0}{B_0} \frac{dB}{dx}(0) D_x \frac{\Delta E}{E_0} + P_0 \frac{D_x \Delta E}{\rho_0 E_0} \right) ds$$

□ Expanding also $U(\Delta E)$ linearly we have

$$U(\Delta E) = U_0 + \frac{dU}{d(\Delta E)}(0)\Delta E = U_0 + \left[\frac{1}{c} \oint \left(\frac{2P_0}{E_0} + \frac{2P_0}{B_0 E_0} \frac{dB}{dx}(0) D_x + P_0 \frac{D_x}{\rho_0 E_0} \right) ds \right] \Delta E$$

□ Since the integral of $P_0(t)$ is U_0 then

$$U(\Delta E) = U_0 + \left[\frac{2U_0}{E_0} + \frac{1}{c E_0} \oint \left(\frac{2P_0}{B_0} \frac{dB}{dx}(0) D_x + P_0 \frac{D_x}{\rho_0} \right) ds \right] \Delta E$$

Synchrotron radiation (5/6)

□ We define the focusing parameter for gradient fields as

$$k = \frac{\frac{dB}{dx}(0)}{B_0 \rho_0}$$

□ Therefore

$$\begin{aligned} U(\Delta E) &= U_0 + \left[\frac{2U_0}{E_0} + \frac{1}{cE_0} \oint \left(\frac{2P_0}{B_0} \frac{dB}{dx}(0) D_x + P_0 \frac{D_x}{\rho_0} \right) ds \right] \Delta E = U_0 + \left[\frac{2U_0}{E_0} + \frac{1}{cE_0} \oint P_0 D_x \left(2k\rho_0 + \frac{1}{\rho_0} \right) ds \right] \Delta E \\ &= U_0 + D\Delta E = U_0 + \frac{U_0}{E_0} (2 + K)\Delta E \end{aligned}$$

➤ where D is the damping coefficient and, since $P_0 \propto 1/\rho_0^2$,

$$K = \frac{1}{cU_0} \oint P_0 D_x \left(2k\rho_0 + \frac{1}{\rho_0} \right) ds = \frac{\oint P_0 D_x \left(2k\rho_0 + \frac{1}{\rho_0} \right) ds}{\oint P_0 ds} = \frac{\oint D_x \left(\frac{2k}{\rho_0} + \frac{1}{\rho_0^3} \right) ds}{\oint \frac{1}{\rho_0^2} ds}$$

Synchrotron radiation (6/6)

- The quantity K is entirely described by integrals of lattice functions

$$K = \frac{\oint D_x \left(\frac{2k}{\rho_0} + \frac{1}{\rho_0^3} \right) ds}{\oint \frac{1}{\rho_0^2} ds}$$

- Contributions to K come only from bending magnets and wigglers, where $1/\rho_0 \neq 0$.
 - For parallel-edged bending magnets $k \neq 0$ at the entrance and exit of the magnet.
 - This exactly compensates the term $1/\rho_0^3$ above, so that $K = 0$.
 - For sector bending magnets $k = 0$ if the focusing isn't performed by the bending magnets but by dedicated quadrupoles.
- In DAFNE there are parallel-edged magnets, sector magnets and wigglers.
 - Using data from M. Migliorati PhD thesis, $D = 3.66 \times 10^{-5}$ and $U_0 = 9.3$ keV.
 - Assuming $E_0 = 510$ MeV, we can derive an estimation for K

$$K = \frac{E_0}{U_0} D - 2 = 7.1 \times 10^{-3}$$

- Therefore K can be neglected in

$$U(\Delta E) = U_0 + \frac{U_0}{E_0} (2 + K) \Delta E \approx U_0 + \frac{2U_0}{E_0} \Delta E$$

Equations of motion in the code (RF+SR)

□ Including the synchrotron-radiation effect, the equations of motion become

$$\Delta\varphi^{(n+1)} = \Delta\varphi^{(n)} + 2\pi h\alpha_0\delta^{(n)}$$

$$\delta^{(n+1)} = \delta^{(n)} - \frac{U_0}{E_0}(1 + 2\delta^{(n)}) + \frac{e\hat{V}_{rf} \cos \Delta\varphi^{(n+1)}}{E_0}$$

□ The Jacobian becomes

$$J(M) = \begin{vmatrix} \frac{\partial(\Delta\varphi^{(n+1)})}{\partial(\Delta\varphi^{(n)})} & \frac{\partial(\Delta\varphi^{(n+1)})}{\partial(\delta^{(n)})} \\ \frac{\partial(\delta^{(n+1)})}{\partial(\Delta\varphi^{(n)})} & \frac{\partial(\delta^{(n+1)})}{\partial(\delta^{(n)})} \end{vmatrix} = 1 - \frac{2U_0}{E_0} \in (0,1)$$

- The phase-space area enclosed by the bunch (particle) trajectory decreases with time.
 - This is due to the radiation damping, as shown later.

□ Also these equations of motion are decoupled for the different bunches.

- Each bunch can be tracked independently of the others.

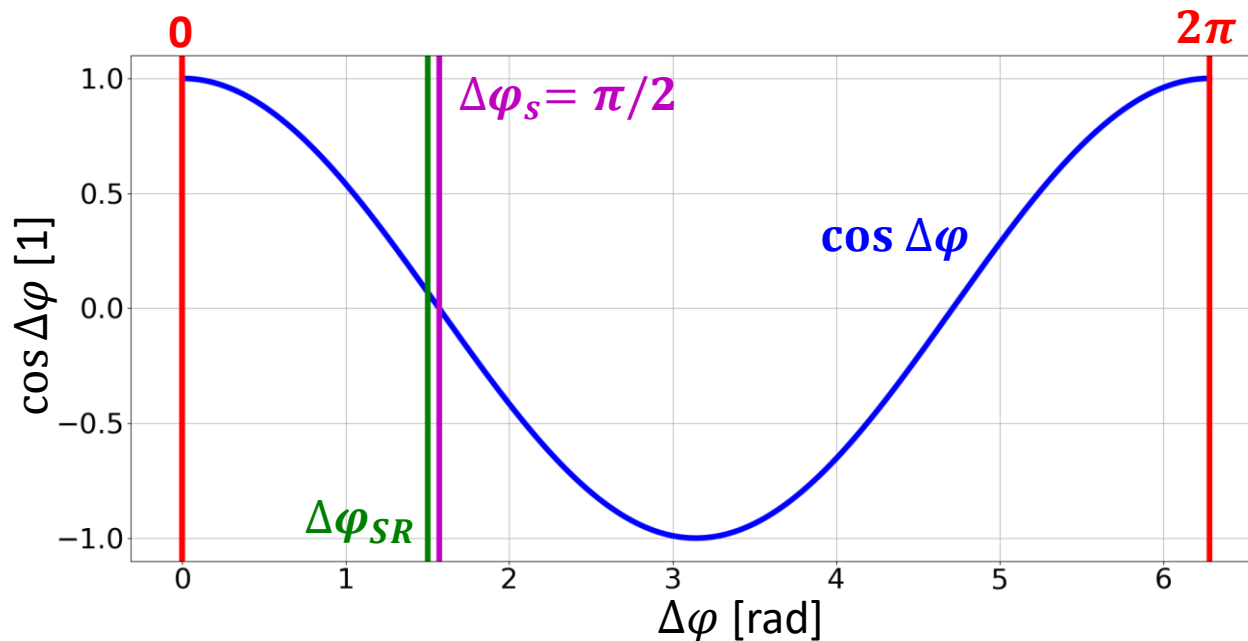
Synchronous phase

- The synchronous particle is the ideal particle which travels along the design (central) orbit at each turn.
 - For this particle $\delta = 0$ at each turn and the corresponding phase $\Delta\varphi_{SR}$ is called synchronous phase.

$$\frac{e\hat{V}_{rf} \cos \Delta\varphi_{SR}}{E_0} - \frac{U_0}{E_0} = 0 \quad \longrightarrow \quad \Delta\varphi_{SR} = \arccos \frac{U_0}{e\hat{V}_{rf}}$$

- The subscript SR indicates that the synchronous phase is evaluated considering the synchrotron radiation.
- $\Delta\varphi_s = \Delta\varphi_{SR}(U_0=0) = \pi/2 = 1.571$ rad is the synchronous phase without considering the synchrotron radiation.

Example of difference between $\Delta\varphi_s$ and $\Delta\varphi_{SR}$ in DAFNE



- $\Delta\varphi_{SR} < \pi/2$, since the corresponding RF voltage must be positive in order to compensate for the energy lost by synchrotron radiation.
- In DAFNE, using $U_0 = 8.88$ keV and $\hat{V}_{rf} = 130$ kV, we have

$$\Delta\varphi_{SR} = 1.502 \text{ rad}$$
- As shown later, $\Delta\varphi_{SR}$ changes when induced voltages are added to the equations of motions.

Small-amplitude synchrotron frequency and damping rate (1/3)

□ We first derive the continuous version of the equations of motion assuming that $dt = T_0$ in the derivative.

$$\Delta\varphi^{(n+1)} = \Delta\varphi^{(n)} + 2\pi h\alpha_0\delta^{(n)}$$

$$\delta^{(n+1)} = \delta^{(n)} + \frac{e\hat{V}_{rf} \cos \Delta\varphi^{(n+1)}}{E_0} - \frac{U_0}{E_0} (1 + 2\delta^{(n)})$$



$$\dot{\Delta\varphi} = \omega_{rf}\alpha_0\delta$$

$$\dot{\delta} = \frac{e\hat{V}_{rf}}{E_0T_0} \cos \Delta\varphi - \frac{U_0}{E_0T_0} (1 + 2\delta)$$

□ We expand $\cos \Delta\varphi$ around $\Delta\varphi_{SR}$ and we assume that the phase displacement φ_0 is small.

$$\cos \Delta\varphi = \cos(\Delta\varphi_{SR} + \varphi_0) \approx \cos \Delta\varphi_{SR} - \sin \Delta\varphi_{SR} \varphi_0$$

□ Since $\dot{\Delta\varphi} = \dot{\varphi}_0$ we have

$$\dot{\varphi}_0 = \omega_{rf}\alpha_0\delta$$

$$\dot{\delta} = \frac{e\hat{V}_{rf}}{E_0T_0} \cos \Delta\varphi_{SR} - \frac{e\hat{V}_{rf}}{E_0T_0} \sin \Delta\varphi_{SR} \varphi_0 - \frac{U_0}{E_0T_0} (1 + 2\delta) = -\frac{e\hat{V}_{rf}}{E_0T_0} \sin \Delta\varphi_{SR} \varphi_0 - \frac{2U_0}{E_0T_0} \delta$$

□ And deriving again

$$\ddot{\delta} = -\frac{e\hat{V}_{rf}}{E_0T_0} \sin \Delta\varphi_{SR} \omega_{rf}\alpha_0\delta - \frac{2U_0}{E_0T_0} \dot{\delta}$$

Small-amplitude synchrotron frequency and damping rate (2/3)

□ Therefore

$$\ddot{\delta} + 2\alpha_{r,SR}\dot{\delta} + \Omega^2\delta = 0$$

➤ where $\alpha_{r,SR}$ and Ω^2 are given by

$$\alpha_{r,SR} = \frac{U_0}{E_0 T_0} \quad \Omega^2 = \frac{e\hat{V}_{rf}\omega_{rf}\alpha_0}{E_0 T_0} \sin \Delta\varphi_{SR}$$

□ The eigenvalues of this differential equation are

$$\lambda^2 + 2\alpha_{r,SR}\lambda + \Omega^2 = 0 \quad \longrightarrow \quad \lambda_{1,2} = -\alpha_{r,SR} \pm j\sqrt{\Omega^2 - \alpha_{r,SR}^2}$$

➤ therefore the solution is

$$\delta(t) = Ae^{-\alpha_{r,SR}t} \cos\left(\sqrt{\Omega^2 - \alpha_{r,SR}^2} t + B\right) \quad \bullet \quad A \text{ and } B \text{ are constants}$$

□ δ decays exponentially oscillating. The small-amplitude damping-rate and synchrotron-frequency are given respectively by

$$\alpha_{r,SR} = \frac{U_0}{E_0 T_0} \quad (= 0 \text{ if } U_0 = 0, \text{ i.e. no damping}) \quad \omega_{s0,SR} = \underbrace{\sqrt{\frac{e\hat{V}_{rf}\omega_{rf}\alpha_0}{E_0 T_0} \sin \Delta\varphi_{SR}}}_{> 0} - \alpha_{r,SR} \quad \left(= \sqrt{\frac{e\hat{V}_{rf}\omega_{rf}\alpha_0}{E_0 T_0}} \text{ if } U_0 = 0 \right)$$

Small-amplitude synchrotron frequency and damping rate (3/3)

□ The constants A and B in

$$\delta(t) = A e^{-\alpha_{r,SR} t} \cos(\omega_{s0,SR} t + B)$$

➤ depend on the initial conditions $\delta(0)$ and $\dot{\delta}(0)$

$$\delta(0) = A \cos B$$

$$\dot{\delta}(0) = -\alpha_{r,SR} A \cos B - \omega_{s0,SR} A \sin B$$

□ If for instance we assume that $\delta(0) = 0$ then

$$\cos B = 0 \quad A \sin B = -\frac{\dot{\delta}(0)}{\omega_{s0,SR}}$$

➤ or

$$B = \pm \frac{\pi}{2} \quad A = \mp \frac{\dot{\delta}(0)}{\omega_{s0,SR}}$$

➤ therefore, using the relation between $\dot{\delta}(0)$ and $\varphi_0(0)$, we obtain

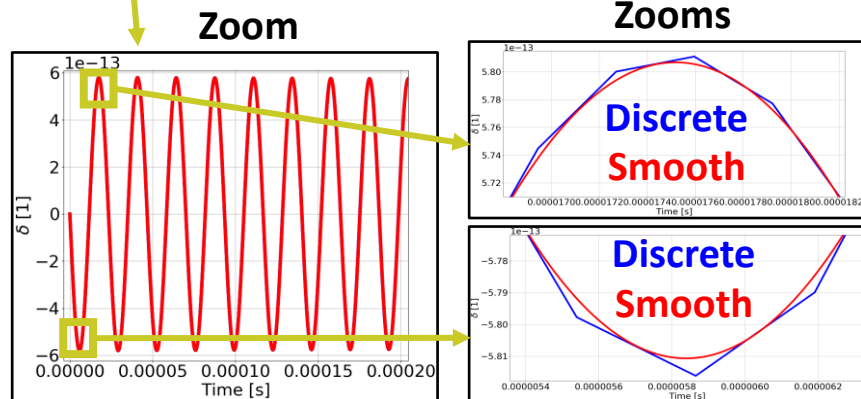
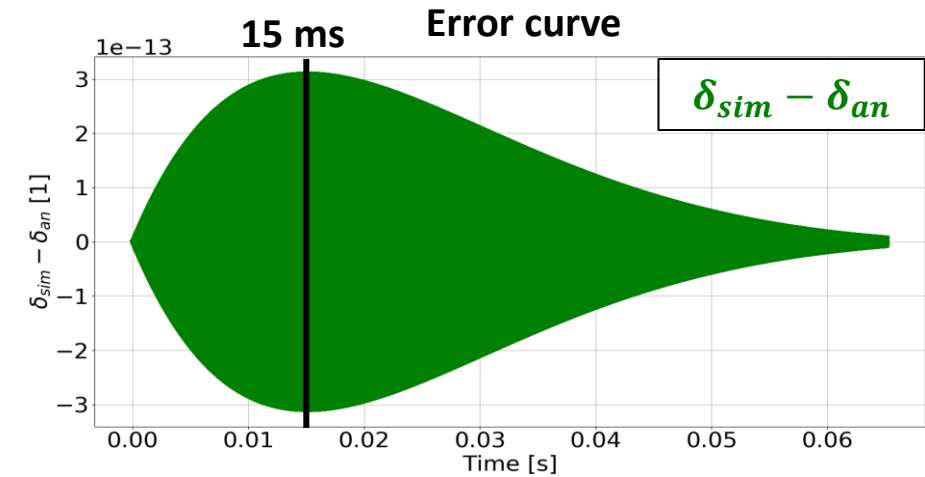
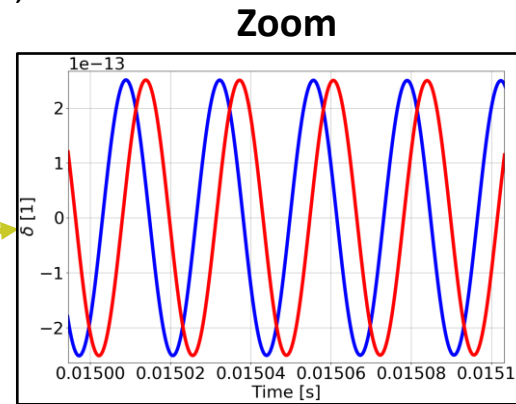
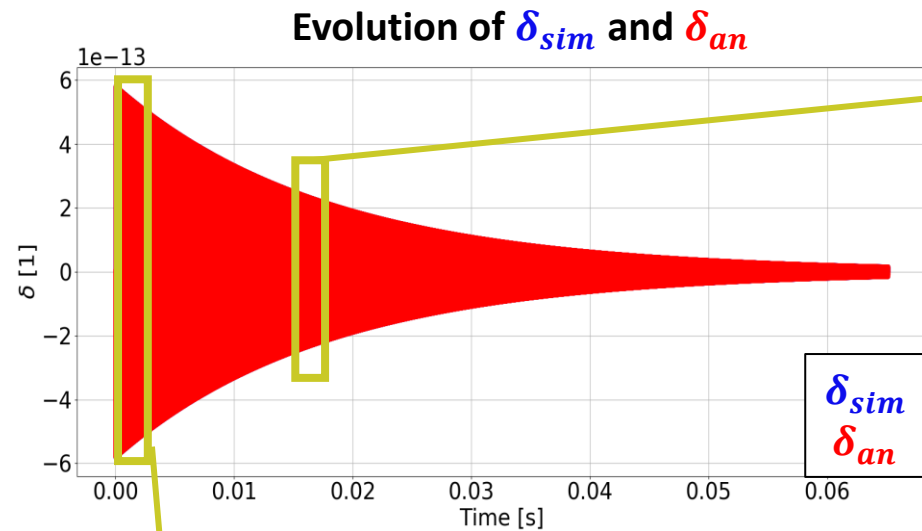
$$\delta(t) = \frac{\dot{\delta}(0)}{\omega_{s0,SR}} e^{-\alpha_{r,SR} t} \sin(\omega_{s0,SR} t) = -\frac{e\hat{V}_{rf} \sin \Delta\varphi_{SR} \varphi_0(0)}{E_0 T_0 \omega_{s0,SR}} e^{-\alpha_{r,SR} t} \sin(\omega_{s0,SR} t)$$

Comparison between simulation and analytical formula (1/2)

Comparison between δ evolutions from single-bunch simulation (δ_{sim}) and analytical formula (δ_{an}).

Used parameters:

- $U_0 = 9.3$ keV, $E_0 = 510$ MeV, $\hat{V}_{rf} = 260$ kV, $\alpha_0 = 0.02$;
- $\varphi_0(0) = 10^{-10}$ rad, $\delta(0) = 0$;
- 200000 turns are simulated.



- The two curves have the same amplitude of oscillations (exponential envelope).
 - However the phase-difference between the two curves can be large.
 - The curves are out of phase by almost $\pi/2$ at 15 ms.

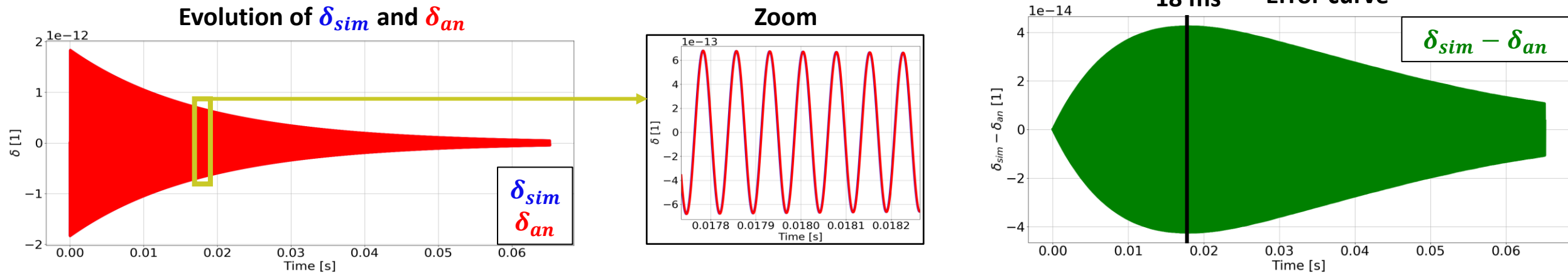
- This phase-difference comes from the fact that the equations of motion in the code are discrete while the analytical formula is continuous.
 - The equations of motion are correct, the analytical formula is an approximation.
 - As shown later, the phase-space orbits associated to the equations of motion are tilted ellipses, while the analytical formula provides non-tilted ellipses.

- For example, the error can decrease by just decreasing α_0 .

- $f_{S0,SR}$ decreases, therefore the discretized curve converges to the smooth one.

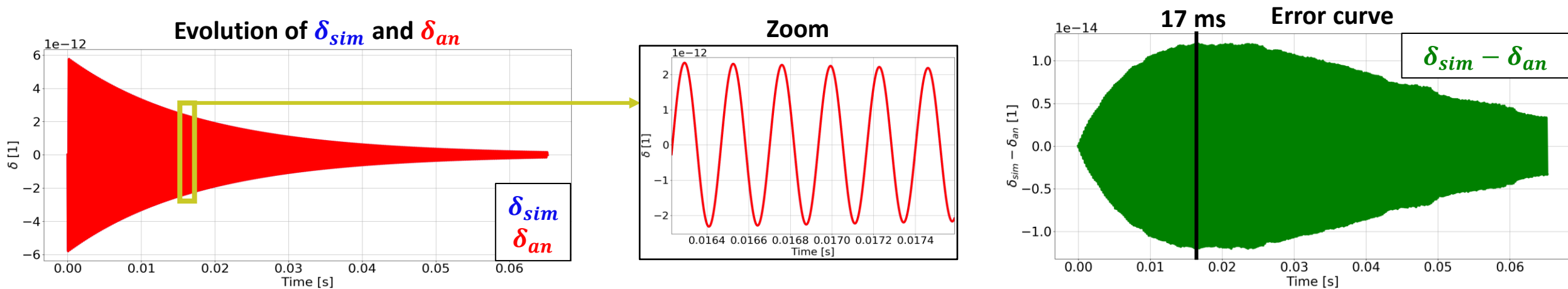
Comparison between simulation and analytical formula (2/2)

- α_0 is decreased from 0.02 to 0.002.



- The phase difference is barely visible. The maximum error is reduced from $3 \cdot 10^{-13}$ to $4 \cdot 10^{-14}$.

- α_0 is decreased from even more, from 0.002 to 0.0002.



- The phase difference isn't visible anymore. The maximum error is reduced from $4 \cdot 10^{-14}$ to $1.2 \cdot 10^{-14}$.

Amplitude of motion for small oscillations (1/2)

□ We start from the discrete equations of motion

$$\Delta\varphi^{(n+1)} = \Delta\varphi^{(n)} + 2\pi h\alpha_0\delta^{(n)}$$

$$\delta^{(n+1)} = \delta^{(n)} + \frac{e\hat{V}_{rf} \cos \Delta\varphi^{(n+1)}}{E_0} - \frac{U_0}{E_0} (1 + 2\delta^{(n)})$$

□ We change variable $\Delta\varphi = \Delta\varphi_{SR} + \varphi_0 \rightarrow \varphi_0$ and we linearly expand $\cos \Delta\varphi$ around $\Delta\varphi_{SR}$ for small φ_0

$$\varphi_0^{(n+1)} = \varphi_0^{(n)} + 2\pi h\alpha_0\delta^{(n)}$$

$$\begin{aligned} \delta^{(n+1)} &= \delta^{(n)} + \frac{e\hat{V}_{rf}}{E_0} \left(\cos \Delta\varphi_{SR} - \sin \Delta\varphi_{SR} \varphi_0^{(n+1)} \right) - \frac{U_0}{E_0} (1 + 2\delta^{(n)}) \\ &= \delta^{(n)} - \frac{e\hat{V}_{rf} \sin \Delta\varphi_{SR}}{E_0} \left(\varphi_0^{(n)} + 2\pi h\alpha_0\delta^{(n)} \right) - \frac{2U_0}{E_0} \delta^{(n)} \\ &= -\frac{e\hat{V}_{rf} \sin \Delta\varphi_{SR}}{E_0} \varphi_0^{(n)} + \left(1 - \frac{2\pi h\alpha_0 e\hat{V}_{rf} \sin \Delta\varphi_{SR}}{E_0} - \frac{2U_0}{E_0} \right) \delta^{(n)} \end{aligned}$$

Amplitude of motion for small oscillations (2/2)

- We can write these two equations in matrix form

$$\begin{pmatrix} \varphi_0^{(n+1)} \\ \delta^{(n+1)} \end{pmatrix} = \begin{pmatrix} 1 & 2\pi h \alpha_0 \\ -\frac{e\hat{V}_{rf} \sin \Delta\varphi_{SR}}{E_0} & 1 - \frac{2\pi h \alpha_0 e\hat{V}_{rf} \sin \Delta\varphi_{SR}}{E_0} - \frac{2U_0}{E_0} \end{pmatrix} \begin{pmatrix} \varphi_0^{(n)} \\ \delta^{(n)} \end{pmatrix}$$

- The 2x2 matrix can be written as

$$\begin{pmatrix} 1 & 2\pi h \alpha_0 \\ -\frac{e\hat{V}_{rf} \sin \Delta\varphi_{SR}}{E_0} & 1 - \frac{2\pi h \alpha_0 e\hat{V}_{rf} \sin \Delta\varphi_{SR}}{E_0} - \frac{2U_0}{E_0} \end{pmatrix} = \begin{pmatrix} \cos \mu_x + \alpha_x \sin \mu_x & \beta_x \sin \mu_x \\ -\gamma_x \sin \mu_x & \cos \mu_x - \alpha_x \sin \mu_x \end{pmatrix}$$

- where

$$\cos \mu_x = 1 - \frac{\pi h \alpha_0 e\hat{V}_{rf} \sin \Delta\varphi_{SR}}{E_0} - \frac{U_0}{E_0} \quad \sin \mu_x = \sqrt{1 - \cos^2 \mu_x} \quad \alpha_x = \frac{1 - \cos \mu_x}{\sin \mu_x} \quad \beta_x = \frac{2\pi h \alpha_0}{\sin \mu_x} \quad \gamma_x = \frac{e\hat{V}_{rf} \sin \Delta\varphi_{SR}}{E_0 \sin \mu_x}$$

- This matrix representation indicates that the phase-space orbits are tilted ellipses with equations

$$\varepsilon = \gamma_x \varphi_0^2 + 2\alpha_x \varphi_0 \delta + \beta_x \delta^2$$

- and the amplitude of motion is proportional to

$$\sqrt{\varepsilon} = \sqrt{\gamma_x \varphi_0^2 + 2\alpha_x \varphi_0 \delta + \beta_x \delta^2}$$

- This formula is used in the code to evaluate how the bunch amplitude of motion evolves with time.

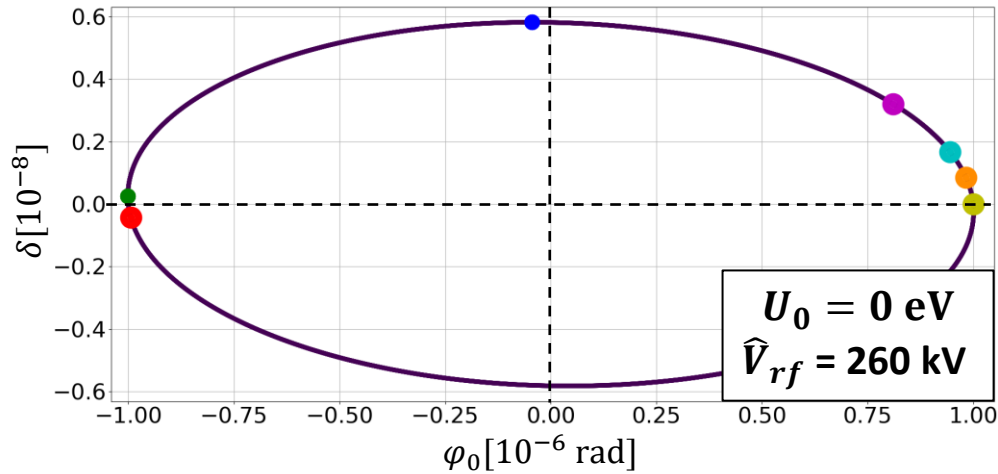
- This idea of matrix representation comes from transverse beam dynamics, where μ_x is the phase advance and $\alpha_x, \beta_x, \gamma_x$ are the Twiss parameters.

Example: amplitude of motion for small oscillations

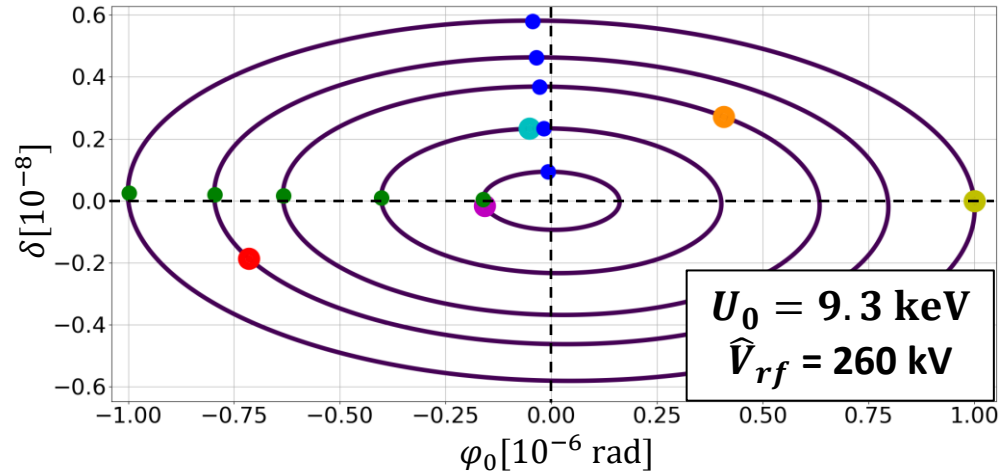
□ Single-bunch simulations are performed with the code to verify that the bunch-orbits in phase-space are indeed titled ellipses.

➤ Parameters used in simulations: $E_0 = 510$ MeV, $\alpha_0 = 0.02$, $\varphi_0(0) = 10^{-6}$ rad, $\hat{V}_{rf} = 260$ kV.

Non-damped motion, slightly tilted ellipse

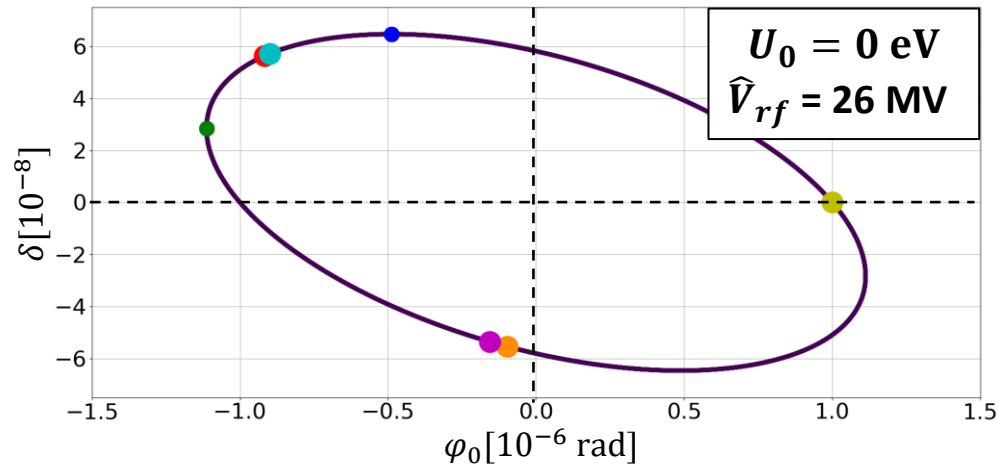


Damped motion, slightly tilted ellipses

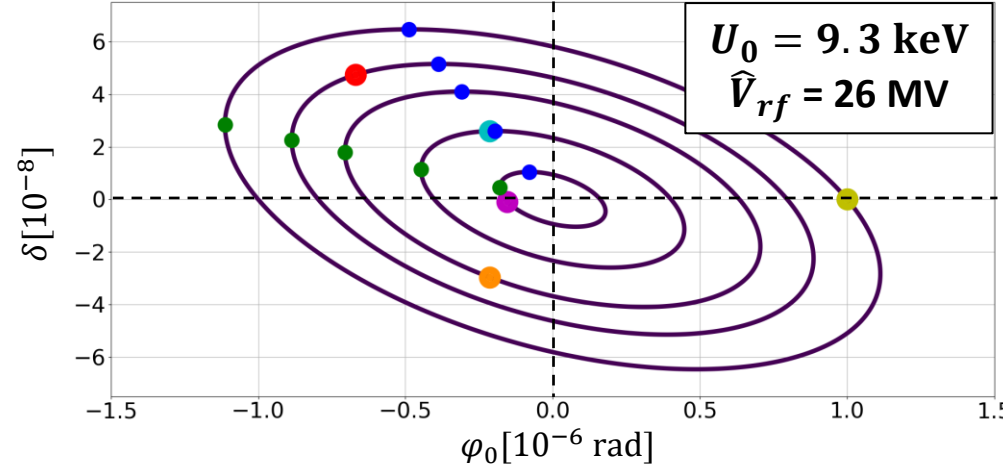


□ Unrealistically we increase the voltage to $\hat{V}_{rf} = 26$ MV to see better that the ellipses are tilted.

Non-damped motion, very tilted ellipse



Damped motion, very tilted ellipses



Ellipse-point with largest δ

$$\bullet \left(-\alpha_x \sqrt{\frac{\varepsilon}{\gamma_x}}, \sqrt{\varepsilon \gamma_x} \right)$$

Ellipse-point with smaller φ_0

$$\bullet \left(-\sqrt{\varepsilon \beta_x}, \alpha_x \sqrt{\frac{\varepsilon}{\beta_x}} \right)$$

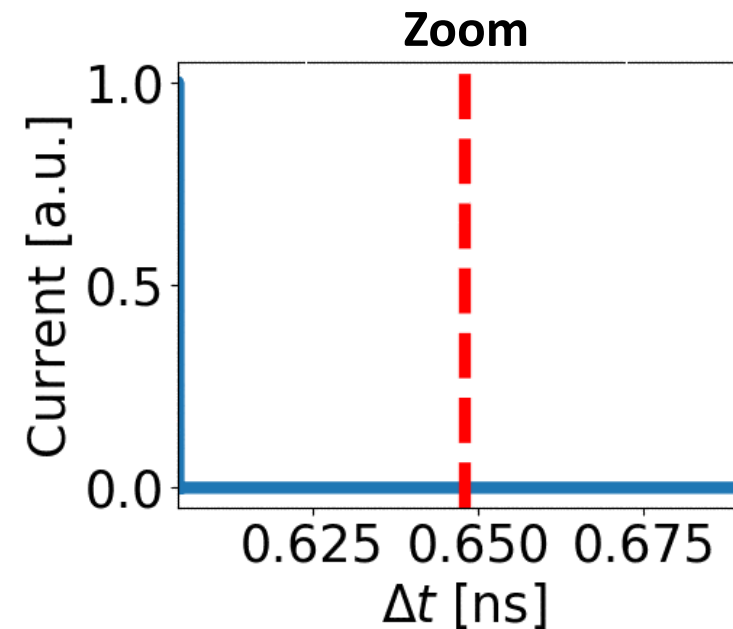
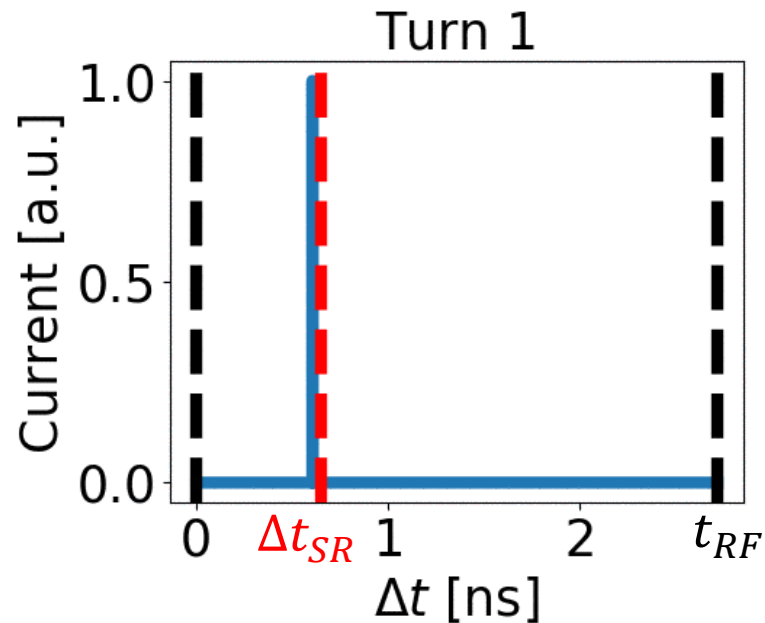
Simulated bunch at

- turn 0
- turn 12500
- turn 25000
- turn 50000
- turn 100000

Example: bunch profile (delta) performing synchrotron oscillations

□ Simulation of a Dirac-delta bunch-profile performing synchrotron oscillations in DAFNE.

- Used parameters: $E_0 = 510$ MeV, $U_0 = 9.3$ keV, $\hat{V}_{rf} = 130$ kV, $\alpha_0 = 0.018$, initial oscillation-amplitude of 0.1 rad.
- From these parameters we derive $f_0 = 3.07$ MHz, $f_{RF} = 368.26$ MHz and $f_{s0,SR} = 28.69$ kHz.
- The inverse of the synchrotron tune $1/Q_s = f_0/f_{s0} \approx 107$ corresponds to the number of revolution turns necessary to perform one synchrotron period in phase space.
- We simulate exactly one synchrotron period.



□ What is the spectrum of a bunch-profile performing synchrotron oscillations?

- Doing numerically a Discrete Fourier Transform (DFT) of the time-domain bunch-profile is computationally expensive.
- We can recur to analytical evaluations.

Spectrum of one bunch performing synchrotron oscillations

- We need these three general properties, two concerning the Dirac-delta function $\delta(x)$ and the last one related to a series-expansion of a complex exponential.

$$\delta(x) = \frac{1}{2\pi} \int_{-\infty}^{+\infty} e^{jxt} dt$$

$$\sum_{k=-\infty}^{+\infty} \delta(t - kT) \stackrel{\text{Dirac comb}}{=} \frac{1}{T} \sum_{q=-\infty}^{+\infty} e^{j2\pi q \frac{t}{T}} \quad \text{Period}$$

$$e^{-jx \cos \theta} = \sum_{n=-\infty}^{+\infty} j^{-n} J_n(x) e^{jn\theta} \quad \text{n-th Bessel function of the first kind}$$

- We assume that the bunch-profile is a delta arriving at a given machine-spot at time $t^{(k)} = kT_0 + A_s \cos[\omega_s t^{(k)}]$, k integer.
- A_s is the synchrotron-oscillation amplitude, which we assume constant (no synchrotron radiation).
 - The bunch current and spectrum can be written as

$$\begin{aligned} \lambda(t) &\propto \sum_{k=-\infty}^{+\infty} \delta(t - kT_0 - A_s \cos[\omega_s t]) \propto \sum_{q=-\infty}^{+\infty} e^{j\omega_0 q(t - A_s \cos[\omega_s t])} = \sum_{q=-\infty}^{+\infty} e^{j\omega_0 q t} e^{-j\omega_0 q A_s \cos(\omega_s t)} \\ &= \sum_{q=-\infty}^{+\infty} e^{j\omega_0 q t} \sum_{n=-\infty}^{+\infty} j^{-n} J_n(\omega_0 q A_s) e^{jn\omega_s t} = \sum_{q=-\infty}^{+\infty} \sum_{n=-\infty}^{+\infty} j^{-n} J_n(\omega_0 q A_s) e^{j(q\omega_0 + n\omega_s)t} \\ S(\omega) &= \int_{-\infty}^{+\infty} \lambda(t) e^{-j\omega t} dt \propto \sum_{q=-\infty}^{+\infty} \sum_{n=-\infty}^{+\infty} j^{-n} J_n(\omega_0 q A_s) \int_{-\infty}^{+\infty} e^{j(q\omega_0 + n\omega_s - \omega)t} dt \propto \sum_{q=-\infty}^{+\infty} \sum_{n=-\infty}^{+\infty} j^{-n} J_n(\omega_0 q A_s) \delta(q\omega_0 + n\omega_s - \omega) \end{aligned}$$

- The bunch-spectrum is therefore discrete and its lines are at $\omega_{q,n} = q\omega_0 + n\omega_s$.

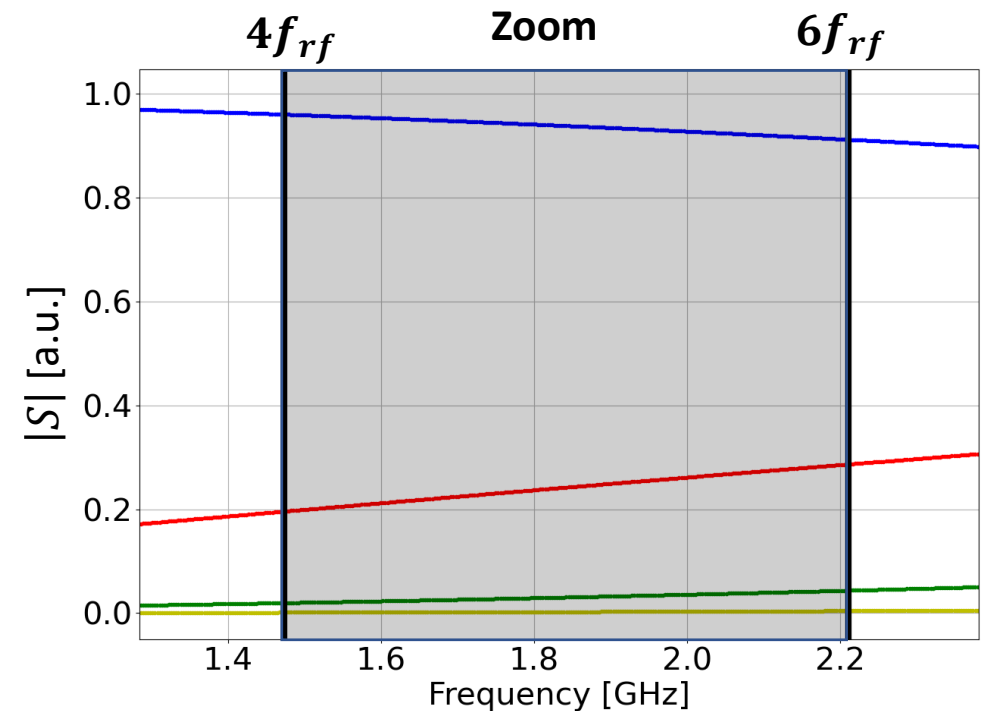
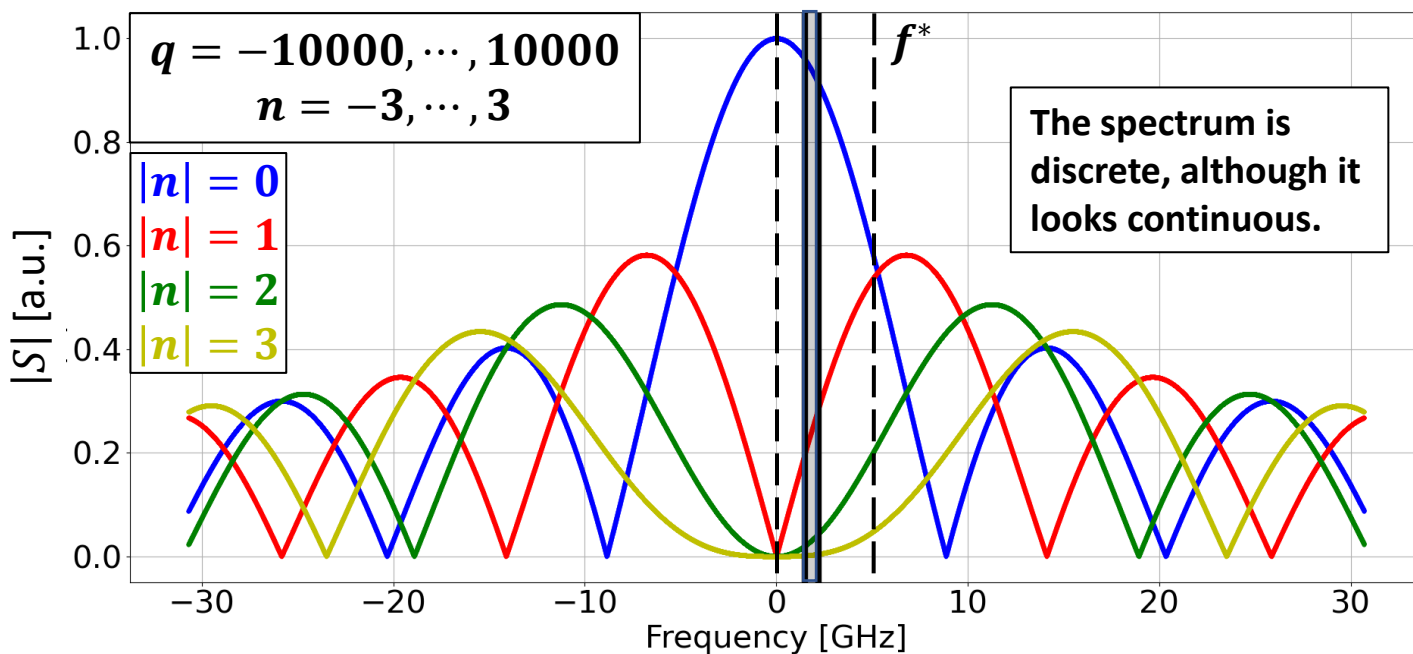
Example: spectrum of bunch performing synchrotron oscillations

- We consider again the last example, where the simulated bunch-profile was a delta performing synchrotron oscillations.
 - Parameters: $1/Q_S \approx 107$, $f_{s0,SR} = 28.69$ kHz, $f_0 = 3.07$ MHz, $f_{rf} = 368.26$ MHz, $A_S = 0.1$ rad/ ω_{RF} .

- We can use Python to evaluate the bunch spectrum

$$S(f) \propto \sum_{q=-\infty}^{+\infty} \sum_{n=-\infty}^{+\infty} j^{-n} J_n(2\pi f_0 q A_S) \delta(qf_0 + n f_{s0,SR} - f)$$

Bunch spectrum versus frequency



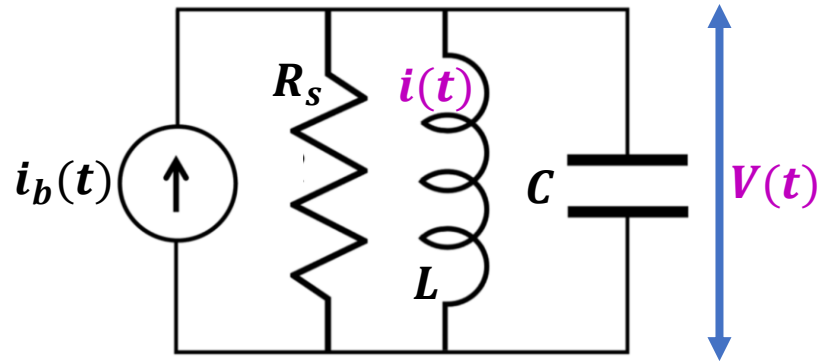
- Given a frequency in $(0, f^*)$, the spectrum-amplitudes strongly decrease as $|n|$ increases.
 - As an example, the zoom shows that the spectrum-amplitudes for $|n| = 3$ are essentially zero in the range $[4f_{rf}, 6f_{rf}]$.

Contents

- ❑ Introduction.
- ❑ Single-particle longitudinal beam-dynamics with synchrotron radiation.
 - Equations of motion, synchrotron radiation, small-amplitude synchrotron oscillations, ...
- ❑ Longitudinal beam-dynamics with synchrotron radiation and Higher Order Modes (HOMs).
 - HOM induced voltage, synchronous phase shift, HOM initial conditions, coupled-bunch instabilities, ...
- ❑ Longitudinal beam-dynamics with synchrotron radiation, HOMs and bunch-by-bunch feedback.
 - Models of the feedback components, growth and damping-rates, cavity-kicker, ideal and real corrections, ...
- ❑ Conclusions and suggested next steps.
- ❑ Appendices.
 - Execution of the new-Python and old-Fortran codes, structure of the code, exponential fits in Python, ...
- ❑ References.

HOM induced voltage (derivation)

- If $\beta=1$, each HOM of the accelerating cavity can be treated as a parallel RLC circuit driven by a point charge current.



$$i_b(t) = Q_b \delta(t) \quad (\delta \text{ is the Dirac delta function})$$

R_s : shunt impedance

L : inductance

C : capacitance

$V(t)$: voltage across the capacitance at time t

$i(t)$: current in the inductance at time t

- $i_b(t)$ charges the capacitance with the charge Q_b at $t = 0$.
- This leads to a voltage across the capacitance.
- Applying the Kirchhoff's law to the currents flowing across the three branches of the circuit

$$\frac{V(t)}{R_s} + \frac{1}{L} \int_0^t V(s) ds + C \frac{dV(t)}{dt} = 0$$

- Deriving

$$\ddot{V} + 2\Gamma \dot{V} + \omega_r^2 V = 0$$

$$\Gamma = \frac{1}{2CR_s}$$

$$\omega_r = \frac{1}{\sqrt{CL}}$$

HOM induced voltage (derivation)

- The eigenvalues are

$$\lambda_{1,2} = -\Gamma \pm j\sqrt{\omega_r^2 - \Gamma^2} = -\frac{\omega_r}{2Q} \pm j\omega_n \quad Q = \frac{\omega_r}{2\Gamma} \quad \omega_n = \sqrt{\omega_r^2 - \Gamma^2}$$

- The solution of the differential equation gives free oscillations of the kind

$$V(t) = e^{-\frac{\omega_r}{2Q}t} [A_1 \cos(\omega_n t) + B_1 \sin(\omega_n t)]$$

- ω_r and Q are respectively the angular resonant frequency and the quality factor of the HOM.

- The current in the inductance satisfies the equation

$$V(t) = L \frac{di(t)}{dt}$$

- direct verification shows that $i(t)$ is of the kind

$$i(t) = e^{-\frac{\omega_r}{2Q}t} [A_2 \cos(\omega_n t) + B_2 \sin(\omega_n t)]$$

HOM induced voltage (derivation)

□ We need to find the constants A_1 , B_1 , A_2 and B_2 .

➤ A_1 and A_2 are immediately computed

$$V(0) = V_0$$

$$A_1 = V_0$$

$$i(0) = i_0$$

$$A_2 = i_0$$

➤ As for B_2

$$V_0 = L \frac{di}{dt}(0) = -\frac{L\omega_r}{2Q} i_0 + L\omega_n B_2$$

$$B_2 = \frac{1}{L\omega_n} V_0 + \frac{\omega_r}{2Q\omega_n} i_0 = \frac{\omega_r Q}{R_s \omega_n} V_0 + \frac{\omega_r}{2Q\omega_n} i_0$$

➤ As for B_1

$$-\frac{V_0}{R_s} - i_0 = C \frac{dV}{dt}(0) = -\frac{C\omega_r}{2Q} V_0 + C\omega_n B_1$$

$$B_1 = \frac{\frac{C\omega_r}{2Q} - \frac{1}{R_s}}{C\omega_n} V_0 - \frac{1}{C\omega_n} i_0 = -\frac{\omega_r}{2Q\omega_n} V_0 - \frac{R_s \omega_r}{Q\omega_n} i_0$$

□ The solution is therefore

$$V(t) = e^{-\frac{\omega_r t}{2Q}} \left[V_0 \cos(\omega_n t) + \left(-\frac{\omega_r}{2Q\omega_n} V_0 - \frac{R_s \omega_r}{Q\omega_n} i_0 \right) \sin(\omega_n t) \right] = e^{-\frac{\omega_r t}{2Q}} \left[\left(\cos(\omega_n t) - \frac{\omega_r}{2Q\omega_n} \sin(\omega_n t) \right) V_0 - \frac{R_s \omega_r}{Q\omega_n} \sin(\omega_n t) i_0 \right]$$

$$i(t) = e^{-\frac{\omega_r t}{2Q}} \left[i_0 \cos(\omega_n t) + \left(\frac{\omega_r Q}{R_s \omega_n} V_0 + \frac{\omega_r}{2Q\omega_n} i_0 \right) \sin(\omega_n t) \right] = e^{-\frac{\omega_r t}{2Q}} \left[\frac{\omega_r Q}{R_s \omega_n} \sin(\omega_n t) V_0 + \left(\cos(\omega_n t) + \frac{\omega_r}{2Q\omega_n} \sin(\omega_n t) \right) i_0 \right]$$

HOM induced voltage (derivation)

□ In matrix form

$$\begin{pmatrix} V(t) \\ i(t) \end{pmatrix} = e^{-\frac{\omega_r}{2Q}t} \begin{pmatrix} \cos(\omega_n t) - \frac{\omega_r}{2Q\omega_n} \sin(\omega_n t) & -\frac{R_s \omega_r}{Q\omega_n} \sin(\omega_n t) \\ \frac{\omega_r Q}{R_s \omega_n} \sin(\omega_n t) & \cos(\omega_n t) + \frac{\omega_r}{2Q\omega_n} \sin(\omega_n t) \end{pmatrix} \begin{pmatrix} V_0 \\ i_0 \end{pmatrix} = e^{-\frac{\omega_r}{2Q}t} \begin{pmatrix} A_{11}(t) & A_{12}(t) \\ A_{21}(t) & A_{22}(t) \end{pmatrix} \begin{pmatrix} V_0 \\ i_0 \end{pmatrix} = W(t) \begin{pmatrix} V_0 \\ i_0 \end{pmatrix}$$

□ Let's suppose that the HOM is unloaded at $t = 0^-$, i.e. $V(0^-) = 0$ and $i(0^-) = 0$.

➤ Let's suppose that a charge Q_b crosses the accelerating cavity at $t=0$. The charge induces the voltage ΔV on the HOM

$$\Delta V = -\frac{Q_b}{C} = -\frac{R_s \omega_r}{Q} Q_b$$

➤ According to the beam-loading theorem, the energy change of the particle due to the voltage induced by itself is

$$\Delta E = Q_b \frac{\Delta V}{2} = -\frac{R_s \omega_r}{2Q} Q_b^2 < 0$$

➤ The bunch therefore loses energy due to the HOM.

➤ The current does not change at $t=0$ and therefore $V_0 = \Delta V$, $i_0 = 0$.

HOM induced voltage (derivation)

□ Let's suppose that a second charge Q_b crosses the accelerating cavity at $t = t_1 > 0$.

➤ The voltage and current of the HOM at $t = t_1$ are
$$\begin{pmatrix} V(t_1) \\ i(t_1) \end{pmatrix} = W(t_1) \begin{pmatrix} V_0 \\ i_0 \end{pmatrix} + \begin{pmatrix} \Delta V \\ 0 \end{pmatrix}$$

➤ The voltage seen by the particle at $t = t_1$ is
$$\left[W(t^*) \begin{pmatrix} V_0 \\ i_0 \end{pmatrix} \right]_{first\ row} + \frac{\Delta V}{2}$$

□ Let's suppose that a third charge Q_b crosses the accelerating cavity at $t = t_2 > t_1$.

➤ The voltage and current of the HOM at $t = t_2$ are
$$\begin{pmatrix} V(t_2) \\ i(t_2) \end{pmatrix} = W(t_2 - t_1) \begin{pmatrix} V(t_1) \\ i(t_1) \end{pmatrix} + \begin{pmatrix} \Delta V \\ 0 \end{pmatrix}$$

➤ The voltage seen by the particle at $t = t_2$ is
$$\left[W(t_2 - t_1) \begin{pmatrix} V(t_1) \\ i(t_1) \end{pmatrix} \right]_{first\ row} + \frac{\Delta V}{2}$$

□ And so on for the other charges...

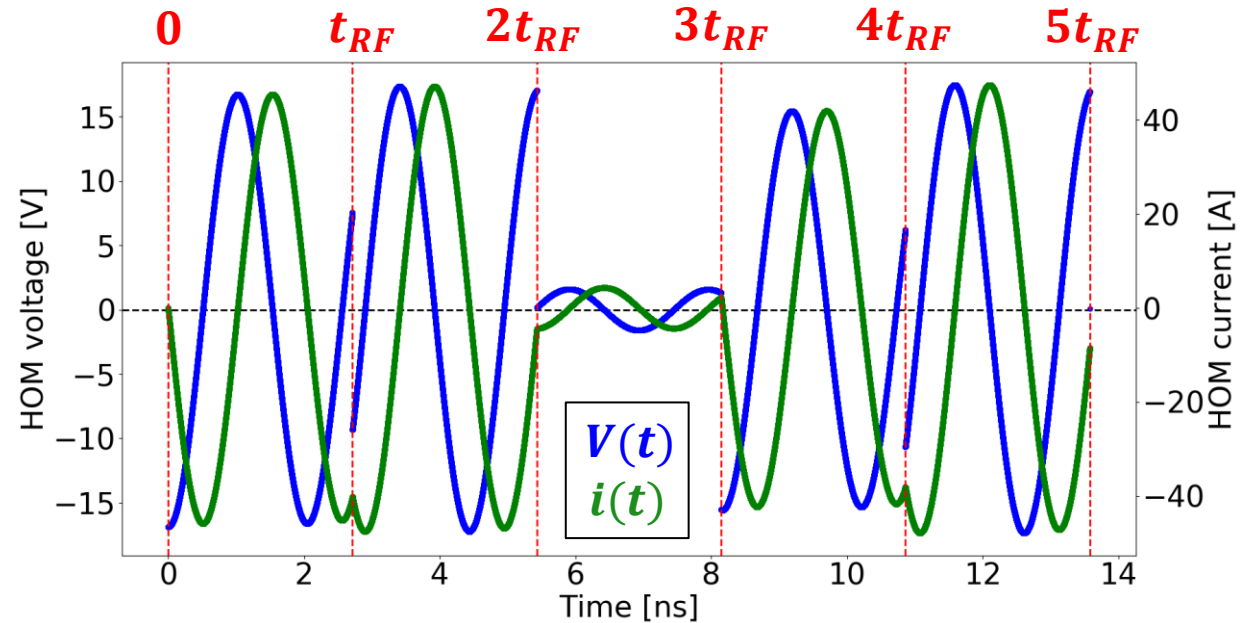
HOM induced voltage (notes)

□ Note 1:

- The voltage of the HOM is discontinuous at the times of passage of the charges
- The current of the HOM is continuous everywhere but not differentiable at the times of passage of the charges

$$V(t) = L \frac{di(t)}{dt}$$

- Example on the right: DAFNE case, one HOM.



□ Note 2: propagation property of the matrix. If t_1 and t_2 are positive, then

$$\begin{pmatrix} V(t_1 + t_2) \\ i(t_1 + t_2) \end{pmatrix} = e^{-\frac{\omega_r}{2Q}(t_1+t_2)} \begin{pmatrix} A_{11}(t_1 + t_2) & A_{12}(t_1 + t_2) \\ A_{21}(t_1 + t_2) & A_{22}(t_1 + t_2) \end{pmatrix} \begin{pmatrix} V(0) \\ i(0) \end{pmatrix} = e^{-\frac{\omega_r}{2Q}t_2} \begin{pmatrix} A_{11}(t_2) & A_{12}(t_2) \\ A_{21}(t_2) & A_{22}(t_2) \end{pmatrix} \begin{pmatrix} V(t_1) \\ i(t_1) \end{pmatrix}$$

$$= e^{-\frac{\omega_r}{2Q}t_2} \begin{pmatrix} A_{11}(t_2) & A_{12}(t_2) \\ A_{21}(t_2) & A_{22}(t_2) \end{pmatrix} e^{-\frac{\omega_r}{2Q}t_1} \begin{pmatrix} A_{11}(t_1) & A_{12}(t_1) \\ A_{21}(t_1) & A_{22}(t_1) \end{pmatrix} \begin{pmatrix} V(0) \\ i(0) \end{pmatrix} = e^{-\frac{\omega_r}{2Q}(t_1+t_2)} \begin{pmatrix} A_{11}(t_2) & A_{12}(t_2) \\ A_{21}(t_2) & A_{22}(t_2) \end{pmatrix} \begin{pmatrix} A_{11}(t_1) & A_{12}(t_1) \\ A_{21}(t_1) & A_{22}(t_1) \end{pmatrix} \begin{pmatrix} V(0) \\ i(0) \end{pmatrix}$$

- This property is useful to keep track of the HOM voltage and current as bunches traverse the cavity at different times.

HOM induced voltage (notes)

□ **Note 3:** if the HOM voltage and current are freely oscillating at $t < t_1$ due to the passage of the first bunch at $t = 0$ and if the second bunch Q_b arrives at time t_1 , then, using Note 2,

$$\begin{pmatrix} V(t_1 + t_2) \\ i(t_1 + t_2) \end{pmatrix} = e^{-\frac{\omega_r}{2Q}t_2} \begin{pmatrix} A_{11}(t_2) & A_{12}(t_2) \\ A_{21}(t_2) & A_{22}(t_2) \end{pmatrix} \begin{pmatrix} V(t_1^-) + \Delta V \\ i(t_1^-) \end{pmatrix} = e^{-\frac{\omega_r}{2Q}(t_1+t_2)} \begin{pmatrix} A_{11}(t_1 + t_2) & A_{12}(t_1 + t_2) \\ A_{21}(t_1 + t_2) & A_{22}(t_1 + t_2) \end{pmatrix} \begin{pmatrix} \Delta V \\ 0 \end{pmatrix} + e^{-\frac{\omega_r}{2Q}t_2} \begin{pmatrix} A_{11}(t_2) & A_{12}(t_2) \\ A_{21}(t_2) & A_{22}(t_2) \end{pmatrix} \begin{pmatrix} \Delta V \\ 0 \end{pmatrix}$$

contribution from first bunch

contribution from second bunch

- The voltage and current at time $t_1 + t_2$ can be decomposed as sum of two free oscillations: the first comes from the first bunch (free oscillation for $t_1 + t_2$), the second comes from the second bunch (free oscillation for t_2).
- This can be generalized to the passage of more than two bunches.

□ **Note 4:** if the HOM is unloaded and a charge Q_b passes through the accelerating cavity at $t = 0$, then, before the passage of the second charge, we have

$$\begin{pmatrix} V(t) \\ i(t) \end{pmatrix} = W(t) \begin{pmatrix} \Delta V \\ 0 \end{pmatrix} \quad \longrightarrow \quad V(t) = -Q_b \frac{R_s \omega_r}{Q} e^{-\frac{\omega_r}{2Q}t} \left[\cos(\omega_n t) - \frac{\omega_r}{2Q \omega_n} \sin(\omega_n t) \right]$$

- This $V(t)$ expression is the well-known one. Why we need to also consider the HOM current and the matrix propagation?
 - If the matrix is not used, then another method is to consider the first row of the expansion in Note 3, i.e. to add the freely oscillating voltages produced by the previous charges. This is inefficient as the number of charges increases.
 - Another possibility is to save into memory the future voltage as the sum of the past and current voltages. A voltage decay-time must be defined (first approximation) and interpolations are needed (second approximation).

□ **Note 5:** if we have more HOMs, then each HOM is treated separately, i.e. the traversing charge drives separately each HOM.

- Since we suppose that the HOMs are in series, the traversing charge sees the sum of the HOM voltages.

Equations of motion in the code (RF+SR+HOM)

□ The equations of motion for the bunch k ($k = 1, \dots, N_b$) become

$$\Delta\varphi_k^{(n+1)} = \Delta\varphi_k^{(n)} + 2\pi h\alpha_0 \delta_k^{(n)}$$

$$\delta_k^{(n+1)} = \delta_k^{(n)} - \frac{U_0}{E_0} (1 + 2\delta_k^{(n)}) + \frac{e\hat{V}_{rf} \cos \Delta\varphi_k^{(n+1)}}{E_0} + \frac{e}{E_0} \sum_{j=1}^{N_{HOM}} [V_{k,j,RES}^{(n+1)} + V_{k,j,IND}]$$

➤ where N_{HOM} is the number of HOMs,

➤ where $V_{k,j,RES}^{(n+1)}$ is the residual voltage present in the HOM j and which the bunch k sees at turn $n + 1$

• $k = 2, \dots, N_b$

$$V_{k,j,RES}^{(n+1)} = W_j \left(\bar{t}_{k-1,k}^{(n+1)} \right) \begin{pmatrix} V_{k-1,j,RES}^{(n+1)} + \Delta V_{k-1,j} \\ i_{k-1,j,RES}^{(n+1)} \end{pmatrix}$$

$$\bar{t}_{k-1,k}^{(n+1)} = \frac{(\Delta\varphi_k^{(n+1)} - \Delta\varphi_{k-1}^{(n+1)})}{\omega_{rf}} + T_{rf} d_{k-1,k}$$

time distance between
the bunches $k - 1$ and k
($d_{k-1,k}$ is the distance in
buckets)

$$\Delta V_{k-1,j} = -\frac{R_{s,j}\omega_{r,j}}{Q_j} Q_{b,k-1}$$

voltage induced by
the charge $k - 1$
on the HOM j

Equations of motion in the code (RF+SR+HOM)

$$\Delta\varphi_k^{(n+1)} = \Delta\varphi_k^{(n)} + 2\pi h \alpha_0 \delta_k^{(n)}$$

$$\delta_k^{(n+1)} = \delta_k^{(n)} - \frac{U_0}{E_0} (1 + 2\delta_k^{(n)}) + \frac{e\hat{V}_{rf} \cos \Delta\varphi_k^{(n+1)}}{E_0} + \frac{e}{E_0} \sum_{j=1}^{N_{HOM}} [V_{k,j,RES}^{(n+1)} + V_{k,j,IND}]$$

- $k = 1$

$$V_{1,j,RES}^{(n+1)} = W_j \left(\bar{t}_{N_b,1}^{(n+1)} \right) \begin{pmatrix} V_{N_b,j,RES}^{(n+1)} + \Delta V_{N_b,j} \\ i_{N_b,j,RES}^{(n+1)} \end{pmatrix}$$

$$\bar{t}_{N_b,1}^{(n+1)} = \frac{(\Delta\varphi_1^{(n+1)} - \Delta\varphi_{N_b}^{(n)})}{\omega_{rf}} + T_{rf} d_{N_b,1}$$

time distance between the bunches N_b and 1, at turn n and $n+1$ respectively ($d_{N_b,1}$ is the distance in buckets)

$$\Delta V_{N_b,j} = -\frac{R_{s,j} \omega_{r,j}}{Q_j} Q_{b,N_b}$$

voltage induced by the charge N_b on the HOM j

- where $V_{k,j,IND}$ derives from the beam loading theorem: the charge k sees half of the voltage that the charge itself induces on the HOM j

$$V_{k,j,IND} = \frac{\Delta V_{k,j}}{2} = -\frac{R_{s,j} \omega_{r,j}}{2Q_j} Q_{b,k}$$

Synchronous phase considering also the HOMs

□ Imposing $\delta_k^{(n)} = \delta_k^{(n+1)} = 0$, the synchronous phase $\Delta\varphi_{HOM,k}$ is the solution of

$$0 = -\frac{U_0}{E_0} + \frac{e\hat{V}_{rf} \cos \Delta\varphi_{HOM,k}}{E_0} + \frac{e}{E_0} \sum_{j=1}^{N_{HOM}} \left(V_{k,j,RES}^{(n+1)} + V_{k,j,IND} \right)$$

➤ if all the HOM voltages are zero, i.e. $V_{k,j,RES}^{(n+1)} = V_{k,j,IND} = 0$, then

$$\Delta\varphi_{HOM,k} = \Delta\varphi_{SR} = \cos^{-1} \frac{U_0}{e\hat{V}_{rf}}$$

➤ if all the HOM residual voltages are zero, i.e. $V_{k,j,RES}^{(n+1)} = 0$, then

$$\Delta\varphi_{HOM,k} = \cos^{-1} \frac{U_0 - e \sum_{j=1}^{N_{HOM}} V_{k,j,IND}}{e\hat{V}_{rf}}$$

- note that $V_{k,j,IND} < 0$, indeed the RF cavities must now compensate for U_0 plus the energy lost by the particle due to the beam loading theorem

➤ we need an iterative procedure to find $\Delta\varphi_{HOM,k}$ in the general case, see below.

HOM initial conditions (unloaded vs loaded)

□ In the code the HOMs can be either 'unloaded' or 'loaded'.

- **Unloaded:** the HOM residual voltage and current are both zero at the start of the simulation.
 - Useful to study transient effects, however in this case the injection process has to be simulated as well.
- **Loaded:** the HOM voltage and current satisfy a stationarity condition, as if the bunches were already circulating for a long time in the ring at the start of the simulation.
 - Useful to neglect the injection and transient phases, allowing at the same time perturbative studies where the bunches are positioned close to their synchronous phases in phase-space.

□ Stationarity condition for a loaded HOM:

- When a charge traverses the RF cavity, the induced ΔV must compensate the decay of $V(t)$ during the previous period T_0 , while the current must remain constant. Normalizing with respect to Q_b , this condition reads

$$\begin{pmatrix} V(t_0)/Q_b \\ i(t_0)/Q_b \end{pmatrix} = e^{-\frac{\omega_r T_0}{2Q}} \begin{pmatrix} A_{11}(T_0) & A_{12}(T_0) \\ A_{21}(T_0) & A_{22}(T_0) \end{pmatrix} \begin{pmatrix} V(t_0)/Q_b \\ i(t_0)/Q_b \end{pmatrix} + \begin{pmatrix} \Delta V/Q_b \\ 0 \end{pmatrix}$$

□ Solving with respect to $V(t_0)/Q_b$ and $i(t_0)/Q_b$, we obtain

$$\frac{V(t_0)}{Q_b} = \frac{-R_s \omega_r / Q}{1 - \left(A_{11}(T_0) + \frac{A_{12}(T_0) A_{21}(T_0)}{e^{\Gamma T_0} - A_{22}(T_0)} \right) / e^{\Gamma T_0}} = \bar{a}_V(T_0) \quad \frac{i(t_0)}{Q_b} = \frac{A_{21}(T_0)}{e^{\Gamma T_0} - A_{22}(T_0)} \bar{a}_V(T_0) = \bar{a}_i(T_0)$$

HOM initial conditions (unloaded vs loaded)

□ In order to start the tracking of the bunches in the code, we need

- The initial phases $\Delta\varphi_k^{(0)}$ of the bunches
- The energy-deviations $\delta_k^{(0)}$ of the bunches
- The residual voltage $V_{1,j,RES}^{(0)}$ and current $i_{1,j,RES}^{(0)}$ of the j^{th} HOM when the first bunch traverses the RF cavity.

□ **Case of unloaded HOM.**

- The Fortran code allows to set the initial phases of the bunches to values close to $\Delta\varphi_{SR} = \cos^{-1}(U_0/\hat{V}_{rf})$

$$\Delta\varphi_k^{(0)} \approx \Delta\varphi_{SR}$$

- The Fortran code allows to set the initial energy-deviations of the bunches to values close to 0

$$\delta_k^{(0)} \approx 0$$

- The residual voltage and current are 0 for the first bunch at turn 0

$$V_{1,j,RES}^{(0)} = i_{1,j,RES}^{(0)} = 0$$

- **NOTE 1:** if intensity effects are large, then the difference between $\Delta\varphi_{HOM,k}$ and $\Delta\varphi_{SR}$ is large, therefore the bunches close to $(\Delta\varphi_{SR}, 0)$ are far from their equilibrium positions and can display unwanted large initial dipole oscillations.
- **NOTE 2:** even if bunches are at $(\Delta\varphi_{HOM,k}, 0)$, dipole oscillations are still visible since the HOM is unloaded and $\Delta\varphi_{HOM,k}$ assumes that the HOM is loaded. However these dipole oscillations are lower than the ones obtained when the bunches are at $(\Delta\varphi_{SR}, 0)$.

HOM initial conditions (unloaded vs loaded)

□ Case of loaded HOM.

- The Fortran code allows to set the initial phases of the bunches to values close to $\Delta\varphi_{SR} = \cos^{-1}(U_0/\hat{V}_{rf})$.

$$\Delta\varphi_k^{(0)} \approx \Delta\varphi_{SR}$$

- The Fortran code allows to set the initial energy-deviations of the bunches to values close to 0.

$$\delta_k^{(0)} \approx 0$$

- In the Fortran code, the residual voltage and current for the first bunch at turn 0 are computed as

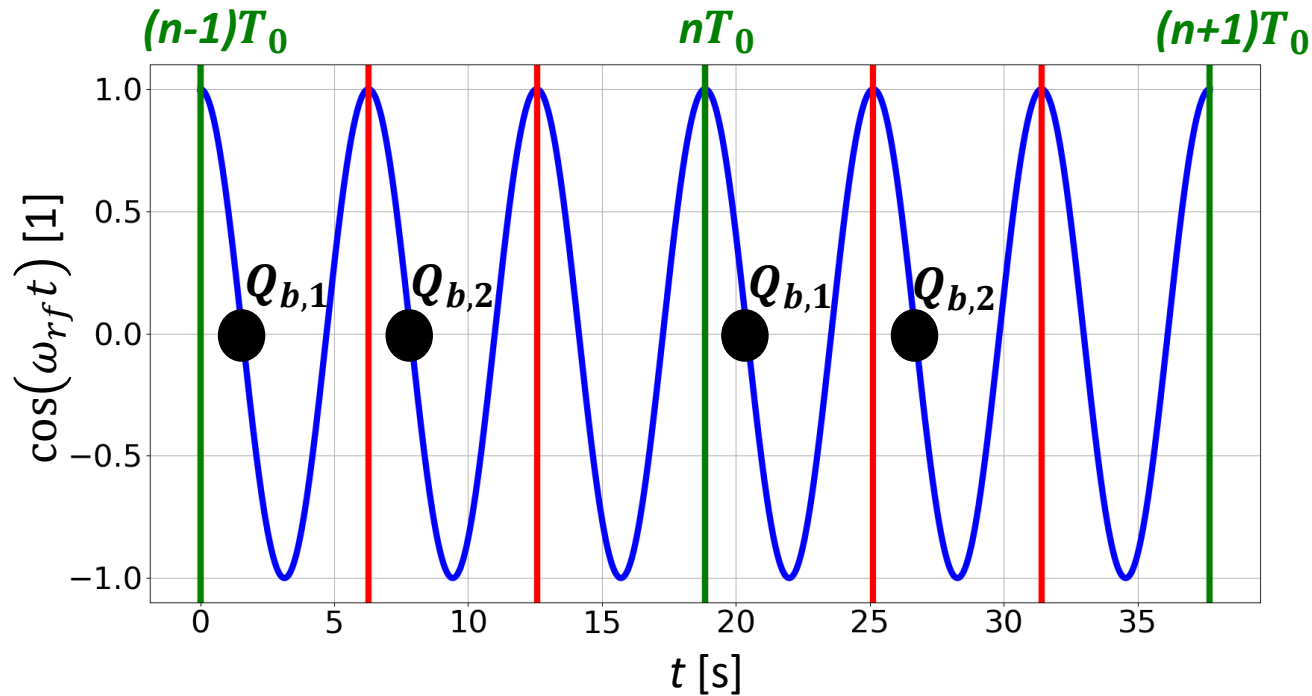
$$\begin{pmatrix} V_{1,j,RES}^{(0)} \\ i_{1,j,RES}^{(0)} \end{pmatrix} = \sum_{i=1}^{N_b} W(t_{i1}) \begin{pmatrix} \bar{a}_V(T_0) Q_{b,i} \\ \bar{a}_i(T_0) Q_{b,i} \end{pmatrix}$$

-> $t_{i1} = T_{rf}(\mathbf{h} - \mathbf{d}_{1i})$ is the time distance between the bunch i at the previous turn and the bunch 1 at the current turn.
 -> \mathbf{d}_{1i} is the distance in number of buckets between the first and the i^{th} bunches.

- This equation represents the sum of residual voltages and currents generated by the N_b bunches during the last turn.
 - As desired, this equation implies that the HOM voltage and current are T_0 -periodic for each bunch (see below).
 - The sum in the equation should be extended to all the previous turns, however the propagation properties of W listed above and the stationarity condition allow to restrict the sum to just the last revolution period.
 - **NOTE 1:** a strong assumption was made, i.e. that all the bunches are in $\Delta\varphi_{SR}$, with time distances which are multiple of T_{rf} . However the actual equilibrium phases are $\Delta\varphi_{HOM,k} \neq \Delta\varphi_{SR}$ and the time distances aren't multiple of T_{rf} .
- **NOTE 2:** if intensity effects are large, then the difference between $\Delta\varphi_{HOM,k}$ and $\Delta\varphi_{SR}$ is large, therefore the bunches close to $(\Delta\varphi_{SR}, 0)$ are far from their equilibrium positions and can display unwanted large initial dipole oscillations.

T_0 -periodicity of voltage and current for loaded HOMs

- By definition, the voltage of a loaded HOM are T_0 - periodic if there is only one bunch in the ring.
- The T_0 -periodicity works also for more bunches.
 - Example: two bunches on a $h=3$ ring with one HOM.



$$\begin{aligned} \begin{pmatrix} V_1^{(n-1)} \\ i_1^{(n-1)} \end{pmatrix} &= \begin{pmatrix} \Delta V_1 \\ 0 \end{pmatrix} + W(T_0) \begin{pmatrix} \bar{a}_V(T_0) Q_{b,1} \\ \bar{a}_i(T_0) Q_{b,1} \end{pmatrix} \\ &+ W\left(T_0 - \frac{2\pi}{\omega_{rf}}\right) \begin{pmatrix} \bar{a}_V(T_0) Q_{b,2} \\ \bar{a}_i(T_0) Q_{b,2} \end{pmatrix} \\ &= \begin{pmatrix} \bar{a}_V(T_0) Q_{b,1} \\ \bar{a}_i(T_0) Q_{b,1} \end{pmatrix} + W\left(T_0 - \frac{2\pi}{\omega_{rf}}\right) \begin{pmatrix} \bar{a}_V(T_0) Q_{b,2} \\ \bar{a}_i(T_0) Q_{b,2} \end{pmatrix} \\ &\quad \text{perturbation from second bunch} \end{aligned}$$

$$\begin{aligned} \begin{pmatrix} V_2^{(n-1)} \\ i_2^{(n-1)} \end{pmatrix} &= \begin{pmatrix} \Delta V_2 \\ 0 \end{pmatrix} + W\left(\frac{2\pi}{\omega_{rf}}\right) \begin{pmatrix} V_1^{(n-1)} \\ i_1^{(n-1)} \end{pmatrix} \\ &= \begin{pmatrix} \bar{a}_V(T_0) Q_{b,2} \\ \bar{a}_i(T_0) Q_{b,2} \end{pmatrix} + W\left(\frac{2\pi}{\omega_{rf}}\right) \begin{pmatrix} \bar{a}_V(T_0) Q_{b,1} \\ \bar{a}_i(T_0) Q_{b,1} \end{pmatrix} \\ &\quad \text{perturbation from first bunch} \end{aligned}$$

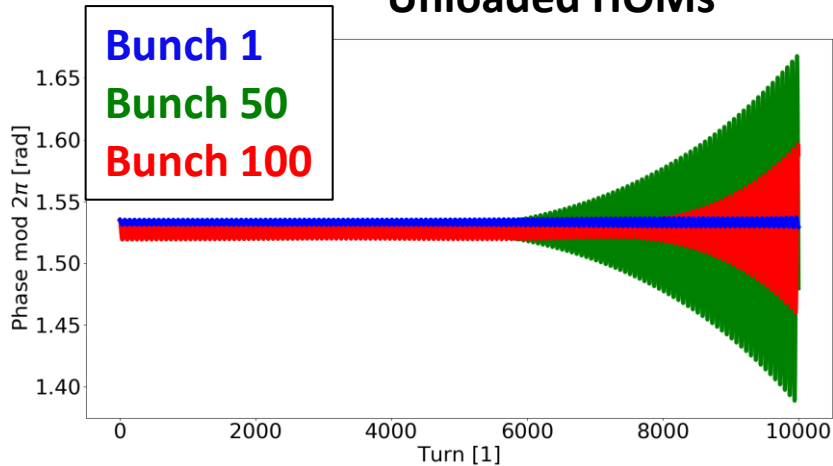
$$\begin{pmatrix} V_1^{(n)} \\ i_1^{(n)} \end{pmatrix} = \begin{pmatrix} \Delta V_1 \\ 0 \end{pmatrix} + W\left(T_0 - \frac{2\pi}{\omega_{rf}}\right) \begin{pmatrix} V_2^{(n-1)} \\ i_2^{(n-1)} \end{pmatrix} = \begin{pmatrix} \bar{a}_V(T_0) Q_{b,1} \\ \bar{a}_i(T_0) Q_{b,1} \end{pmatrix} + W\left(T_0 - \frac{2\pi}{\omega_{rf}}\right) \begin{pmatrix} \bar{a}_V(T_0) Q_{b,2} \\ \bar{a}_i(T_0) Q_{b,2} \end{pmatrix} = \begin{pmatrix} V_1^{(n-1)} \\ i_1^{(n-1)} \end{pmatrix} \quad \text{\textbf{\color{red} } } T_0\text{-periodicity is verified.}$$

perturbation from second bunch

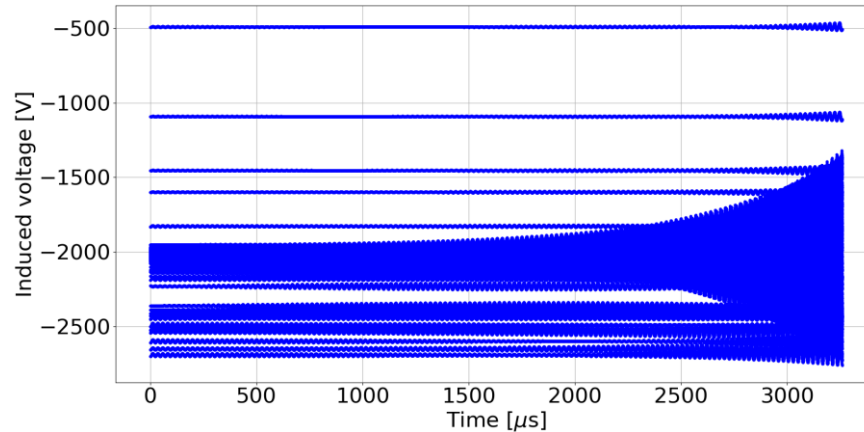
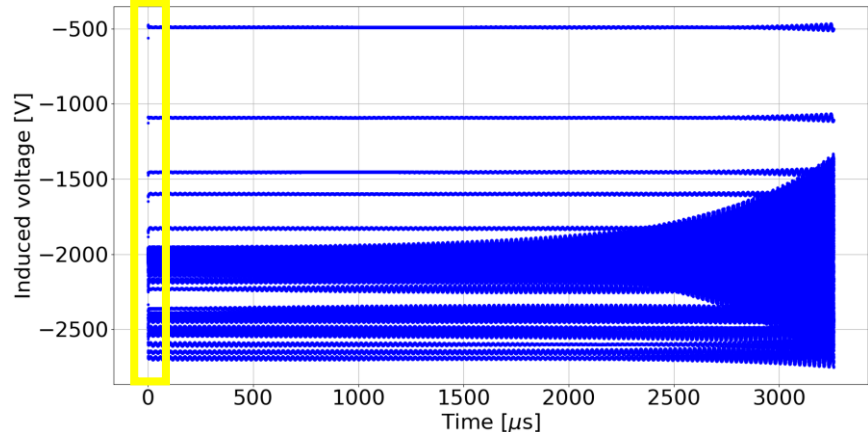
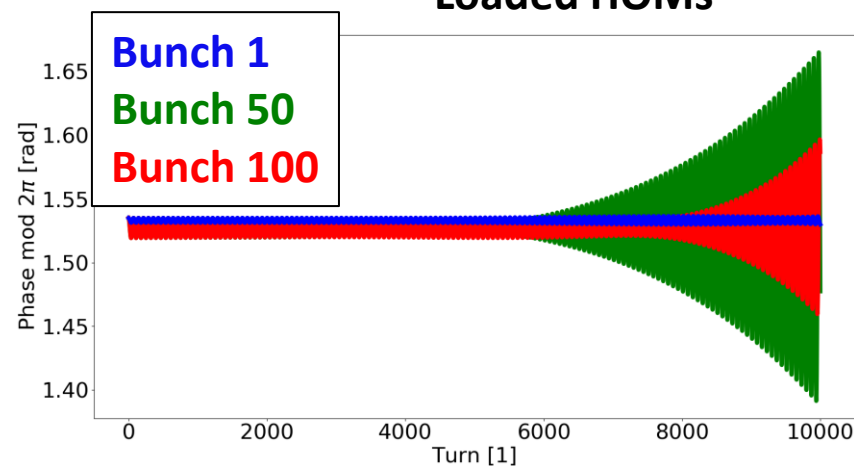
Example of simulation using unloaded and loaded HOMs

- DAFNE case: $E_0 = 510$ MeV, $U_0 = 9.3$ keV, $V_{rf} = 260$ kV, 14 HOMs, 100 bunches with $Q_b = 15$ nC in buckets 1, 2, ..., 100.
- The initial phases and energy-deviations are respectively $\Delta\varphi_k^{(0)} = \Delta\varphi_{SR}$ and $\delta_k^{(0)} = \mathbf{0}$.
- We plot the dipole oscillations for the bunches 1, 50 and 100 along 10000 turns.
- We plot the HOM voltages seen by the bunches along 10000 turns.

Unloaded HOMs



Loaded HOMs



- The dipole oscillations remain practically the same when the HOMs are loaded.
- The voltages seen by the bunches when the HOMs are unloaded converge rapidly to the voltages seen by the bunches when the HOMs are loaded.
- We need a better algorithm to compute the stationary voltages of loaded HOMs.
 - The stable phases are $\Delta\varphi_{HOM,k}$ and not $\Delta\varphi_{SR}$ and so the time-distances between bunches are not multiple of T_{rf} .
 - Finding $\Delta\varphi_{HOM,k}$ allows also to position the bunches close to their equilibrium points at turn 0.

Improvement of the loaded-HOM algorithm

$\Delta\varphi_{HOM,1} = \Delta\varphi_{HOM,2} = \Delta\varphi_{SR}$ -> First guess for $\Delta\varphi_{HOM,1}$ and $\Delta\varphi_{HOM,2}$

$V_{1,RES}^{(0)} = V_{2,RES}^{(0)} = 0$ -> First guess for $V_{1,RES}^{(0)}$ and $V_{2,RES}^{(0)}$

for $j = 1, \dots, n_{iter}$ -> n_{iter} is the chosen number of iterations

$$t_{11} = hT_{rf}, t_{21} = T_{rf}(h - d_{12}) + (\Delta\varphi_{HOM,1} - \Delta\varphi_{HOM,2})/\omega_{rf}$$

$$\begin{pmatrix} V_{1,RES,NEW}^{(0)} \\ i_{1,RES}^{(0)} \end{pmatrix} = W(t_{11}) \begin{pmatrix} \bar{a}_V(T_0)Q_{b,1} \\ \bar{a}_i(T_0)Q_{b,1} \end{pmatrix} + W(t_{21}) \begin{pmatrix} \bar{a}_V(T_0)Q_{b,2} \\ \bar{a}_i(T_0)Q_{b,2} \end{pmatrix}$$

Compute residual voltage and current for first bunch

$$t_{12} = T_{rf}d_{12} + (\Delta\varphi_{HOM,2} - \Delta\varphi_{HOM,1})/\omega_{rf}$$

$$\begin{pmatrix} V_{2,RES,NEW}^{(0)} \\ i_{2,RES}^{(0)} \end{pmatrix} = W(t_{12}) \begin{pmatrix} V_{1,RES,NEW}^{(0)} + \Delta V_1 \\ i_{1,RES}^{(0)} \end{pmatrix}$$

Compute residual voltage and current for second bunch

$$\text{error} = \sqrt{|V_{1,RES,NEW}^{(0)} - V_{1,RES}^{(0)}|^2 + |V_{2,RES,NEW}^{(0)} - V_{2,RES}^{(0)}|^2} \rightarrow L_2 \text{ norm}$$

$$\Delta\varphi_{HOM,1} = \arccos \left[\left(U_0 - \Delta V_1/2 - V_{1,RES,NEW}^{(0)} \right) / V_{rf} \right]$$

$$\Delta\varphi_{HOM,2} = \arccos \left[\left(U_0 - \Delta V_2/2 - V_{2,RES,NEW}^{(0)} \right) / V_{rf} \right]$$

Compute updated values for $\Delta\varphi_{HOM,1}$ and $\Delta\varphi_{HOM,2}$

$V_{1,RES}^{(0)} = V_{1,RES,NEW}^{(0)}, V_{2,RES}^{(0)} = V_{2,RES,NEW}^{(0)}$ -> save voltages to compute error at iter. $j+1$

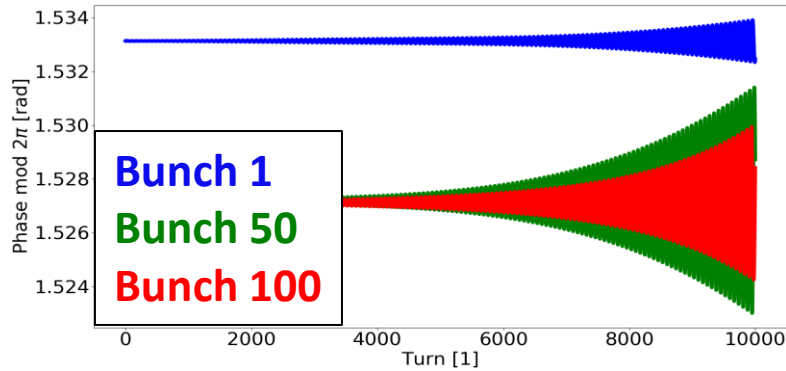
return $\Delta\varphi_{HOM,1}, \Delta\varphi_{HOM,2}, V_{1,RES}^{(0)}, i_{1,RES}^{(0)}, V_{2,RES}^{(0)}, i_{2,RES}^{(0)}$ -> outputs

- ❑ Example with only two bunches and one HOM.
- ❑ The routine provides as output $\Delta\varphi_{HOM,1}, \Delta\varphi_{HOM,2}, V_{1,RES}^{(0)}, i_{1,RES}^{(0)}, V_{2,RES}^{(0)}, i_{2,RES}^{(0)}$.
- ❑ The routine is an iterative algorithm: at each iteration j the error is expected to diminish.
- ❑ The routine is launched one time before the main tracking loop.
- ❑ Idea behind the algorithm:
 - Guess $\Delta\varphi_{HOM,1}$ and $\Delta\varphi_{HOM,2}$
 - $V_{1,RES}^{(0)}$ and $V_{2,RES}^{(0)}$ are determined
 - $\Delta\varphi_{HOM,1}$ and $\Delta\varphi_{HOM,2}$ are determined ...
- ❑ The routine can be also used to compute $\Delta\varphi_{HOM,1}$ and $\Delta\varphi_{HOM,2}$ for unloaded HOMs.
- ❑ The Fortran loaded-HOM routine is obtained setting $n_{iter}=1$ and $\Delta\varphi_{HOM,i} = \Delta\varphi_{SR}$ for all the bunches.

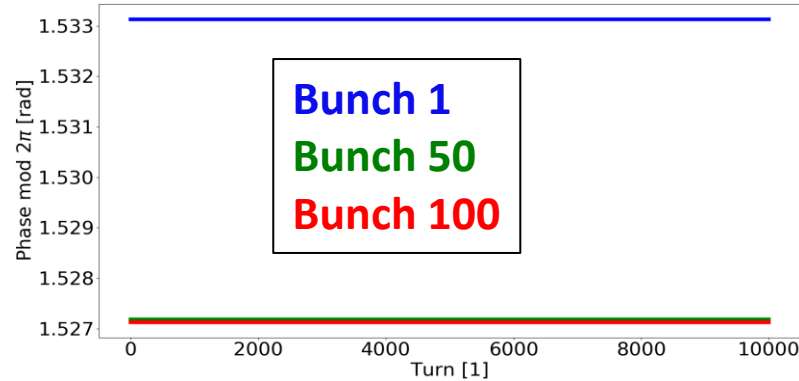
Previous simulation using improved routine for loaded HOMs

- ❑ DAFNE case: $E_0 = 510$ MeV, $U_0 = 9.3$ keV, $V_{rf} = 260$ kV, 14 HOMs, 100 bunches with $Q_b=15$ nC in buckets 1, 2, ..., 100.
- ❑ The initial phases and energy-deviations are respectively $\Delta\varphi_k^{(0)} = \Delta\varphi_{HOM,k}$ and $\delta_k^{(0)} = \mathbf{0}$.
- ❑ Unloaded HOMs: $V_{1,j,RES}^{(0)} = i_{1,j,RES}^{(0)} = \mathbf{0}$.
 - As desired, the dipole oscillations are significantly lower than the ones obtained when $\Delta\varphi_k^{(0)} = \Delta\varphi_{SR}$.
- ❑ Loaded HOMs: $V_{1,j,RES}^{(0)}$ and $i_{1,j,RES}^{(0)}$ come from the outputs of the improved routine.
 - As desired, there are no dipole oscillations and the voltages seen by each bunch are constant in time.

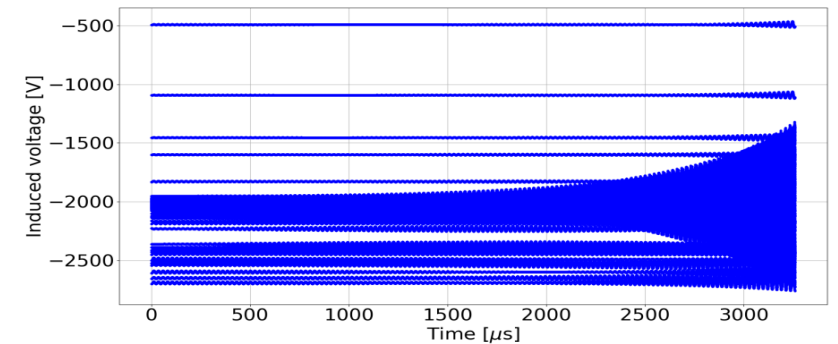
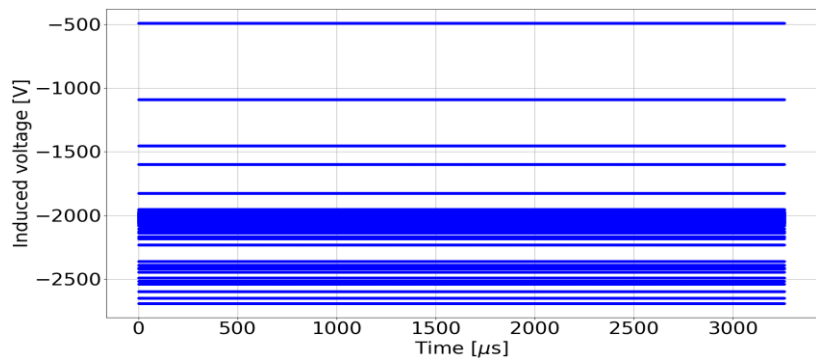
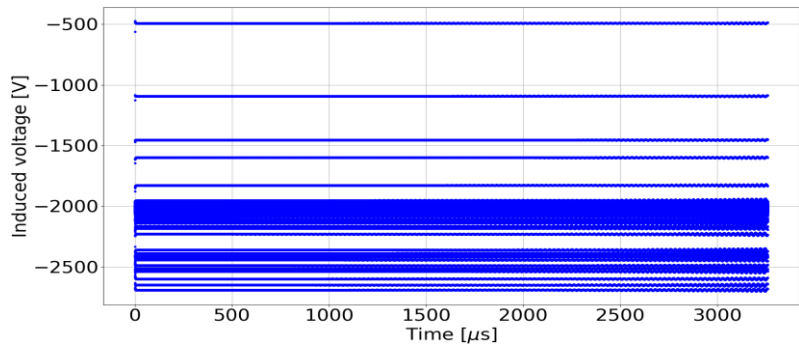
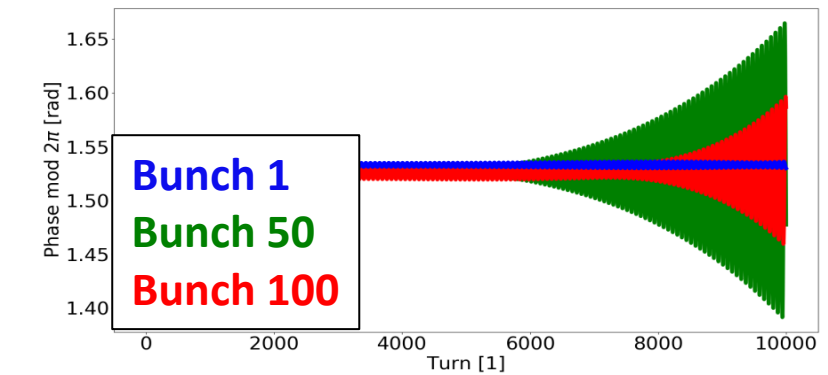
Unloaded HOMs (improved routine)



Loaded HOMs (improved routine)



Loaded HOMs (Fortran routine)



Effects of the bunch length on HOM-voltage computations

□ In the code, each bunch is represented by just one macroparticle.

□ How to take into account the actual bunch length σ_t in the HOM voltage calculations?

➤ In the code, the R_s of each HOM is multiplied by $e^{-\frac{\omega_r^2 \sigma_t^2}{2}}$ and then computations are done as for a single particle. Why?

□ If $\lambda(t) = Q_b \delta_d(t)$ is the longitudinal line-density of a particle-bunch crossing the RF cavity, then the residual voltage in the cavity is given by

$$V(t) = -Q_b \frac{R_s \omega_r}{Q} e^{-\frac{\omega_r^2 \sigma_t^2}{2}} \left[\cos(\omega_n t) - \frac{\omega_r}{2Q\omega_n} \sin(\omega_n t) \right] = -Q_b w_{\parallel}(t)$$

➤ where $w_{\parallel}(t)$ [V/C] is the wakefield of the HOM.

□ In general, given an arbitrary $\lambda(t)$, the residual voltage in the RF cavity is given by the convolution of λ and w_{\parallel}

$$V(t) = -\lambda(t) * w_{\parallel}(t) = -\int_0^{\infty} \lambda(t - \tau) w_{\parallel}(\tau) d\tau \quad \text{NOTE: } V(t)/Q_b \text{ is called wake function or wake potential}$$

➤ where $\lambda(t - \tau)$ is the charge at $t - \tau$ which affects the charge at t . The particles at the head of the bunch have lower t .

➤ The formula is indeed true if $\lambda(t) = Q_b \delta_d(t)$

$$V(t) = -\int_0^{\infty} Q_b \delta_d(t - \tau) w_{\parallel}(\tau) d\tau = -Q_b w_{\parallel}(t)$$

Effects of the bunch length on HOM-voltage computations

□ Applying the Fourier transform \mathcal{F} and using its inverse \mathcal{F}^{-1} we obtain

$$\mathcal{F}(V) = -\mathcal{F}(\lambda) \mathcal{F}(w_{\parallel}) = -S(\omega)Z(\omega) \quad \text{or} \quad V = -\mathcal{F}^{-1}[\mathcal{F}(\lambda) \mathcal{F}(w_{\parallel})] = -\mathcal{F}^{-1}[S(\omega)Z(\omega)]$$

➤ where S is the bunch spectrum and Z is the longitudinal coupling impedance of the HOM

$$Z(\omega) = \frac{R_s}{1 + jQ \left(\frac{\omega}{\omega_r} - \frac{\omega_r}{\omega} \right)}$$

➤ The formula is indeed true if $\lambda(t) = Q_b \delta_d(t)$

$$V(t) = -\mathcal{F}^{-1}[\mathcal{F}(\lambda) \mathcal{F}(w_{\parallel})] = -Q_b \mathcal{F}^{-1}[\mathcal{F}(w_{\parallel})] = -Q_b w_{\parallel}(t)$$

➤ If $\lambda(t)$ is Gaussian, then

$$\lambda(t) = \frac{Q_b}{\sigma_t \sqrt{2\pi}} e^{-\frac{t^2}{2\sigma_t^2}} \quad S(\omega) = Q_b e^{-\frac{\omega^2 \sigma_t^2}{2}} \quad V(t) = -\mathcal{F}^{-1}[\mathcal{F}(\lambda) \mathcal{F}(w_{\parallel})] = -Q_b \mathcal{F}^{-1} \left[e^{-\frac{\omega^2 \sigma_t^2}{2}} \mathcal{F}(w_{\parallel}) \right]$$

$$V(t) = -Q_b \mathcal{F}^{-1} \left[e^{-\frac{\omega^2 \sigma_t^2}{2}} \mathcal{F}(w_{\parallel}) \right] \approx -Q_b e^{-\frac{\omega_r^2 \sigma_t^2}{2}} w_{\parallel}(t) = -Q_b \frac{\tilde{R}_s \omega_r}{Q} e^{-\frac{\omega_r}{2Q} t} \left[\cos(\omega_n t) - \frac{\omega_r}{2Q \omega_n} \sin(\omega_n t) \right] \quad \tilde{R}_s = e^{-\frac{\omega_r^2 \sigma_t^2}{2}} R_s$$

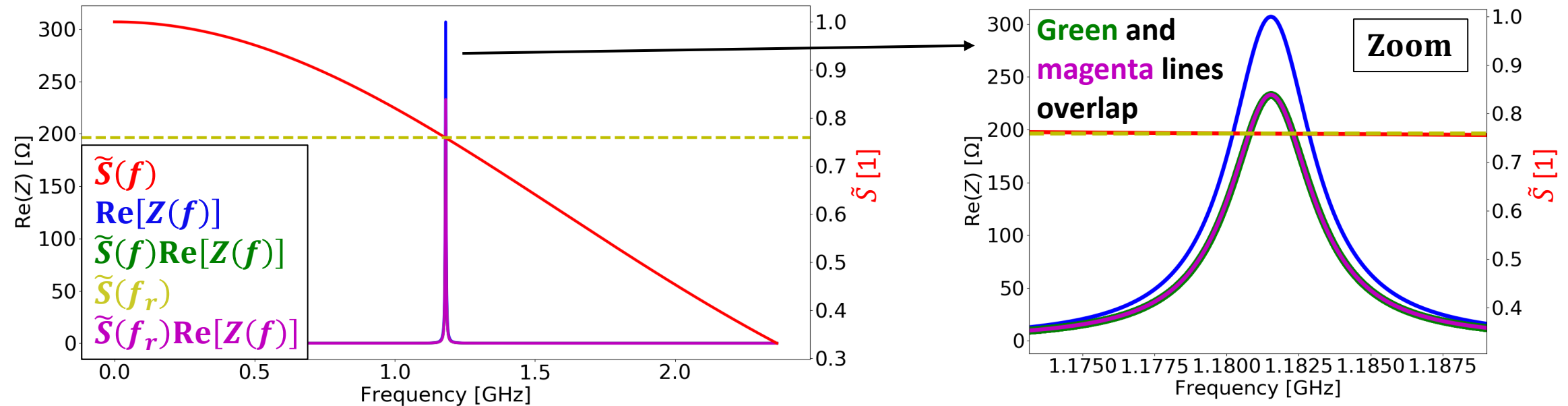
Is this approximation ok?

Effects of the bunch length on HOM-voltage computations

□ Let's check if the following approximation can be done

$$\mathcal{F}^{-1}\left(e^{-\frac{\omega^2\sigma_t^2}{2}}\mathcal{F}(w_{\parallel})\right) \approx \mathcal{F}^{-1}\left(e^{-\frac{\omega_r^2\sigma_t^2}{2}}\mathcal{F}(w_{\parallel})\right) \quad \text{or} \quad \mathcal{F}^{-1}[S(\omega)Z(\omega)] \approx \mathcal{F}^{-1}[S(\omega_r)Z(\omega)] \quad \text{or} \quad S(\omega)Z(\omega) \approx S(\omega_r)Z(\omega)$$

□ We take as an example one HOM of the DAFNE RF cavity and we consider a Gaussian bunch with $\sigma_z = 30$ mm ($\tilde{S} = S/Q_b$).



□ Close to f_r , $\tilde{S}(f) \approx \tilde{S}(f_r)$ since the HOM bandwidth is small.



$$\tilde{S}(f)\text{Re}[Z(f)] \approx \tilde{S}(f_r)\text{Re}[Z(f)]$$

□ Far from f_r , $\tilde{S}(f)$ significantly differs from $\tilde{S}(f_r)$, but $\text{Re}[Z(f)] \approx 0$



$$\tilde{S}(f)\text{Re}[Z(f)] \approx \tilde{S}(f_r)\text{Re}[Z(f)] \approx 0$$

Coupled-bunch instabilities (1/12)

- Let's suppose to have N_b equally-spaced bunches, each with charge Q_b , circulating in a ring with circumference C_r .
 - We assume that each bunch is described by only one macroparticle.

- For each bunch $n = 0, \dots, N_b - 1$, the continuous equations of motion are

$$\dot{\Delta\varphi}_n = \omega_{rf}\alpha_0\delta_n \quad \dot{\delta}_n = -\frac{U_0}{E_0T_0}(1 + 2\delta_n) + \frac{eV_{W,n}^{tot}}{E_0T_0} + \frac{e\hat{V}_{rf}}{E_0T_0}\cos\Delta\varphi_n$$

- where $V_{W,n}^{tot}$ is the induced-voltage seen by the bunch n and induced by all the charges circulating in the ring.

- Deriving and substituting

$$\ddot{\Delta\varphi}_n = -\frac{\omega_{rf}\alpha_0U_0}{E_0T_0}\left(1 + 2\frac{\dot{\Delta\varphi}_n}{\omega_{rf}\alpha_0}\right) + \frac{\omega_{rf}\alpha_0eV_{W,n}^{tot}}{E_0T_0} + \frac{\omega_{rf}\alpha_0e\hat{V}_{rf}}{E_0T_0}\cos\Delta\varphi_n$$

- Changing variable from $\Delta\varphi_n$ to $\varphi_{0,n} = \Delta\varphi_n - \Delta\varphi_{HOM,n}$, and then from $\varphi_{0,n}$ to $z_{0,n} = -c\varphi_{0,n}/\omega_{rf}$, we obtain

$$\ddot{z}_{0,n} = \frac{c\alpha_0U_0}{E_0T_0} - \frac{D}{T_0}\dot{z}_{0,n} - \frac{c\alpha_0eV_{W,n}^{tot}}{E_0T_0} - \frac{c\alpha_0e\hat{V}_{rf}}{E_0T_0}\cos\left(\Delta\varphi_{HOM,n} - \frac{2\pi h}{C_r}z_{0,n}\right)$$

Coupled-bunch instabilities (2/12)

□ $V_{W,n}^{tot}$ can be obtained summing wake-function contributions over all the past revolution turns q and over all the bunches h

$$V_{W,n}^{tot}(t) = -Q_b \sum_{h=0}^{N_b-1} \sum_{q=0}^{+\infty} w_{\parallel} \left\{ \left(q + \frac{n}{N_b} - \frac{h}{N_b} \right) C_r + z_{0,h} \left[t - \left(q + \frac{n}{N_b} - \frac{h}{N_b} \right) T_0 \right] - z_{0,n}(t) - \frac{c}{\omega_{rf}} (\Delta\varphi_{HOM,h} - \Delta\varphi_{HOM,n}) \right\}$$

➤ where $w_{\parallel}(z) = 0$ for $z < 0$ and the $\Delta\varphi_{HOM,h}$ are mod(2π).

□ The $\Delta\varphi_{HOM,h}$ must be all equal due to the symmetrical position of the full buckets in the ring. We call $\Delta\varphi_{HOM}$ the common value.

□ Therefore, expanding $V_{W,n}^{tot}$ linearly with respect to the equilibrium positions $z_{0,h} = z_{0,n} = 0$, we obtain

$$V_{W,n}^{tot}(t) = -Q_b \sum_{h=0}^{N_b-1} \sum_{q=0}^{+\infty} \left(w_{\parallel} \left\{ \left(q + \frac{n}{N_b} - \frac{h}{N_b} \right) C_r \right\} + \frac{dw_{\parallel}}{dz} \left[z_{0,h} \left(t - \left(q + \frac{n}{N_b} - \frac{h}{N_b} \right) T_0 \right) - z_{0,n}(t) \right] \right)$$

➤ where

$$\frac{dw_{\parallel}}{dz} = \frac{dw_{\parallel}}{dz} \Big|_{\left(q + \frac{n}{N_b} - \frac{h}{N_b} \right) C_r} \quad \text{and} \quad \frac{dw_{\parallel}(z)}{dz} = \frac{R_s \omega_r}{Q} e^{-\frac{\omega_r z}{2Qc}} \left[-\frac{\omega_r}{Qc} \cos\left(\omega_n \frac{z}{c}\right) + \left(\frac{\omega_r^2}{4Q^2 c \omega_n} - \frac{\omega_n}{c} \right) \sin\left(\omega_n \frac{z}{c}\right) \right]$$

□ We linearly expand the accelerating voltage as well

$$\hat{V}_{rf} \cos\left(\Delta\varphi_{HOM} - \frac{2\pi h}{C_r} z_{0,n}\right) = \hat{V}_{rf} \cos(\Delta\varphi_{HOM}) + \frac{2\pi h \hat{V}_{rf}}{C_r} \sin(\Delta\varphi_{HOM}) z_{0,n}$$

Coupled-bunch instabilities (3/12)

□ Substituting into the differential equation we obtain

$$\ddot{z}_{0,n} = \frac{c\alpha_0 U_0}{E_0 T_0} - \frac{D}{T_0} \dot{z}_{0,n} - \frac{c\alpha_0 e \hat{V}_{rf}}{E_0 T_0} \cos \Delta\varphi_{HOM} - \left(\frac{2\pi h c \alpha_0 e \hat{V}_{rf}}{C_r E_0 T_0} \sin \Delta\varphi_{HOM} + \frac{Q_b c \alpha_0 e}{E_0 T_0} \sum_{h=0}^{N_b-1} \sum_{q=0}^{+\infty} \frac{dw_{\parallel}}{dz} \right) z_{0,n}$$

$$+ \frac{Q_b c \alpha_0 e}{E_0 T_0} \sum_{h=0}^{N_b-1} \sum_{q=0}^{+\infty} w_{\parallel} \left\{ \left(q + \frac{n}{N_b} - \frac{h}{N_b} \right) C_r \right\} + \frac{Q_b c \alpha_0 e}{E_0 T_0} \sum_{h=0}^{N_b-1} \sum_{q=0}^{+\infty} \frac{dw_{\parallel}}{dz} z_{0,h} \left(t - \left(q + \frac{n}{N_b} - \frac{h}{N_b} \right) T_0 \right)$$

□ Therefore

$$\ddot{z}_{0,n} + \frac{D}{T_0} \dot{z}_{0,n} + \omega_{s,HOM}^2 z_{0,n} = \frac{Q_b c \alpha_0 e}{E_0 T_0} \sum_{h=0}^{N_b-1} \sum_{q=0}^{+\infty} \frac{dw_{\parallel}}{dz} z_{0,h} \left(t - \left(q + \frac{n}{N_b} - \frac{h}{N_b} \right) T_0 \right)$$

➤ where, setting for instance $n = 0$ due to the symmetry of the charge distribution,

$$\omega_{s,HOM}^2 = \frac{c\alpha_0 e}{E_0 T_0} \left(\frac{2\pi h \hat{V}_{rf}}{C_r} \sin \Delta\varphi_{HOM} + Q_b \sum_{h=0}^{N_b-1} \sum_{q=0}^{+\infty} \frac{dw_{\parallel}}{dz} \Big|_{\left(q - \frac{h}{N_b} \right) C_r} \right)$$

For $Q_b \approx 0$ we obtain the zero-intensity zero-amplitude synchrotron frequency with synchrotron radiation

$$\omega_{s0,SR}^2 = \frac{\alpha_0 \omega_{rf} e \hat{V}_{rf}}{E_0 T_0} \sin \Delta\varphi_{SR}$$

➤ and

$$U_0 = e \hat{V}_{rf} \cos \Delta\varphi_{HOM} - Q_b e \sum_{h=0}^{N_b-1} \sum_{q=0}^{+\infty} w_{\parallel} \left\{ \left(q - \frac{h}{N_b} \right) C_r \right\}$$

This equation can be used to compute $\Delta\varphi_{HOM}$.

Coupled-bunch instabilities (4/12)

□ We have to solve a system of n coupled second-order differential equations with the forcing term being a linear combination of the solutions themselves computed at different times.

□ We find a solution of the type

$$z_{0,n}(t) = a_n e^{j\Omega t}$$

➤ with a_n and Ω complex quantities to be determined.

□ Substituting into the differential equation we obtain

$$\left(\Omega^2 - \frac{jD}{T_0} \Omega - \omega_{S,HOM}^2 \right) a_n = - \frac{Q_b c \alpha_0 e}{E_0 T_0} \sum_{h=0}^{N_b-1} a_h \sum_{q=-\infty}^{+\infty} \frac{dw_{\parallel}}{dz} \Big|_{\left(q + \frac{n}{N_b} - \frac{h}{N_b} \right) C_r} e^{-j\Omega T_0 \left(q + \frac{n}{N_b} - \frac{h}{N_b} \right)}$$

➤ where the sum over q could be extended for negative values since $w_{\parallel}(z) = 0$ if $z < 0$.

□ From the definition of the longitudinal coupling impedance we have

$$\frac{dw_{\parallel}}{dz} \Big|_{\left(q + \frac{n}{N_b} - \frac{h}{N_b} \right) C_r} = - \frac{j}{2\pi c} \int_{-\infty}^{+\infty} \omega Z_{\parallel}(\omega) e^{-j\omega T_0 \left(q + \frac{n}{N_b} - \frac{h}{N_b} \right)} d\omega$$

Coupled-bunch instabilities (5/12)

□ Multiplying by the exponential, summing over q and using one property of the delta function, we have

$$\begin{aligned}
 \sum_{q=-\infty}^{+\infty} \frac{dw_{\parallel}}{dz} e^{-j\Omega T_0 \left(q + \frac{n}{N_b} - \frac{h}{N_b} \right)} &= -\frac{j}{2\pi c} \int_{-\infty}^{+\infty} \omega Z_{\parallel}(\omega) e^{-j(\omega+\Omega) \left(\frac{n}{N_b} - \frac{h}{N_b} \right) T_0} \sum_{q=-\infty}^{+\infty} e^{-j(\omega+\Omega)qT_0} d\omega \\
 &= -\frac{j}{C_r} \sum_{p=-\infty}^{+\infty} \int_{-\infty}^{+\infty} \omega Z_{\parallel}(\omega) e^{-j(\omega+\Omega) \left(\frac{n}{N_b} - \frac{h}{N_b} \right) T_0} \delta \left(\omega + \Omega - p \frac{2\pi}{T_0} \right) d\omega \\
 &= -\frac{j}{C_r} \sum_{p=-\infty}^{+\infty} (\omega_0 p - \Omega) Z_{\parallel}(\omega_0 p - \Omega) e^{-2\pi j \left(\frac{n}{N_b} - \frac{h}{N_b} \right) p}
 \end{aligned}$$

□ Substituting

$$\left(\Omega^2 - \frac{jD}{T_0} \Omega - \omega_{s,HOM}^2 \right) a_n = \frac{jQ_b c \alpha_0 e}{C_r E_0 T_0} \sum_{h=0}^{N_b-1} a_h \sum_{p=-\infty}^{+\infty} (\omega_0 p - \Omega) Z_{\parallel}(\omega_0 p - \Omega) e^{-2\pi j \left(\frac{n}{N_b} - \frac{h}{N_b} \right) p}$$

□ Defining

$$\lambda(\Omega) = \frac{1}{Q_b} \left(\Omega^2 - \frac{jD}{T_0} \Omega - \omega_{s,HOM}^2 \right) \quad b_n = Q_b a_n \quad M_{n,h}(\Omega) = \frac{j c \alpha_0 e}{C_r E_0 T_0} \sum_{p=-\infty}^{+\infty} (\omega_0 p - \Omega) Z_{\parallel}(\omega_0 p - \Omega) e^{-2\pi j \left(\frac{n}{N_b} - \frac{h}{N_b} \right) p}$$

Coupled-bunch instabilities (6/12)

➤ we obtain the system of linear equations

$$\bar{\lambda} b_n = \sum_{h=0}^{N_b-1} M_{n,h}(\Omega) b_h \quad n = 0, \dots, N_b - 1$$

➤ where we imposed that all the $\lambda(\Omega)$ are equal, calling $\bar{\lambda}$ the common value.

□ From linear algebra, we know that this system of equations has N_b complex eigenvalues $\bar{\lambda}_\mu$, $\mu = 0, \dots, N_b - 1$.

➤ A set of N_b eigenvectors b_h ($h = 0, \dots, N_b - 1$) is associated to each $\bar{\lambda}_\mu$.

□ The square matrix $\|M_{n,h}\|$ is said circular since it satisfies the property

$$\|M_{n,h}\| = \begin{pmatrix} M_{0,0} & M_{0,1} & M_{0,2} & \cdots & M_{0,N_b-1} \\ M_{1,0} & M_{1,1} & M_{1,2} & \cdots & M_{1,N_b-1} \\ \vdots & \vdots & \vdots & \ddots & \vdots \\ M_{N_b-1,0} & M_{N_b-1,1} & M_{N_b-1,2} & \cdots & M_{N_b-1,N_b-1} \end{pmatrix} = \begin{pmatrix} M_{0,0} & M_{0,1} & M_{0,2} & \cdots & M_{0,N_b-1} \\ M_{0,N_b-1} & M_{0,0} & M_{0,1} & \cdots & M_{0,N_b-2} \\ \vdots & \vdots & \vdots & \ddots & \vdots \\ M_{0,1} & M_{0,2} & M_{0,3} & \cdots & M_{0,0} \end{pmatrix}$$

□ Since $\|M_{n,h}\|$ is circular, then the N_b eigenvalues are given by

$$\bar{\lambda}_\mu = \sum_{h=0}^{N_b-1} M_{0,h}(\Omega) e^{j\frac{2\pi}{N_b}h\mu} = \frac{jc\alpha_0 e}{C_r E_0 T_0} \sum_{p=-\infty}^{+\infty} (\omega_0 p - \Omega) Z_{\parallel}(\omega_0 p - \Omega) \sum_{h=0}^{N_b-1} e^{j\frac{2\pi}{N_b}h(p+\mu)}$$

Coupled-bunch instabilities (7/12)

□ If $(p + \mu)$ is a multiple of N_b ($p + \mu = lN_b, l$ integer), then the last sum is equal to N_b , otherwise

$$\sum_{h=0}^{N_b-1} e^{j\frac{2\pi}{N_b}h(p+\mu)} = \sum_{h=0}^{N_b-1} \left(e^{j\frac{2\pi}{N_b}(p+\mu)} \right)^h = \frac{1 - e^{j2\pi(p+\mu)}}{1 - e^{j\frac{2\pi}{N_b}(p+\mu)}} = 0 \quad \Rightarrow \quad \sum_{h=0}^{N_b-1} e^{j\frac{2\pi}{N_b}h(p+\mu)} = N_b \delta_{p+\mu, lN_b}$$

□ Therefore the N_b eigenvalues are

$$\bar{\lambda}_\mu = \frac{j c \alpha_0 e N_b}{C_r E_0 T_0} \sum_{l=-\infty}^{+\infty} [(lN_b - \mu)\omega_0 - \Omega] Z_{\parallel} [(lN_b - \mu)\omega_0 - \Omega]$$

➤ where $\mu = 0, \dots, N_b - 1$ is called coupled-bunch mode.

□ Given a certain μ , an important property of the corresponding eigenvectors can be obtained from

$$\sum_{h=0}^{N_b-1} M_{0,h} e^{j\frac{2\pi}{N_b}h\mu} b_n^{(\mu)} = \sum_{p=0}^{N_b-1} M_{n,p} b_p^{(\mu)} = \sum_{p=0}^{N_b-1} M_{0, N_b - n + p} b_p^{(\mu)} \quad n = 0, \dots, N_b - 1$$

□ It follows that

$$e^{j\frac{2\pi}{N_b}h\mu} b_n^{(\mu)} = b_{h+n-N_b}^{(\mu)} \quad b_n^{(\mu)} = b_{h+n-N_b}^{(\mu)} e^{-j\frac{2\pi}{N_b}h\mu} \quad \Rightarrow \quad b_n^{(\mu)} = b_0^{(\mu)} e^{j\frac{2\pi}{N_b}n\mu}$$

Coupled-bunch instabilities (8/12)

□ Given $\mu = 0, \dots, N_b - 1$, the solutions of the original differential equation are

$$z_{0,n}^{(\mu)}(t) = a_0^{(\mu)} e^{j\left(\Omega^{(\mu)}t + \frac{2\pi}{N_b}n\mu\right)} = a_0^{(\mu)} e^{-\text{Im}(\Omega^{(\mu)})t} e^{j\left[\text{Re}(\Omega^{(\mu)})t + \frac{2\pi}{N_b}n\mu\right]} \quad n = 0, \dots, N_b - 1$$

➤ where we highlighted the dependency of Ω from μ , since Ω is the solution of

$$\frac{1}{Q_b} \left(\Omega^2 - \frac{jD}{T_0} \Omega - \omega_{s,HOM}^2 \right) = \frac{j c \alpha_0 e N_b}{C_r E_0 T_0} \sum_{l=-\infty}^{+\infty} [(lN_b - \mu)\omega_0 - \Omega] Z_{\parallel} [(lN_b - \mu)\omega_0 - \Omega]$$

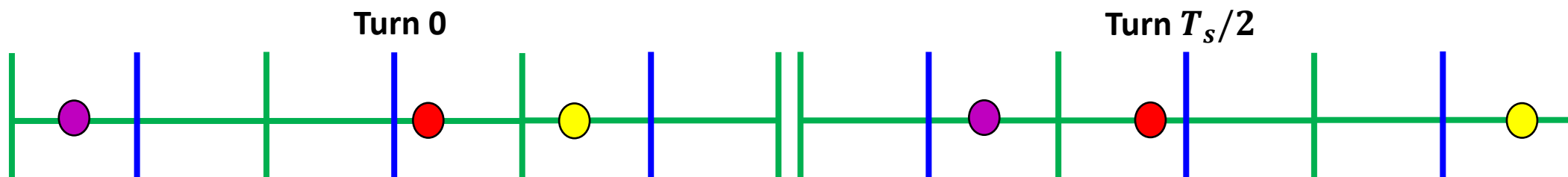
➤ If $\Omega^{(\mu)}$ is complex with negative imaginary part, then $z_{0,n}^{(\mu)}(t)$ grows exponentially in time and the bunch is unstable.

□ Given $\mu = 0, \dots, N_b - 1$, the phase-shift between consecutive bunches is given by

$$\Delta\phi_{\mu} = \frac{2\pi}{N_b} \mu$$

- If e.g. $\mu = 0$, then $\Delta\phi_0 = 0$ and all the bunches oscillate in phase (“0 mode”);
- If e.g. $\mu = N_b/2$ with N_b even, then $\Delta\phi_{N_b/2} = \pi$ and pairs of consecutive bunches oscillate in antiphase (“ π mode”);
- For $\mu = 1, \dots, N_b - 1$, it occurs that $\Delta\phi_{N_b-\mu} = -\Delta\phi_{\mu} \text{ mod}(2\pi)$.

➤ Example of “ π mode” scheme for 3 bunches:



Coupled-bunch instabilities (9/12)

□ To estimate the grow-rates of the unstable bunches, we assume that $\Omega \approx \omega_{s,HOM}$.

$$Q_b \lambda(\Omega) = \Omega^2 - \frac{jD}{T_0} \Omega - \omega_{s,HOM}^2 \approx 2\omega_{s,HOM}(\Omega - \omega_{s,HOM}) - \frac{jD}{T_0} \omega_{s,HOM} = 2\omega_{s,HOM} \left(\Omega - \omega_{s,HOM} - \frac{jD}{2T_0} \right)$$

□ Therefore, rearranging the terms,

$$\Omega = \omega_{s,HOM} + \frac{jD}{2T_0} + \frac{j c \alpha_0 e N_b Q_b}{2 C_r E_0 T_0 \omega_{s,HOM}} \sum_{l=-\infty}^{+\infty} [(lN_b - \mu)\omega_0 - \omega_{s,HOM}] Z_{\parallel} [(lN_b - \mu)\omega_0 - \omega_{s,HOM}]$$

□ Taking the real and imaginary parts of Ω

$$\text{Re}[\Omega^{(\mu)}] = \omega_{s,HOM} - \frac{c \alpha_0 e N_b Q_b}{2 C_r E_0 T_0 \omega_{s,HOM}} \sum_{l=-\infty}^{+\infty} [(lN_b - \mu)\omega_0 - \omega_{s,HOM}] \text{Im}\{Z_{\parallel} [(lN_b - \mu)\omega_0 - \omega_{s,HOM}]\} = \omega_{s,HOM} - \Delta\omega^{(\mu)}$$

$$\text{Im}[\Omega^{(\mu)}] = \frac{U_0}{E_0 T_0} + \frac{c \alpha_0 e N_b Q_b}{2 C_r E_0 T_0 \omega_{s,HOM}} \sum_{l=-\infty}^{+\infty} [(lN_b - \mu)\omega_0 - \omega_{s,HOM}] \text{Re}\{Z_{\parallel} [(lN_b - \mu)\omega_0 - \omega_{s,HOM}]\} = \alpha_{r,SR} + \alpha_{r,HOM}^{(\mu)}$$

□ The imaginary part of the impedance leads only to a shift of the angular frequency of the bunch oscillation.

□ Since $\text{Re}(Z_{\parallel}) \geq 0$ for all frequencies, the bunch instability is caused by the real part of the impedance with $l \leq 0$.

Coupled-bunch instabilities (10/12)

□ To summarize, for a given μ , we have

$$z_{0,n}^{(\mu)}(t) = a_0^{(\mu)} e^{-\left(\alpha_{r,SR} + \alpha_{r,HOM}^{(\mu)}\right)t} e^{j\left[\left(\omega_{s,HOM} - \Delta\omega^{(\mu)}\right)t + \frac{2\pi}{N_b}n\mu\right]}$$

□ The bunches are unstable if and only if

$$\alpha_{r,HOM}^{(\mu)} = \frac{c\alpha_0 e N_b Q_b}{2C_r E_0 T_0 \omega_{s,HOM}} \sum_{l=-\infty}^{+\infty} \left[(lN_b - \mu)\omega_0 - \omega_{s,HOM} \right] \operatorname{Re}\{Z_{\parallel}[(lN_b - \mu)\omega_0 - \omega_{s,HOM}]\} < -\alpha_{r,SR}$$

□ If Z_{\parallel} is given by a resonator impedance, then $\omega \operatorname{Re}[Z(\omega)] = \frac{\omega R_s}{1 + Q^2 \left(\frac{\omega}{\omega_r} - \frac{\omega_r}{\omega}\right)^2} = \frac{\omega_r^2 R_s \omega^3}{\omega_r^2 \omega^2 + Q^2 (\omega^2 - \omega_r^2)^2} \xrightarrow{\omega \rightarrow \pm\infty} 0$

- Therefore we can compute numerically $\alpha_{r,HOM}^{(\mu)}$ limiting the sum to indices $l \in [-l_{max}, l_{max}]$, with l_{max} sufficiently large.
- After having computed $\Delta\varphi_{HOM}$ with the formula shown earlier, $\omega_{s,HOM}$ can be evaluated with

$$\omega_{s,HOM} = \sqrt{\frac{c\alpha_0 e}{E_0 T_0} \left(\frac{2\pi h \hat{V}_{rf}}{C_r} \sin \Delta\varphi_{HOM} + Q_b \sum_{h=0}^{N_b-1} \sum_{q=0}^{+\infty} \frac{dw_{\parallel}}{dz} \Big|_{\left(q - \frac{h}{N_b}\right) C_r} \right)}$$

Coupled-bunch instabilities (11/12)

□ The expression for $\alpha_{r,HOM}^{(\mu)}$ assumes that each bunch is represented by just one macroparticle.

- This assumption is also done in the macroparticle code and therefore there is consistency.
- However, as explained earlier, all the HOM shunt-impedances were rescaled in the code to take into account that bunches have a Gaussian profile.

$$R_s \longrightarrow e^{-\frac{\omega_r^2 \sigma_t^2}{2}} R_s$$

➤ To have again consistency, we need to correct $\alpha_{r,HOM}^{(\mu)}$ assuming that bunches have a Gaussian profile.

- All the steps done previously to arrive at $\alpha_{r,HOM}^{(\mu)}$ can be repeated changing

$$w_{\parallel}(z) \longrightarrow V_w(z) \quad \text{or equivalently} \quad Z_{\parallel}(\omega) \longrightarrow Z_{\parallel}(\omega) e^{-\frac{\omega^2 \sigma_t^2}{2}}$$

- where $V_w(z)$ is the voltage induced by a Gaussian bunch at a distance z from its centre of mass.

□ Therefore the $\alpha_{r,HOM}^{(\mu)}$ can be corrected as

$$\alpha_{r,HOM}^{(\mu)} = \frac{c \alpha_0 e N_b Q_b}{2 C_r E_0 T_0 \omega_{s,HOM}} \sum_{l=-\infty}^{+\infty} [(l N_b - \mu) \omega_0 - \omega_{s,HOM}] \operatorname{Re}\{Z_{\parallel}[(l N_b - \mu) \omega_0 - \omega_{s,HOM}]\} e^{-\frac{[(l N_b - \mu) \omega_0 - \omega_{s,HOM}]^2 \sigma_t^2}{2}}$$

- This expression can be refined even more using a correction factor involving a Bessel function (derivation from Vlasov equation).
 - However, the proposed exponential factor is more consistent with the type of shunt-impedance rescaling done in the code.

□ The assumption that $\Omega \approx \omega_{s,HOM}$ in the argument of Z_{\parallel} can be strong since Z_{\parallel} varies rapidly with frequency due to the high Q .

- If the beam-spectrum couples with Z_{\parallel} at essentially just one frequency, then we can solve directly the equation for Ω .

Coupled-bunch instabilities (12/12)

□ Indeed, calling l_1 the index associated to the unique coupling frequency, the equation to solve is

$$\Omega = A + \frac{j c \alpha_0 e N_b Q_b}{2 C_r E_0 T_0 \omega_{s,HOM}} (q \omega_0 - \Omega) Z_{\parallel} [q \omega_0 - \Omega] e^{-\frac{[q \omega_0 - \omega_{s,HOM}]^2 \sigma_t^2}{2}} \quad \triangleright \text{ where } \quad A = \omega_{s,HOM} + \frac{j U_0}{E_0 T_0} \quad q = l_1 N_b - \mu$$

□ Assuming that $|\Omega| \ll \omega_r$ and that $q \omega_0 \approx \omega_r$, the impedance term can be expressed as

$$Z_{\parallel} [q \omega_0 - \Omega] = \frac{R_s}{1 + jQ \left(\frac{q \omega_0 - \Omega}{\omega_r} - \frac{\omega_r}{q \omega_0 - \Omega} \right)} = \frac{R_s}{1 + jQ \left(\frac{q \omega_0}{\omega_r} - \frac{\Omega}{\omega_r} - \frac{\omega_r}{q \omega_0} - \frac{\omega_r^2}{q^2 \omega_0^2} \frac{\Omega}{\omega_r} \right)} = \frac{R_s}{1 + jQ \left(\frac{q \omega_0}{\omega_r} - \frac{\omega_r}{q \omega_0} \right) - \frac{jQ}{\omega_r} \left(1 + \frac{\omega_r^2}{q^2 \omega_0^2} \right) \Omega}$$

□ Therefore

$$\Omega = A + \frac{j c \alpha_0 e N_b Q_b}{2 C_r E_0 T_0 \omega_{s,HOM}} (q \omega_0 - \Omega) \frac{R_s}{1 + jQ \left(\frac{q \omega_0}{\omega_r} - \frac{\omega_r}{q \omega_0} \right) - \frac{jQ}{\omega_r} \left(1 + \frac{\omega_r^2}{q^2 \omega_0^2} \right) \Omega} e^{-\frac{[q \omega_0 - \omega_{s,HOM}]^2 \sigma_t^2}{2}} = A + \frac{B(q \omega_0 - \Omega)}{C - D \Omega}$$

► where the complex constants B , C and D are

$$B = \frac{j c \alpha_0 e N_b Q_b R_s}{2 C_r E_0 T_0 \omega_{s,HOM}} e^{-\frac{[q \omega_0 - \omega_{s,HOM}]^2 \sigma_t^2}{2}} \quad C = 1 + jQ \left(\frac{q f_0}{f_r} - \frac{f_r}{q f_0} \right) \quad D = \frac{jQ}{\omega_r} \left(1 + \frac{f_r^2}{q^2 f_0^2} \right)$$

□ Rearranging the terms we obtain this quadratic equation in Ω

$$D \Omega^2 - (C + AD + B) \Omega + AC + B q \omega_0 = 0$$

► and the desired Ω is the smallest solution in absolute value. The grow-rate is the imaginary part of Ω .

Coupled-bunch oscillations: beam spectrum (1/2)

□ We fix the coupled-bunch mode μ and we assume that each bunch-profile is a delta function.

□ At turn k , the bunch h arrives at a fixed point of the ring at time

$$t^{(k)} = kT_0 + h \frac{T_0}{N_b} + A_s \cos \left[\text{Re}(\Omega^{(\mu)}) t^{(k)} + \frac{2\pi}{N_b} h\mu \right]$$

➤ where we assume that all the bunches have the same oscillation amplitude A_s .

□ The beam current can be written as

$$\begin{aligned} \lambda(t) &\propto \sum_{k=-\infty}^{+\infty} \sum_{h=0}^{N_b-1} \delta \left(t - kT_0 - h \frac{T_0}{N_b} - A_s \cos \left[\text{Re}(\Omega^{(\mu)}) t + \frac{2\pi}{N_b} h\mu \right] \right) \propto \sum_{q=-\infty}^{+\infty} \sum_{h=0}^{N_b-1} e^{jq\omega_0 t} e^{-jqh \frac{2\pi}{N_b}} e^{-jq\omega_0 A_s \cos \left[\text{Re}(\Omega^{(\mu)}) t + \frac{2\pi}{N_b} h\mu \right]} \\ &= \sum_{q=-\infty}^{+\infty} \sum_{h=0}^{N_b-1} e^{jq\omega_0 t} e^{-jqh \frac{2\pi}{N_b}} \sum_{m=-\infty}^{\infty} j^{-m} J_m(q\omega_0 A_s) e^{-jm \left[\text{Re}(\Omega^{(\mu)}) t + \frac{2\pi}{N_b} h\mu \right]} = \sum_{q=-\infty}^{+\infty} \sum_{m=-\infty}^{\infty} j^{-m} J_m(q\omega_0 A_s) e^{jt(q\omega_0 - m \text{Re}(\Omega^{(\mu)}))} \sum_{h=0}^{N_b-1} e^{-jh \frac{2\pi}{N_b} (q+m\mu)} \\ &\propto \sum_{l=-\infty}^{+\infty} \sum_{m=-\infty}^{\infty} j^{-m} J_m[(lN_b - m\mu)\omega_0 A_s] e^{jt[(lN_b - m\mu)\omega_0 - m \text{Re}(\Omega^{(\mu)})]} \end{aligned}$$

Coupled-bunch oscillations: beam spectrum (2/2)

□ Therefore the beam spectrum can be written as

$$S(\omega) = \int_{-\infty}^{+\infty} \lambda(t) e^{-j\omega t} dt \propto \sum_{l=-\infty}^{+\infty} \sum_{m=-\infty}^{\infty} j^{-m} J_m[(lN_b - m\mu)\omega_0 A_s] \int_{-\infty}^{+\infty} e^{jt[(lN_b - m\mu)\omega_0 - m\text{Re}(\Omega^{(\mu)}) - \omega]} dt$$

$$\propto \sum_{l=-\infty}^{+\infty} \sum_{m=-\infty}^{\infty} j^{-m} J_m[(lN_b - m\mu)\omega_0 A_s] \delta\left((lN_b - m\mu)\omega_0 - m\text{Re}(\Omega^{(\mu)}) - \omega\right)$$

□ The beam spectrum is discrete and its lines are situated at $\omega = (lN_b - m\mu)\omega_0 - m\text{Re}(\Omega^{(\mu)})$.

➤ If $N_b = 1$, then $\mu = 0$ and the lines are at $\omega = l\omega_0 - m\text{Re}(\Omega^{(0)}) \approx l\omega_0 - m\omega_{s,HOM}$.

□ We saw that, for bunches having a delta profile, the grow-rate of the coupled-bunch instability is

$$\alpha_{r,HOM}^{(\mu)} \propto \sum_{l=-\infty}^{+\infty} [(lN_b - \mu)\omega_0 - \omega_{s,HOM}] \text{Re}\{Z_{\parallel}[(lN_b - \mu)\omega_0 - \omega_{s,HOM}]\} \propto \sum_{l=-\infty}^{+\infty} \int_{-\infty}^{+\infty} \omega \text{Re}\{Z_{\parallel}[\omega]\} \delta\left((lN_b - \mu)\omega_0 - \omega_{s,HOM} - \omega\right) d\omega \propto S(\omega) \Big|_{m=1}$$

➤ The electromagnetic interaction between the different bunches is due to the multiplication of the beam coupling-impedance Z_{\parallel} with the beam spectrum S with $m = 1$.

- Only the beam spectrum-lines with $m = 1$ (dipolar motion) are significant to evaluate the coupled-bunch instability.
- This is consistent with the adopted macroparticle model, where each bunch has no internal structure and therefore the spectrum lines with $m \neq 1$ (quadrupolar motion etc.) can't be excited.

Example for the DAFNE ring: coupled-bunch instability (1/7)

□ $\alpha_0 = 0.018$, $U_0 = 8.88$ keV, $V_{rf} = 130$ kV, $f_{rf} = 369$ MHz, $f_0 = 3$ MHz, $f_{s0} = 29$ kHz.

□ $N_b = 4$ equally-spaced bunches, bunch-current $I_b = Q_b/T_0 = 15$ mA, $\sigma_z = 20$ mm.

□ 4 coupled-modes $\mu = 0, 1, 2, 3$. The phase between consecutive bunches is $\Delta\phi_\mu = \frac{\pi}{2}\mu$.

□ One HOM of the accelerating cavity has $f_r = 796.8$ MHz, $R_s = 20$ k Ω , $Q = 40000$.

➤ We want to excite a certain coupled-bunch mode with this HOM.

- R_s and Q are always kept constant, whereas f_r is shifted to obtain the desired coupling between beam-spectrum and impedance.

□ The critical frequencies which can lead to instability are negative and given by

$$f_{l,\mu} = (4l - \mu)f_0 - f_{s,HOM} \quad l \leq 0 \quad \mu = 0, 1, 2, 3$$

➤ We want to excite only the mode μ_1 through the line at f_{l_1,μ_1} , with $l_1 \leq 0$.

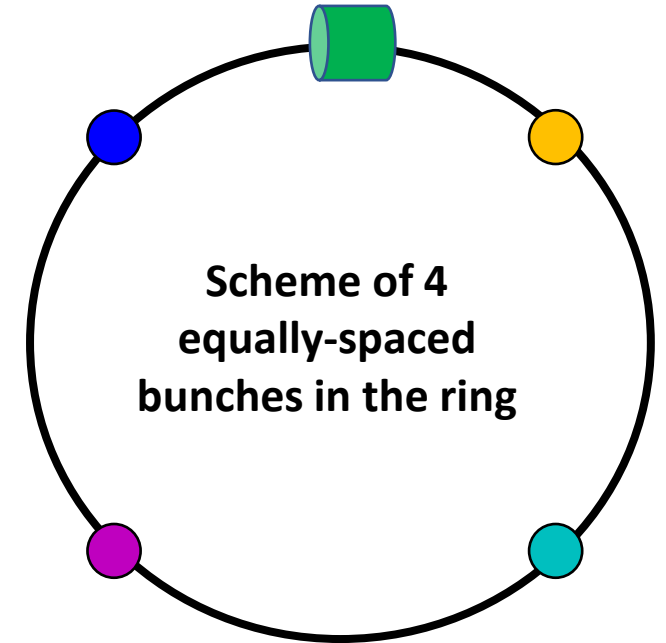
- Since $\text{Re}(Z_{\parallel})$ is symmetric with respect to the axis $f = 0$, and assuming that $f_{s,HOM} \approx f_{s0}$, we set f_r at

$$-f_{l_1,\mu_1} \approx f_r = [4(1 - l_1) - (4 - \mu_1)]f_0 + f_{s0} = (4l_2 - \mu_2)f_0 + f_{s0}$$

➤ f_{l_2,μ_2} is the line-frequency closest to f_r and some coupling could occur, although the Q is quite large.

- In any case $l_2 = 1 - l_1 > 0$ and therefore the mode $\mu_2 = 4 - \mu_1 \pmod{4}$ is damped and not excited.

Accelerating cavity



Example for the DAFNE ring: coupled-bunch instability (2/7)

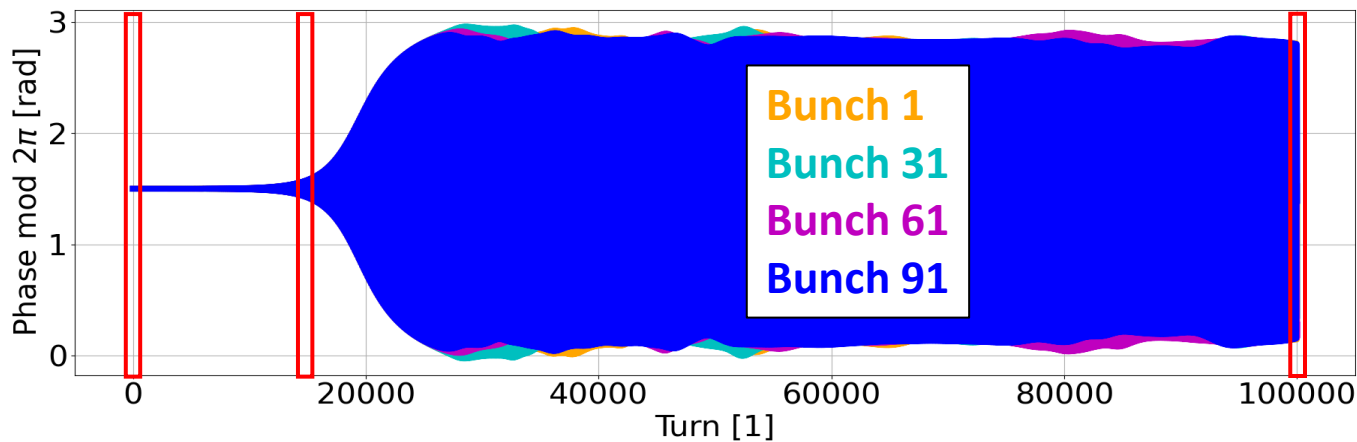
□ We want to excite $\mu_1 = 0$.

- If $l_1 = -66$, then $f_r = 264f_0 + f_{s0} = 811.05$ MHz.
- The high Q leads to a small coupling (damping) of $\mu_2 = 0$.

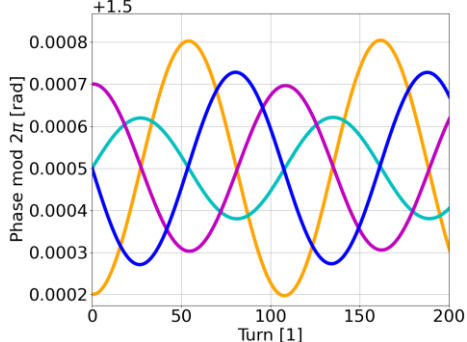
□ At turn 0, the four bunches start with different initial conditions.

- The maximum oscillation amplitude is 0.3 mrad = 0.13 ps.

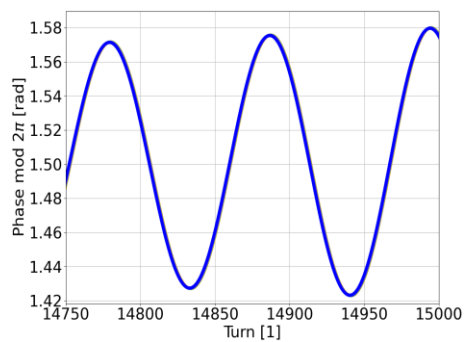
Phase oscillations of the four bunches along the first 100000 turns



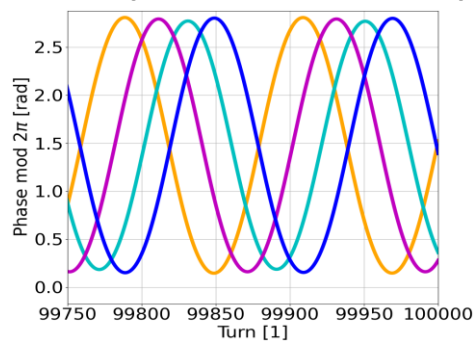
Zoom (0-200 turns)



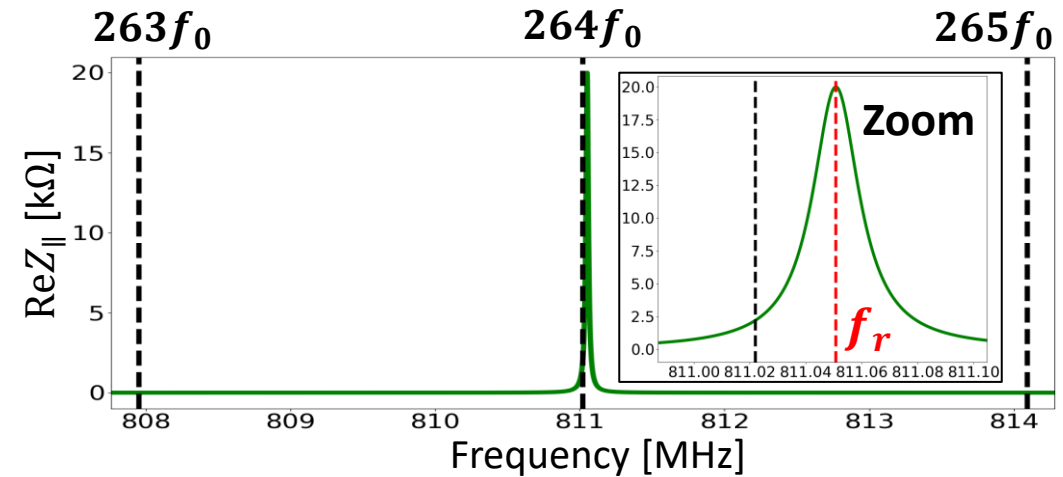
Zoom (14.75k-15k turns)



Zoom (99.75k-100k turns)



Real part of the HOM longitudinal impedance



□ Exponential growth of oscillations in the first roughly 15000 turns, then convergence to an equilibrium due to wake-field/RF-voltage non-linearities and synchrotron radiation.

□ At equilibrium the four bunches oscillate with roughly the same amplitude of 1.32 rad = 570 ps.

- The instability is fast and strong.

□ After a certain transient time and during the exponential growth, the bunches oscillate in phase, i.e. $\Delta\phi_0 = 0$.

- The bunches aren't in phase anymore at equilibrium.

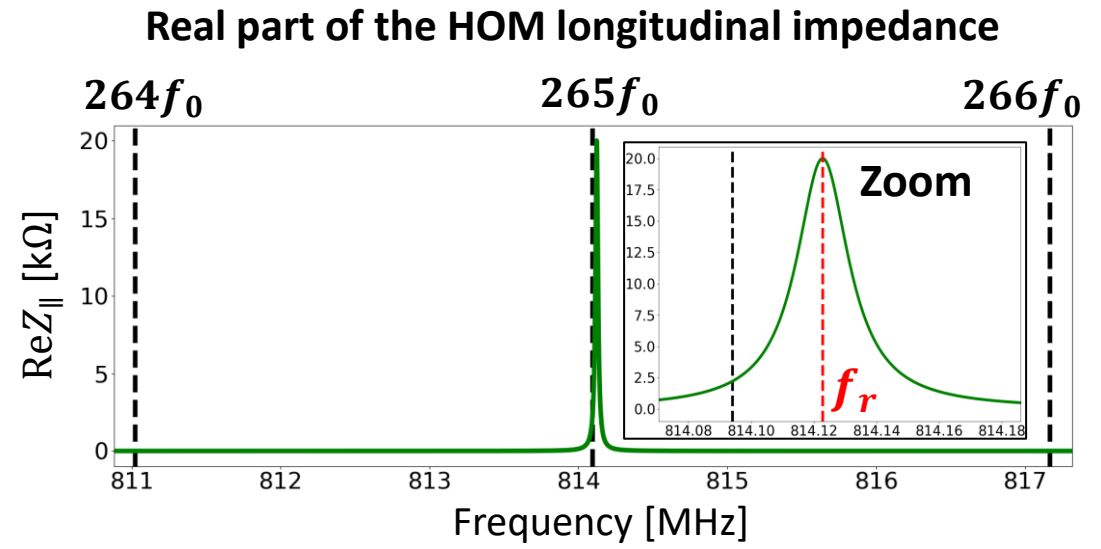
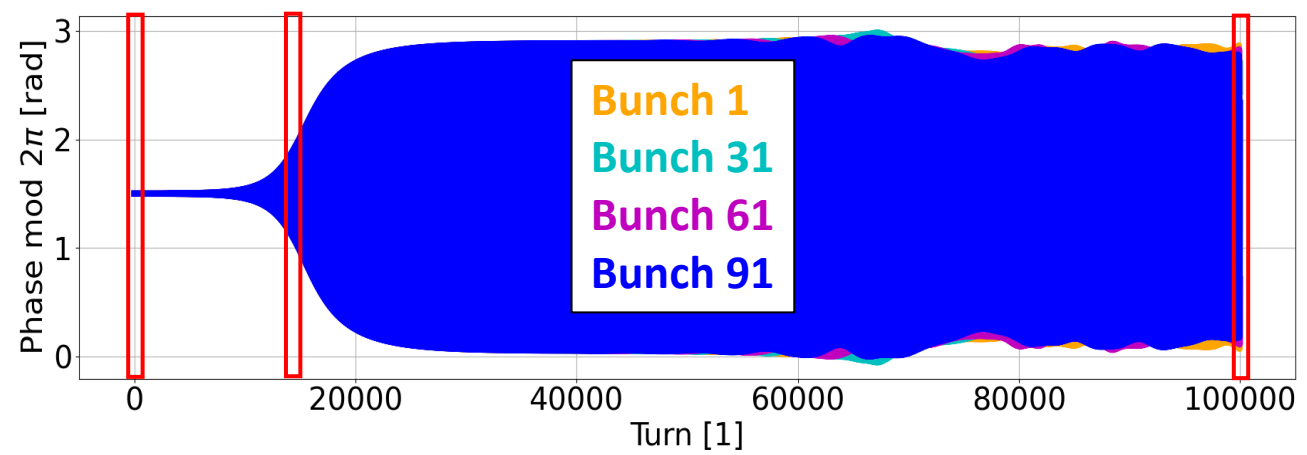
Example for the DAFNE ring: coupled-bunch instability (3/7) ⁷²

□ We want to excite $\mu_1 = 1$.

- If $l_1 = -66$, then $f_r = 265f_0 + f_{s0} = 814.12$ MHz.
- The high Q leads to a small coupling (damping) of $\mu_2 = 3$.

□ The initial conditions of the bunches are the same as those chosen for $\mu_1 = 0$ (the maximum oscillation-amplitude is 0.3 mrad = 0.13 ps.)

Phase oscillations of the four bunches along the first 100000 turns



□ Exponential growth of oscillations in the first roughly 12000 turns, then convergence to an equilibrium due to wake-field/RF-voltage non-linearities and synchrotron radiation.

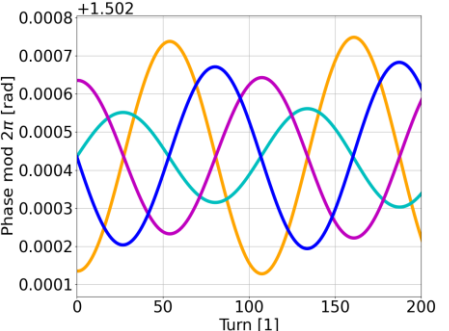
□ At equilibrium the four bunches oscillate with roughly the same amplitude of 1.40 rad = 604 ps.

- Instability even faster and stronger than for $\mu_1 = 0$.

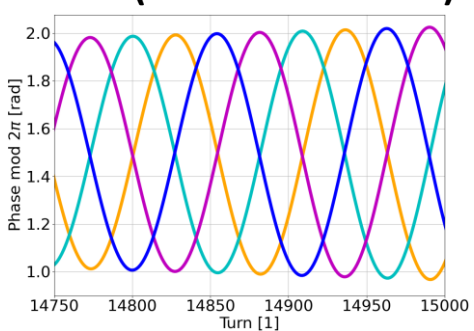
□ After a certain transient time, consecutive bunches oscillate in quadrature, i.e. $\Delta\phi_1 = \pi/2$.

- This phase difference isn't preserved at equilibrium.

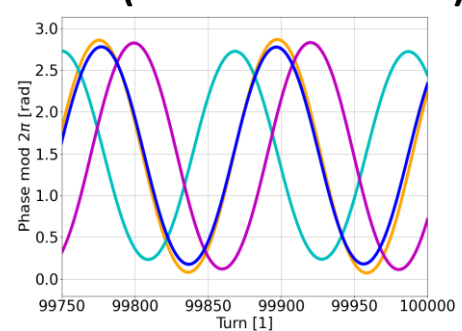
Zoom (0-200 turns)



Zoom (14.75k-15k turns)



Zoom (99.75k-100k turns)



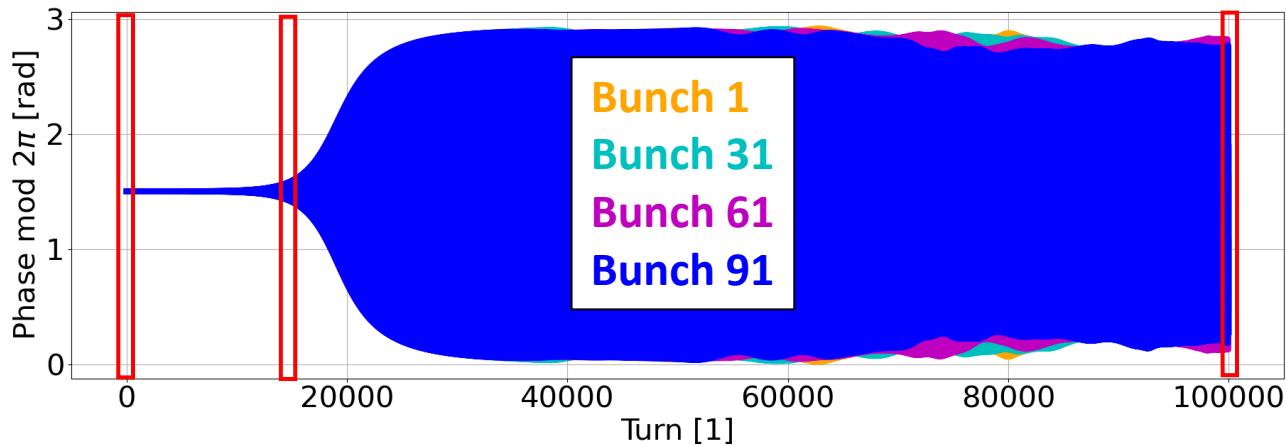
Example for the DAFNE ring: coupled-bunch instability (4/7)

□ We want to excite $\mu_1 = 2$.

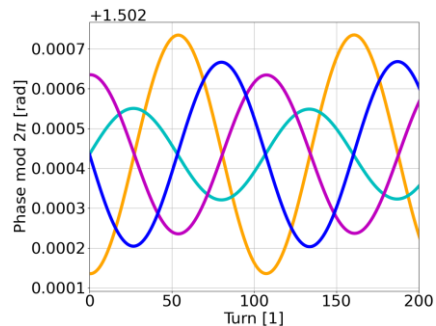
- If $l_1 = -66$, then $f_r = 266f_0 + f_{s0} = 817.19$ MHz.
- The high Q leads to a small coupling (damping) of $\mu_2 = 2$.

□ The initial conditions of the bunches are the same as those chosen for $\mu_1 = 0$ (the maximum oscillation-amplitude is 0.3 mrad = 0.13 ps.)

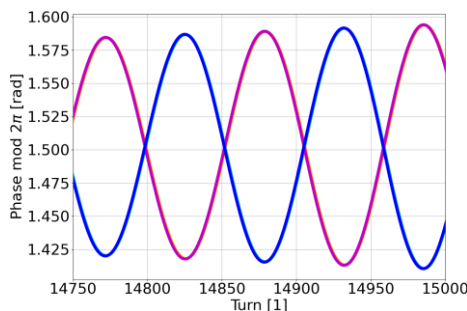
Phase oscillations of the four bunches along the first 100000 turns



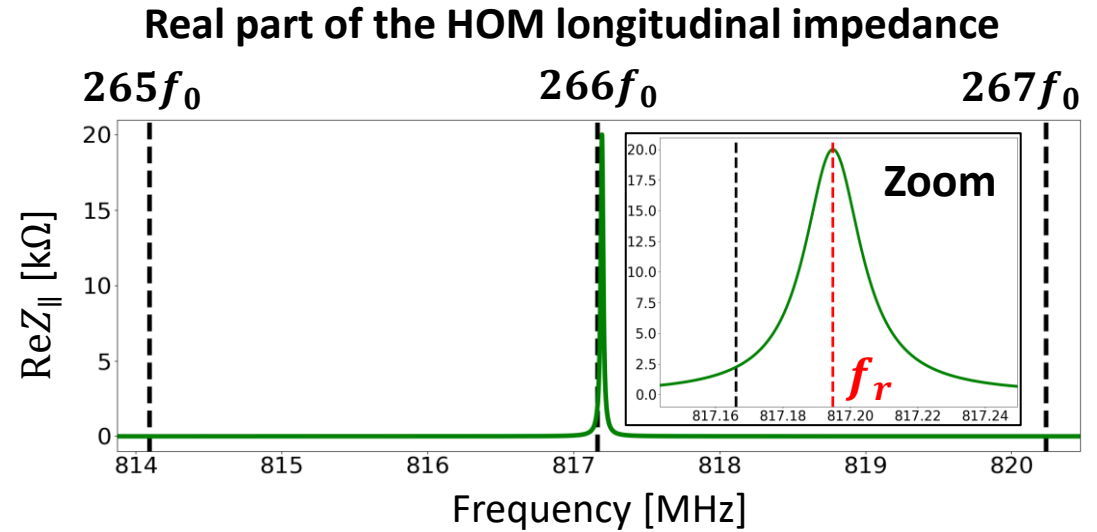
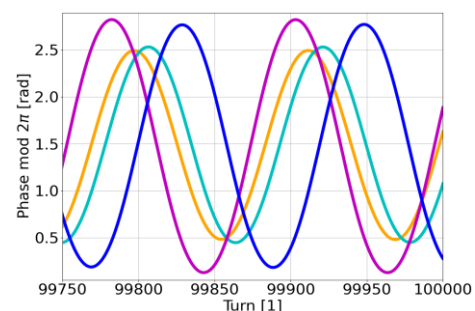
Zoom (0-200 turns)



Zoom (14.75k-15k turns)



Zoom (99.75k-100k turns)



□ Exponential growth of oscillations in the first roughly 15000 turns, then convergence to an equilibrium due to wake-field/RF-voltage non-linearities and synchrotron radiation.

□ At equilibrium the bunches 61 and 91 have the largest oscillation amplitude of 1.31 rad = 566 ps.

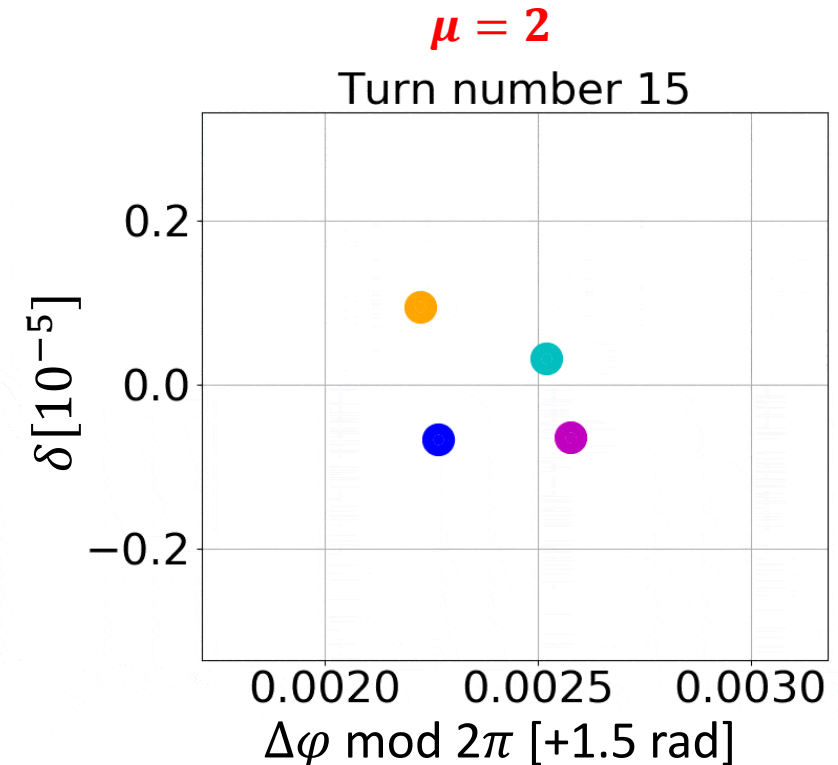
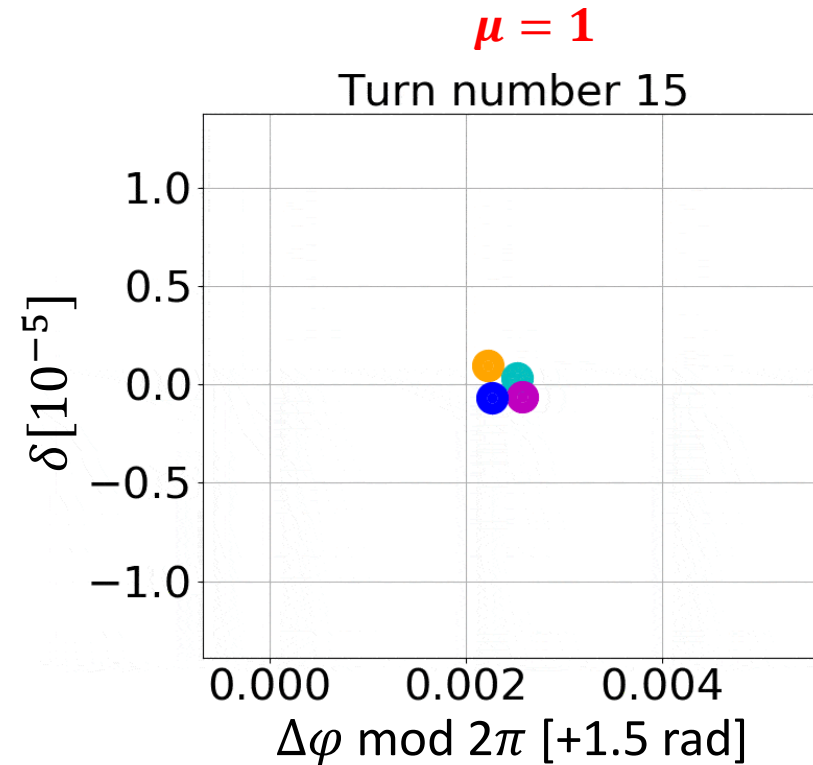
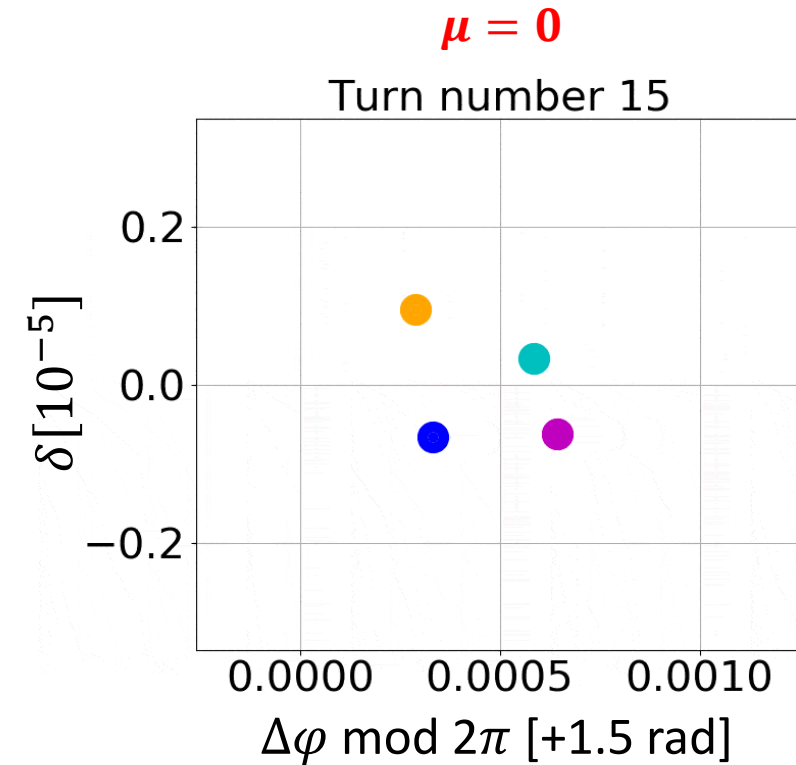
- Instability comparable to that obtained for $\mu_1 = 0$.

□ After a certain transient time and during the exponential growth, the bunches oscillate in antiphase, i.e. $\Delta\phi_2 = \pi$.

- This phase difference isn't preserved at equilibrium.

Example for the DAFNE ring: coupled-bunch instability (5/7)⁷⁴

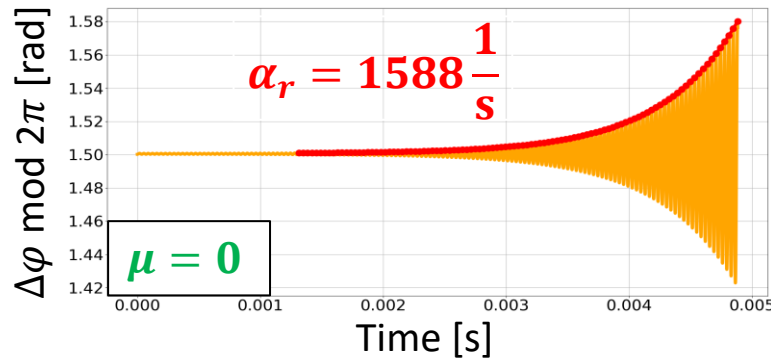
- For each analysed case ($\mu = 0, 1, 2$) we plot the longitudinal phase space for the first 15000 turns.
 - The oscillation amplitudes grow exponentially (the value-limits on the axes are modified every 5000 turns for better visualization).
 - All the phases are mod 2π so that the evolution of the different bunches can be seen on the same bucket.
- After a certain number of turns:
 - $\mu = 0$: Consecutive bunches oscillate in phase ($\Delta\phi_0 = 0$) and the four bunches are superimposed.
 - $\mu = 1$: Consecutive bunches oscillate in quadrature ($\Delta\phi_1 = \pi/2$) and the four bunches coincide with vertices of squares.
 - $\mu = 2$: Consecutive bunches oscillate in antiphase ($\Delta\phi_2 = \pi$), bunches 1 and 61 are superimposed, bunches 31 and 91 are superimposed.



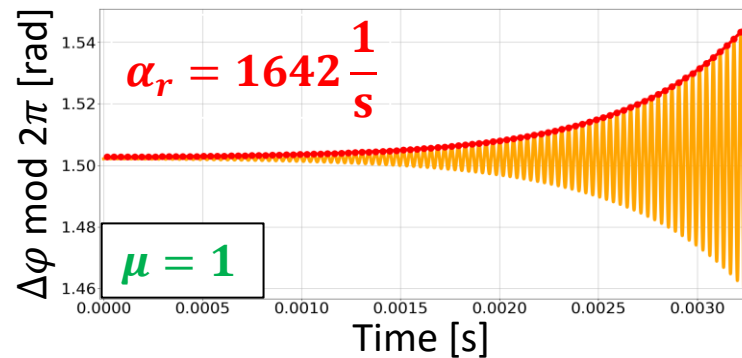
Example for the DAFNE ring: coupled-bunch instability (6/7)⁷⁵

- Finally we compute in simulation the grow-rate of bunch oscillations and compare them with analytical estimations.
 - As an example we consider the following six cases in simulation.

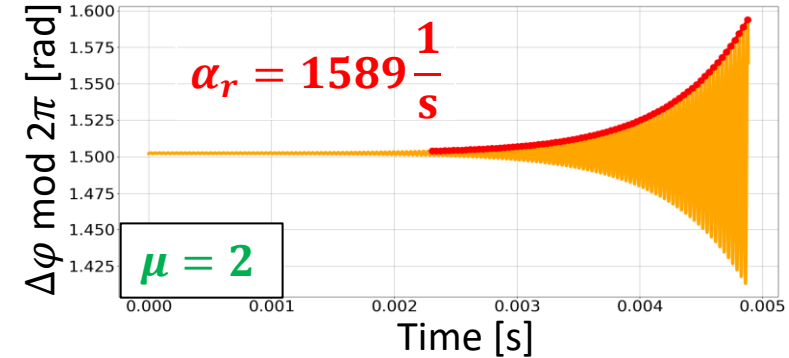
Bunch 1, fit from turn 4k to 15k



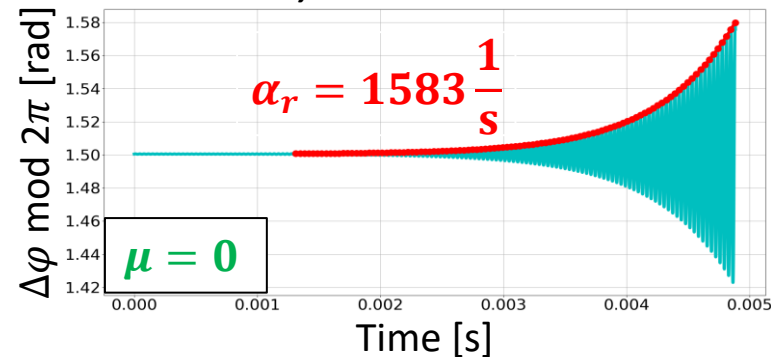
Bunch 1, fit from turn 0 to 10k



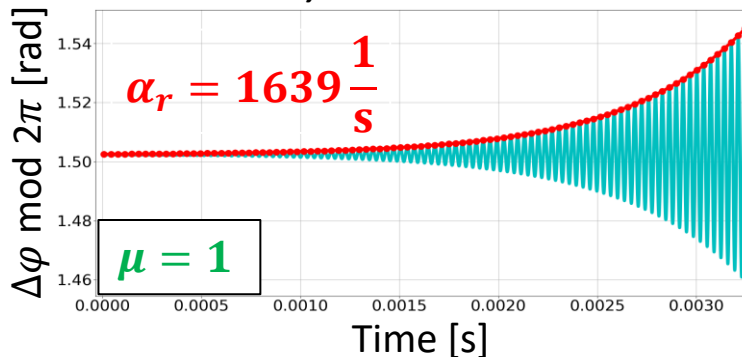
Bunch 1, fit from turn 7k to 15k



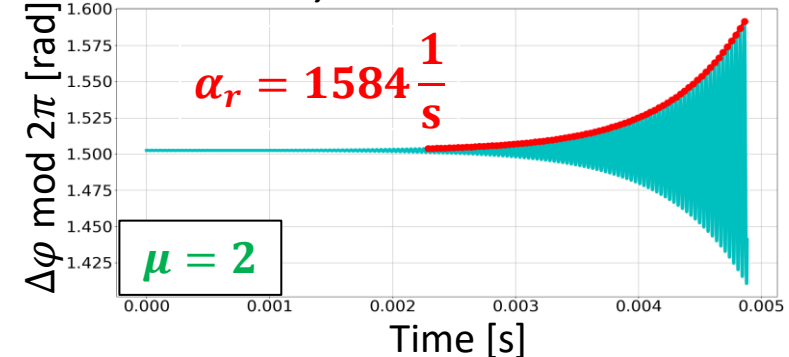
Bunch 31, fit from turn 4k to 15k



Bunch 31, fit from turn 0 to 10k



Bunch 31, fit from turn 7k to 15k



- As expected from theory, given a certain μ the grow-rates are practically the same for all the bunches.
- As already seen, the largest grow-rate occurs for $\mu = 1$, whereas the grow-rates for $\mu = 0$ and $\mu = 2$ are essentially the same.

- The analytical damping-rate due to synchrotron radiation is $\alpha_{r,SR} = 53 \frac{1}{s}$ (≈ 57400 turns).

Example for the DAFNE ring: coupled-bunch instability (7/7)

□ To analytically estimate the total grow-rate (including synchrotron radiation) we use the two formulas discussed earlier

➤ **'Explicit' formula**

It's safe to set $|l| \leq 100$
since the critical l is -66

$$\alpha_r = -\frac{U_0}{E_0 T_0} - \frac{c \alpha_0 e N_b Q_b}{2 C_r E_0 T_0 \omega_{s,HOM}} \sum_{l=-100}^{+100} [(l N_b - \mu) \omega_0 - \omega_{s,HOM}] \operatorname{Re}\{Z_{\parallel}[(l N_b - \mu) \omega_0 - \omega_{s,HOM}]\}$$

➤ **'Implicit' formula**

The Ω with the smallest
magnitude is considered

$$\Omega = A + \frac{j c \alpha_0 e N_b Q_b}{2 C_r E_0 T_0 \omega_{s,HOM}} (q \omega_0 - \Omega) Z_{\parallel} [q \omega_0 - \Omega] e^{-\frac{[q \omega_0 - \omega_{s,HOM}]^2 \sigma_t^2}{2}} \quad \alpha_r = -\operatorname{Im}[\Omega]$$

□ Comparison of α_r values from simulations and analytical estimations.

➤ The discrepancies between α_r from simulations and analytical estimations are in %.

	α_r [1/s] for $\mu = 0$	α_r [1/s] for $\mu = 1$	α_r [1/s] for $\mu = 2$
From simulation	1588, 1583	1642, 1639	1589, 1584
Analyt. explicit	1542 (2.8%)	1588 (3.3%)	1542 (2.8%)
Analyt. implicit	1636 (3.1%)	1631 (0.6%)	1635 (3.0%)

➤ Why the implicit formula, expected to be precise, overestimate α_r if $\mu = 0$ or $\mu = 2$?

- If $\mu_1 = 0$ then $\mu_2 = 0$ and if $\mu_1 = 2$ then $\mu_2 = 2$, so the implicit formula neglects the line at positive frequencies which contributes to a small damping of the mode and to a decrease of α_r .
- If $\mu_1 = 1$ then $\mu_2 = 3$, so in this case the neglected damping refers to mode 3 and therefore doesn't affect the mode 1.

➤ If the implicit formula has to consider also the line at positive frequencies, then a cubic equation in Ω must be solved.

➤ The explicit formula confirms that α_r is the largest for $\mu = 1$ and that α_r is the same for $\mu = 0$ and $\mu = 2$.

- **These values are lower than those found in simulations by just 3%.**

➤ The implicit formula provides essentially the same α_r for each μ .

- **The maximum discrepancy with simulations is just 3%.**

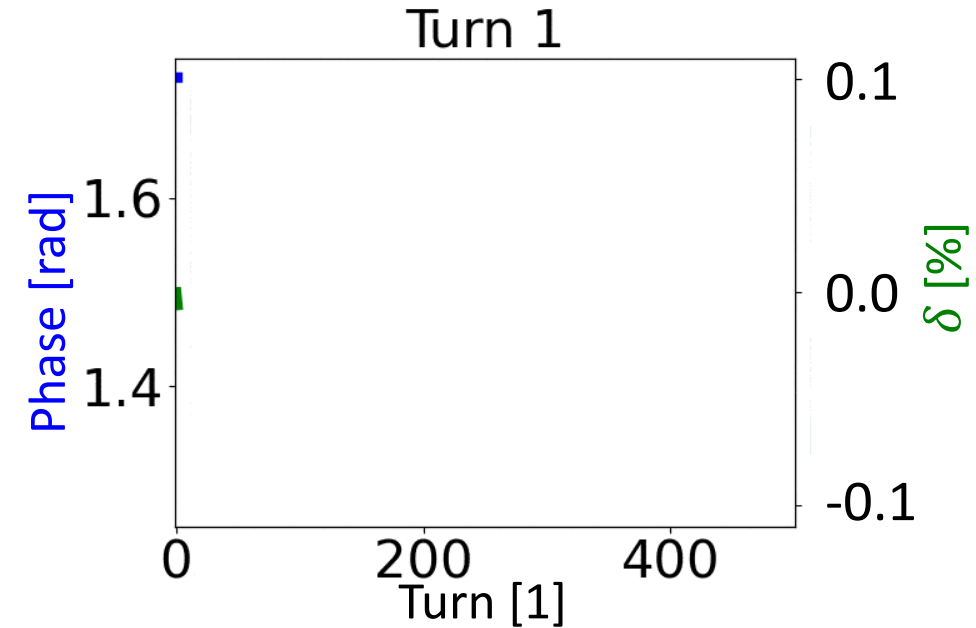
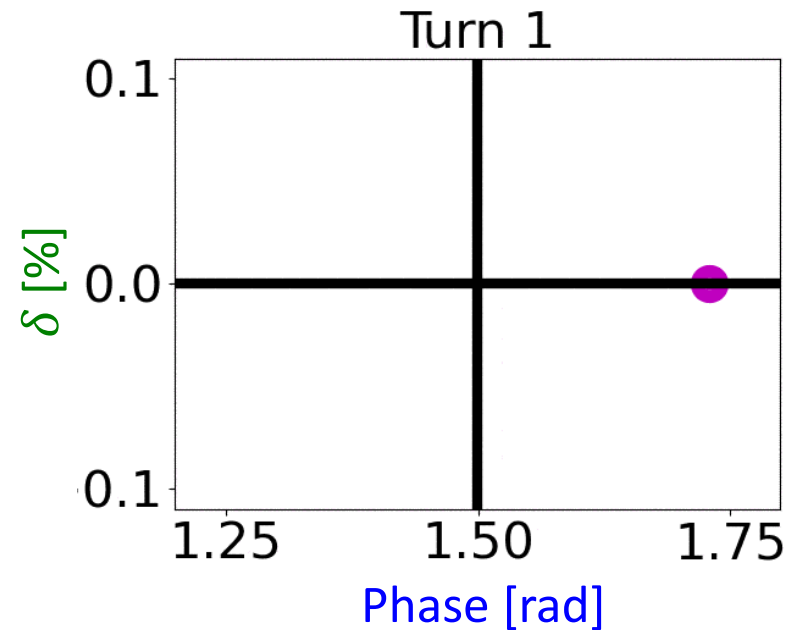
Contents

- ❑ Introduction.
- ❑ Single-particle longitudinal beam-dynamics with synchrotron radiation.
 - Equations of motion, synchrotron radiation, small-amplitude synchrotron oscillations, ...
- ❑ Longitudinal beam-dynamics with synchrotron radiation and Higher Order Modes (HOMs).
 - HOM induced voltage, synchronous phase shift, HOM initial conditions, coupled-bunch instabilities, ...
- ❑ Longitudinal beam-dynamics with synchrotron radiation, HOMs and bunch-by-bunch feedback.
 - Models of the feedback components, grow and damping-rates, cavity-kicker, ideal and real corrections, ...
- ❑ Conclusions and suggested next steps.
- ❑ Appendices.
 - Execution of the new-Python and old-Fortran codes, structure of the code, exponential fits in Python, ...
- ❑ References.

Bunch-by-bunch longitudinal feedback

- Let's suppose that
 - We have only one bunch circulating in the DAFNE ring.
 - The bunch intensity is very low, so that the induced voltages can be neglected.
 - The bunch is injected into the ring with a phase error of 0.23 rad with respect to $\Delta\varphi_{SR} = \arccos \frac{U_0}{e\hat{V}_{rf}}$.

- The particle performs synchrotron oscillations in phase space.
- The phase and energy oscillations are sinusoidal functions with initial phases which differ by $\pi/2$.
- How to actively damp these phase and energy oscillations?



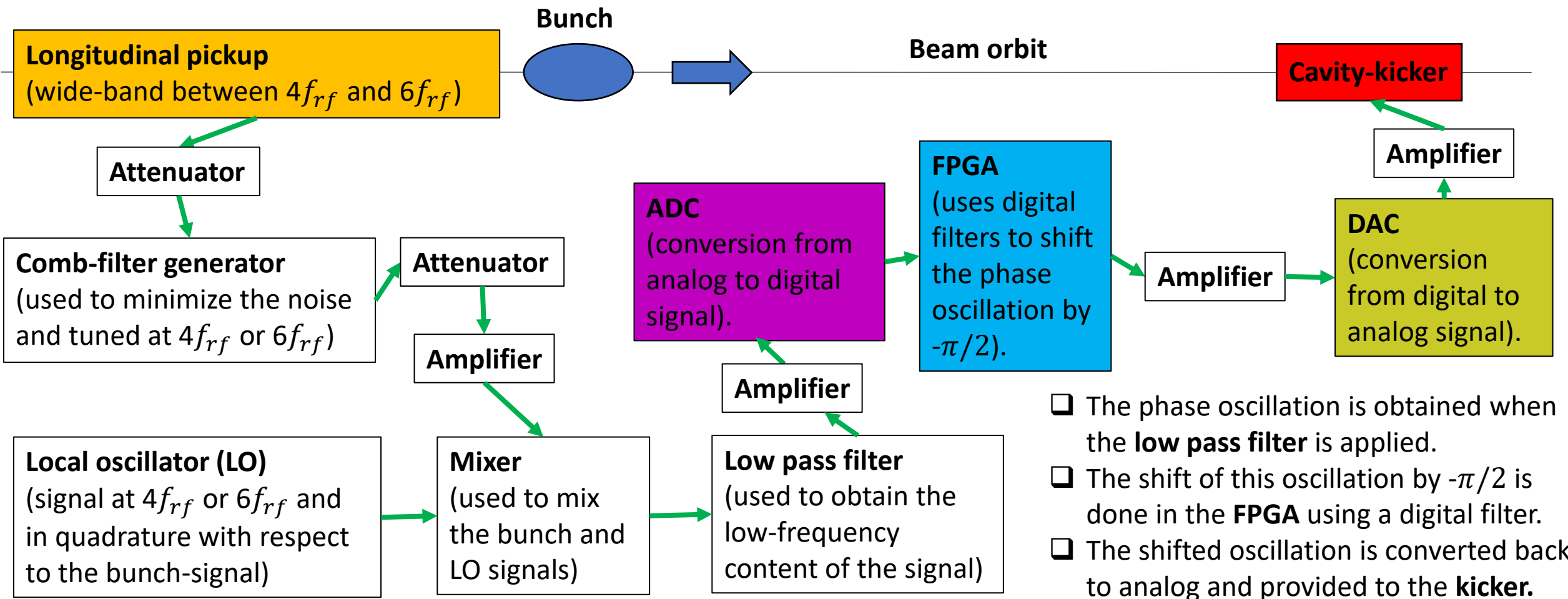
- Simplifying a lot, the DAFNE bunch-by-bunch longitudinal feedback
 - measures the last synchrotron oscillation of the bunch phases;
 - shifts this synchrotron oscillation by $-\pi/2$ to obtain a sinusoidal function in anti-phase with respect to the δ oscillation.
 - applies this shifted synchrotron oscillation as an energy correction to the bunch during the next synchrotron oscillation.

Bunch-by-bunch longitudinal feedback in DAFNE

❑ The energy correction is provided by a so-called kicker, which can be an RF cavity, as in DAFNE, or a stripline structure.

❑ Here is a simplified scheme of the bunch-by-bunch longitudinal feedback used in DAFNE.

➤ When multiple bunches circulate in the ring, the feedback acts on each bunch independently from the other bunches.



Longitudinal pickup: special-button BPM

- ❑ The Beam Position Monitors (BPMs) are the main diagnostic tools in DAFNE.
 - They consist of four “button” electrodes mounted flush with the vacuum pipe.
- ❑ In each DAFNE ring, special-button BPMs can measure individual time offset on a bunch-by-bunch basis, i.e. without memory of the preceding bunch.
- ❑ These special-button BPMs must
 - have a reasonably high transfer impedance Z_b and shouldn't have narrow-band resonances in the frequency-range of interest:
 - in DAFNE the frequencies of interest are between $4f_{rf} = 1.47$ GHz (~ 30 bunch operation) and $6f_{rf} = 2.21$ GHz (~ 120 bunch operation);
 - the necessary design value of Z_b is $0.3 \div 0.4 \Omega$ in the region $1.3 \div 2.2$ GHz.
 - keep the beam coupling impedance and parasitic losses within acceptably low values.
 - **NOTE:** in general these two impedances grow together (e.g. with the increase of the button radius), so a compromise must be found.
- ❑ For the longitudinal feedback, one special-button BPM is chosen out of two available.
 - this BPM measures the bunch current summing together the signals coming from the four button electrodes.

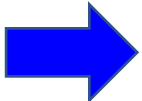
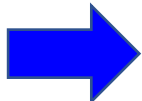
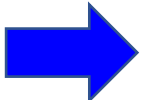
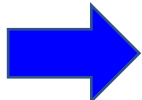
Analytical formulae for the electrode impedances

- The transfer impedance of a button electrode is the complex ratio between the voltage induced by a centred beam at the external termination of the detector circuit and the beam current.

$$Z_b(\omega) = \frac{V_b(\omega)}{I_b(\omega)} = \left(\phi R_0 \frac{\omega_1}{\omega_2} \right) \frac{j\omega/\omega_1}{1 + j\omega/\omega_1}$$

- where $\phi = r/4b$ is the so-called coverage factor, with r and b the button and beam-pipe radii;
- R_0 is the characteristic impedance of the coaxial cable connecting the button to the detector circuit;
- $\omega_1 = 1/R_0 C_b$, with C_b the electrode capacitance; $\omega_2 = c/2r$ is the inverse of the electrode traversal time.

- The frequency response of Z_b is of the high-pass type since

- For low frequencies $\omega \ll \omega_1$  $Z_b(\omega) = \left(\frac{\phi R_0}{\omega_2} \right) j\omega$ 
 - Multiplication by $j\omega$.
 - The electrode acts like a time differentiator.
- For high frequencies $\omega \gg \omega_2$:  $Z_b(\omega) = \phi R_0 \frac{\omega_1}{\omega_2}$ 
 - The asymptotic response is purely resistive.
 - The electrode voltage is in phase and proportional to the beam current.

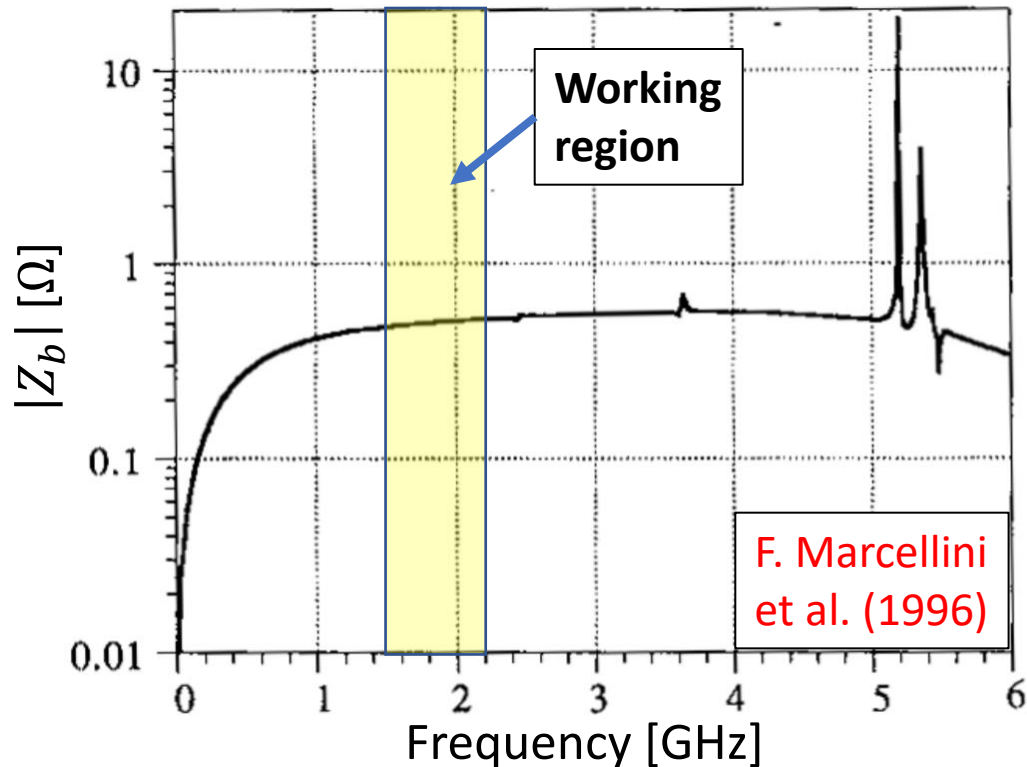
- In first approximation, the coupling impedance is simply

$$Z_{\parallel}(\omega) = \left(\phi \frac{\omega_1}{\omega_2} \right) Z_b(\omega)$$

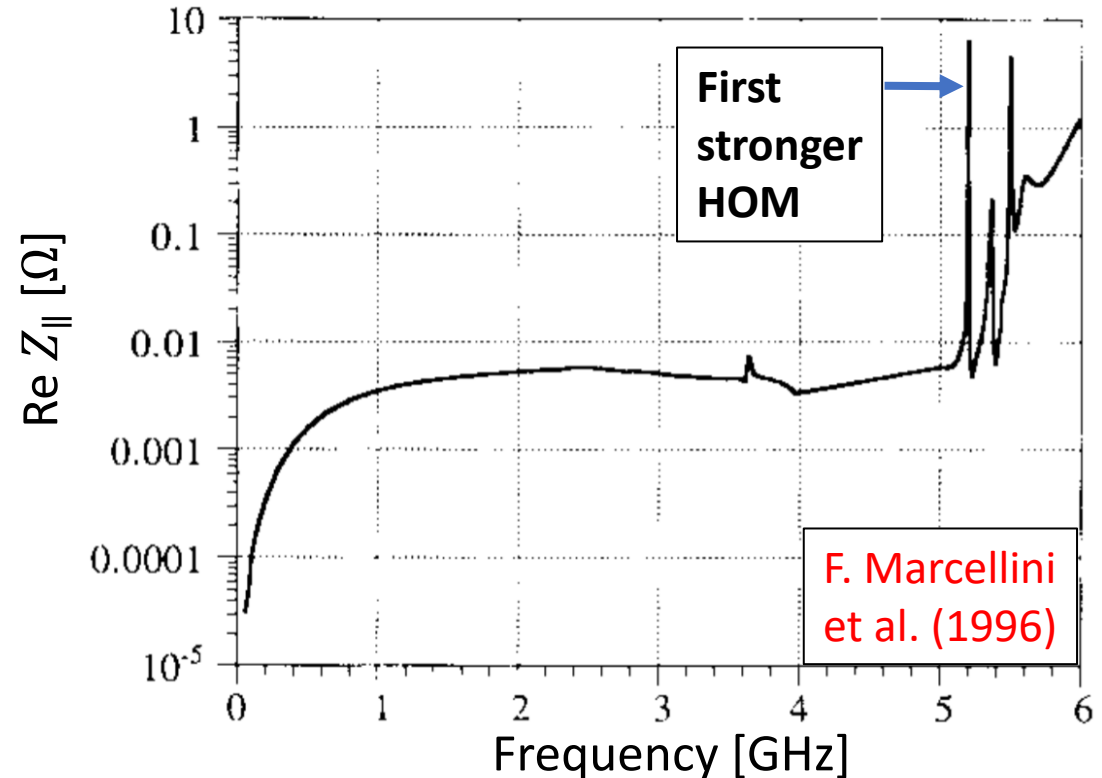
Longitudinal pickup: transfer and coupling impedances

- Simulations were performed in 1996 to estimate the transfer and coupling impedances of the DAFNE special-button BPMs .

Button transfer impedance from the HFSS code



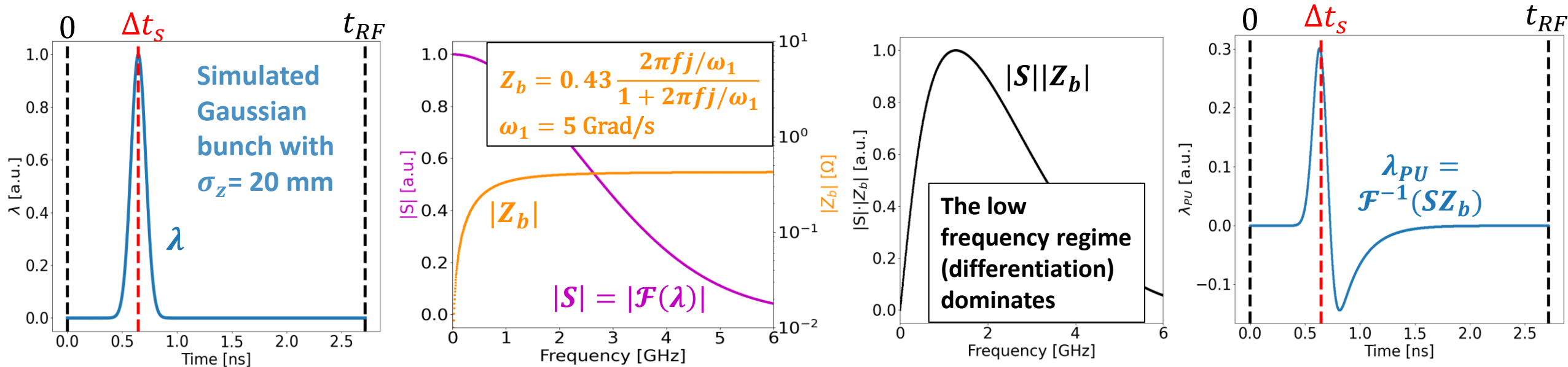
BPM coupling impedance from the HFSS code



- The coupling impedance is indeed roughly proportional to the transfer impedance.
- In the working region the button transfer impedance is sufficiently flat with a satisfactory value of **0.43 Ω**.
- The button low-frequency impedance is relatively small and is acceptable from the beam dynamics point of view.
- The first stronger HOM at 5.2 GHz is not dangerous to the multibunch instabilities due to its low R_s .

Phase detection for a signal coming from the pickup

- The analog front-end of the longitudinal feedback is designed to measure τ , which is the time of arrival of each bunch relative to the RF master oscillator clock.
 - Equivalently, the goal is to measure $\varphi_0 = \Delta\varphi - \Delta\varphi_{rf} = \omega_{rf}\tau$, i.e. the difference between the bunch phase and the synchronous phase.
- The bunch-signal coming from the pickup is a short differentiated pulse.
 - We can numerically reproduce the electrode transfer function and apply it to the typical DAFNE bunch current.

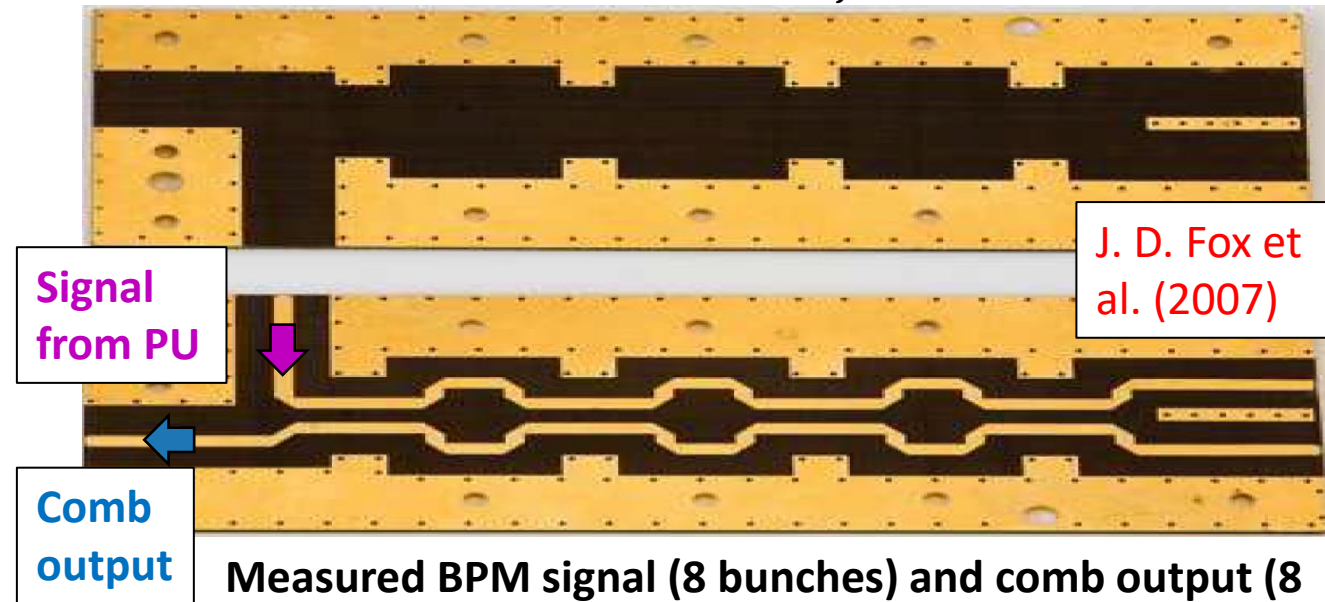


- If such a short pulse is used for phase detection, the obtained signal will be also a short baseband pulse.
 - The sampling of this signal by the ADC clock will be very sensitive to pulse and clock timings.

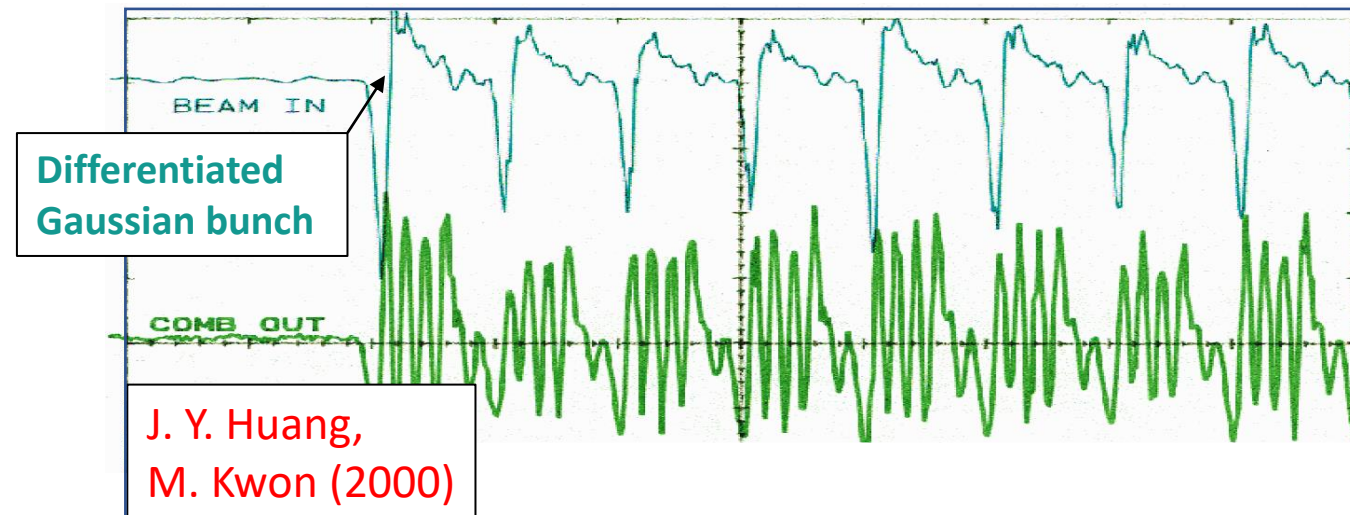
Stripline comb generator

- ❑ To avoid this sampling sensitivity, the pickup signal is 'lengthened' by feeding it into a comb generator.
 - Planar stripline circuit made from a copper-clad teflon material and then gold plated to lower the losses.
- ❑ The comb generator converts the pickup signal of a bunch into a tone burst of a few cycles at an harmonic of f_{rf} .
- ❑ When the bunch-spacing is T_{rf} , 4-cycle tone bursts at $6f_{rf}$ are often used (as in PEP-II, PLS).
 - The tone burst must be shorter than the bunch spacing to minimize the interbunch crosstalk.
 - Some margin is left since the actual bunch-spacing can be less than T_{rf} : adjacent bunches
 - have non-zero bunch length;
 - can oscillate not in phase.
- ❑ When a burst is phase-detected, the baseband phase-signal has a rectangular envelope with duration equal to that of the input burst.
 - The sampling of the phase-signal is less sensitive to pulse and clock timings.

4-cycle comb generator at $6f_{rf}$ used for PEP-II



Measured BPM signal (8 bunches) and comb output (8 4-cycle tone bursts at $6f_{rf}$) at PLS, South Korea



Stripline comb generator at $4f_{rf}$: measurements (1/2)

Measurements of the frequency response of DAFNE comb-generators were performed at INFN using a VNA (G. Franzini, D. Pellegrini, D. Quartullo).

- Considered frequencies between 300 kHz and 8.5 GHz (maximum possible).

First measured comb generator: 5-tone-burst at $4f_{rf} = 1.47$ GHz.

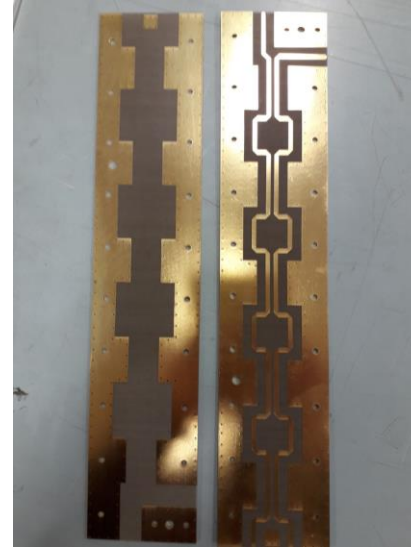
The frequency response is made of sinc-like functions at 1.50 GHz ($\approx 4f_{rf}$), 4.47 GHz ($\approx 12f_{rf} = 4.42$ GHz), 7.44 GHz ($\approx 20f_{rf} = 7.37$ GHz).

We reproduce in simulation the comb-filter in time and frequency domain.

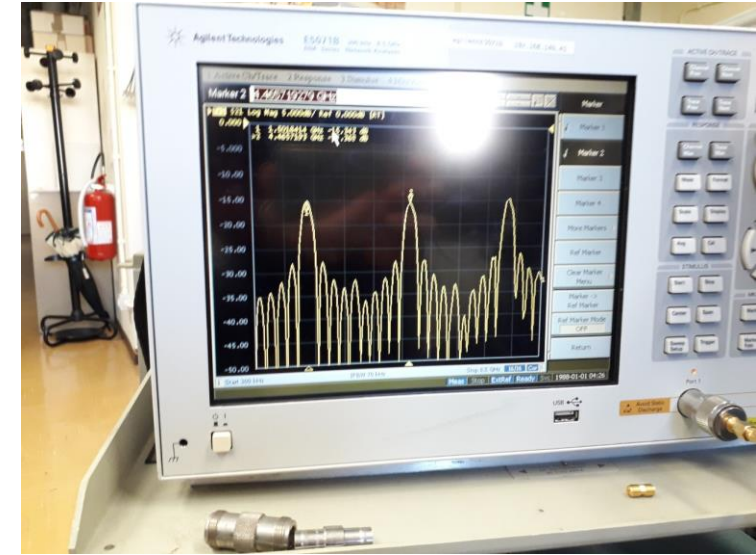
- We suppose that the comb-filter in time domain is 'a smoothing' of the derivative of a 1.47 GHz square-wave.
 - Sinc functions at $4(2k+1)f_{rf}$ ($k=0,\dots$) in frequency domain.

Good agreement between measurements and simulations.

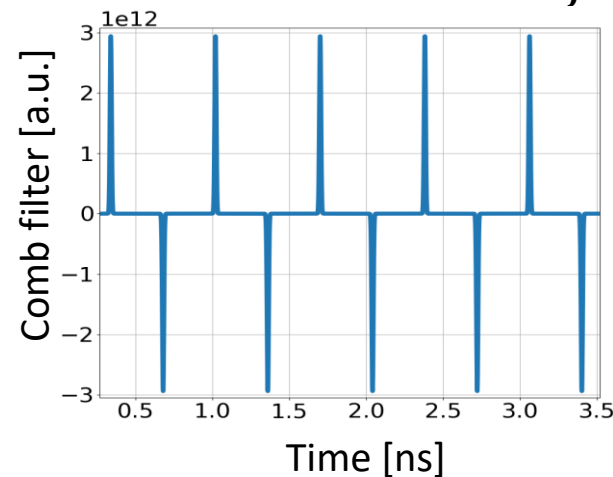
5-cycle comb generator at $4f_{rf}$



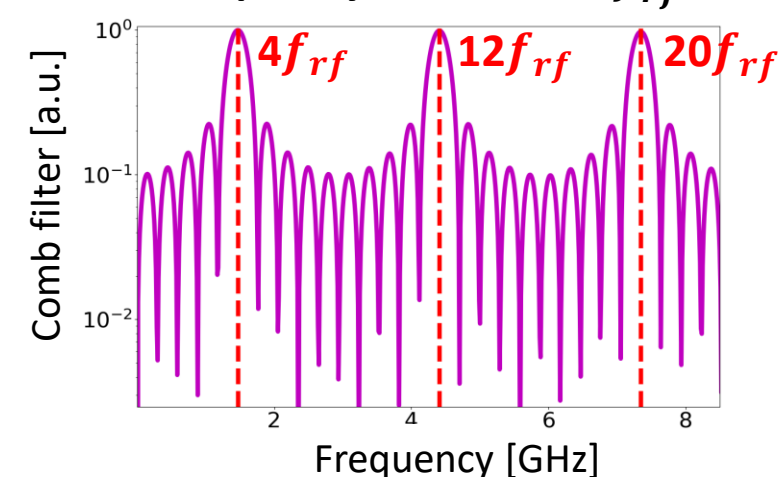
Measured frequency response



Simulated comb-filter in time domain at $4f_{rf}$



Simulated comb-filter in frequency domain at $4f_{rf}$



Stripline comb generator at $4f_{rf}$: measurements (2/2)

- Measurements of the response of the comb-generator in time domain were then performed.

- An impulse-generator and an oscilloscope were used.

- A pulse of 456 ps length was generated and sent to the comb-generator.

- It was not possible to have shorter pulses without decreasing the signal amplitude.

- The pulse length was $2/3$ of the square-wave period (equal to 680 ps).

- The oscilloscope provides as output a sine-like 5-cycle tone burst with period of 678 ps or frequency of $4f_{rf}$.

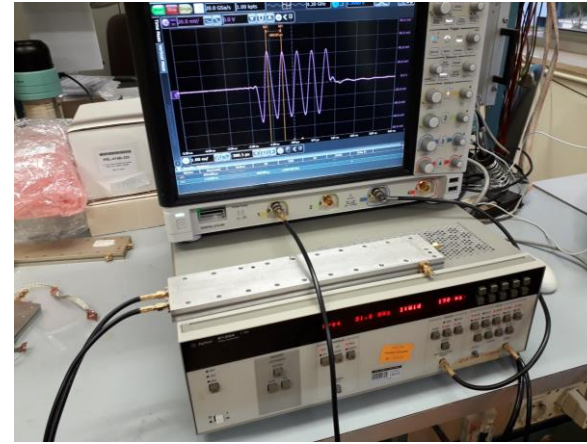
- This output is reproduced in simulation convolving the reconstructed pulse with the comb-filter in time domain.

- The pulse acts like a low-pass filter which keeps only the sinc at $4f_{rf}$.

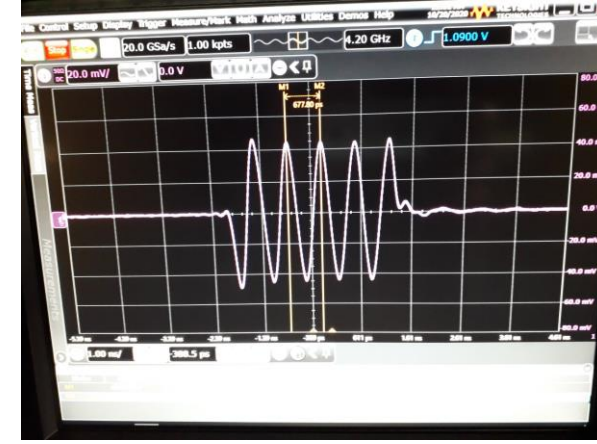
Impulse of length 456 ps



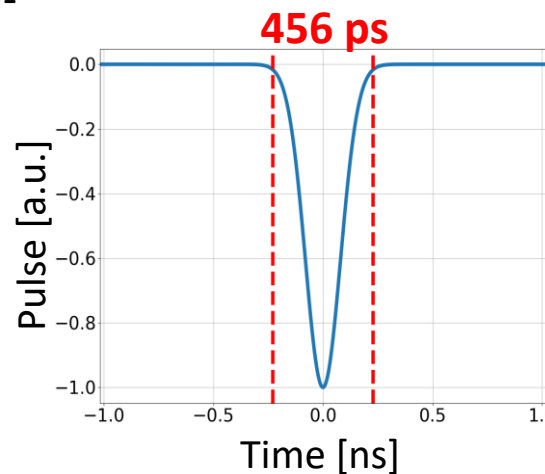
Setup with generator (down), comb (middle), oscilloscope (top)



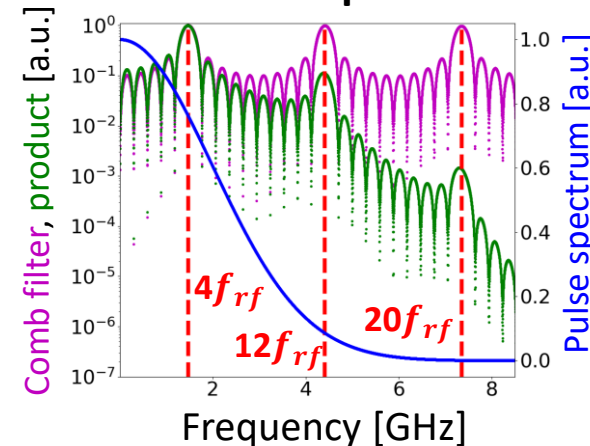
Zoom on the output of the oscilloscope



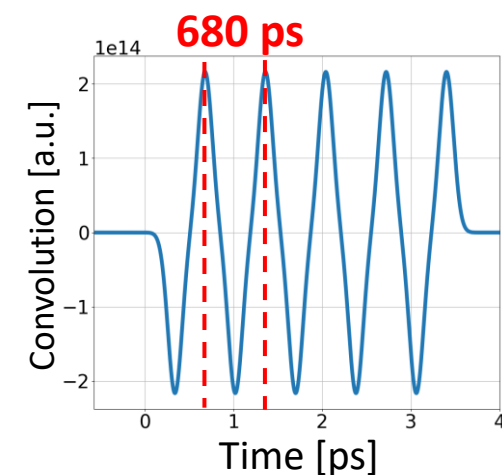
Simulated pulse with 456 ps end-to-end length



Simulated pulse spectrum, comb filter and their product



Convolution between simulated pulse and comb filter in time domain



Stripline comb generator at $6f_{rf}$: measurements (1/2)

- Measurements were then repeated for another comb generator: 5-tone-burst at $6f_{rf} = 2.21$ GHz.
- The frequency response is made of sinc-like functions with frequencies at 2.27 GHz ($\approx 6f_{rf}$), 6.76 GHz ($\approx 18f_{rf} = 6.64$ GHz).
- We reproduce in simulation the comb-filter in time and frequency domain.
 - We suppose that the comb-filter in time domain is 'a smoothing' of the derivative of a 2.21 GHz square wave.
 - Sinc functions at $6(2k+1)f_{rf}$ ($k=0,\dots$) in frequency domain.
- Good agreement between measurements and simulations.

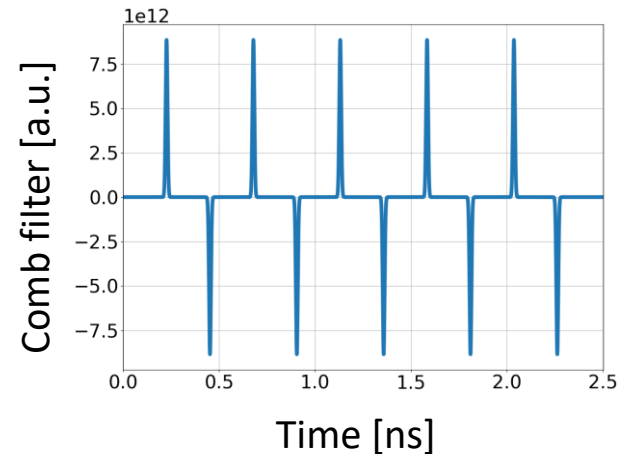
5-cycle comb generator at $6f_{rf}$



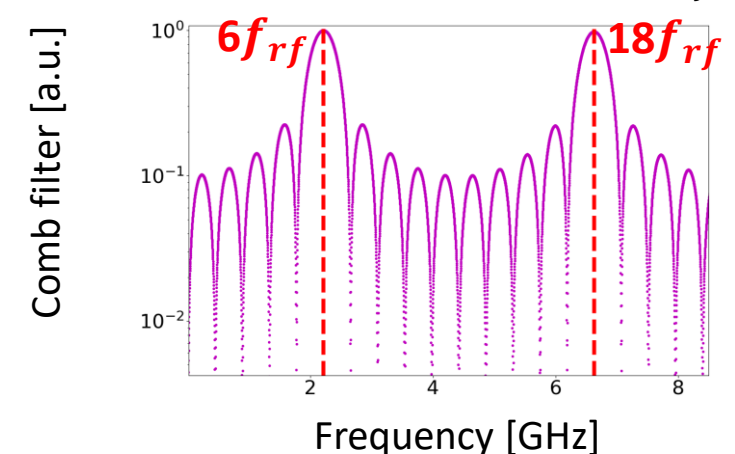
Measured frequency response



Simulated comb-filter in time domain at $6f_{rf}$



Simulated comb-filter in frequency domain at $6f_{rf}$



Stripline comb generator at $6f_{rf}$: measurements (2/2)

□ Measurements of the response of the comb-generator in time domain were then performed.

□ A pulse of 456 ps length was generated and sent to the comb-generator.

- The pulse length was comparable to the square-wave period (equal to 452 ps).

□ The oscilloscope provides as output a sine-like 5-cycle tone burst with period of 439 ps or frequency of $6f_{rf}$.

□ This output is reproduced in simulation convolving the reconstructed pulse with the comb-filter in time domain.

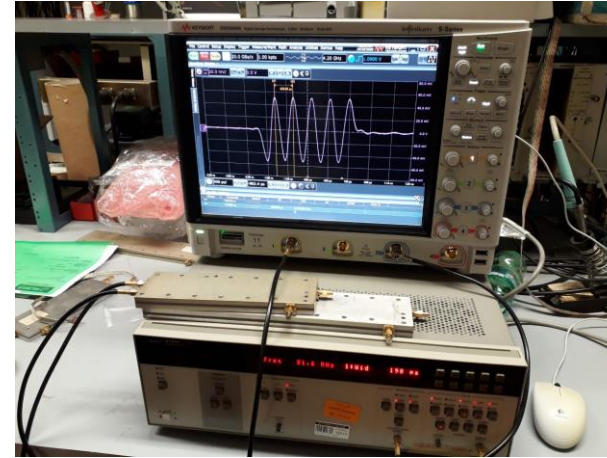
- The pulse acts like a low-pass filter which keeps only the sinc at $6f_{rf}$.

□ Good agreement between measurements and simulations, as for the case of the comb at $4f_{rf}$.

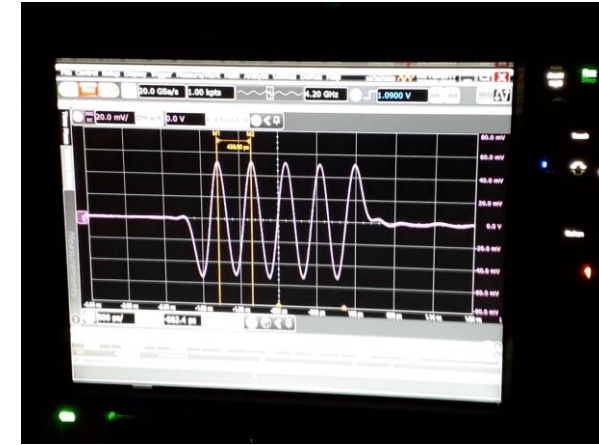
Impulse of length 456 ps



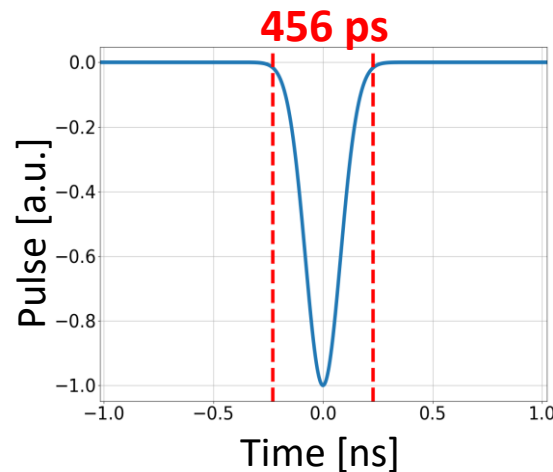
Setup with generator (down), comb (middle), oscilloscope (top)



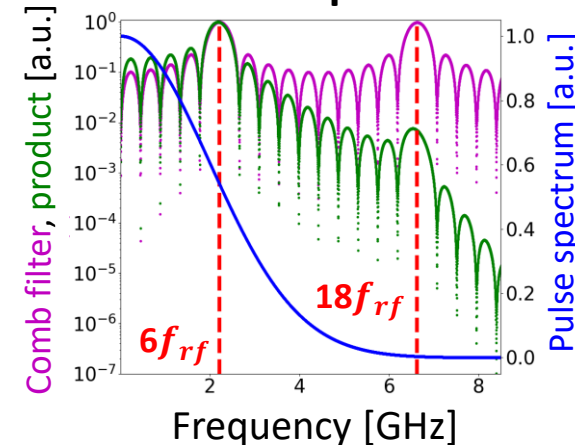
Zoom on the output of the oscilloscope



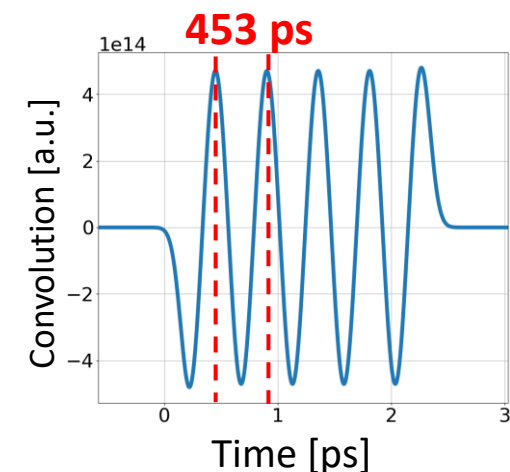
Simulated pulse with 456 ps end-to-end length



Simulated pulse spectrum, comb filter and their product



Convolution between simulated pulse and comb filter in time domain



Comb-generator as a filter

- The simulated comb-filter, confirmed by measurements (see before), was applied in simulation to the signal coming from the pickup.

- As an example, we considered a 4-cycle comb-filter at $6f_{rf}$.

- The bandwidth of a sinc is equal to

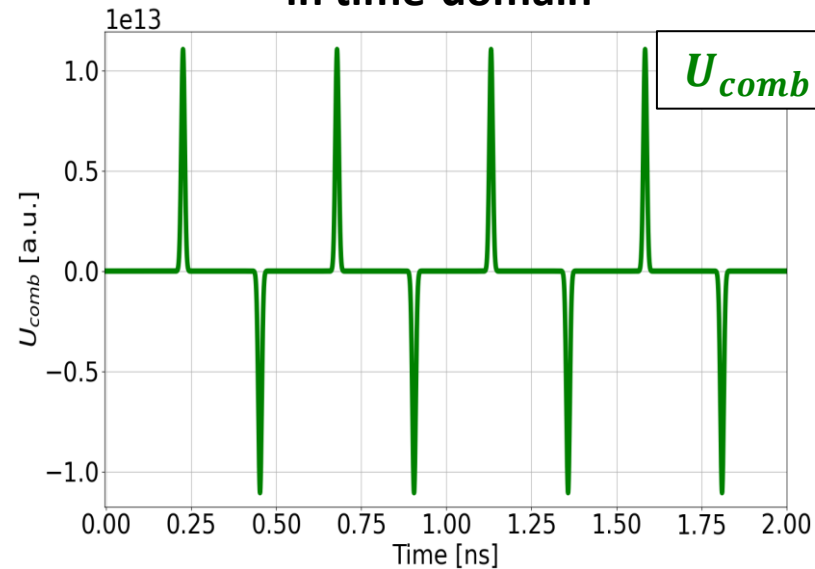
$$\Delta f_{BW} = 2 \frac{1}{4T_{6f_{rf}}} = 3f_{rf}$$

- Therefore in DAFNE the actual bunch current (\sim Gaussian) is filtered first by the pickup and then by the comb generator.

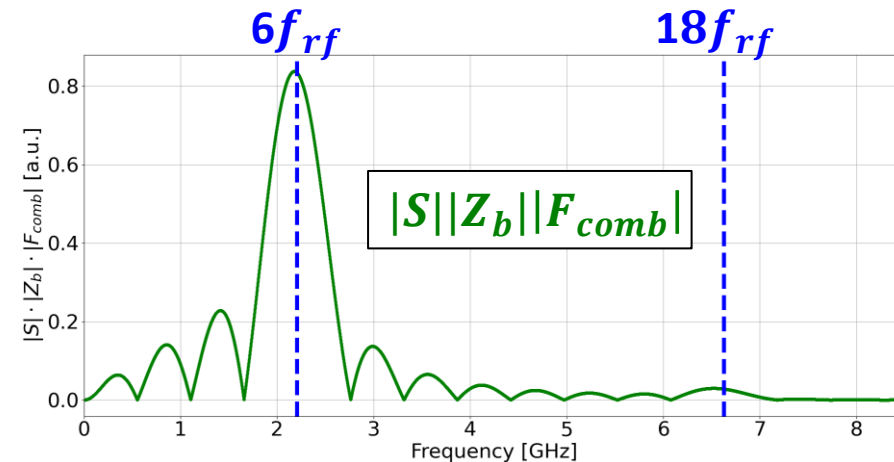
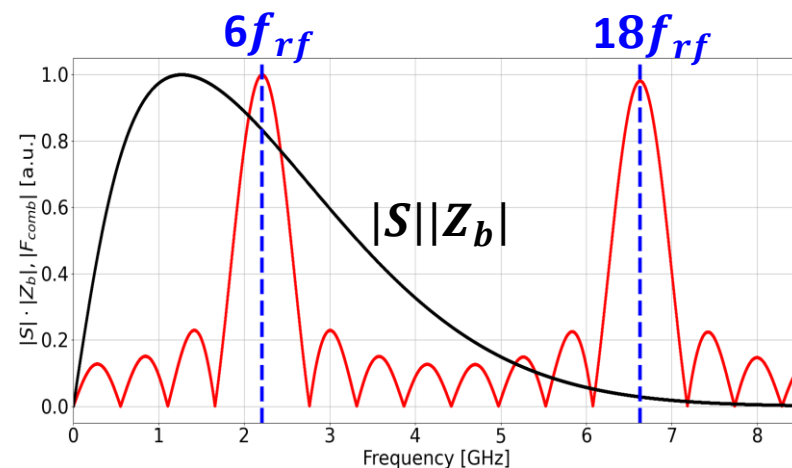
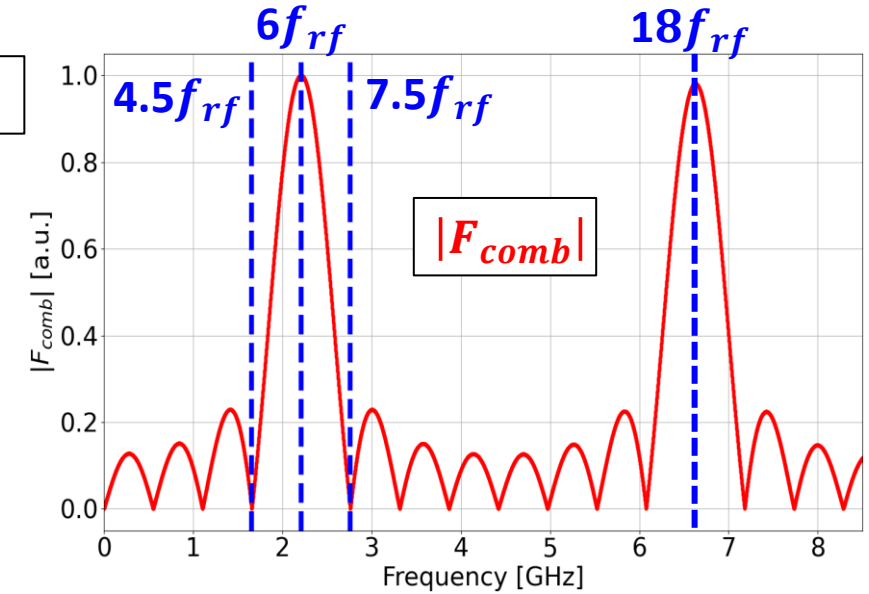
$$V_{comb}(t) \propto \mathcal{F}^{-1}(S \times Z_b \times F_{comb})$$

- The signal coming from the pickup acts as a band-pass filter which keeps only the sinc at $6f_{rf}$.

Simulated comb-filter
in time-domain



Simulated comb-filter in frequency-domain



Time signal before and after the comb generator (1/3)

- We consider one synchrotron period in DAFNE and we simulate the output-signal coming from the comb-generator.
 - Three different input-signals are used.
 - The macroparticle code is not used here. Synchrotron oscillations are obtained by simply shifting the input signal by

$$\tau = A \cos(\omega_s k T_0)$$

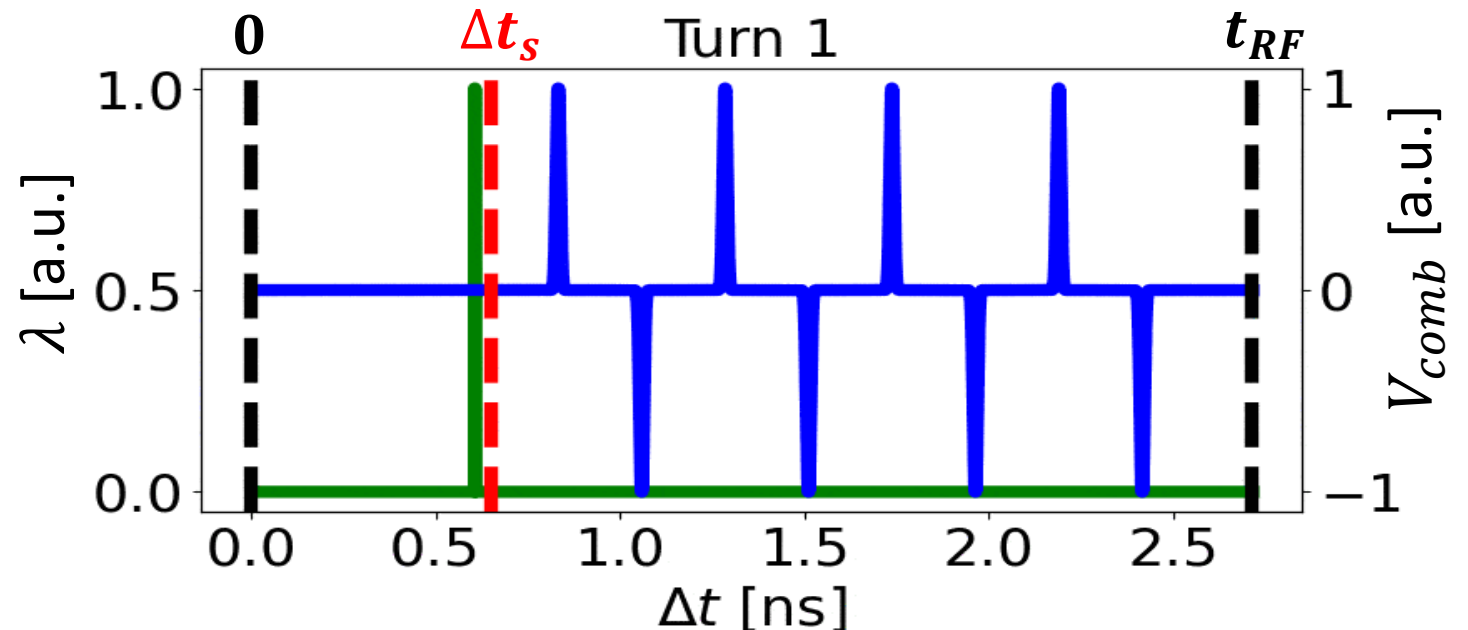
A: oscillation amplitude = 0.1 rad

k: turn number

- **First example:** We obtain V_{comb} by convolving the numerically reconstructed comb-filter in time domain with a delta signal arriving at time $\Delta t_s + \tau$.

$$\lambda(t) = \delta(t - \Delta t_s - \tau) \quad \Rightarrow \quad V_{comb}(t) \propto \lambda(t) * U_{comb}(t) = \int_0^{+\infty} \delta(t - a - \Delta t_s - \tau) U_{comb}(a) da = U_{comb}(t - \Delta t_s - \tau)$$

- The output from the comb generator is the filter itself shifted by $\Delta t_s + \tau$.
- The relative phase between λ and V_{comb} is preserved over time.
 - Required for phase detection.
- This model is not realistic since the signal entering the comb-generator is not a delta function, as shown before.



Time signal before and after the comb generator (2/3)

□ **Second example:** The input signal is Gaussian with mean $\Delta t_s + \tau$ and with $\sigma_z = 20$ mm or 30 mm.

➤ We obtain V_{comb} by convolving this signal with the comb-filter in time domain

$$V_{comb}(t) \propto \lambda(t) * U_{comb}(t) = \int_0^{+\infty} e^{-\frac{(t-a-\Delta t_s-\tau)^2}{2\sigma_t^2}} U_{comb}(a) da \approx |A(t)| \sin[6\omega_{rf}(t + t_a - \Delta t_s - \tau)]$$

➤ The output of the comb generator is sinusoidal with frequency $6f_{rf}$.

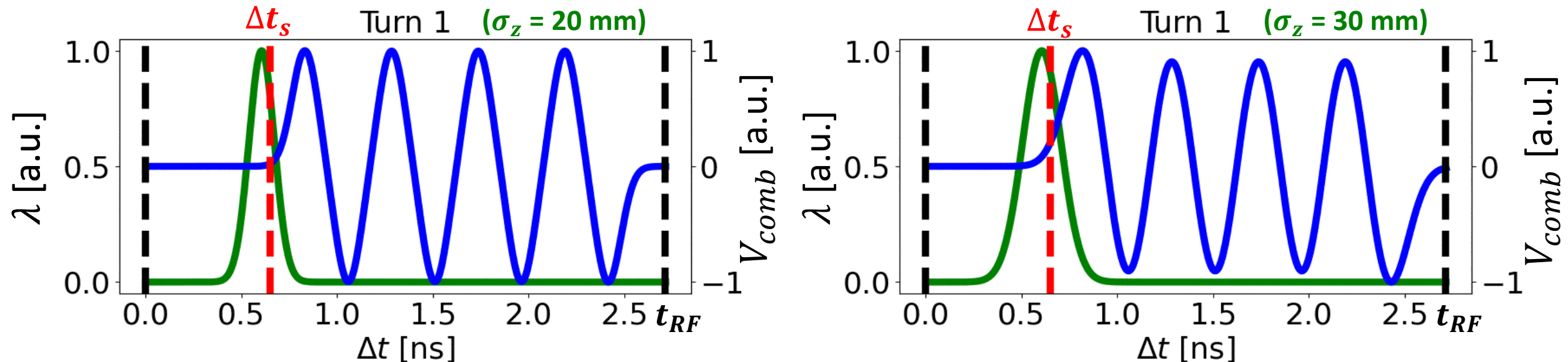
- The filter sinc-functions at higher frequencies are made negligible by the Gaussian spectrum.

➤ The relative phase between λ and V_{comb} is preserved over time. This is essential for phase detection.

- With respect to the mean of λ , this phase difference is equal to $6\omega_{rf}t_a$ and is larger for longer bunches.

➤ For large σ_z , V_{comb} is amplitude-modulated in correspondence of the first and fourth periods (amplitude $|A(t)|$).

➤ This better model is not realistic yet since the comb-generator input is not Gaussian, but a differentiated Gaussian.



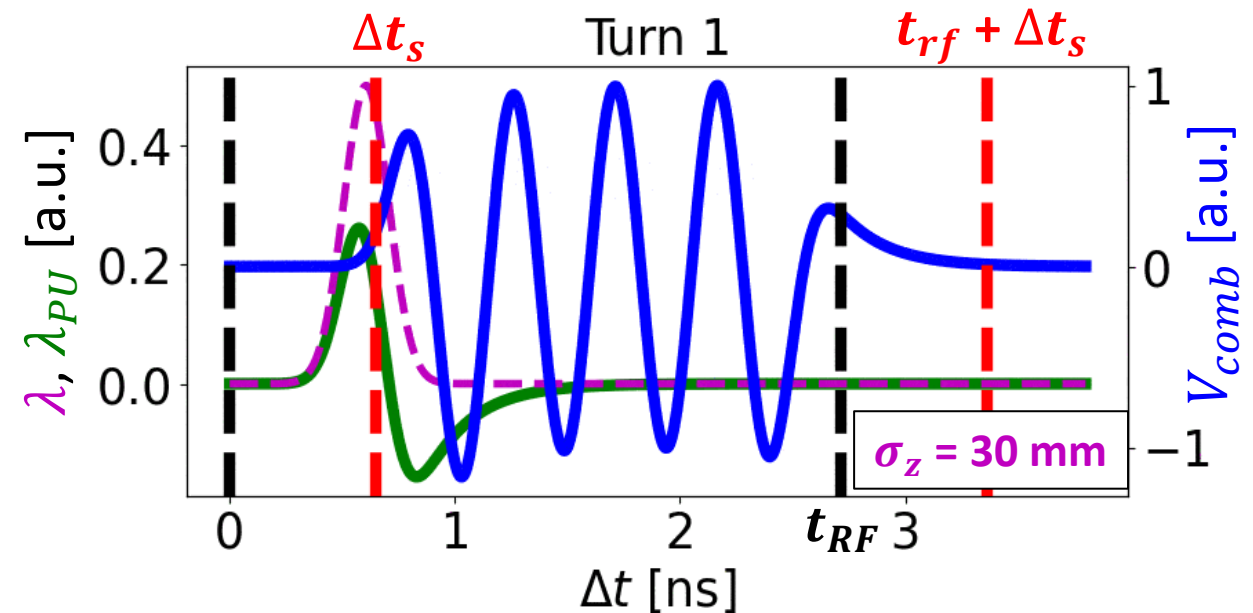
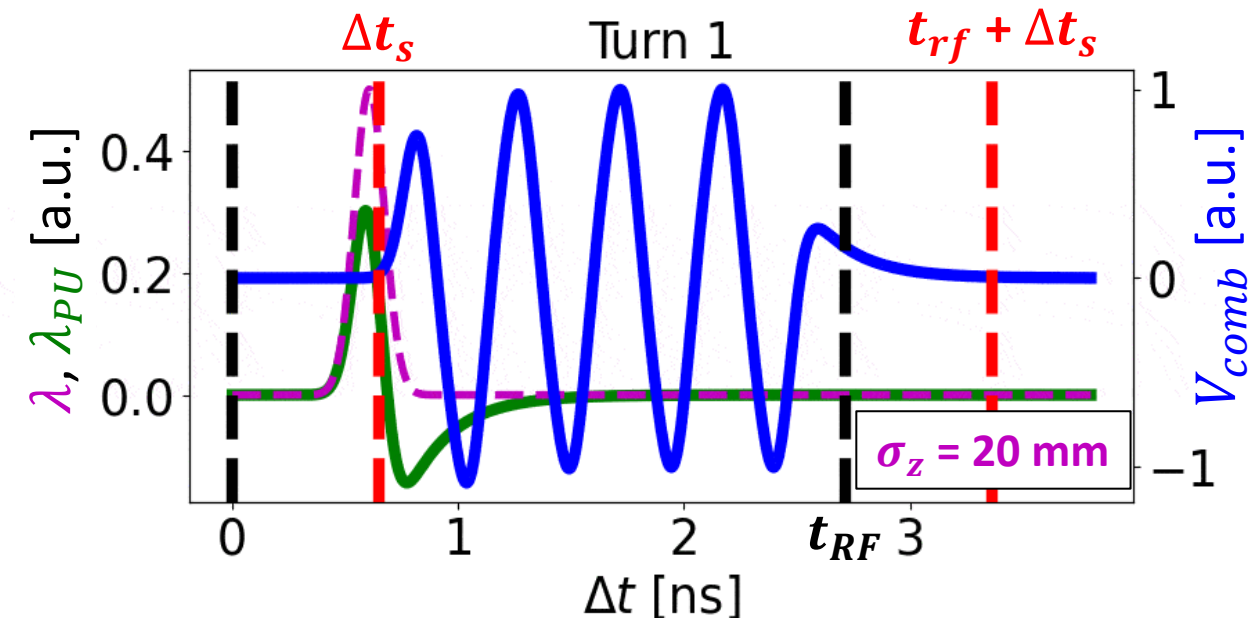
Time signal before and after the comb generator (3/3)

□ **Third example (realistic):** The input signal is a differentiated Gaussian.

- This signal is obtained by applying Z_b to a Gaussian profile with mean $\Delta t_s + \tau$ and with $\sigma_z = 20$ mm or 30 mm.
- We obtain V_{comb} by convolving the input signal with the comb-filter in time domain.

$$V_{comb}(t) \propto \lambda(t) * U_{comb}(t) = \int_0^{+\infty} \lambda(t-a) U_{comb}(a) da \propto |B(t)| \sin[6\omega_{rf}(t + t'_a - \Delta t_s - \tau)]$$

- V_{comb} has essentially the same features of the V_{comb} computed for Gaussian inputs (second example).
 - It is sinusoidal with frequency $6f_{rf}$.
 - The phase difference between V_{comb} and the mean of the Gaussian profile is $6\omega_{rf}t'_a$ and constant over time.
 - V_{comb} extends to the adjacent bucket, leading to possible coupling between phases of consecutive bunches.



Voltage from the comb generator

- The signal exiting the comb generator goes through an attenuator, which is followed by an amplifier.
- Characterizing better the proportionality factor, V_{comb} is equal to:

$$V_{comb}(t) = \frac{Q_b}{T_0} |Z_b| g_p g_c g_a |B(t)| \sin[6\omega_{rf}(t + t'_a - \Delta t_s - \tau)]$$

➤ V_{comb} is proportional to:

- the total bunch current Q_b/T_0 ;
- the magnitude of the button transfer impedance $|Z_b|$, which is constant ($= 0.43 \Omega$) in the working region, i.e. around $4f_{rf}$ or $6f_{rf}$;
- the coefficient g_p , accounting for the attenuation provided by the pickup-attenuator, which is able to control the level of signal measured by the pickup;
- the coefficient g_c , which accounts for the attenuation-level provided by the comb-generator and the attenuator placed after it;
- the gain g_a of the amplifier placed after the comb generator;
- the amplitude modulation $|B(t)|$, which can be different from 1 in correspondence of the first and fourth periods of the sinusoidal tone burst.

Local oscillator and mixer

□ The local oscillator is locked to the ring RF clock and produces a sinusoidal signal with frequency $6f_{rf}$

$$V_{lo}(t) = \sin[6(\omega_{rf}t + \phi_{lo})]$$

➤ where $\phi_{lo} = \phi_{lo1} + \phi_{lo2}$ is adjusted by using a phase shifter (servo), so that

- V_{lo} is in quadrature with respect to the sinusoidal V_{comb} ;
- ϕ_{lo2} is the phase advance of the comb-voltage relative to the bunch centre of mass minus the synchronous phase

$$6\phi_{lo1} = -\pi/2 \qquad \phi_{lo2} = \omega_{rf}(t'_a - \Delta t_s)$$

□ Therefore

$$V_{lo}(t) = -\cos[6\omega_{rf}(t + t'_a - \Delta t_s)]$$

□ V_{comb} and V_{lo} are multiplied together in the mixer

$$\begin{aligned} V_{mix}(t) &= -\frac{Q_b}{T_0} |Z_b| g_p g_c g_a |B(t)| \sin[6\omega_{rf}(t + t'_a - \Delta t_s - \tau)] \cos[6\omega_{rf}(t + t'_a - \Delta t_s)] \\ &= -\frac{Q_b}{2T_0} |Z_b| g_p g_c g_a |B(t)| [\sin(-6\omega_{rf}\tau) + \sin(12\omega_{rf}(t + t'_a - \Delta t_s) - 6\omega_{rf}\tau)] \end{aligned}$$

Low-pass filter

□ A low-pass filter is then applied to V_{mix} to eliminate the high-frequency component of the mixer output

$$V_{lpf}(t) = \frac{Q_b}{2T_0} |Z_b| g_p g_c g_a |B(t)| \sin(6\varphi_0) \approx \frac{3Q_b}{T_0} |Z_b| g_p g_c g_a |B(t)| \varphi_0$$

↑
For small phases

□ More in general we have

$$V_{lpf}(t) = \frac{Q_b}{T_0} |Z_b| g_m g_p g_c g_a |B(t)| \sin(g_l \tilde{\varphi}_0)$$

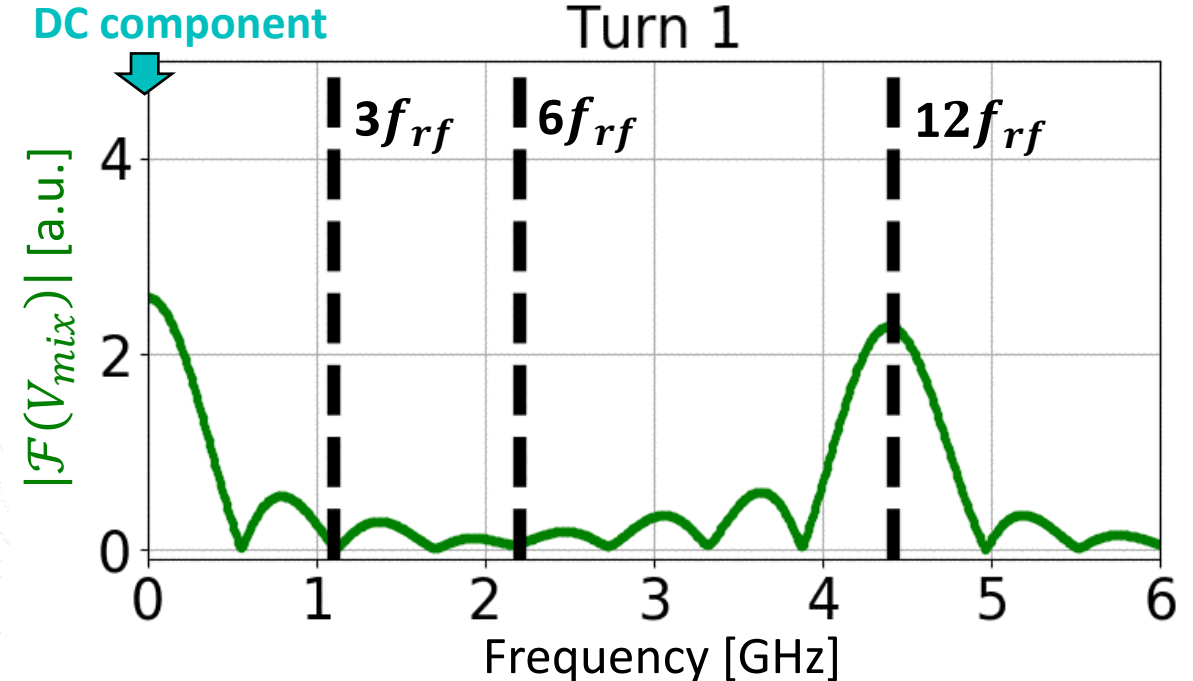
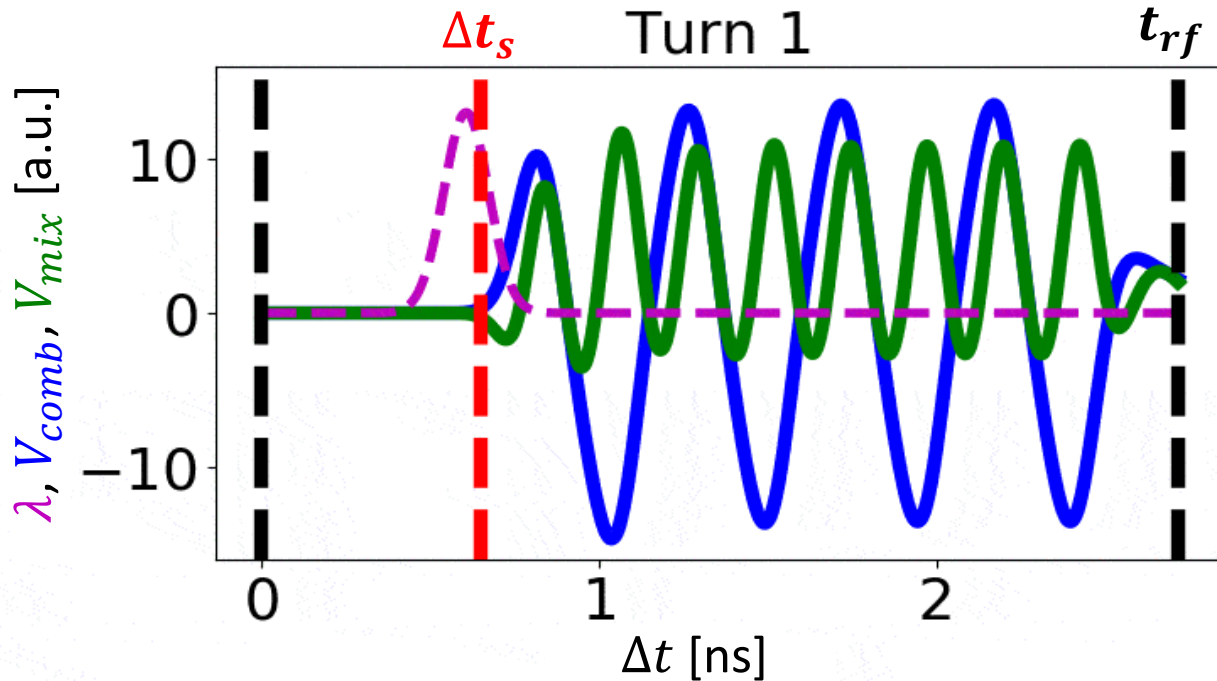
- where $g_m \leq 0.5$ is the conversion efficiency of the mixer;
- where $g_l = 4$ or 6 depending on the DAFNE operation mode;
- where

$$\tilde{\varphi}_0 = \varphi_0 + \varphi_{cl} + \varphi_{err} + \varphi_{off}$$

- being φ_{cl} an error phase accounting for the possible coupling between consecutive bunches when a tone burst reaches the adjacent bucket (as shown earlier);
- being φ_{err} an error phase present when the phase advance of the comb-voltage relative to the bunch centre of mass is not compensated (as shown earlier);
- being φ_{off} a phase offset which one can adjust to compensate the other phase errors.

Example continued: mixer

- **Third example continued:** V_{comb} is the comb-generator output when the input is a differentiated Gaussian signal, $\sigma_z = 20$ mm.
 - We suppose first that the local oscillator can't compensate for t'_a .
 - We compute numerically V_{mix} and its Fourier transform along one synchrotron period.



- Qualitatively

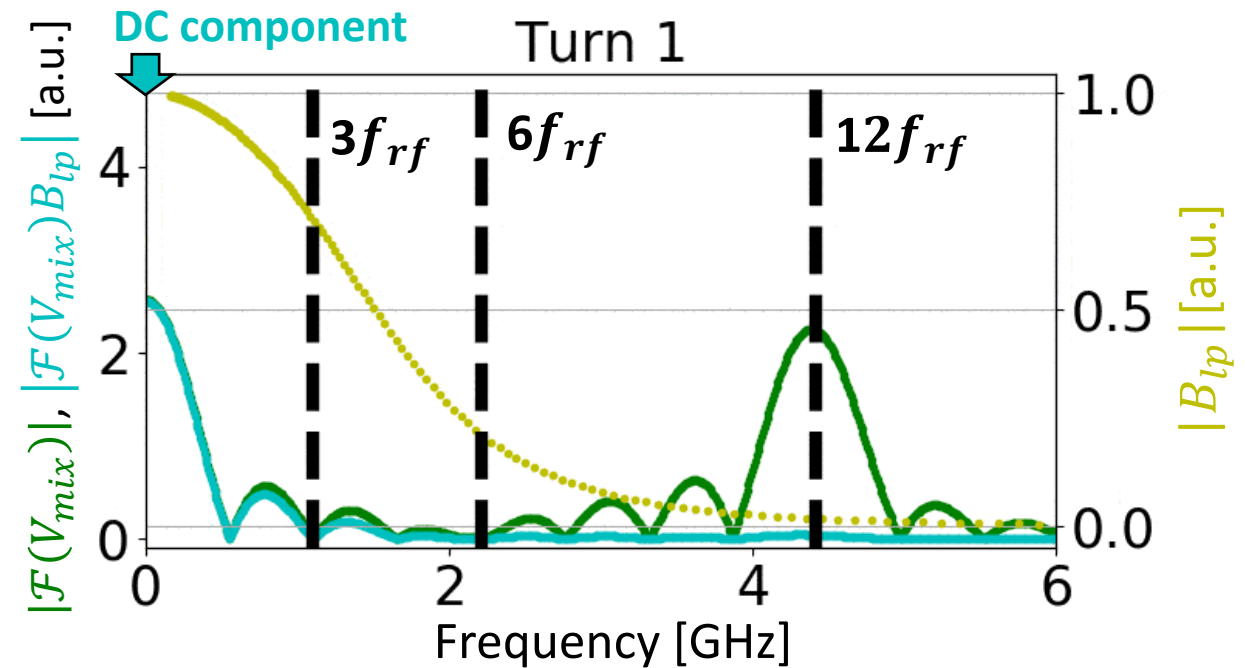
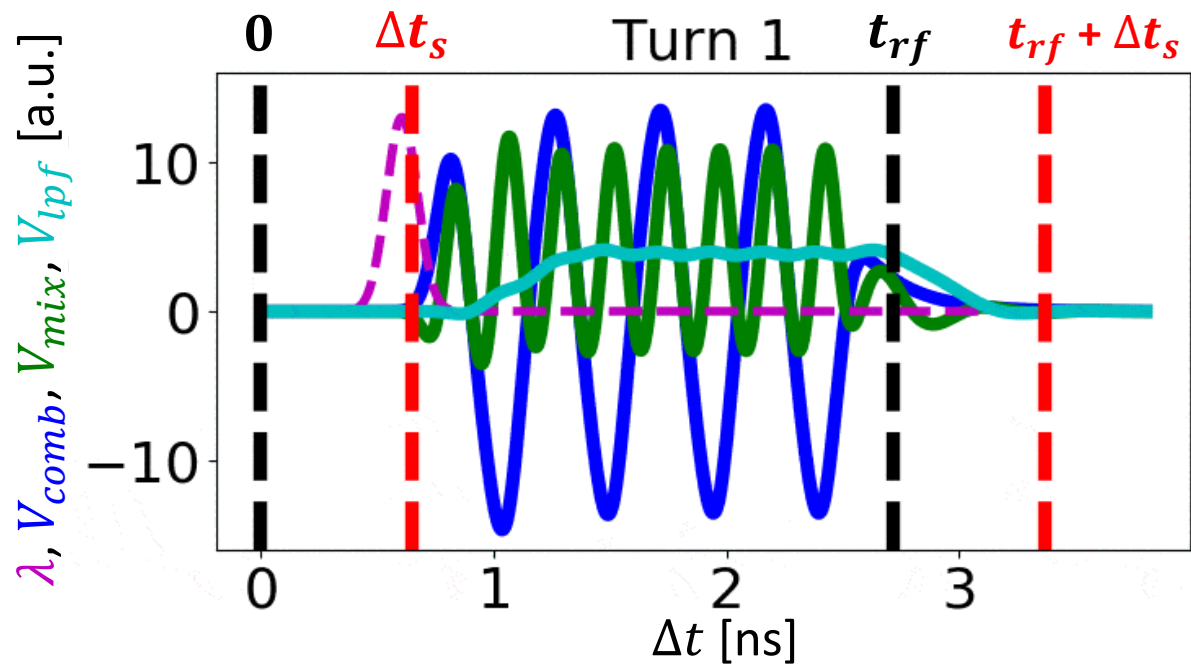
$$\begin{aligned}
 V_{mix}(t) &\propto -|B(t)| \sin[6\omega_{rf}(t + t'_a - \Delta t_s - \tau)] \cos[6\omega_{rf}(t - \Delta t_s)] \\
 &= \underbrace{\frac{|B(t)|}{2} \sin[6\omega_{rf}(\tau - t'_a)]}_{\text{DC component (signal average)}} - \underbrace{\frac{|B(t)|}{2} \sin[12\omega_{rf}(t - \Delta t_s) + 6\omega_{rf}(t'_a - \tau)]}_{\text{High-frequency component at } 12f_{rf}}
 \end{aligned}$$

DC component (signal average)

High-frequency component at $12f_{rf}$

Example continued: low-pass filter

- We apply a Bessel low-pass filter B_{lp} to V_{mix} in order to obtain only the DC component of V_{mix} .
 - A baseband Bessel low-pass filter was used at PEP-II.
 - In simulation the filter has order 4 and the gain magnitude is -3 dB at $3f_{rf}$.



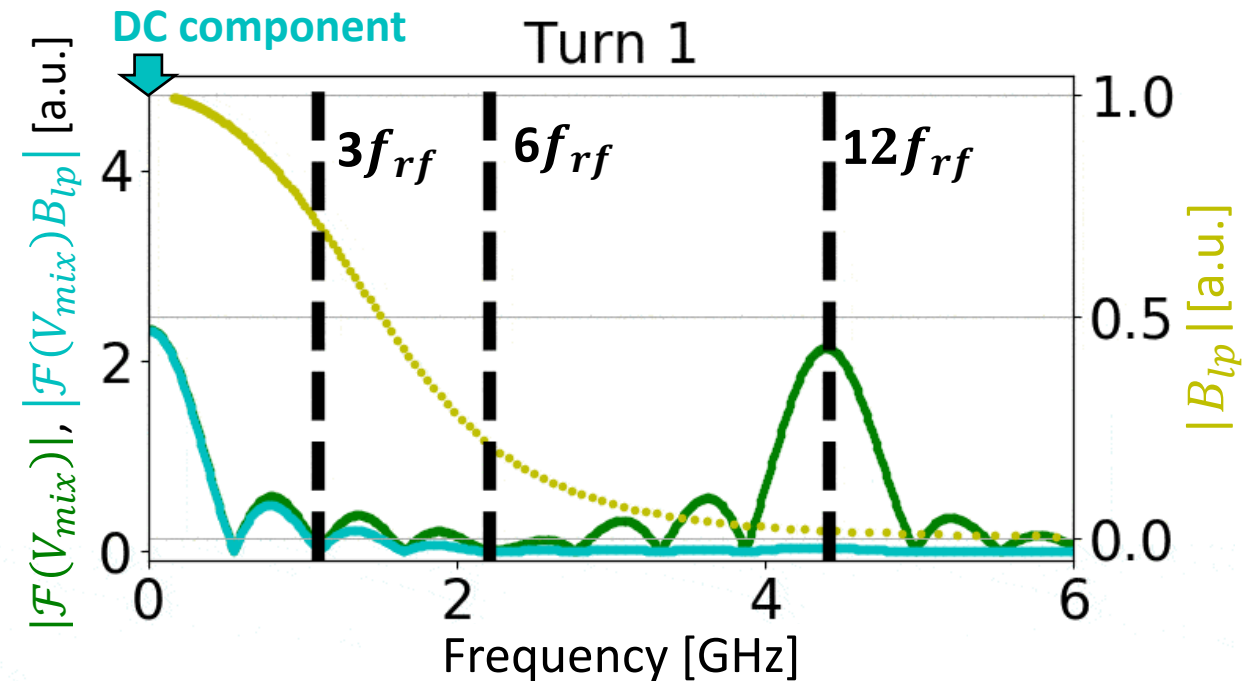
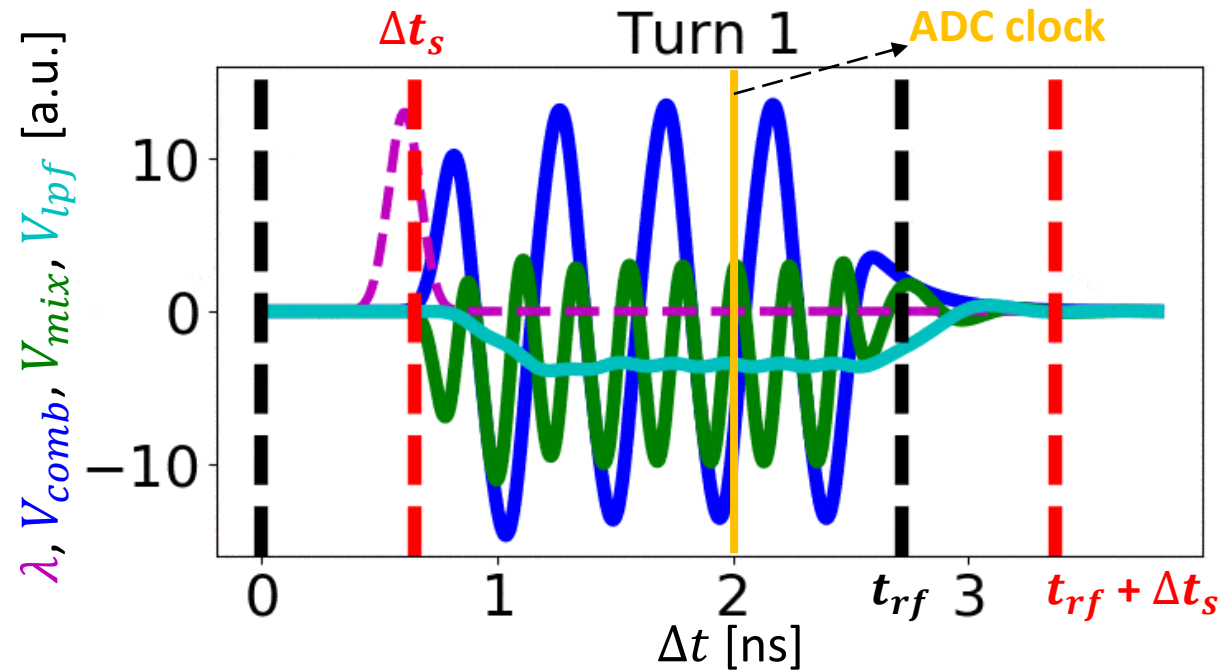
- Qualitatively

$$V_{lpf}(t) \propto \frac{|B(t)|}{2} \sin[6\omega_{rf}(\tau - t'_a)]$$

- V_{lpf} doesn't oscillate around zero due to the lack of compensation for t'_a .
- V_{lpf} extends to the adjacent bucket, leading to potential coupling in phase detection.

Example continued: phase compensation

- If the reference signal from the local oscillator can compensate for the phase error $6\omega_{rf}t'_a$ then V_{lpf} oscillates around zero and consequently the phase detection is correct.



- Qualitatively

$$V_{lpf}(t) \propto \sin(6\omega_{rf}t)$$

- At each turn, the time-span where V_{lpf} is constant is relatively large thanks to the tone-burst technique.
 - In this time-span $|B(t)| \approx 1$ (no amplitude modulation in V_{comb}), therefore we assume that $|B(t)| = 1$.
 - The ADC clock could for instance sample in correspondence of the orange line at each turn.
- V_{lpf} still extends to the adjacent bucket, leading to potential coupling in phase detection.

Phase detection and input for ADC

- In the macroparticle code $\varphi_0 = \Delta\varphi - \Delta\varphi_{SR}$ is already known at each turn,
 - $\Delta\varphi$ is known from the tracking and the constant $\Delta\varphi_{SR}$ can be easily computed.
 - The signal manipulations shown in the last slides (Gaussian profile, button transfer impedance, comb-generator, etc.) can't be directly applied in the code since each bunch is represented by just a macroparticle.
 - However the Python routines able to perform these signal manipulations are available for separate analysis.

- In the code we directly compute

$$V_{lpf} = \frac{Q_b}{T_0} |Z_b| g_m g_p g_c g_a \sin[g_l(\varphi_0 + \varphi_{cl} + \varphi_{err} + \varphi_{off})]$$

- where phase errors can be included through φ_{cl} (bunch coupling) and φ_{err} (phase advance of the comb-voltage).

- If intensity effects are large, then the synchronous phase is $\Delta\varphi_{HOM} \neq \Delta\varphi_{SR}$ and this shift can't be neglected. Therefore, from

$$V_{lpf} = \frac{Q_b}{T_0} |Z_b| g_m g_p g_c g_a \sin[g_l(\Delta\varphi - \Delta\varphi_{HOM} + (\Delta\varphi_{HOM} - \Delta\varphi_{SR}) + \varphi_{cl} + \varphi_{err})]$$

- we see that, even when $\varphi_{cl} = \varphi_{err} = 0$, we have to compensate the synchronous-phase shift due to the HOMs.
 - This can be done in the code since $\Delta\varphi_{HOM}$ can be computed with the new Python routine;
 - In operation, an input-offset can be set in the phase-servo-loop panel in order to obtain the desired compensation.

- Before entering into the ADC, V_{lpf} passes through an amplifier with gain g_{a2} .

- Noise can also be added in the code and the input voltage for the ADC is $V_{ADC} = g_{a2}V_{lpf} + \mathcal{N}(0, \sigma_N)$, where \mathcal{N} is a sample from a Gaussian distribution with mean 0 and rms σ_N .

ADC processing

□ Let's suppose that the number of bits for the ADC is $n_{bit,ADC}$.

□ With $n_{bit,ADC}$ we can represent the $2^{n_{bit,ADC}}$ signed numbers

$$\{-(2^{n_{bit,ADC}-1} - 1), -(2^{n_{bit,ADC}-1} - 1) + 1, \dots, -2, -1, 0, 1, 2, \dots, 2^{n_{bit,ADC}-1} - 1, 2^{n_{bit,ADC}-1}\}$$

□ The ADC converts a mixer-voltage V_{ADC} (real number) into an output n_{oADC} (integer number)

$$V_{ADC} \in]-\infty, +\infty[$$



$$n_{oADC}$$

∩

$$\{-(2^{n_{bit,ADC}-1} - 1), -(2^{n_{bit,ADC}-1} - 1) + 1, \dots, -2, -1, 0, 1, 2, \dots, 2^{n_{bit,ADC}-1} - 1, 2^{n_{bit,ADC}-1}\}$$

□ Calling $V_{max,ADC}$ the maximum input voltage for the ADC

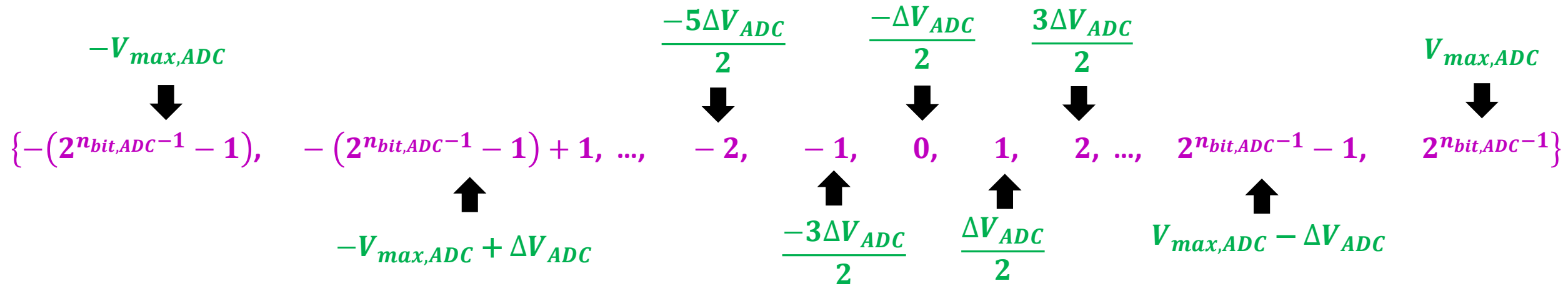
$$]-\infty, -V_{max,ADC}] \ni V_{ADC} \longrightarrow -(2^{n_{bit,ADC}-1} - 1) \quad [V_{max,ADC}, +\infty[\ni V_{ADC} \longrightarrow 2^{n_{bit,ADC}-1}$$

□ For other values of V_{ADC} , we divide the interval $[-V_{max,ADC}, V_{max,ADC}]$ into sub-intervals with length ΔV_{ADC}

$$\Delta V_{ADC} = \frac{V_{max,ADC} - [-V_{max,ADC}]}{2^{n_{bit,ADC}-1} - [-(2^{n_{bit,ADC}-1} - 1)]} = \frac{2V_{max,ADC}}{2^{n_{bit,ADC}} - 1}$$

ADC processing

□ Therefore we have the correspondences



□ The relations are

$$\frac{\Delta V_{ADC}}{2} (2^{n_{oADC}} - 1) = V_{ADC, n_{oADC}} \longrightarrow n_{oADC} = \frac{V_{ADC, n_{oADC}}}{\Delta V_{ADC}} + \frac{1}{2}$$

□ If $V_{ADC} \neq V_{ADC, n_{oADC}}$, then the above relation yields a non-integer number and we take the integer part of it

$$n_{oADC} = \text{int} \left(\frac{V_{ADC}}{\Delta V_{ADC}} + \frac{1}{2} \right) = \text{int} \left(\frac{2^{n_{bit,ADC}} - 1}{2} \frac{V_{ADC}}{V_{max,ADC}} + \frac{1}{2} \right)$$

□ In DAFNE $n_{bit,ADC} = 8$ and therefore the conversion formula is

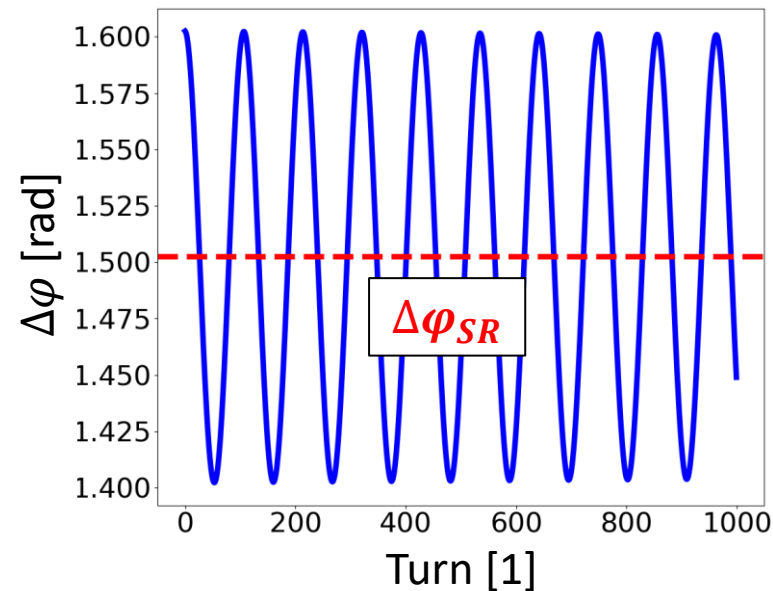
$$n_{oADC} = \text{int} \left(127.5 \frac{V_{ADC}}{V_{max,ADC}} + 0.5 \right)$$

NOTE: bug in the Fortran code, the formula on the left is used even when $n_{bit,ADC} \neq 8$

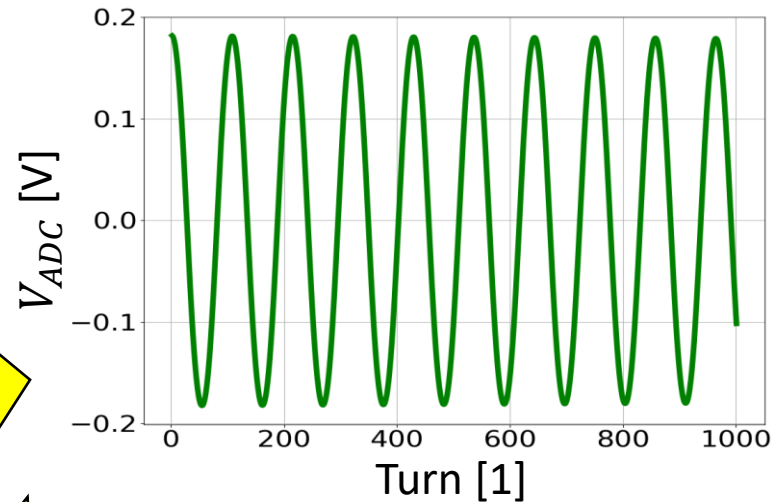
ADC processing: DAFNE examples

- Simulation of an oscillating bunch. Phase amplitude of 0.1 rad, no intensity effects, no action of the feedback.
 - We plot the voltage signal entering the ADC and the ADC output ($V_{max,ADC} = 200$ mV).

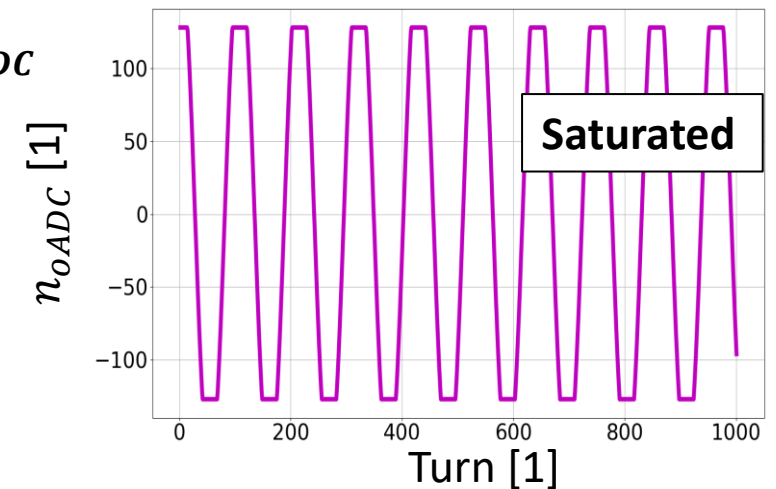
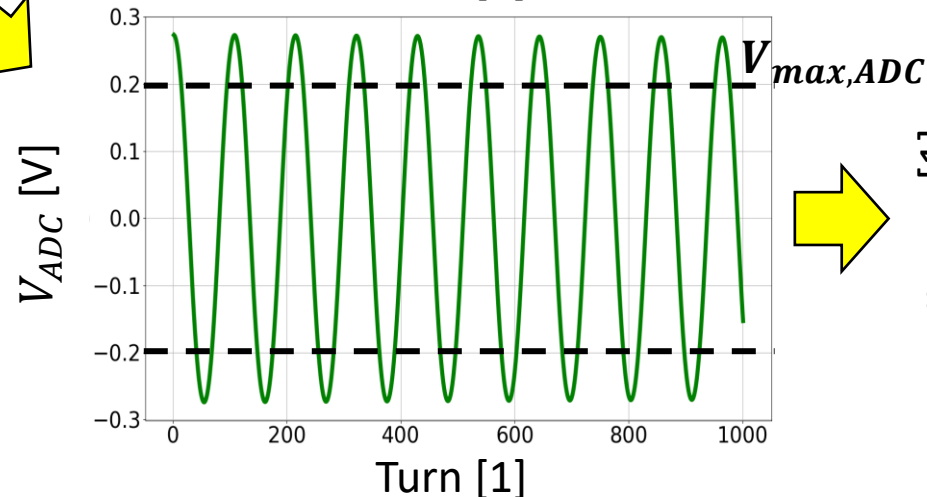
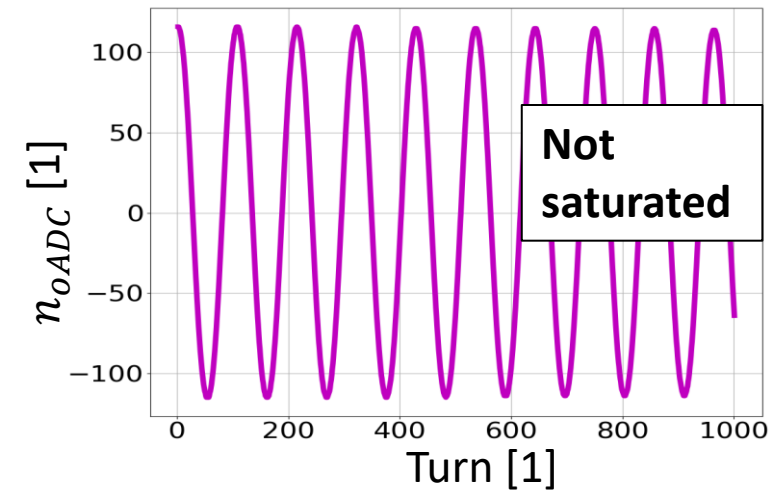
Phase oscillations around $\Delta\phi_{SR}$



Input voltage for ADC between ± 200 mV



ADC output between -127 and 128



- Too high gains can lead to signal saturation in the ADC.

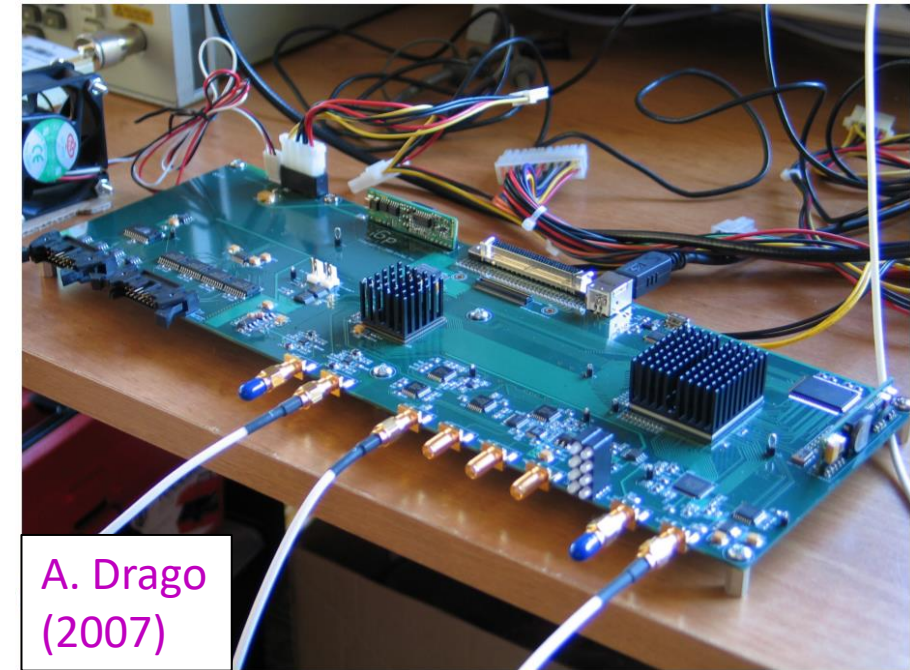
FPGA: introduction

Xilinx FPGA used in DAFNE

- ❑ The ADC output n_{oADC} is processed by the FPGA (Field Programmable Gate Array), which is a configurable integrated circuit.
- ❑ The goal of the FPGA is to shift the n_{oADC} signal by $\pi/2$, so that the output signal is in anti-phase with respect to the energy oscillation of the bunch.
- ❑ The shift by $\pi/2$ is performed applying a FIR (Finite Impulse Response) filter to the n_{oADC} signal.
 - FIR: the filter is not recursive, i.e. the output is not used in the input.
- ❑ Different filters can be programmed in the FPGA, although the sinusoidal one is generally used in DAFNE operation.
- ❑ Concerning the sinusoidal filter, a convolution is performed between the n_{oADC} signal, evaluated along the last synchrotron period, and the sinusoidal function f_{FIR} with angular frequency ω_{s0} and phase ϕ_2 . At time t_k , the FPGA output is

$$n_{oFPGA}(t_k) = g_{FPGA} n_{oADC} * f_{FIR} = g_{FPGA} \sum_{i=0}^{N_{tap}-1} n_{oADC}[t_{k-i}] f_{FIR,i} = g_{FPGA} \sum_{i=0}^{N_{tap}-1} n_{oADC}[t_{k-i}] \sin(\omega_{s0} \Delta t_{DSF} i + \phi_2)$$

- where g_{FPGA} is the gain of the FPGA;
- $t_{k-N_{tap}+1}, \dots, t_k$ are equidistant bunch arrival-times when the feedback operates (we call Δt_{DSF} the time interval);
- N_{tap} is the number of filter taps and is such that $n_{oADC}[t_k] \approx n_{oADC}[t_{k-N_{tap}}]$.



A. Drago
(2007)

FPGA: shift of the input-signal using a convolution

□ Why this convolution is able to shift the n_{oADC} signal by $\pi/2$? We start from the expression

$$n_{oFPGA}(t_k) = \frac{g_{FPGA}}{\Delta t_{DSF}} \sum_{i=0}^{N_{tap}-1} n_{oADC}[t_{k-i}] \sin(\omega_{s0} \Delta t_{DSF} i + \phi_2) \Delta t_{DSF}$$

□ If Δt_{DSF} is small, this expression can be approximated with an integral

$$n_{oFPGA}(t) = \frac{g_{FPGA} A_{oADC}}{\Delta t_{DSF}} \int_{t-kT_{s0}}^t \sin[\omega_{s0}(t-\tau) + \phi_1] \sin(\omega_{s0}\tau + \phi_2) d\tau =$$

$$= \frac{g_{FPGA} A_{oADC}}{2\Delta t_{DSF}} \int_{t-kT_{s0}}^t [\cos(\omega_{s0}t - 2\omega_{s0}\tau + \phi_1 - \phi_2) - \cos(\omega_{s0}t + \phi_1 + \phi_2)] d\tau = -\frac{g_{FPGA} A_{oADC} kT_{s0}}{2\Delta t_{DSF}} \cos(\omega_{s0}t + \phi_1 + \phi_2)$$

- where $k \geq 1$ is the number of synchrotron periods along which n_{oADC} and f_{FIR} are evaluated;
- where A_{oADC} and ϕ_1 are respectively the amplitude and phase of n_{oADC} .

□ Therefore we have the transformation

$$n_{oADC}(t) = A_{oADC} \sin(\omega_{s0}t + \phi_1) \quad \longrightarrow \quad n_{oFPGA}(t) = \frac{g_{FPGA} A_{oADC} kT_{s0}}{2\Delta t_{DSF}} \sin\left(\omega_{s0}t + \phi_1 + \phi_2 - \frac{\pi}{2}\right)$$

- if $\phi_2 = 0$, then n_{oADC} is shifted by $\pi/2$ as desired.

FPGA: frequency response of the sinusoidal filter

□ We compute the frequency response of the filter, **assuming an arbitrary small time-step.**

➤ We take as an example DAFNE with $f_{s0} = 28.72$ kHz. The filter has phase $\phi_2 = 0$.

□ The absolute value of the filter Fourier-transform is a sinc-like function.

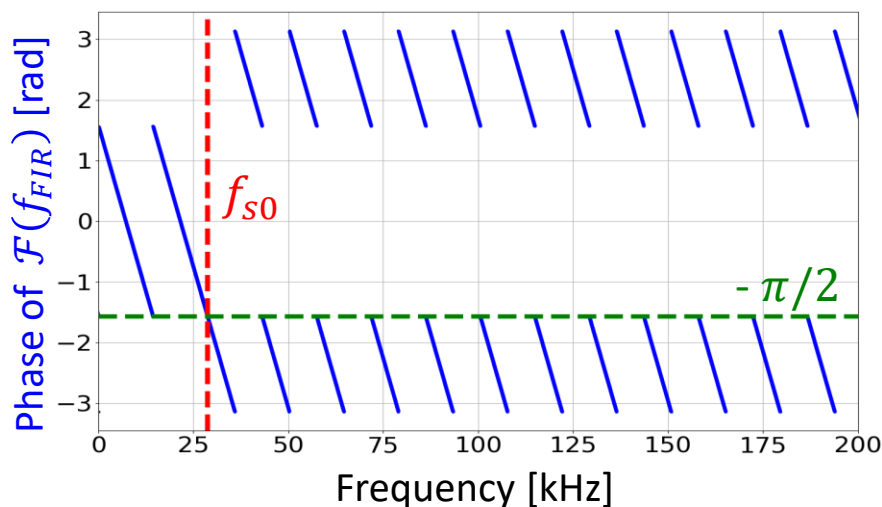
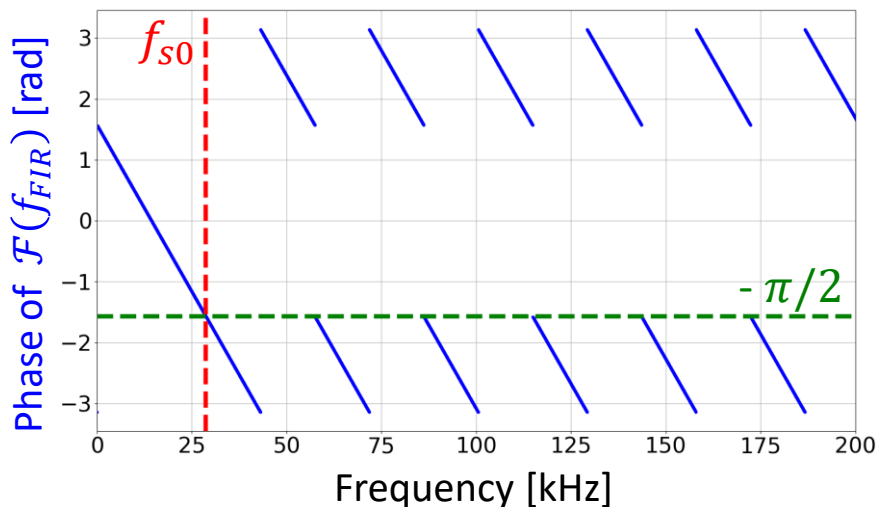
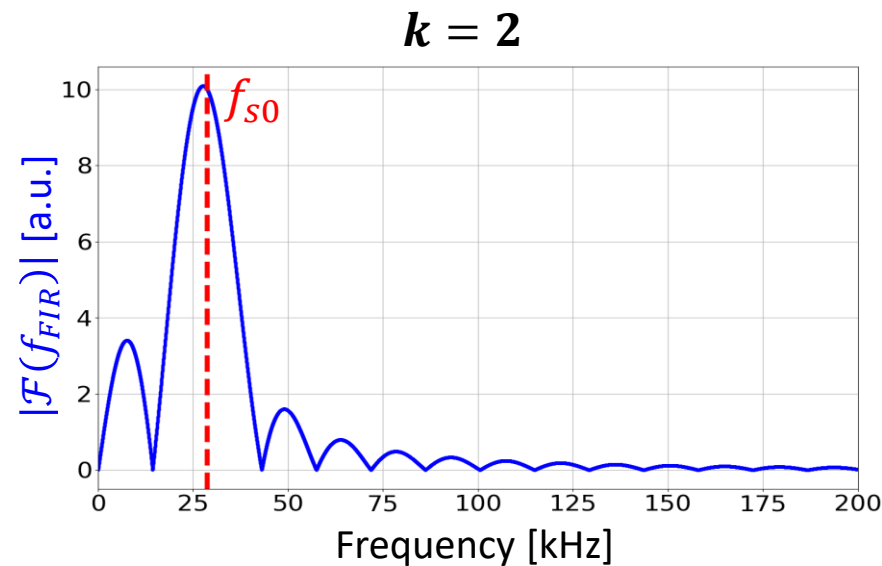
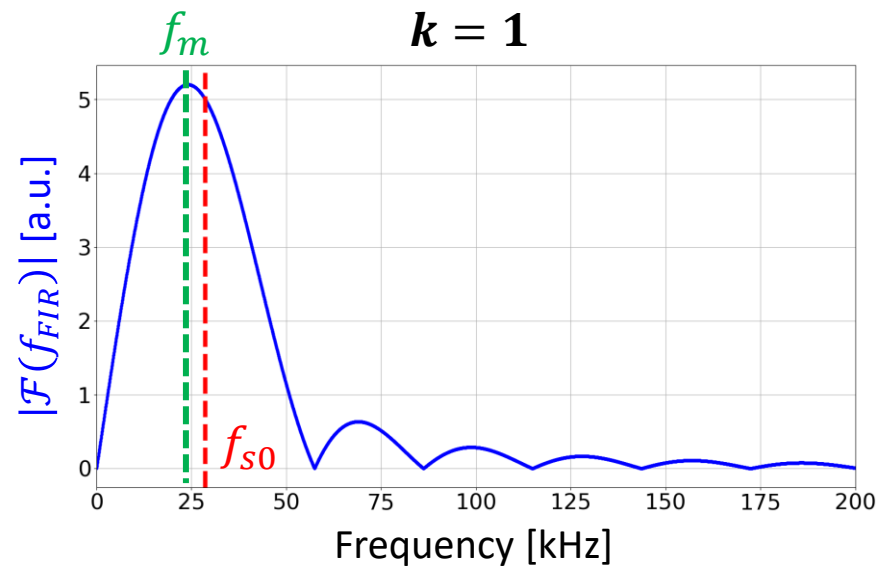
➤ The maximum value occurs at $f_m < f_{s0}$ and f_m approaches f_{s0} as k increases.

□ The phase decreases linearly with frequency and has discontinuities where $|\mathcal{F}(f_{FIR})| = 0$.

➤ The phase is $-\pi/2$ in correspondence of f_{s0} as expected.

□ If the input signal has $f_s \approx f_{s0}$, then the phase has to be as close as possible to $-\pi/2$.

➤ $k = 1$ is preferable to $k = 2$ since the phase slope is higher.



FPGA: down sampling factor (1/5)

- ❑ Let's suppose that the feedback operates every d_{DSF} turns. $d_{DSF} \geq 1$ is an integer called **down-sampling factor**.
- ❑ Using a down-sampling factor larger than 1 has pros and cons.
- ❑ **Advantage:** the number of operations per unit-time performed in the FPGA is reduced by factor d_{DSF}^2 .
 - Computations on $1/d_{DSF}$ of the original data, moreover the time available to do the computations is d_{DSF} times longer.
 - The saved computational time can be used to do more complicated filter-calculations and/or treat more bunches.
- ❑ **Disadvantage:** the feedback doesn't provide the proper correction at each revolution turn, but just every d_{DSF} turns.
 - The last computed correction is given until a new correction is evaluated.
- ❑ In theory, according to the Nyquist theorem, Δt_{DSF} can be as low as $T_{s0}/2$ in order to properly reconstruct the sinusoidal synchrotron oscillation of the bunch.
 - Two samples per period ($N_{tap} = 2$) are sufficient to detect amplitude and phase of the synchrotron oscillation.
- ❑ In practice, the synchrotron oscillations are not perfectly sinusoidal, for instance when the bunch is far from the synchronous phase or when intensity effects are high.
 - Moreover, the two samples are useless if they are close to zero.
 - This can happen when the sampling times are close to the zero crossings of the sine function.
- ❑ Usually in operation $N_{tap} \geq 5$.

FPGA: down sampling factor (2/5)

- As seen earlier, n_{oADC} is shifted by $-\pi/2$ when convolved with f_{FIR} .
 - Both signals should extend over one synchrotron period and ϕ_2 should be zero.
- Using N_{tap} taps means to divide the synchrotron period T_{s0} into N_{tap} intervals, each with length $\Delta t_{DSF} = d_{DSF}T_0$.
- $1/Q_s$ is the number of revolution turns necessary for a particle to perform one synchrotron period.
 - Assuming that $1/Q_s$ is an integer multiple of N_{tap} , then

$$\frac{1}{Q_s}T_0 = T_{s0} = N_{tap}\Delta t_{DSF} = N_{tap}(d_{DSF}T_0) \quad \Rightarrow \quad d_{DSF}N_{tap} = \frac{1}{Q_s}$$

- Therefore the following three expressions are all equivalent

$$\begin{aligned} n_{oFPGA}(t_k) &= g_{FPGA} \sum_{i=0}^{N_{tap}-1} n_{oADC}[t_{k-i}] \sin(\omega_{s0} i d_{DSF} T_0) = g_{FPGA} \sum_{i=0}^{N_{tap}-1} n_{oADC}[t_{k-i}] \sin(2\pi i d_{DSF} Q_s) \\ &= g_{FPGA} \sum_{i=0}^{N_{tap}-1} n_{oADC}[t_{k-i}] \sin\left(\frac{2\pi i}{N_{tap}}\right) \end{aligned}$$

- When (as usual) $1/Q_s$ isn't an integer multiple of N_{tap} , we use the first of these three expressions.
 - The time step of f_{FIR} is $d_{DSF}T_0$, which is also the time step of n_{oADC} . This is required to perform a proper convolution.
 - However it's usually not possible to cover exactly one T_{s0} using this expression, as instead it occurs using the third one.

FPGA: down sampling factor (3/5)

- ❑ The previous formula doesn't take into account the following two delays.
 - **Feedback delay:** the feedback-correction computed at turn n is not provided to the bunch at turn n .
 - In the macroparticle code we assume that this correction is given at turn $n + 1$.
 - **Hold-buffer delay:** The feedback-correction computed at turn $kd_{DSF}T_0$ is the one given to the bunch for all the times between $kd_{DSF}T_0$ and $(k + 1)d_{DSF}T_0$.
 - The feedback-correction at turn $kd_{DSF}T_0$ is computed as if the turn is not $kd_{DSF}T_0$ but $kd_{DSF}T_0 + \Delta t_{DSF}/2$.

- ❑ The filter sinusoidal function has to compensate these two delays with a constant phase offset ϕ_2

$$f_{FIR,i} = \sin(\omega_{s0} i d_{DSF} T_0 + \phi_2) = \sin\left(\omega_{s0} i d_{DSF} T_0 + \omega_{s0} T_0 \uparrow \text{Feedback delay} + \omega_{s0} \frac{d_{DSF} T_0}{2} \uparrow \text{Hold-buffer delay}\right)$$

- ❑ The filter sinusoidal function is not supposed to add DC components to the output signal.
 - Even if the integral of the sine function on one period is zero, discretizations can add a non-zero DC component.
 - Therefore the average of the N_{tap} filter-coefficients is subtracted from each $f_{FIR,i}$.

- ❑ Therefore we have

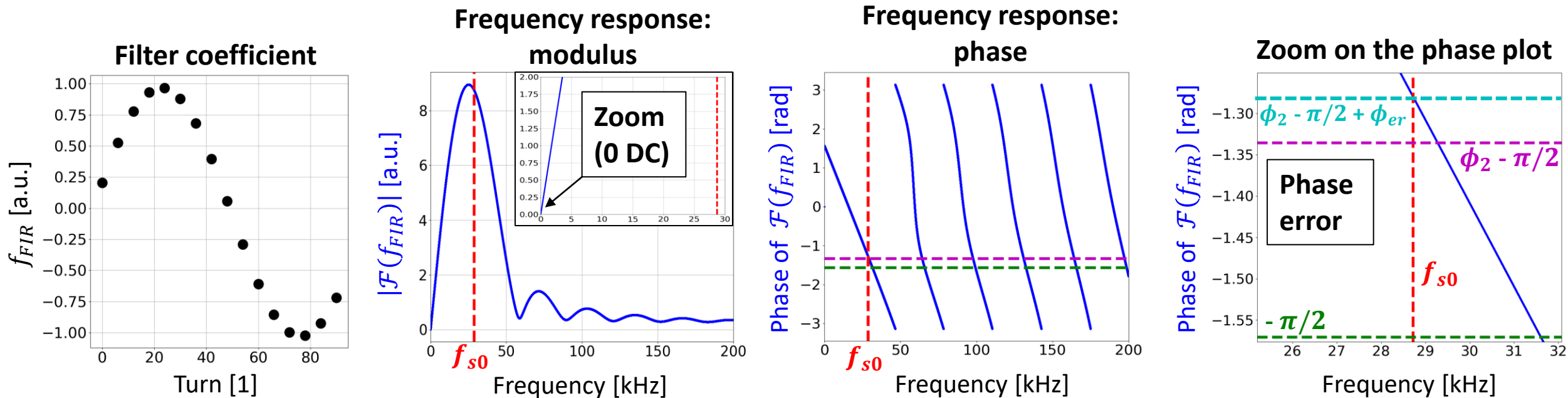
$$n_{oFPGA}(t_k) = g_{FPGA} \sum_{i=0}^{N_{tap}-1} n_{oADC}[t_{k-i}] \left\{ \sin\left[\omega_{s0} i d_{DSF} T_0 + \omega_{s0} T_0 \left(1 + \frac{d_{DSF}}{2}\right)\right] - \frac{1}{N_{tap}} \sum_{j=0}^{N_{tap}-1} f_{FIR,j} \right\}$$

FPGA: down sampling factor (4/5)

❑ There is still one correction to be added to ϕ_2 .

❑ To see this, we compute again the frequency response of the sinusoidal filter.

- This time we take into account the two delays in ϕ_2 and the fact that the samples are taken every d_{DSF} turns.
- Used parameters in this example: T_0 from DAFNE, $f_{s0} = 28.7$ kHz, $d_{DSF} = 6$, $N_{tap} = 16$, $\phi_2 = \omega_{s0} T_0 \left(1 + \frac{d_{DSF}}{2}\right)$.



➤ ϕ_{er} is due to two independent reasons:

- the filter function can't cover exactly one T_{s0} ($|\phi_{er}| > 0$ even if ideally the time step is arbitrarily small);
- the time step is not arbitrarily small ($|\phi_{er}| > 0$ even if ideally one T_{s0} is exactly covered).

FPGA: down sampling factor (5/5)

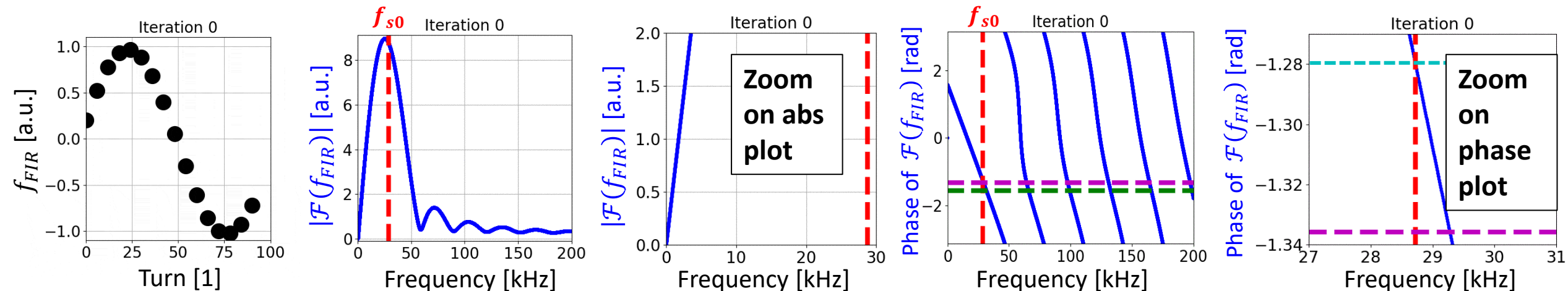
Iterative procedure in the new Python code to compensate for this phase error:

- **Iteration 1:** ϕ_{er} is subtracted from ϕ_2 , i.e. the new ϕ_2 is $\tilde{\phi}_2 = \phi_2 - \phi_{er}$.
 - In this way the phase frequency-response at f_{s0} becomes ϕ_2 as desired.
 - However, since the time step is not arbitrarily small, changing ϕ_2 leads to a non-zero DC component.
- **Iteration 2:** the average of the filter coefficients is subtracted from the coefficients themselves.
 - In this way the DC component is zero.
 - However, this subtraction changes the phase frequency-response at f_{s0} which is not ϕ_2 anymore.
- **Iteration 3:** the new ϕ'_{er} is subtracted from $\tilde{\phi}_2$, i.e. the new ϕ_2 is $\tilde{\phi}_2 = \phi_2 - \phi_{er} - \phi'_{er}$.
- **Iteration 4:** ...

The iterations repeat until the filter has zero DC component and the phase frequency-response at f_{s0} is sufficiently close to ϕ_2 .

➤ Usually few iterations are needed to reach convergence.

- In our example 10 iterations diminish the phase error from $5.6 \cdot 10^{-2}$ rad to $1.3 \cdot 10^{-5}$.



DAC processing and ideal voltage

- The DAC (digital-to-analog converter) converts the digital output of the FPGA into analog values.
 - The inputs of the DAC must be integers between $-(2^{n_{bit,DAC}-1} - 1)$ and $2^{n_{bit,DAC}-1}$, where $n_{bit,DAC}$ is the number of bit for the DAC (in DAFNE $n_{bit,DAC} = 8$).
 - As a function of time, the output of the DAC is a continuous piecewise-constant function.
 - The discontinuities are located in correspondence of the bunch arrival-times when the feedback operates, i.e. those times which are multiple of $d_{DSF}T_0$.
- If $V_{MAXkick}$ represents the maximum voltage which the cavity-kicker can provide to the bunch, then the analog values given by the DAC represent the fractions of $V_{MAXkick}$ which the cavity-kicker should provide to the bunch to damp its oscillations.
 - The feedback provides the values of the requested voltages, whereas the actual voltages are produced by the cavity kicker and its generator.
 - We denote the voltage values requested by the feedback with V_{FBkick} .
 - As shown later, these values are ideal since the bunch can see in reality only approximations of them.
- The output of the DAC and V_{FBkick} are given by

$$n_{oDAC} = \frac{\text{int}(g_{DAC}n_{oFPGA})}{2^{n_{bit,DAC}-1}} \quad V_{FBkick} = n_{oDAC}V_{MAXkick}$$

- where g_{DAC} is the gain of the DAC and the operator $\text{int}()$ takes the integer part of $g_{DAC}n_{oFPGA}$;
- if $\text{int}(g_{DAC}n_{oFPGA}) > 2^{n_{bit,DAC}-1}$, then $n_{oDAC} = 1$;
- if $\text{int}(g_{DAC}n_{oFPGA}) < -(2^{n_{bit,DAC}-1} - 1)$, then $n_{oDAC} = -1 + 1/2^{n_{bit,DAC}-1}$.

Equations of motion in the code: RF+SR+HOM+FB (simplified)

□ If we assume that the cavity-kicker can provide exactly the voltage requested by the feedback, the equations of motion are

$$\Delta\varphi_k^{(n+1)} = \Delta\varphi_k^{(n)} + 2\pi h\alpha_0\delta_k^{(n)}$$

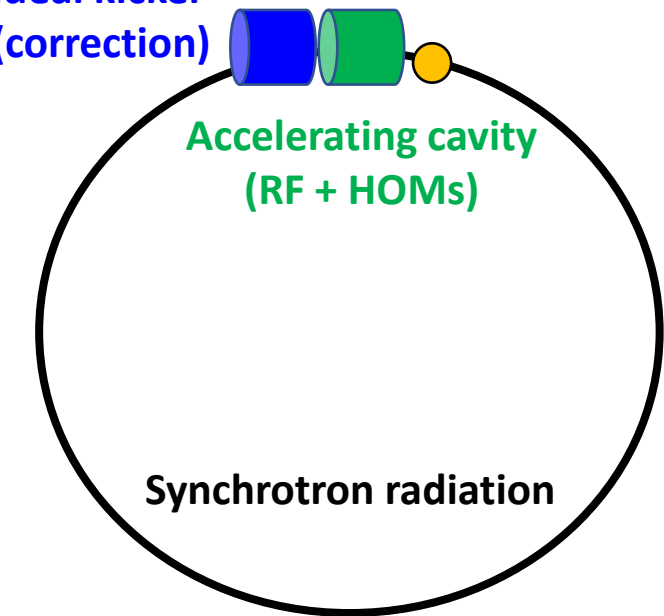
$$\delta_k^{(n+1)} = \delta_k^{(n)} - \frac{U_0}{E_0} (1 + 2\delta_k^{(n)}) + \frac{eV_{FBkick,k}^{(n)}}{E_0} + \frac{e\hat{V}_{rf} \cos \Delta\varphi_k^{(n+1)}}{E_0} + \frac{e}{E_0} \sum_{j=1}^{N_{HOM}} [V_{k,j,RES}^{(n+1)} + V_{k,j,IND}]$$

- where $V_{FBkick,k}^{(n)}$ is the voltage provided by the kicker to the bunch k at turn $(n + 1)$.
 - $V_{FBkick,k}^{(n)}$ usually changes from bunch to bunch and, for a given bunch, changes every $d_{DSF}T_0$ turns.
 - If for instance $d_{DSF} = 1$, then $V_{FBkick,k}^{(n)}$ is evaluated using $\Delta\varphi_k^{(n)}$ and not $\Delta\varphi_k^{(n+1)}$ since the feedback-kicker system acts with a delay of one turn.

Ideal kicker
(correction)

Accelerating cavity
(RF + HOMs)

Synchrotron radiation



- The equations of motion assume that the two cavities are point-like and placed at the same spot in the ring. The bunch starts at the exit of the accelerating cavity and in order
- drifts along the ring (first equation of motion);
 - loses energy by synchrotron radiation;
 - receives the energy-kick from the cavity-kicker;
 - receives the energy-kicks (accelerating and HOM-induced) from the accelerating cavity.

- Small bug in the Fortran code: the kicker voltage applied to the last bunch is wrong if the first bucket is empty.

Small amplitude synchrotron frequency with SR and FB (1/3)

□ We neglect collective effects and we assume that

- $d_{DSF} = 1$;
- the feedback-kicker system acts with no delay;
- T_0 is small relative to T_{s0} .

□ The discrete equations of motion can be made continuous as

$$\Delta\dot{\varphi} = \omega_{rf}\alpha_0\delta \qquad \dot{\delta} = -\frac{U_0}{E_0T_0}(1+2\delta) + \frac{eV_{FBkick}(\Delta\varphi)}{E_0T_0} + \frac{e\hat{V}_{rf}}{E_0T_0}\cos\Delta\varphi$$

□ Deriving again with respect to time

$$\Delta\ddot{\varphi} = -\frac{\omega_{rf}\alpha_0U_0}{E_0T_0}(1+2\delta) + \frac{\omega_{rf}\alpha_0eV_{FBkick}(\Delta\varphi)}{E_0T_0} + \frac{\omega_{rf}\alpha_0e\hat{V}_{rf}}{E_0T_0}\cos\Delta\varphi$$

□ Expanding around $\Delta\varphi_{SR}$ we have

$$\ddot{\varphi}_0 = -\frac{\omega_{rf}\alpha_0U_0}{E_0T_0}\left(1+2\frac{\dot{\varphi}_0}{\omega_{rf}\alpha_0}\right) + \frac{\omega_{rf}\alpha_0eV_{FBkick}(\varphi_0)}{E_0T_0} + \frac{\omega_{rf}\alpha_0e\hat{V}_{rf}}{E_0T_0}(\cos\Delta\varphi_{SR} - \sin\Delta\varphi_{SR}\varphi_0)$$

Small amplitude synchrotron frequency with SR and FB (2/3)

□ Simplifying and rearranging the terms we obtain

$$\ddot{\varphi}_0 + \frac{2U_0}{E_0 T_0} \dot{\varphi}_0 - \frac{\omega_{rf} \alpha_0 e V_{FBkick}(\varphi_0)}{E_0 T_0} + \frac{\omega_{rf} \alpha_0 e \hat{V}_{rf}}{E_0 T_0} \sin \Delta\varphi_{SR} \varphi_0 = 0$$

□ We assume that the feedback shifts φ_0 by $-\pi/2$ as desired.

- This requires that no saturation has to occur in the feedback, i.e.
 - The input of the ADC is always in the range $[-V_{max,ADC}, V_{max,ADC}]$.
 - The input of the DAC is always in the range $[-(2^{n_{bit,DAC}} - 1), 2^{n_{bit,DAC}} - 1]$.
- Grouping all the feedback gains in one expression, we have

$$\varphi_0(t) = A \sin(\omega_{s0} t + \phi_1)$$



Phase detection

ADC

FPGA

DAC

Kicker max
voltage

$$V_{FBkick}(t) = -A \frac{Q_b}{T_0} |Z_b| g_m g_p g_c g_a g_l g_{a2} \frac{2^{n_{bit,ADC}} - 1}{2V_{max,ADC}} \frac{g_{FPGA} T_{s0}}{2T_0} \frac{g_{DAC}}{2^{n_{bit,DAC}} - 1} V_{MAXkick} \cos(\omega_{s0} t + \phi_1) = -\frac{1}{\omega_{s0}} g_{FBtot} \dot{\varphi}_0(t)$$

- where $g_{FBtot} > 0$ is the total gain of the feedback in volt units

$$g_{FBtot} = \frac{Q_b}{T_0} |Z_b| g_m g_p g_c g_a g_l g_{a2} \frac{2^{n_{bit,ADC}} - 1}{2V_{max,ADC}} \frac{g_{FPGA} T_{s0}}{2T_0} \frac{g_{DAC}}{2^{n_{bit,DAC}} - 1} V_{MAXkick}$$

- **Note 1:** although A should have rad units, in this case A is dimensionless since φ_0 derives from $\sin(\varphi_0) \approx \varphi_0$
- **Note 2:** if $d_{DSF} > 1$ then, at least in first approximation, the FPGA term should be divided by d_{DSF} ($\Delta t_{DSF} = d_{DSF} T_0$ in the convolution)

Small amplitude synchrotron frequency with SR and FB (3/3)

□ The differential equation becomes

$$\ddot{\varphi}_0 + \left(\frac{2U_0}{E_0 T_0} + \frac{\omega_{rf} \alpha_0 e g_{FBtot}}{E_0 T_0 \omega_{s0}} \right) \dot{\varphi}_0 + \frac{\omega_{rf} \alpha_0 e \hat{V}_{rf} \sin \Delta\varphi_{SR}}{E_0 T_0} \varphi_0 = 0$$

□ As expected, the feedback affects the damping-rate of the bunch oscillations. This rate becomes

$$\alpha_{r,SRFB} = \alpha_{r,SR} + \alpha_{r,FB} = \frac{U_0}{E_0 T_0} + \frac{\pi h f_0^2 \alpha_0 e g_{FBtot}}{E_0 \omega_{s0}}$$

□ On the contrary, the feedback doesn't affect the frequency of the oscillations

$$\omega_{s0,SRFB} = \omega_{s0,SR}$$

□ The solution of the differential equation is

$$\varphi_0(t) = A e^{-\alpha_{r,SRFB} t} \cos(\omega_{s0,SR} t + B)$$

□ If, for instance, $\varphi_0(0) = 0$ and $\delta(0) = \hat{\delta}$ then

$$\varphi_0(t) = \frac{\omega_{rf} \alpha_0 \hat{\delta}}{\omega_{s0,SR}} e^{-\alpha_{r,SRFB} t} \sin(\omega_{s0,SR} t)$$

FPGA: DAFNE example (1/5)

□ Assuming $U_0 = 8.88$ keV, $E_0 = 510$ MeV, $\hat{V}_{rf} = 130$ kV and $\alpha_0 = 0.018$, then $1/Q_s = 106.95$.

□ In DAFNE d_{DSF} can vary from 1 to 32, whereas N_{tap} can vary from 1 to 16.

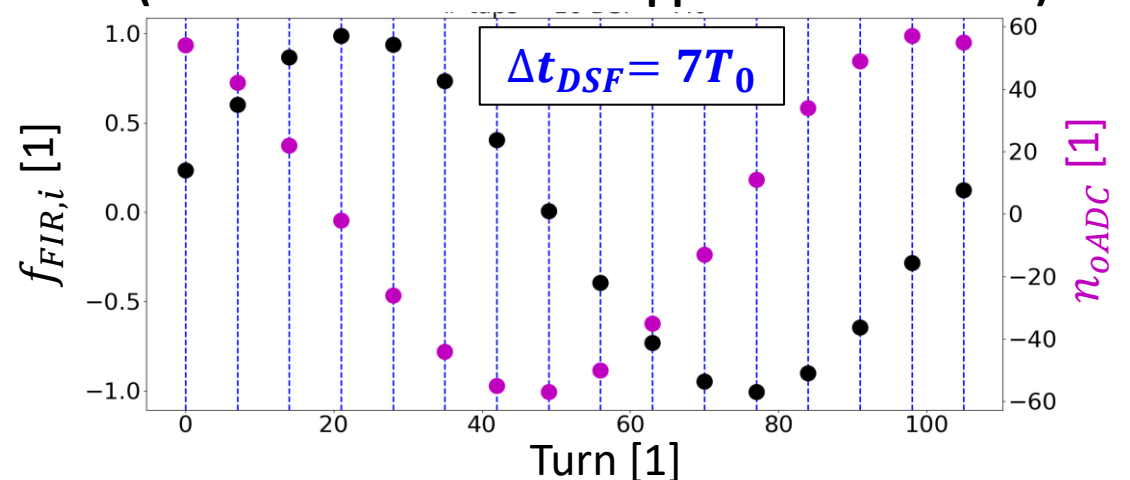
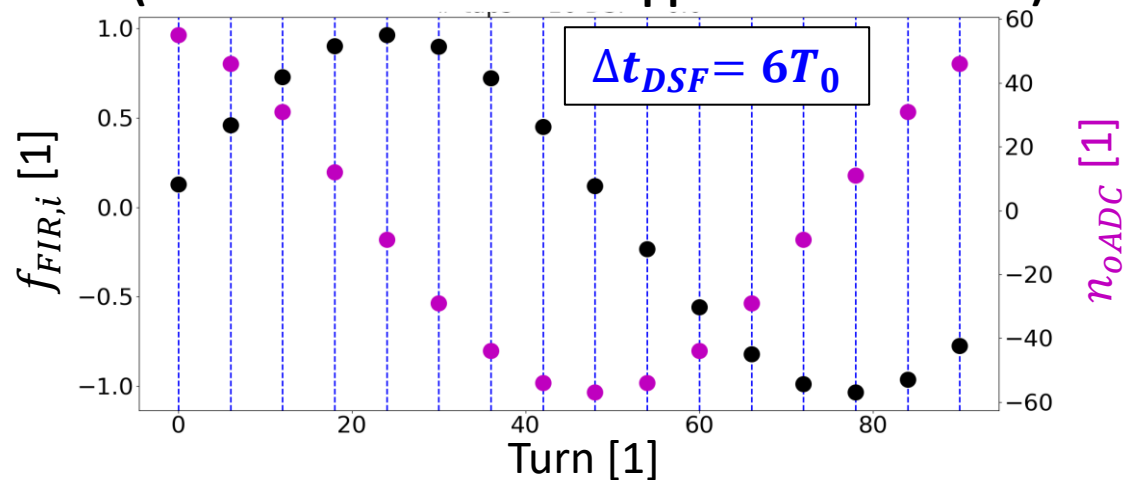
➤ We assume that the maximum number of taps is used, i.e. $N_{tap} = 16$.

➤ In principle the optimal d_{DSF} can be either 6 or 7 since $d_{DSF} = 1/(N_{tap}Q_s) = 6.68$.

□ We do single-bunch simulations without intensity effects to find which d_{DSF} leads to the most efficient feedback-response.

➤ At turn 0 the bunch-phase is displaced by 0.1 rad with respect to $\Delta\phi_{SR}$. 100000 turns are simulated.

$d_{DSF} = 6$: filter with $N_{tap} = 16$ and first 16 samples of n_{oADC} (no feedback-correction applied to the bunch) $d_{DSF} = 7$: filter with $N_{tap} = 16$ and first 16 samples of n_{oADC} (no feedback-correction applied to the bunch)

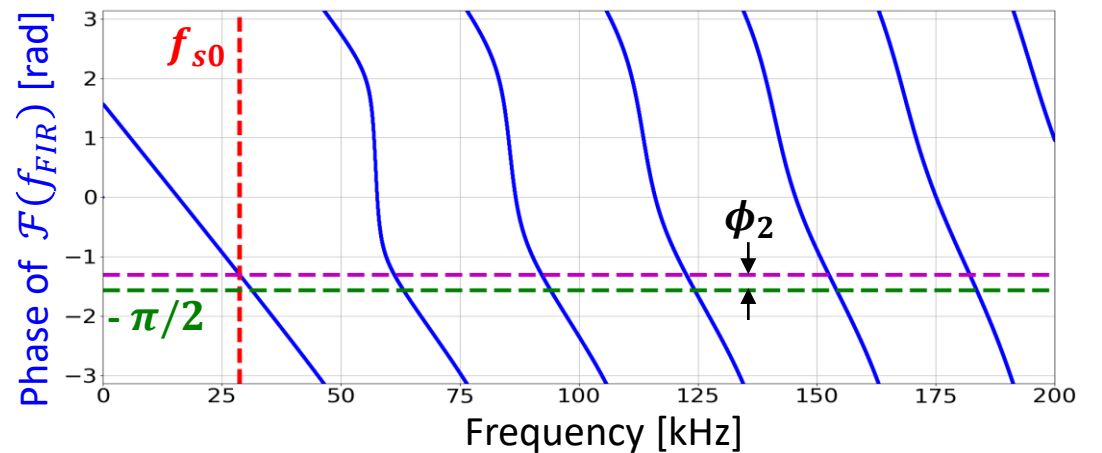
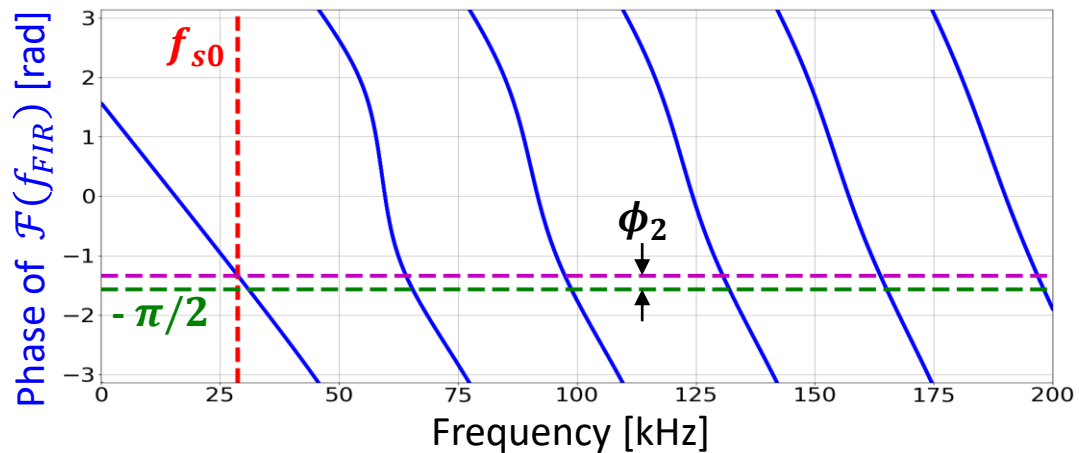
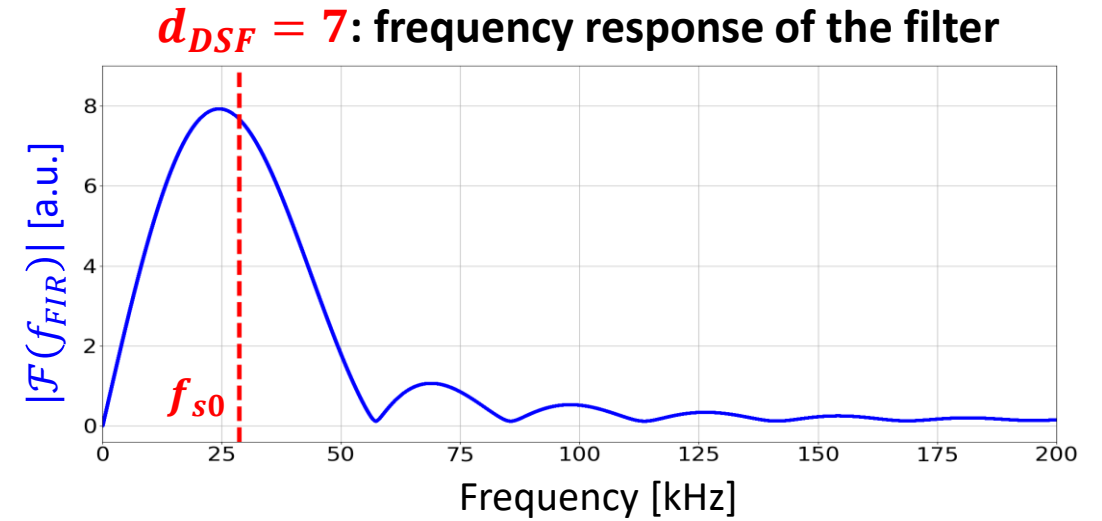
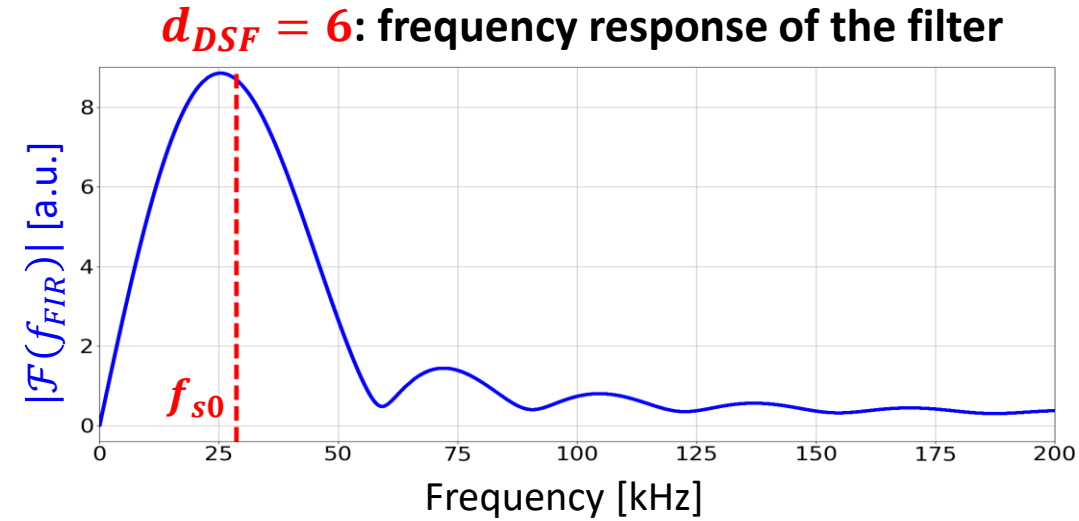


➤ When $d_{DSF} = 6$, then n_{oADC} and $f_{FIR,i}$ cover less than one synchrotron period ($N_{tap}d_{DSF} = 96 < 1/Q_s$).

➤ When $d_{DSF} = 7$, then n_{oADC} and $f_{FIR,i}$ cover more than one synchrotron period ($N_{tap}d_{DSF} = 112 > 1/Q_s$).

FPGA: DAFNE example (2/5)

- We compare the frequency-response of the filter when $d_{DSF} = 6$ and $d_{DSF} = 7$.

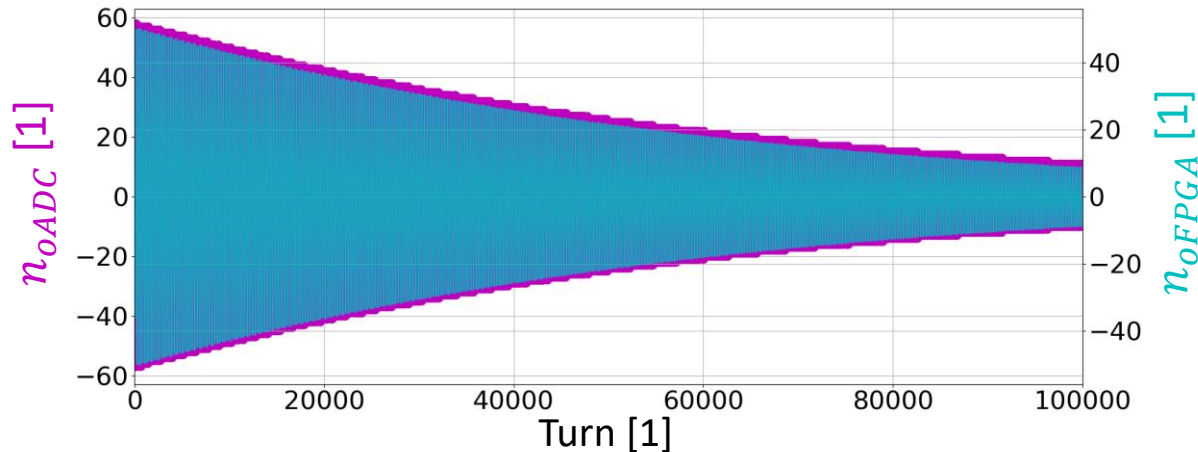


- $\phi_2 = \omega_{s0}T_0(1+d_{DSF}/2)$ is equal to 0.235 rad when $d_{DSF} = 6$, 0.264 rad when $d_{DSF} = 7$.
- The modulus frequency-response around f_{s0} is lower when $d_{DSF} = 7$.

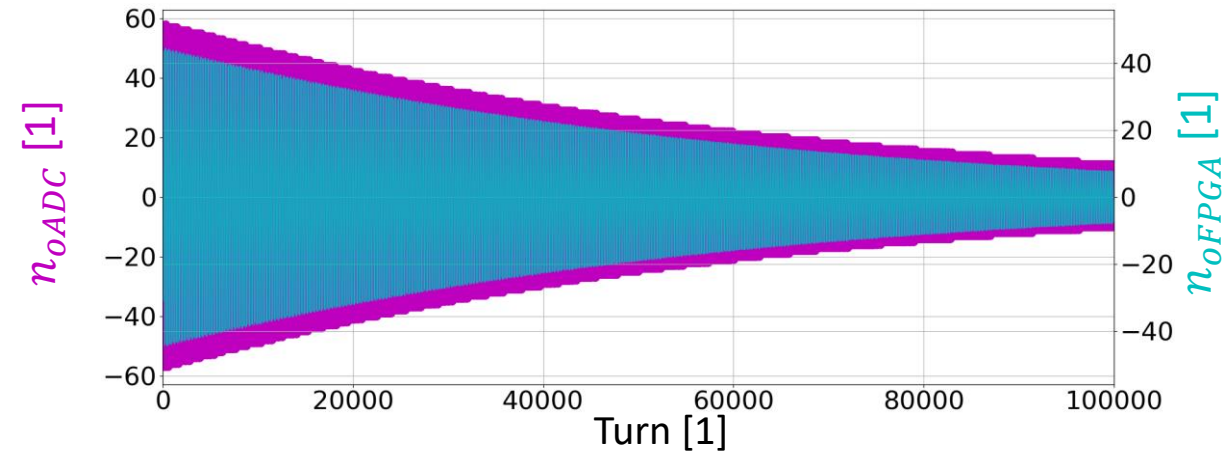
FPGA: DAFNE example (3/5)

- We analyse the evolution of n_{oADC} and n_{oFPGA} without applying the feedback-correction to the bunch.
 - The linear interpolations between consecutive points are plotted only to facilitate the visualization.
 - The decay of the oscillations is due to synchrotron radiation.

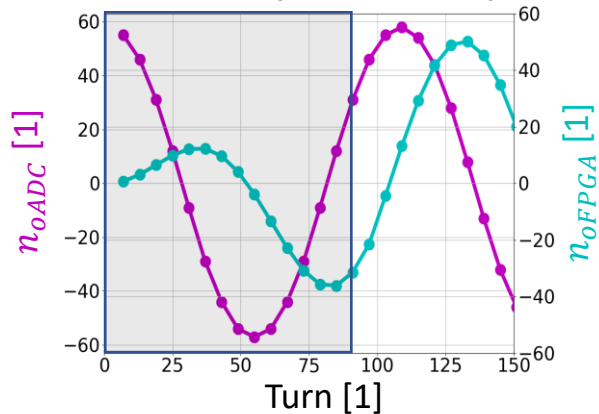
$d_{DSF} = 6: n_{oADC}$ and n_{oFPGA}



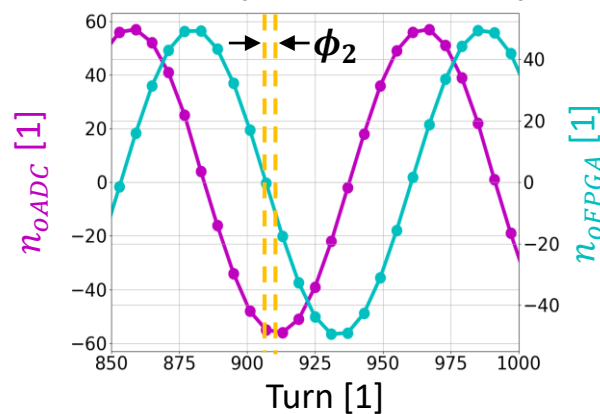
$d_{DSF} = 7: n_{oADC}$ and n_{oFPGA}



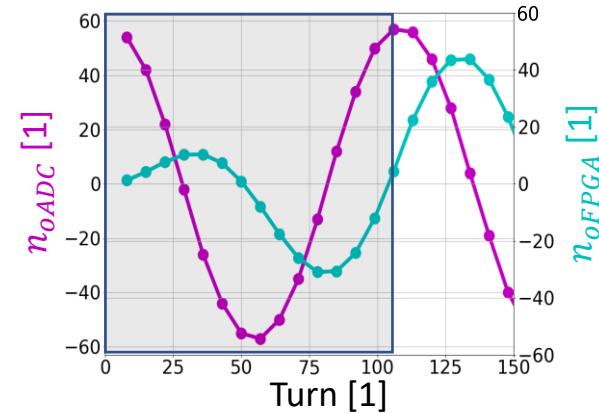
Zoom 1 (0-150 turns)



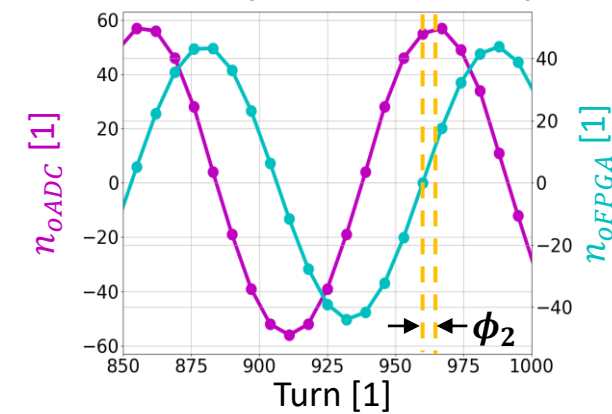
Zoom 2 (850-1000 turns)



Zoom 1 (0-150 turns)



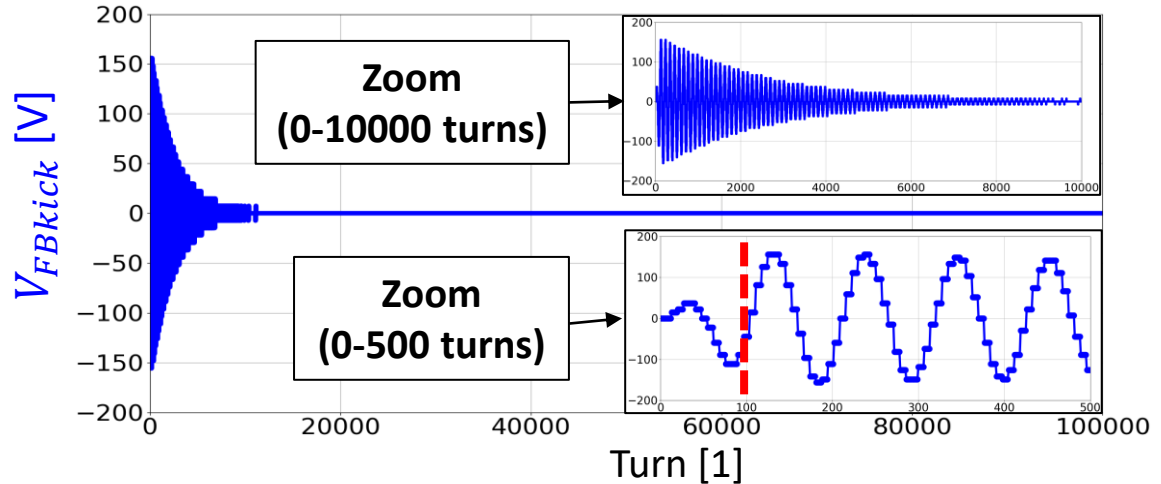
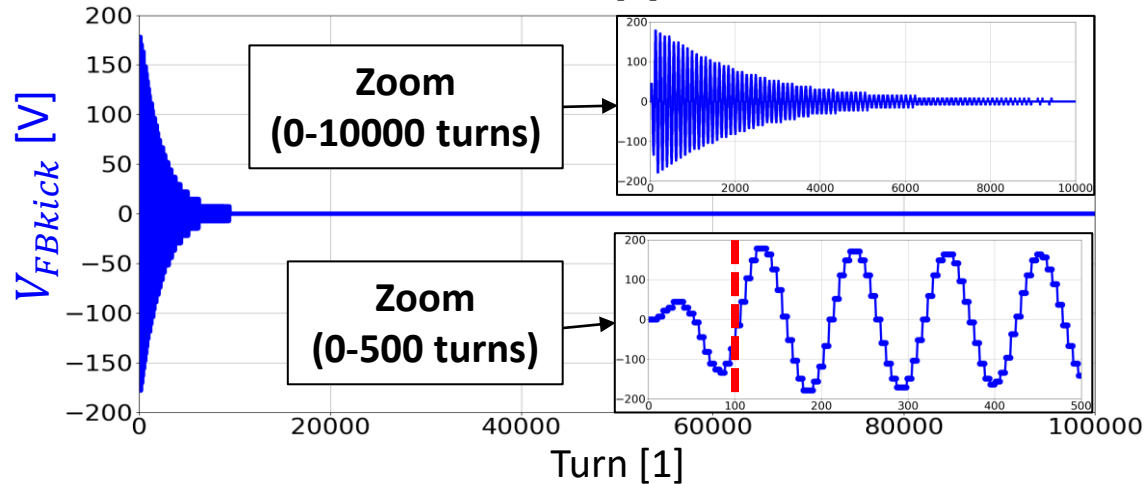
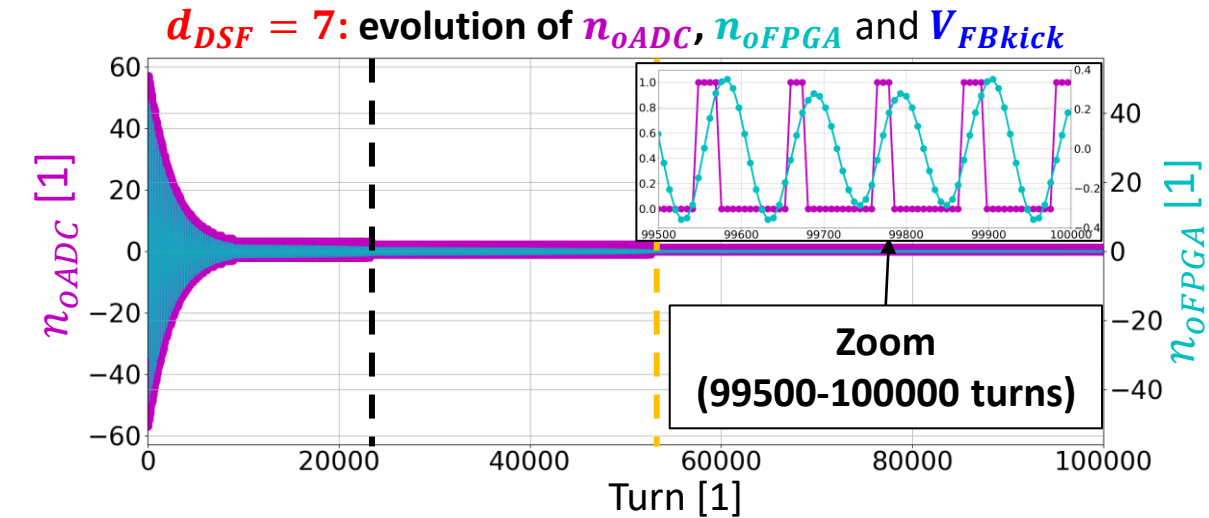
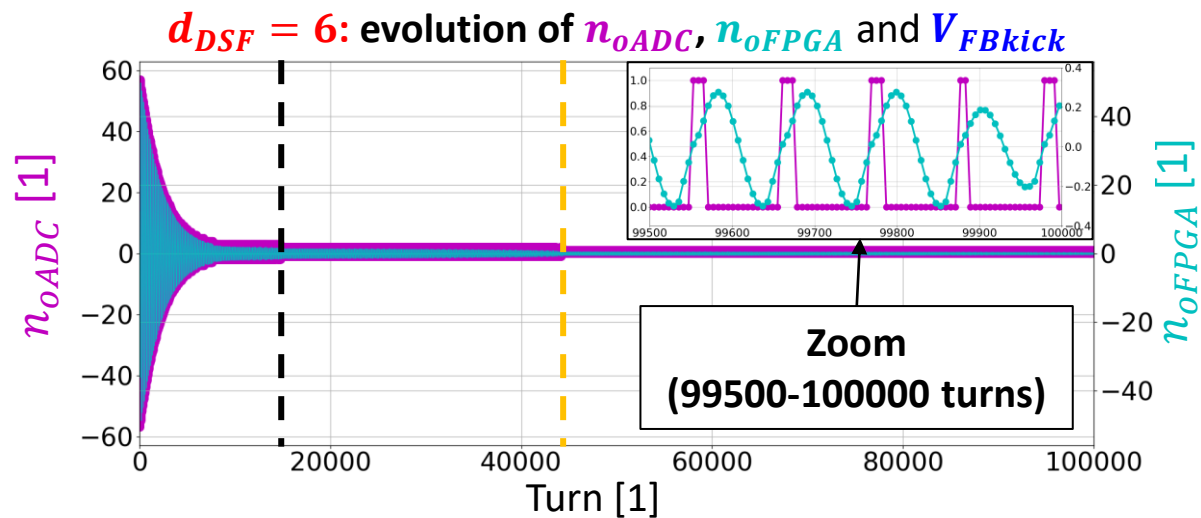
Zoom 2 (850-1000 turns)



- The shaded regions cover the first $N_{tap} - 1 = 15$ samples of n_{oADC} . Here n_{oFPGA} is in transient regime (hold-buffer not full yet).
- The n_{oFPGA} amplitude is lower when $d_{DSF} = 7$. This is due to the lower modulus of the frequency-response around f_{s0} .

FPGA: DAFNE example (4/5)

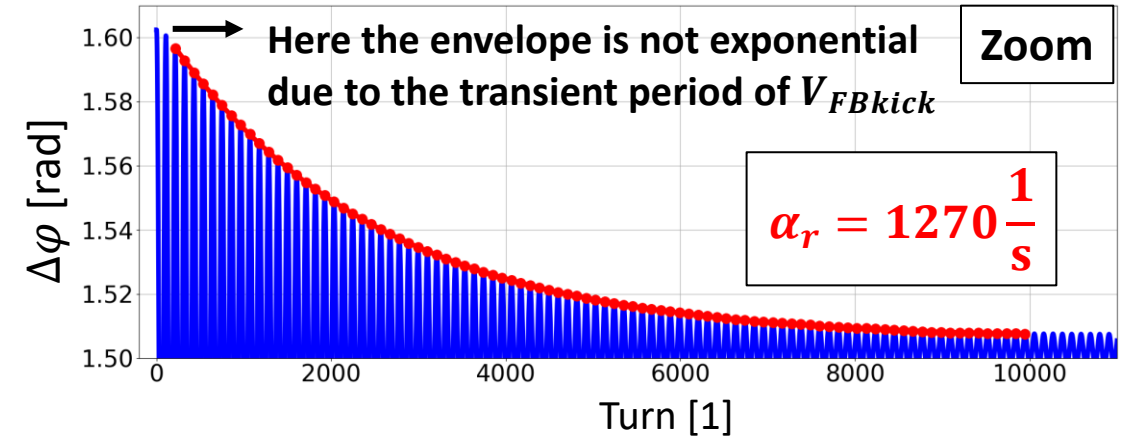
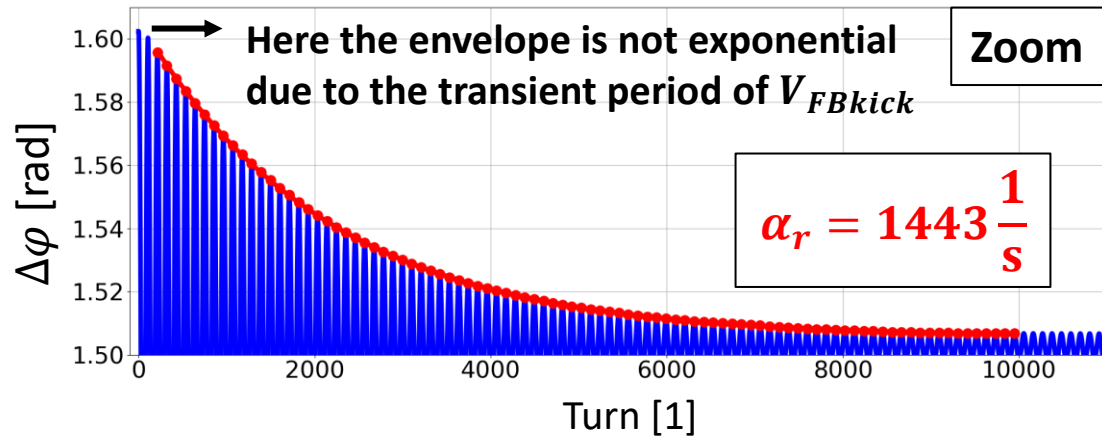
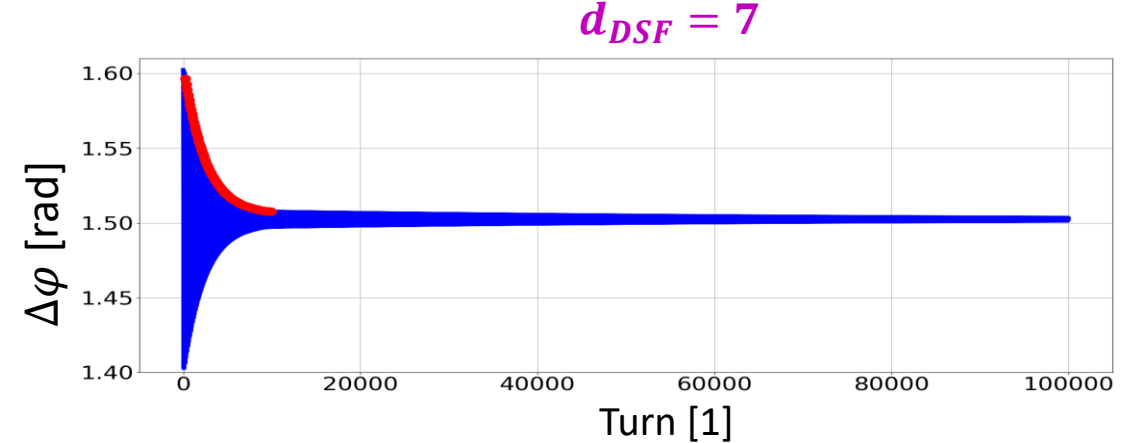
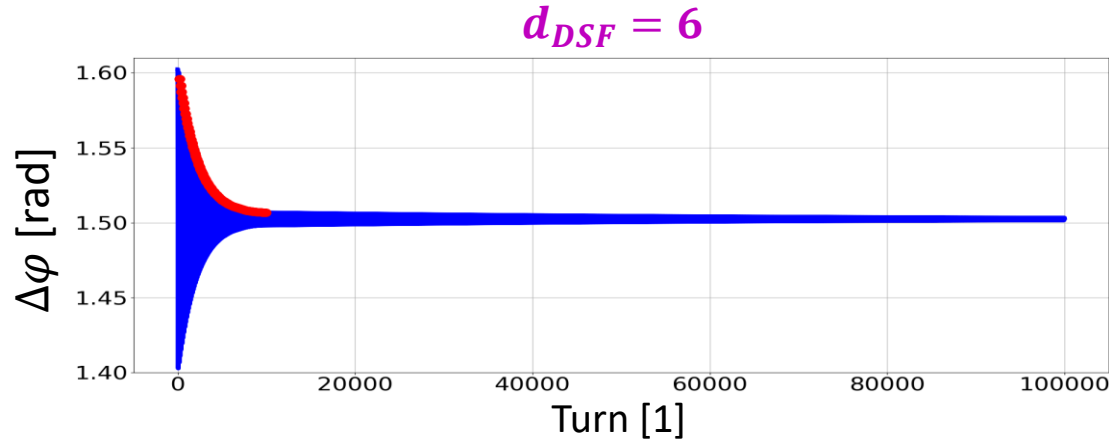
□ We analyse the evolution of n_{oADC} , n_{oFPGA} and V_{FBkick} when the feedback-correction is applied to the bunch.



- When $d_{DSF} = 6$, faster exponential decay of n_{oADC} (black and orange dashed lines) due to the larger amplitude of n_{oFPGA} and V_{FBkick} .
- At the end of the simulations, n_{oADC} takes 0 and 1 values, whereas n_{oFPGA} is sinusoidal like with $|n_{oFPGA}| < 0.4$.
- In this example $g_{DAC} = 0.5$, therefore $V_{FBkick} = 0$ if $|n_{oFPGA}| < 2$, and this occurs after about 10000 turns.
- There is a transient period of about 100 turns for V_{FBkick} .

FPGA: DAFNE example (5/5)

- We analyse the evolution of the bunch-phase $\Delta\phi$ when the feedback-correction is applied to the bunch.



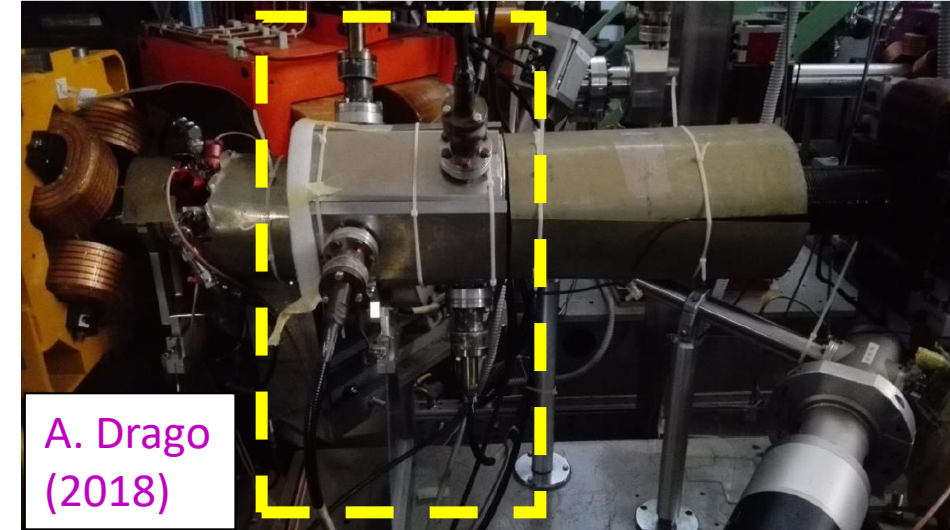
- The simulated damping-rates are $\alpha_r = 1443 \text{ 1/s}$ if $d_{DSF} = 6$, $\alpha_r = 1270 \text{ 1/s}$ if $d_{DSF} = 7$.
- The analytical damping-rates are $\alpha_{r,SRFB} = 1473 \text{ 1/s}$ if $d_{DSF} = 6$, $\alpha_{r,SRFB} = 1270 \text{ 1/s}$ if $d_{DSF} = 7$ (good agreements with simulations).
 - The analytical damping-rate assuming $d_{DSF} = 1$ is $\alpha_{r,SRFB} = 8569 \text{ 1/s}$ ($\alpha_{r,SR} = 53 \text{ 1/s}$, $\alpha_{r,FB} = 8516 \text{ 1/s}$).

- This example shows that $d_{DSF} = 6$ should be preferred to $d_{DSF} = 7$ (an equal α_r is obtained by increasing g_{DAC} by 14% when $d_{DSF} = 7$).

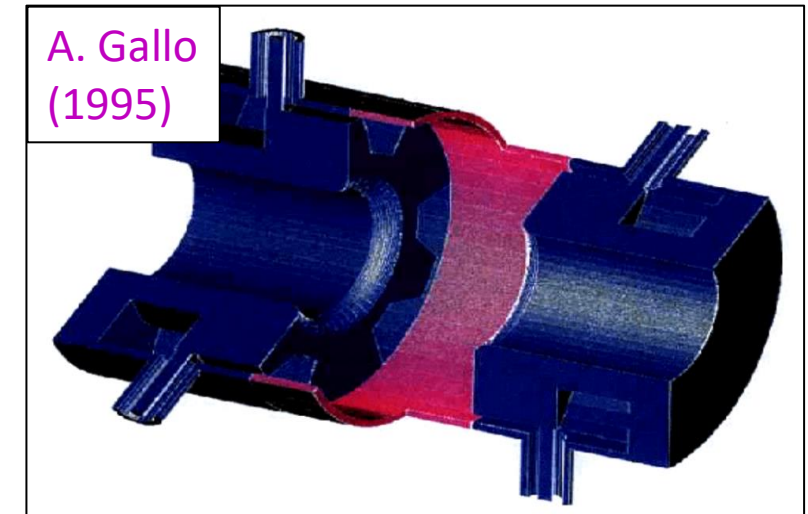
Cavity kicker in DAFNE: introduction

- ❑ The active element of the longitudinal feedback-system is the cavity-kicker.
 - One kicker per DAFNE ring.
- ❑ The kicker is a special 'overdamped' pill-box cavity:
 - The pill-box cavity is 72 mm long and has a diameter of 200 mm (the diameter of the beam-pipe is 88 mm).
- ❑ A large bandwidth is obtained by loading the pill-box cavity with 6 ridged waveguides followed by broadband transitions to standard coaxial cables.
 - The 6 waveguides are placed symmetrically on the pill box, 120° apart from each other.
- ❑ 3 waveguides (ports) are used to inject power into the kicker, the other 3 are terminated onto 50 Ω termination loads.
 - Thanks to the symmetry of the waveguides and the fact that the power dissipated on the loads is much larger than the one dissipated on the cavity walls, the system is in theory perfectly matched at the resonant frequency (zero reflected power by the input ports).
- ❑ There is no need to tune the kicker in operation due to the large bandwidth and no need to cool the kicker since most of the power is dissipated on the loads.
- ❑ The strong waveguide-coupling leads also, as a by-product, to a significant damping of all the kicker HOMs.

Cavity kicker for the DAFNE positron ring



CAD view of the cavity kicker



Kicker parameters (1/3)

□ The kicker must be able to damp the coupled-bunch instabilities due to the HOMs (mostly those of the accelerating RF system).

□ It was shown that, in the presence of coupled-bunch instabilities, the beam-spectrum lines which can be excited are situated at

$$f_{l,m,\mu} = (lN_b - m\mu)f_0 - mf_{s,HOM}$$

➤ where $l \in (-\infty, +\infty)$, $m \in (-\infty, +\infty)$ is the oscillation mode and $\mu = 0, \dots, N_b$ is the coupled-bunch mode.

□ We suppose that the machine is full, i.e. $N_b = h$, and that $m = 1$, since the dipolar mode is usually the most critical for coupled-bunch instabilities. This leads to

$$f_{l,\mu} = lf_{rf} - \mu f_0 - f_{s,HOM}$$

➤ with $f_{s,HOM} \ll f_0$ (in DAFNE they differ by about factor 100).

□ To be able to damp every coupled-bunch mode, it is sufficient that the kicker bandwidth covers for each $\bar{\mu}$ at least one line $f_{l,\bar{\mu}}$.

➤ We want to find the minimum bandwidth able to do this: larger bandwidths would unnecessarily lower the kicker shunt impedance and this, as shown later, would decrease the available kicker-voltage for a given amplifier power.

□ Neglecting in the analysis $f_{s,HOM}$ which is relatively small, and considering that l can be positive and negative, it can be easily verified that the minimum required bandwidth $\Delta f_{BW,min}$ is

$$\Delta f_{BW,min} = \frac{f_{rf}}{2}$$

➤ as long as the resonant frequency is placed at

$$0.25 f_{rf} \quad \text{or} \quad (p \pm 0.25)f_{rf} \quad p \geq 1$$

Kicker parameters (2/3)

- In DAFNE the following resonant frequency was chosen

$$f_r = 3.25f_{rf} = 1198 \text{ MHz}$$

- Since the pillbox cavity is operated in the TM_{010} fundamental mode, the diameter of the pill box cavity can be estimated as

$$d_{pillbox} = \frac{2.405c}{\pi f_r} \approx 200 \text{ mm}$$

- The constraints on the kicker bandwidth Δf_{BW} and the quality factor Q are given by

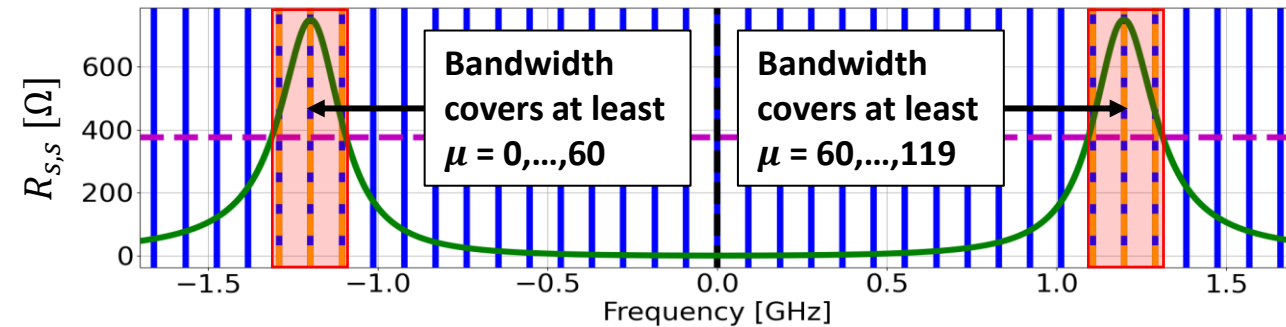
$$\Delta f_{BW} > \Delta f_{BW,min} = \frac{f_{rf}}{2} = 184 \text{ MHz} \quad Q < \frac{f_r}{\Delta f_{BW,min}} = 6.5$$

- In DAFNE the measured and simulated kicker bandwidth and quality factor are

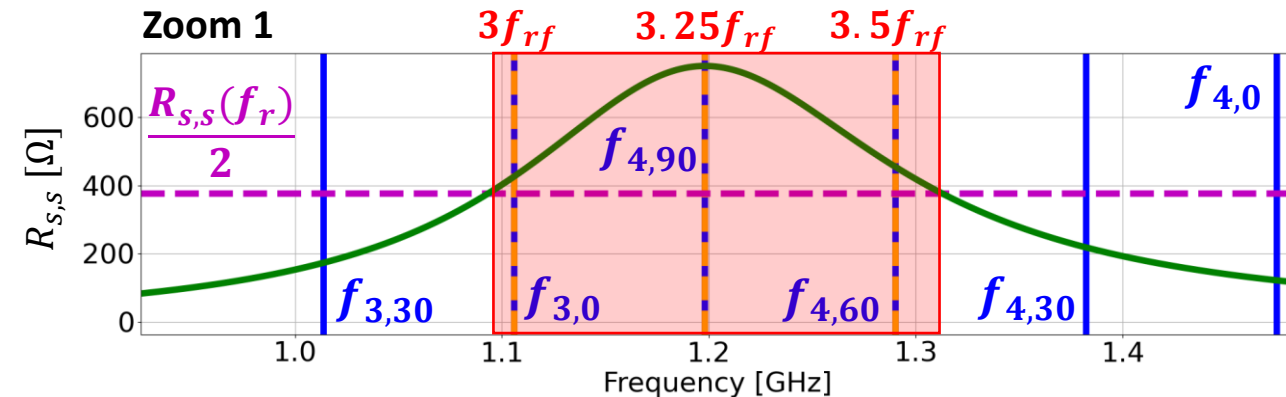
$$\Delta f_{BW} \approx 220 \text{ MHz} \quad Q \approx 5.4$$

- Since each waveguide covers 11% of the available cavity surface, the number of waveguides could be increased to 8 leading to a larger bandwidth.
 - This was not done since the constraints are already satisfied (with some margin) using 6 waveguides.

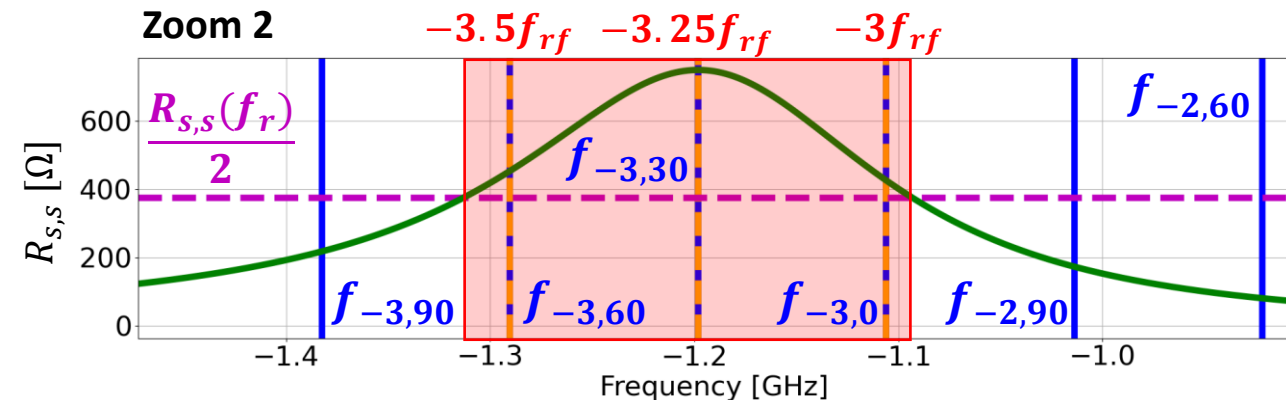
Kicker shunt-impedance reproduced in simulation with some spectrum lines (see next slide for the definition of $R_{s,s}$), $f_{s,HOM} = 30 \text{ kHz}$



Zoom 1



Zoom 2



Kicker parameters (3/3)

- The frequency-dependent kicker shunt-impedance $R_{s,s}(f)$ is defined as

$$R_{s,s}(f) = \frac{|V_g(f)|^2}{2P_{fw}} = \frac{1}{2P_{fw}} \left| \int_{-\frac{L}{2}}^{\frac{L}{2}} E_z(z) e^{j[2\pi f \frac{z}{c} - \phi_z(z)]} dz \right|^2$$

- where V_g , P_{fw} and L are respectively the kicker gap-voltage phasor, the forward-power at the kicker input and the gap length;
- where E_z and ϕ_z are respectively the amplitude and phase of the longitudinal electric-field evaluated on the beam axis and expressed as a phasor:

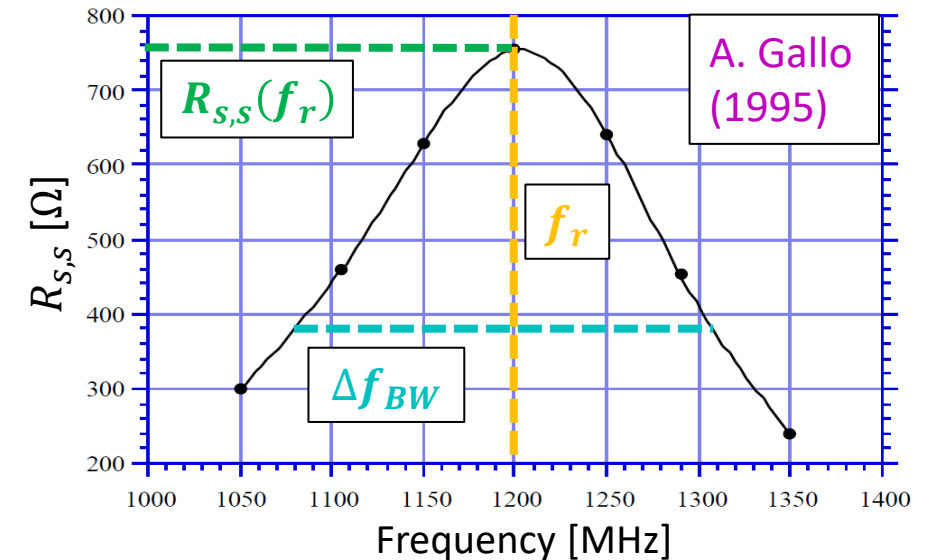
$$E_z(z, t) = \text{Re}\{E_z(z) e^{j[2\pi f t - \phi_z(z)]}\}$$

- $R_{s,s}(f)$ was computed by integrating on the beam-axis the E -field distribution given by a 3D electromagnetic simulation of the kicker.

- Simulations, and also measurement, showed that $R_{s,s}(f_r) \approx 750 \Omega$.
 - The maximum power provided by the kicker amplifiers is 600 W.
 - One 200 W power-amplifier for each input-waveguide.
 - The available gap-voltage when the kicker-generator works at f_r is

$$V_{MAXkick} = |V_g(f_r)| = \sqrt{2P_{fw}R_{s,s}(f_r)} \approx 950 \text{ V}$$

Shunt-impedance obtained from an electromagnetic simulation of the kicker model



- It turns out that $R_{s,s}(f) = 2 \text{ Re}[Z(f)]$, where Z is the beam-coupling impedance of the kicker.
 - The kicker, in addition to providing the voltage-correction to each bunch, contributes as a resonant impedance with parameters

$$f_r = 3.25 f_{rf} \quad Q = 5.4 \quad R_s = R_{s,s}(f_r)/2 = 375 \Omega$$
 - This impedance, not included in the Fortran code, was added in the new Python code.

Kicker coupling-impedance in the code (1/3)

- As shown, the HOMs shunt-impedances were rescaled by an exponential factor to consider the Gaussian profile of the bunches.
 - We show now that this technique can't be properly used for the kicker fundamental-mode due to its relatively small Q .
- We consider the parameters of the kicker fundamental-mode $f_r = 3.25f_{rf}$, $Q = 5.4$, $R_s = 375 \Omega$ and a Gaussian profile of rms σ_t .

- The kicker wake-potential induced by the Gaussian profile at distance $z = ct$ from its centre can be computed analytically as

$$W_1(t) = -R_s \frac{\Gamma}{\omega_n} e^{\left[\frac{1}{2}(\Gamma^2 - \omega_n^2)\sigma_t^2 - \Gamma t\right]} \left\{ \text{Re}[\text{erfc}(A)](\omega_n \cos B + \Gamma \sin B) + \text{Im}[\text{erfc}(A)](\Gamma \cos B - \omega_n \sin B) \right\} \quad t \in (-\infty, +\infty)$$

- where erfc is the complementary error function and

$$\Gamma = \frac{\omega_r}{2Q} \approx \frac{\omega_r}{11} \quad \omega_n = \sqrt{\omega_r^2 - \Gamma^2} \approx \omega_r \quad A = \frac{\Gamma\sigma_t^2 - t + j\omega_n\sigma_t^2}{\sqrt{2}\sigma_t} \quad B = \Gamma\omega_n\sigma_t^2 - \omega_n t$$

- This formula is obtained through profile and wake-function convolution using algebraic routines from the Mathematica software.
- This formula is valid for every resonator impedance.
 - A plot of W_1 has already been shown to verify that the HOM shunt-impedance rescaling was possible.

- As concerns the kicker impedance, we want to compare W_1 with two rescaled wake-functions:

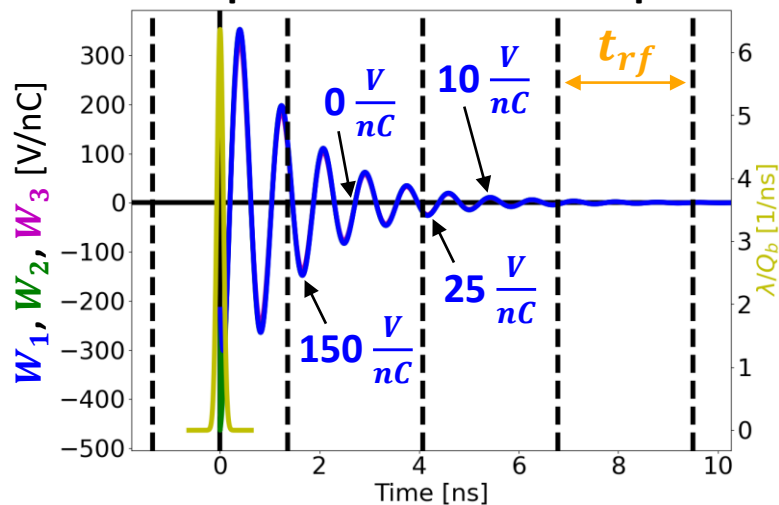
- W_2 : the rescaling is done by using the exponential factor already adopted for the HOMs;
- W_3 : the rescaling factor is such that $W_3(0) = W_1(0)$.

$$W_2(t) = e^{-\frac{\omega_r^2\sigma_t^2}{2}} w_{\parallel}(t) \quad W_3(t) = \frac{W_1(0)}{w_{\parallel}(0)} w_{\parallel}(t) \quad \text{where} \quad w_{\parallel}(t) = -[\text{sgn}(t) + 1] \frac{R_s\omega_r}{2Q} e^{-\frac{\omega_r t}{2Q}} \left[\cos(\omega_n t) - \frac{\omega_r}{2Q\omega_n} \sin(\omega_n t) \right]$$

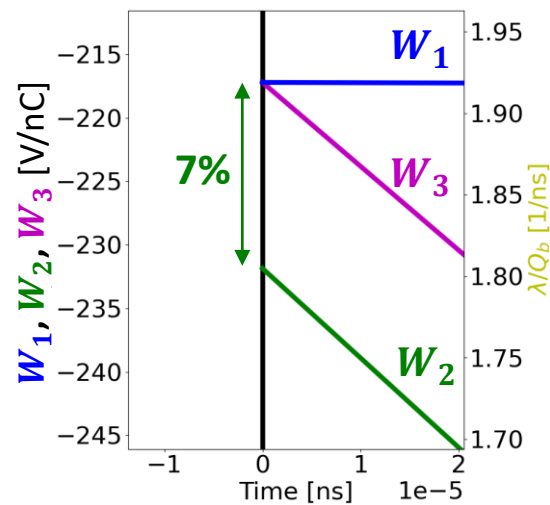
Kicker coupling-impedance in the code (2/3)

□ We show the three potentials for the DAFNE case, using $\sigma_t = 20$ mm.

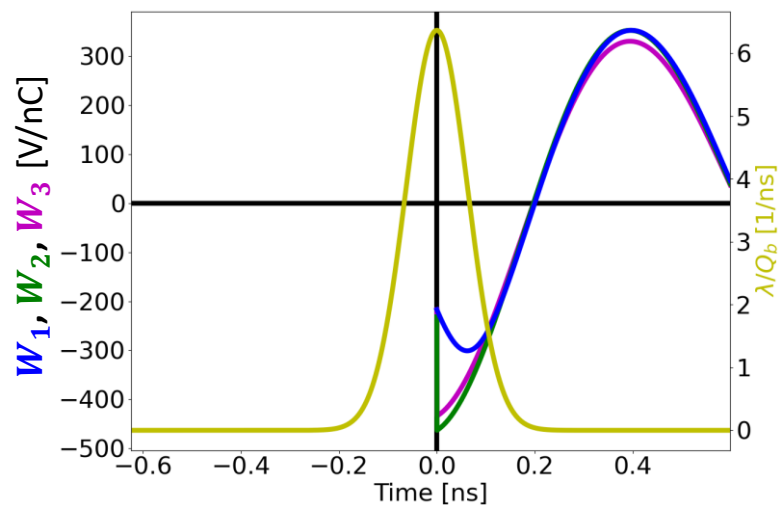
Wake potentials and bunch profile



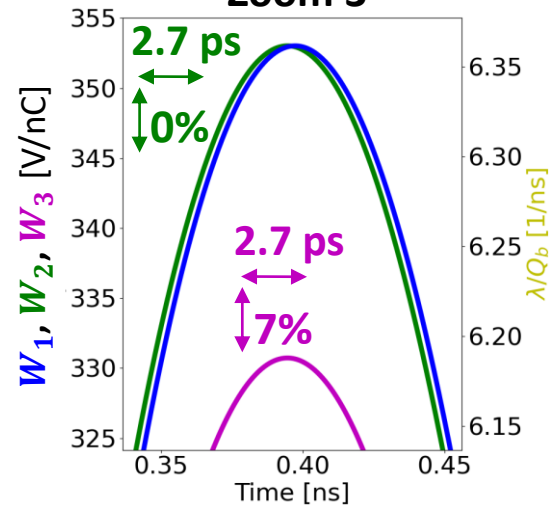
Zoom 2



Zoom 1



Zoom 3



□ W_1 decays to zero after essentially 3 RF periods.

□ At 0 ns the amplitudes of W_1 and W_2 differ by 7%.

After roughly 0.2 ns:

- there is a time-shift of 2.7 ps between W_1 and W_2 ;
- the amplitudes of W_1 and W_2 are the same.

□ At 0 ns the W_1 and W_3 amplitudes coincide by construction.

After roughly 0.2 ns:

- there is a time-shift of 2.7 ps between W_1 and W_3 ;
- the amplitudes of W_1 and W_3 differ by 7%.

□ As for the beam dynamics, we expect that the approximation using W_2 is stronger than the one using W_3 .

- Error using W_2 : always 15 V/nC;
- Worst-case error using W_3 : 7% of 150 V/nC + 7% of 25 V/nC = 12 V/nC.
- If the bunch distances are t_{rf} (e.g. in stable conditions), the error using W_3 is just 7% of 10 V/nC. Indeed the bunch sees zero potential from the last bunch due to the fact that $\omega_n \approx \omega_r = 3.25 \omega_{rf}$.

□ W_2 and W_3 are among the best possible fits for W_1 .

- In any case the constant time-shifts can't be compensated changing the resonator parameters.
- This proves that no resonator can properly fit W_1 .

Kicker coupling-impedance in the code (3/3)

- Being the resonator-fits unprecise, the kicker-impedance contribution was added in the energy equation of motion using directly W_1 .

$$\delta_k^{(n+1)} = \delta_k^{(n)} - \frac{U_0}{E_0} (1 + 2\delta_k^{(n)}) + \frac{eV_{FBkick,k}^{(n)}}{E_0} + \frac{e\hat{V}_{rf} \cos \Delta\varphi_k^{(n+1)}}{E_0} + \frac{e}{E_0} \sum_{j=1}^{N_{HOM}} [V_{k,j,RES}^{(n+1)} + V_{k,j,IND}] + \frac{eV_{kicker,k}^{(n+1)}}{E_0}$$

- where the kicker induced-voltage is given by the sum of the instantaneous voltage and the voltage induced by the last 3 bunches

$$V_{kicker,k}^{(n+1)} = Q_b \left(W_1(0) + W_1 \left(\left[\Delta\varphi_k^{(n+1)} - \Delta\varphi_{k-1}^{(n+1)} \right] / \omega_{rf} \right) + W_1 \left(\left[\Delta\varphi_k^{(n+1)} - \Delta\varphi_{k-2}^{(n+1)} \right] / \omega_{rf} \right) + W_1 \left(\left[\Delta\varphi_k^{(n+1)} - \Delta\varphi_{k-3}^{(n+1)} \right] / \omega_{rf} \right) \right)$$

- Here the phases aren't meant mod 2π , i.e. $c \left(\Delta\varphi_k^{(n+1)} - \Delta\varphi_{k-i}^{(n+1)} \right) / \omega_{rf}$ is the distance between the bunches k and $k - i$.
- As shown, the kicker induced-voltage decays after 3 RF periods, so the contributions from the last 3 bunches are enough.

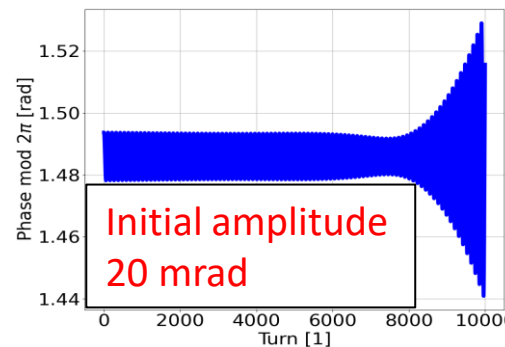
- Since the kicker induced-voltage isn't negligible, it was also necessary to add the kicker-impedance in the beam-matching routine.

- This was done by simply adding the resonator W_3 to the HOMs during the matching procedure.

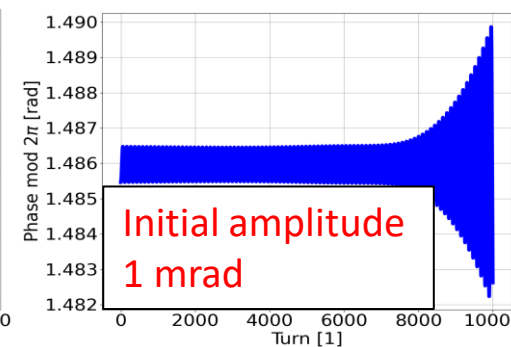
- DAFNE example with 105 contiguous bunches, $I_b = 15$ mA, HOMs + kicker impedances during tracking, feedback off, bunch k starts at $\Delta\varphi_{HOM,k}$.

- Although it's an approximation, the matching with HOMs + W_3 provides a negligible initial oscillation-amplitude for all bunches (as the number 80 here shown).
- The matching with HOMs + W_2 provides less satisfying results, as expected from the observations given in the previous slide.

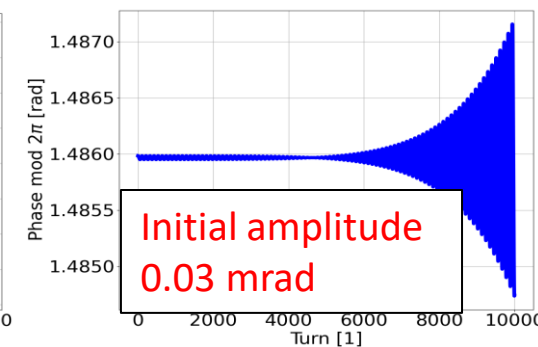
Oscillations of bunch 80, matching with just HOMs



Oscillations of bunch 80, matching with HOMs+ W_2

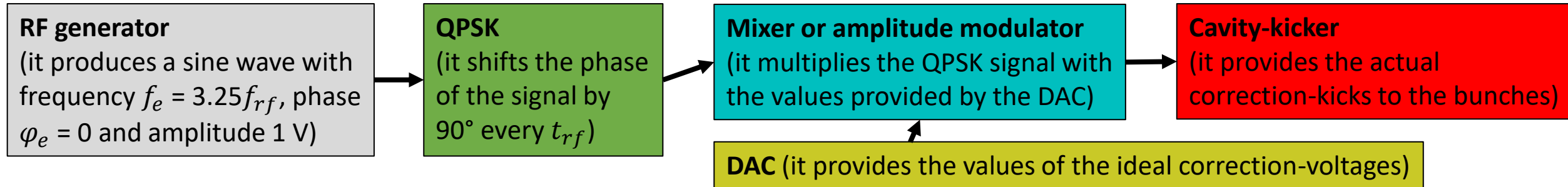


Oscillations of bunch 80, matching with HOMs+ W_3



Kicker correction-voltage

- We now describe the second voltage-contribution of the kicker, i.e. the voltage-corrections given to the bunches.
- The final part of the feedback block-diagram shown earlier can be expanded (and simplified) as

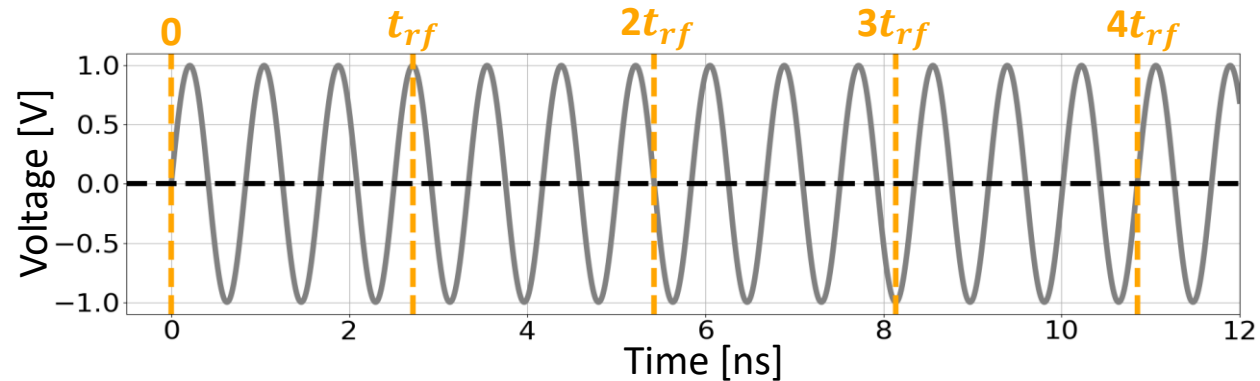


- The DAC provides the values V_{FBkick} of the voltages which should be given to the bunches to have optimal corrections.
- The generator produces a sine wave with frequency $f_e = 3.25f_{rf}$, which is the resonant frequency of the kicker.
 - If this signal is equal to 0 at $t = 0$, then a bunch crossing the kicker at $t = t_{rf}$ sees the maximum of the sine wave, as desired.
 - However, a second bunch crossing the kicker at $t = 2t_{rf}$ sees zero voltage and therefore no correction is applied to that bunch.
 - To solve this problem, the QPSK (Quadrature Phase-Shift Keying) modulation is used to shift the signal by 90° every t_{rf} .
- The mixer multiplies the signal coming from the QPSK with the values V_{FBkick} provided by the DAC.
 - The resulting signal is a piece-wise sinusoidal signal with amplitudes given by the values V_{FBkick} .
- The cavity-kicker, being a resonator with its filling time, modifies the signal coming from the mixer.
 - Because of this, even if everything is perfectly synchronized, the bunches can see just an approximation of the ideal kicks V_{FBkick} .

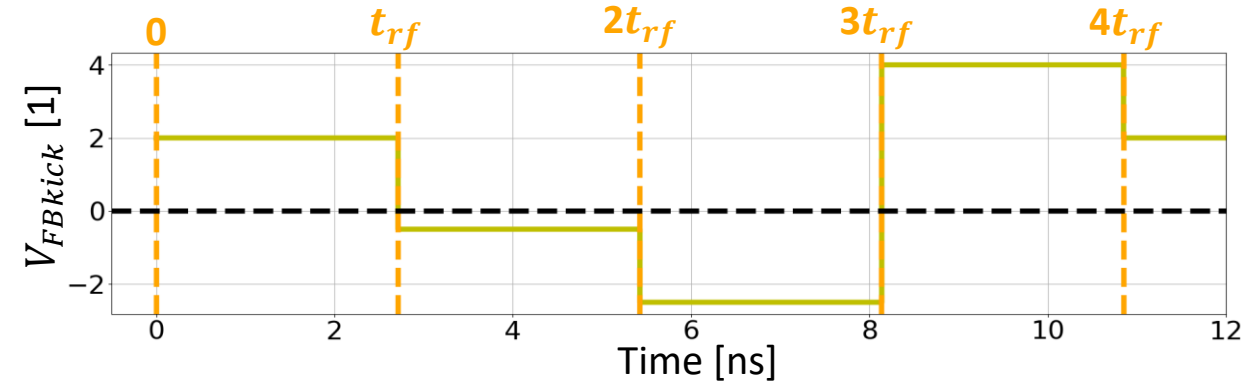
Example: voltage signal from generator to mixer

- Let's suppose that the bunches 1, 2, 3 and 4 circulate in DAFNE ($t_{rf} = 2.71$ ns).
 - At a certain turn n the values V_{FBkick} of the ideal correction-voltages are 2, -0.5, -2.5, 4 respectively for the bunches 1, 2, 3 and 4.
 - The kicker is crossed by the bunch i at it_{rf} , $i = 1, \dots, 4$.
- The mixer-signal is given by the QPSK-signal, which never changes along the turns, multiplied with the DAC signal, which changes every d_{DSF} turns.
 - The voltage from the mixer is discontinuous at the times which are multiple of t_{rf} .
 - As shown later, the voltage-signal from the kicker is continuous at all times and bunches arriving slightly late can still get a proper correction.

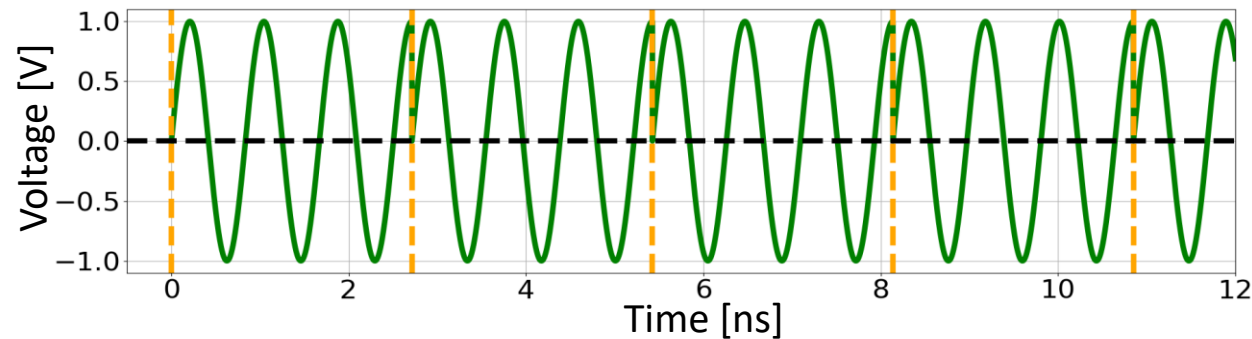
Voltage from the generator



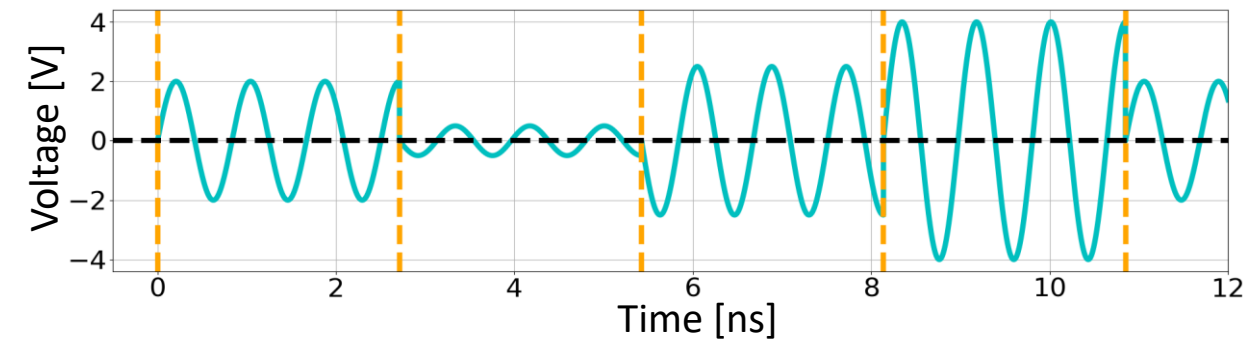
Signal from the DAC at turn n



Voltage from the QPSK



Voltage from the mixer at turn n



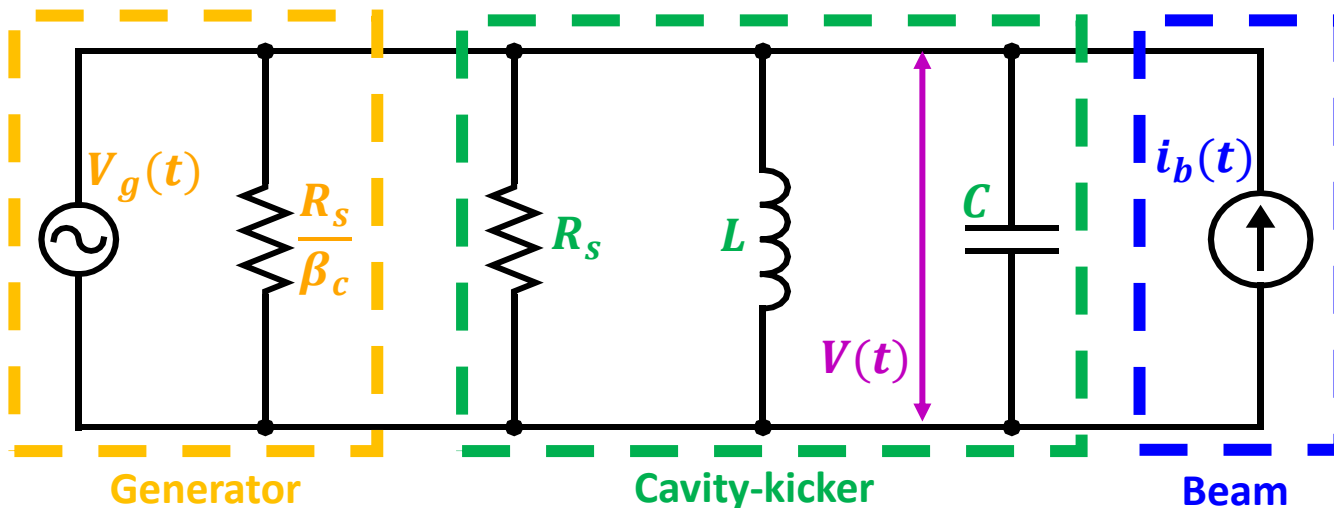
Kicker correction-voltage in the code (1/6)

- The cavity-kicker is modelled as a parallel RLC resonant circuit. This allows to take into account the finite filling-time of the kicker.
- The kicker is excited by the circulating beam-current $i_b(t)$ and by the kicker RF-generator $V_g(t)$.
 - The generator has angular frequency $\omega_e = 2\pi f_e$ and is amplitude-modulated with the V_{FBkick} values coming from the DAC.
 - The generator has inner resistance equal to the shunt impedance of the kicker divided by the coupling factor

$$\beta_c = \frac{P_{ext}}{P_{wall}} \begin{array}{l} \longrightarrow \text{'External' power lost through the waveguides (power-couplers).} \\ \longrightarrow \text{Ohmic power-losses due to the non-perfectly conductive walls of the kicker.} \end{array}$$

- As observed earlier, we assume that the generator-kicker system is perfectly matched when the generator works at f_e , therefore $\beta_c = 1$.

- Since we expect that the bunches cross the kicker at times kt_{rf} , after the passage of the bunch $k - 1$ at $(k - 1)t_{rf}$ the generator-amplitude $V_{FBkick,k-1}$ suddenly changes to the value $V_{FBkick,k}$ pertaining to the bunch k . The QPSK shifts the generator-phase by 90° at times kt_{rf} .



$$\text{Sources} \left\{ \begin{array}{l} V_g(t) = V_{FBkick,k} \sin(\omega_e t) \quad t \in [(k-1)t_{rf}, kt_{rf}[\\ i_b(t) = Q_b \sum_{k \geq 1} \delta(t - kt_{rf}) \end{array} \right. \quad k = 1, 2, \dots$$

Unknown $V(t)$: voltage across the capacitance at time t

- In the following derivation we neglect the beam current ($i_b(t) \equiv 0$) since the corresponding (induced) voltage was already considered.

Kicker correction-voltage in the code (2/6)

- The generator-voltage in the time interval $(k - 1)t_{rf} \leq t < kt_{rf}$ is given by

$$V_g(t) = V_{FBkick,k} \sin(\omega_e t + \varphi_e)$$

- where we consider the more general case with $\varphi_e \neq 0$.

- Applying the Kirchhoff's law for currents, we have

$$\frac{V(t)}{R_s} + \frac{1}{L} \int_0^t V(s) ds + C \frac{dV(t)}{dt} = \frac{V_g(t)}{R_s} = \frac{V_{FBkick,k}}{R_s} \sin(\omega_e t + \varphi_e)$$

- Deriving one time

$$\ddot{V} + 2\Gamma\dot{V} + \omega_r^2 V = F_k \cos(\omega_e t + \varphi_e) \quad \Gamma = \frac{1}{2CR_s} \quad \omega_r = \frac{1}{\sqrt{CL}} \quad F_k = 2\Gamma\omega_e V_{FBkick,k}$$

- The associated homogenous differential equation is

$$\ddot{V}_h + 2\Gamma\dot{V}_h + \omega_r^2 V_h = 0$$

- Its eigenvalues are

$$\lambda_{1,2} = -\Gamma \pm j\sqrt{\omega_r^2 - \Gamma^2} = -\Gamma \pm j\omega_n \quad \omega_n = \sqrt{\omega_r^2 - \Gamma^2}$$

- Its solution is

$$V_h(t) = e^{-\Gamma t} [C_1 \cos(\omega_n t) + C_2 \sin(\omega_n t)]$$

- where the constant C_1 and C_2 depend on $V(0) = V_0$ and $\dot{V}(0) = \dot{V}_0$.

Kicker correction-voltage in the code (3/6)

- The forcing term of the inhomogeneous equation is

$$F_k \cos(\omega_e t + \varphi_e) = \operatorname{Re}\{F_k e^{j(\omega_e t + \varphi_e)}\}$$

- Therefore we find a particular solution of the type

$$V_p(t) = \operatorname{Re}\{X e^{j(\omega_e t + \varphi_e)}\}$$

➤ where X is a complex constant.

- Inserting $F_k e^{j(\omega_e t + \varphi_e)}$ and $X e^{j(\omega_e t + \varphi_e)}$ into the inhomogeneous differential equation we obtain

$$-X\omega_e^2 + 2\Gamma X\omega_e j + \omega_r^2 X = F_k$$

- Solving for X

$$X = \frac{2\Gamma\omega_e V_{FBkick,k}}{\omega_r^2 - \omega_e^2 + 2\Gamma\omega_e j} = \frac{V_{FBkick,k}}{Q\left(\frac{\omega_r}{\omega_e} - \frac{\omega_e}{\omega_r}\right) + j} = \frac{V_{FBkick,k} \left[Q\left(\frac{\omega_r}{\omega_e} - \frac{\omega_e}{\omega_r}\right) - j \right]}{Q^2\left(\frac{\omega_r}{\omega_e} - \frac{\omega_e}{\omega_r}\right)^2 + 1} = V_{FBkick,k}(A - jB)$$

➤ where

$$Q = \frac{\omega_r}{2\Gamma} \quad A = \frac{Q\left(\frac{\omega_r}{\omega_e} - \frac{\omega_e}{\omega_r}\right)}{Q^2\left(\frac{\omega_r}{\omega_e} - \frac{\omega_e}{\omega_r}\right)^2 + 1} \quad B = \frac{1}{Q^2\left(\frac{\omega_r}{\omega_e} - \frac{\omega_e}{\omega_r}\right)^2 + 1}$$

Kicker correction-voltage in the code (4/6)

□ Substituting

$$V_p(t) = V_{FBkick,k} \operatorname{Re}\{(A - jB)e^{j(\omega_e t + \varphi_e)}\} = V_{FBkick,k} [A \cos(\omega_e t + \varphi_e) + B \sin(\omega_e t + \varphi_e)]$$

□ Therefore all the solutions of the inhomogeneous differential equation are given by

$$V(t) = e^{-\Gamma t} [C_1 \cos(\omega_n t) + C_2 \sin(\omega_n t)] + V_{FBkick,k} [A \cos(\omega_e t + \varphi_e) + B \sin(\omega_e t + \varphi_e)]$$

□ C_1 is determined by

$$V_0 = C_1 + V_{FBkick,k} (A \cos \varphi_e + B \sin \varphi_e) \quad \longrightarrow \quad C_1 = V_0 - V_{FBkick,k} (A \cos \varphi_e + B \sin \varphi_e)$$

□ C_2 is determined by

$$\dot{V}_0 = -\Gamma C_1 + C_2 \omega_n + V_{FBkick,k} \omega_e (B \cos \varphi_e - A \sin \varphi_e)$$



$$C_2 = \frac{1}{\omega_n} \dot{V}_0 + \frac{\Gamma}{\omega_n} V_0 - \frac{\Gamma V_{FBkick,k}}{\omega_n} (A \cos \varphi_e + B \sin \varphi_e) - \frac{V_{FBkick,k} \omega_e}{\omega_n} (B \cos \varphi_e - A \sin \varphi_e)$$

Kicker correction-voltage in the code (5/6)

□ Substituting we finally obtain

$$V(t) = e^{-\Gamma t} \left\{ \left[\cos(\omega_n t) + \frac{\Gamma}{\omega_n} \sin(\omega_n t) \right] V_0 + \frac{\sin(\omega_n t)}{\omega_n} \dot{V}_0 \right\} + V_{FBkick,k} f(t)$$

➤ where

$$f(t) = A \cos(\omega_e t + \varphi_e) + B \sin(\omega_e t + \varphi_e) +$$

$$-e^{-\Gamma t} \left\{ (A \cos \varphi_e + B \sin \varphi_e) \cos(\omega_n t) + \frac{(\Gamma A + \omega_e B) \cos \varphi_e + (\Gamma B - \omega_e A) \sin \varphi_e}{\omega_n} \sin(\omega_n t) \right\}$$

□ Deriving $V(t)$ we obtain

$$\dot{V}(t) = e^{-\Gamma t} \left\{ -\frac{\omega_r^2}{\omega_n} \sin(\omega_n t) V_0 + \left[\cos(\omega_n t) - \frac{\Gamma}{\omega_n} \sin(\omega_n t) \right] \dot{V}_0 \right\} + V_{FBkick,k} \dot{f}(t)$$

➤ where

$$\dot{f}(t) = -A\omega_e \sin(\omega_e t + \varphi_e) + B\omega_e \cos(\omega_e t + \varphi_e) +$$

$$e^{-\Gamma t} \left\{ \omega_e (A \sin \varphi_e - B \cos \varphi_e) \cos(\omega_n t) + \frac{(\omega_r^2 A + \Gamma \omega_e B) \cos \varphi_e + (\omega_r^2 B - \Gamma \omega_e A) \sin \varphi_e}{\omega_n} \sin(\omega_n t) \right\}$$

Kicker correction-voltage in the code (6/6)

- Similar to what done for the RLC circuit for the HOMs discussed earlier, in the code V and \dot{V} are computed using the matrix expression

$$\begin{pmatrix} V(t) \\ \dot{V}(t) \end{pmatrix} = e^{-\frac{\omega_r t}{2Q}} \begin{pmatrix} \cos(\omega_n t) + \frac{\omega_r}{2Q\omega_n} \sin(\omega_n t) & \frac{1}{\omega_n} \sin(\omega_n t) \\ -\frac{\omega_r^2}{\omega_n} \sin(\omega_n t) & \cos(\omega_n t) - \frac{\omega_r}{2Q\omega_n} \sin(\omega_n t) \end{pmatrix} \begin{pmatrix} V_0 \\ \dot{V}_0 \end{pmatrix} + V_{FBkick,k} \begin{pmatrix} f(t) \\ \dot{f}(t) \end{pmatrix} \quad 0 \leq t < t_{rf}$$

It decays exponentially with time and accounts for the emptying-process of the kicker.

It oscillates with time and accounts for the generator-voltage and the filling-process of the kicker.

- If the RF generator is perfectly synchronized with the synchronous arrival times of the bunches, then $\varphi_e = 0$ and

$$f(t) = A \cos(\omega_e t) + B \sin(\omega_e t) - e^{-\Gamma t} \left\{ A \cos(\omega_n t) + \frac{\Gamma A + \omega_e B}{\omega_n} \sin(\omega_n t) \right\} \xrightarrow{\text{for large } t} A \cos(\omega_e t) + B \sin(\omega_e t) \neq \sin(\omega_e t)$$

- If $\omega_r = \omega_e = 3.25\omega_{rf}$, as it occurs when the QPSK is active and there are no frequency errors, then $A = 0, B = 1$ and

$$f(t) = \sin(\omega_e t + \varphi_e) - e^{-\Gamma t} \left\{ \sin \varphi_e \cos(\omega_n t) + \frac{\omega_e \cos \varphi_e + \Gamma \sin \varphi_e}{\omega_n} \sin(\omega_n t) \right\} \xrightarrow{\text{for large } t} \sin(\omega_e t + \varphi_e) \neq \sin(\omega_e t)$$

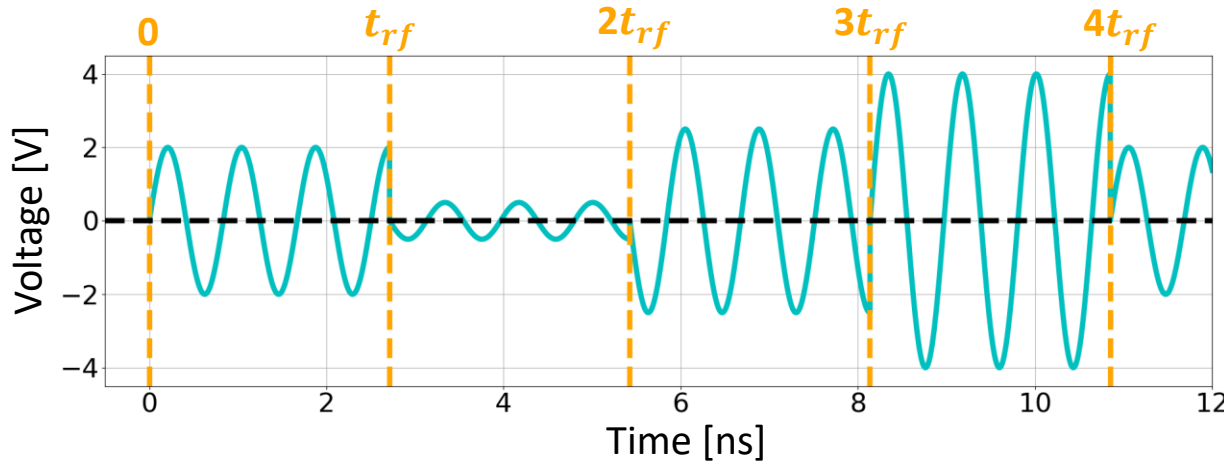
- If $\varphi_e = 0$ and $\omega_r = \omega_e = 3.25\omega_{rf}$ (ideal case), then

$$f(t) = \underbrace{\sin(\omega_e t)}_{\parallel V_g(t)/V_{FBkick,k}} - \underbrace{e^{-\Gamma t} \frac{\omega_e}{\omega_n} \sin(\omega_n t)}_{\text{Filling-process term decaying exponentially with time}} \quad \longrightarrow \quad \underbrace{V_{FBkick,k} f(t_{rf})}_{\text{Desired voltage-kick}} = \underbrace{V_{FBkick,k}}_{\text{Desired voltage-kick}} - \underbrace{V_{FBkick,k} e^{-\Gamma t_{rf}} \frac{\omega_e}{\omega_n} \sin(\omega_n t_{rf})}_{\text{Error term due to filling-process}} \approx e^{-\frac{3.25\pi}{Q}} \quad (\text{since } \omega_n \approx \omega_r)$$

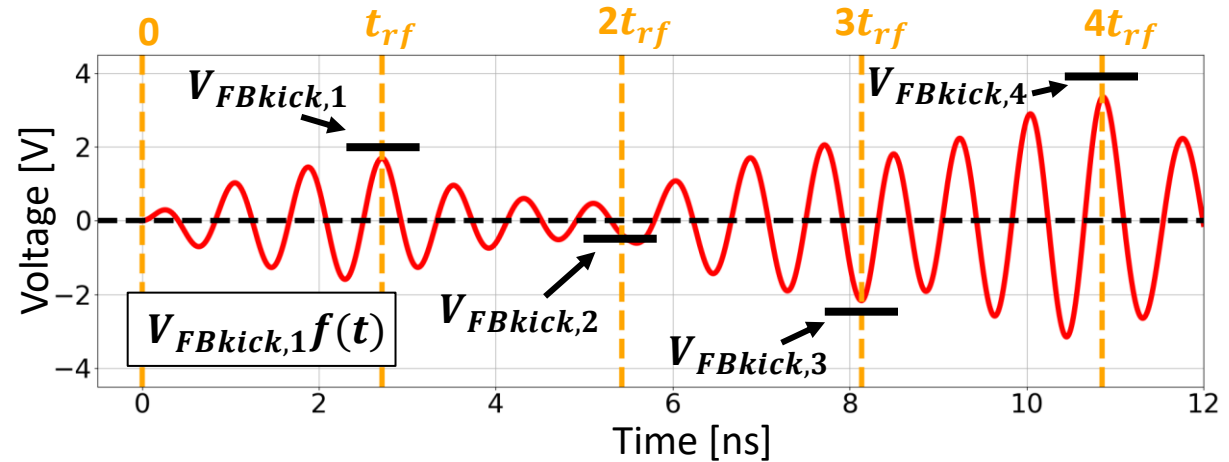
Example continued: voltage signal from mixer to kicker

- We assume that $\varphi_e = 0$ and $\omega_r = \omega_e = 3.25\omega_{rf}$. The voltage from the mixer and the actual kicker-voltage are given respectively by

Voltage from the mixer at turn n



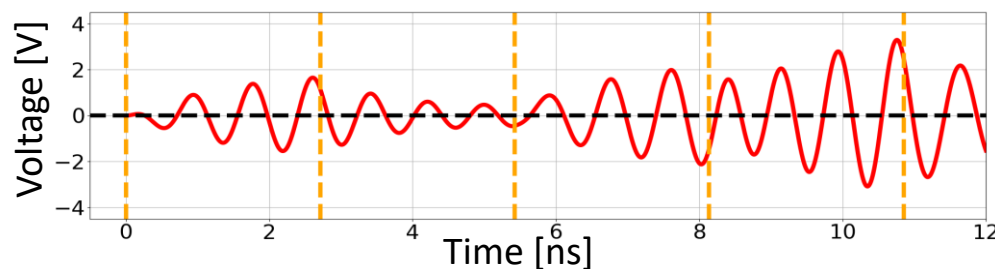
Kicker voltage at turn 1



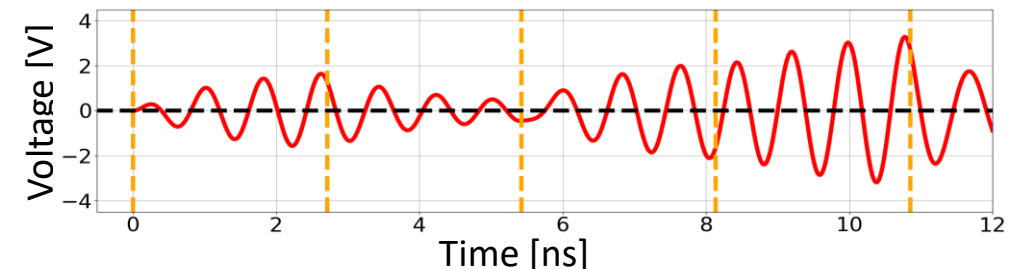
- The voltage from the mixer coincides with the amplitude-modulated generator voltage $V_g(t)$ defined for the kicker circuit-model.
- The kicker-voltage is a continuous function of time, as opposed to the mixer-voltage which is discontinuous at kt_{rf} .
- The kicker-voltages at t_{rf} , $3t_{rf}$ and $4t_{rf}$ are visibly lower than the corresponding $V_{FBkick,k}$.
- In this example, being at turn 1, there isn't residual voltage in the kicker at $t = 0$, therefore $V(t) = V_{FBkick,1}f(t)$ for $0 \leq t \leq t_{rf}$.

- At least for times close to kt_{rf} , a frequency error of 5% is essentially equivalent to a shift of the phase by $\pi/4$.

Kicker voltage at turn n ($\varphi_e = \pi/4$)



Kicker voltage at turn n ($|\omega_r - \omega_e|/(3.25\omega_{rf}) = 5\%$)



Kicker-voltage evaluation for bunches

- The code takes into account the fact that bunches perform synchrotron oscillations around their corresponding synchronous phases.
 - The times kt_{rf} , when the QPSK acts, correspond to the $\Delta\varphi_{SR}$ of the different buckets: a bunch arriving at kt_{rf} has phase $\Delta\varphi_{SR}$.

- Given ω_e , ω_r , φ_e and Q , the matrix equation previously derived can be expressed in functional and compact form as

$$\begin{pmatrix} V(t) \\ \dot{V}(t) \end{pmatrix} = e^{-\frac{\omega_r t}{2Q}} \begin{pmatrix} \cos(\omega_n t) + \frac{\omega_r}{2Q\omega_n} \sin(\omega_n t) & \frac{1}{\omega_n} \sin(\omega_n t) \\ -\frac{\omega_r^2}{\omega_n} \sin(\omega_n t) & \cos(\omega_n t) - \frac{\omega_r}{2Q\omega_n} \sin(\omega_n t) \end{pmatrix} \begin{pmatrix} V_{0,k-1} \\ \dot{V}_{0,k-1} \end{pmatrix} + V_{FBkick,k} \begin{pmatrix} f(t) \\ \dot{f}(t) \end{pmatrix} = p(t, V_{FBkick,k}, V_{0,k-1}, \dot{V}_{0,k-1})$$

- where $V_{0,k-1} = V[(k-1)t_{rf}]$, $\dot{V}_{0,k-1} = \dot{V}[(k-1)t_{rf}]$, $0 \leq t \leq t_{rf}$ and p is the 'propagation' function.

- If the bunch k is **in advance** with respect to $\Delta\varphi_{SR}$ ($\Delta\varphi_k < \Delta\varphi_{SR}$), then the kicker-voltage seen by the bunch k is given by

$$V(t_k) = p(t_k, V_{FBkick,k}, V_{0,k-1}, \dot{V}_{0,k-1}) \Big|_{1^{\circ} \text{ element}} \quad t_k = t_{rf} + \frac{\Delta\varphi_k - \Delta\varphi_{SR}}{\omega_{rf}} < t_{rf}$$

- If the bunch k is **late** with respect to $\Delta\varphi_{SR}$ ($\Delta\varphi_k > \Delta\varphi_{SR}$), then we need first to update the initial conditions and then compute $V(t_k)$

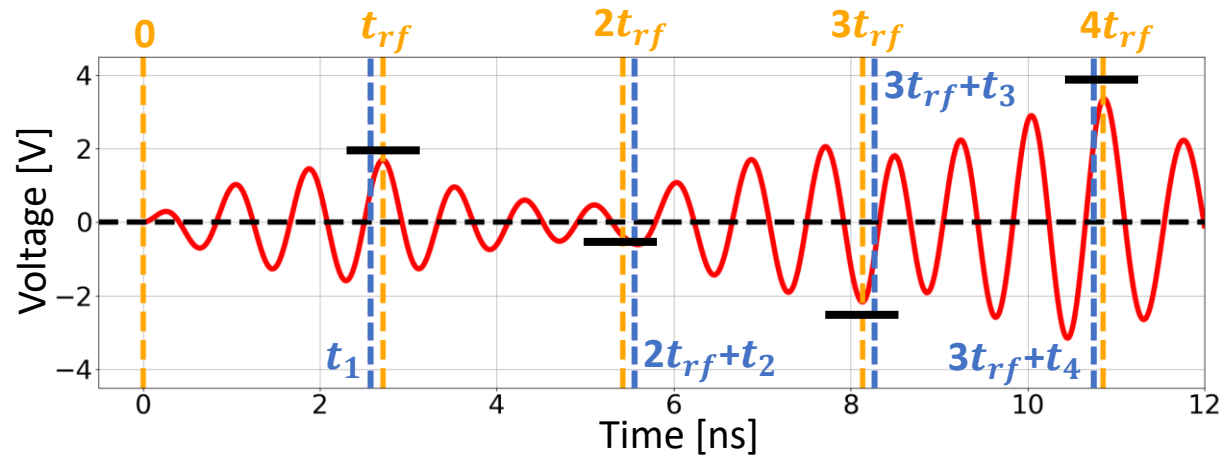
$$\begin{pmatrix} V_{0,k} \\ \dot{V}_{0,k} \end{pmatrix} = p(t_{rf}, V_{FBkick,k}, V_{0,k-1}, \dot{V}_{0,k-1}) \quad V(t_k) = p(t_k, V_{FBkick,k+1}, V_{0,k}, \dot{V}_{0,k}) \Big|_{1^{\circ} \text{ element}} \quad t_k = \frac{\Delta\varphi_k - \Delta\varphi_{SR}}{\omega_{rf}} > 0$$

- If there are empty buckets between two bunches, then the initial conditions must be updated iteratively before computing $V(t_k)$.

Example continued: kicker-voltage seen by bunches

- We consider again the case $\varphi_e = 0$, $\omega_r = \omega_e = 3.25\omega_{rf}$ and we assume that the four bunches traverse the kicker respectively at times t_1 (in advance), $2t_{rf} + t_2$ (late), $3t_{rf} + t_3$ (late), $3t_{rf} + t_4$ (in advance), with $0 < t_k < t_{rf}$.

Kicker voltage at turn 1



- Being the first turn, the kicker residual-voltage is zero at $t = 0$

$$\begin{pmatrix} V(0) \\ \dot{V}(0) \end{pmatrix} = \begin{pmatrix} V_{0,0} \\ \dot{V}_{0,0} \end{pmatrix} = \begin{pmatrix} 0 \\ 0 \end{pmatrix}$$

- $V(t_1)$ can be computed as

$$V(t_1) = p(t_1, V_{FBkick,1}, V_{0,0}, \dot{V}_{0,0}) \Big|_{1^\circ} \quad t_1 = t_{rf} + \frac{\Delta\varphi_1 - \Delta\varphi_{SR}}{\omega_{rf}}$$

- To compute $V(t_2)$ we need to update the initial conditions twice

$$\begin{pmatrix} V_{0,1} \\ \dot{V}_{0,1} \end{pmatrix} = p(t_{rf}, V_{FBkick,1}, V_{0,0}, \dot{V}_{0,0}) \quad \begin{pmatrix} V_{0,2} \\ \dot{V}_{0,2} \end{pmatrix} = p(t_{rf}, V_{FBkick,2}, V_{0,1}, \dot{V}_{0,1}) \quad V(t_2) = p(t_2, V_{FBkick,3}, V_{0,2}, \dot{V}_{0,2}) \Big|_{1^\circ} \quad t_2 = \frac{\Delta\varphi_2 - \Delta\varphi_{SR}}{\omega_{rf}}$$

- To compute $V(t_3)$ and $V(t_4)$ we need to update the initial conditions one time more

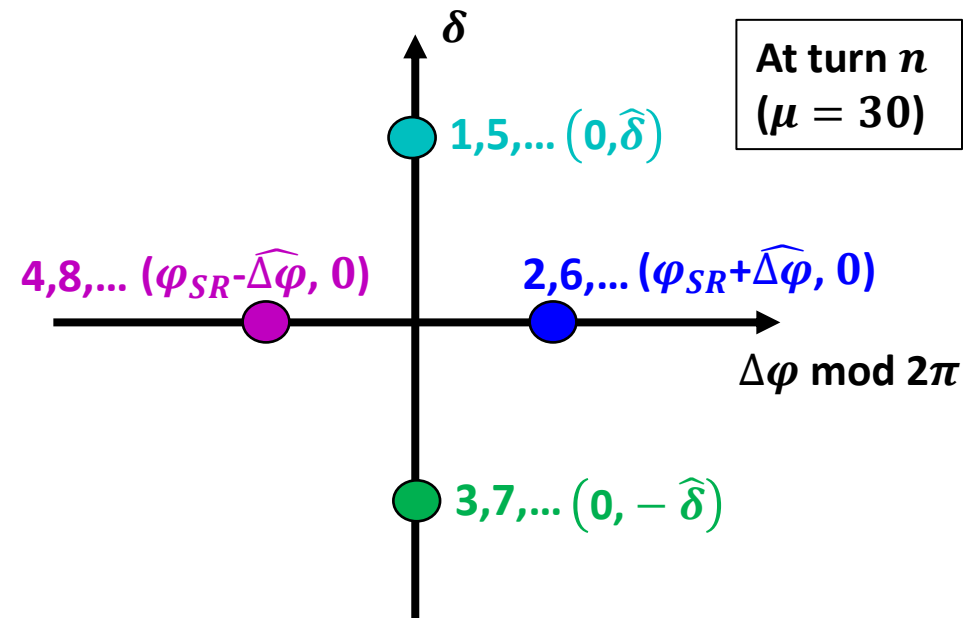
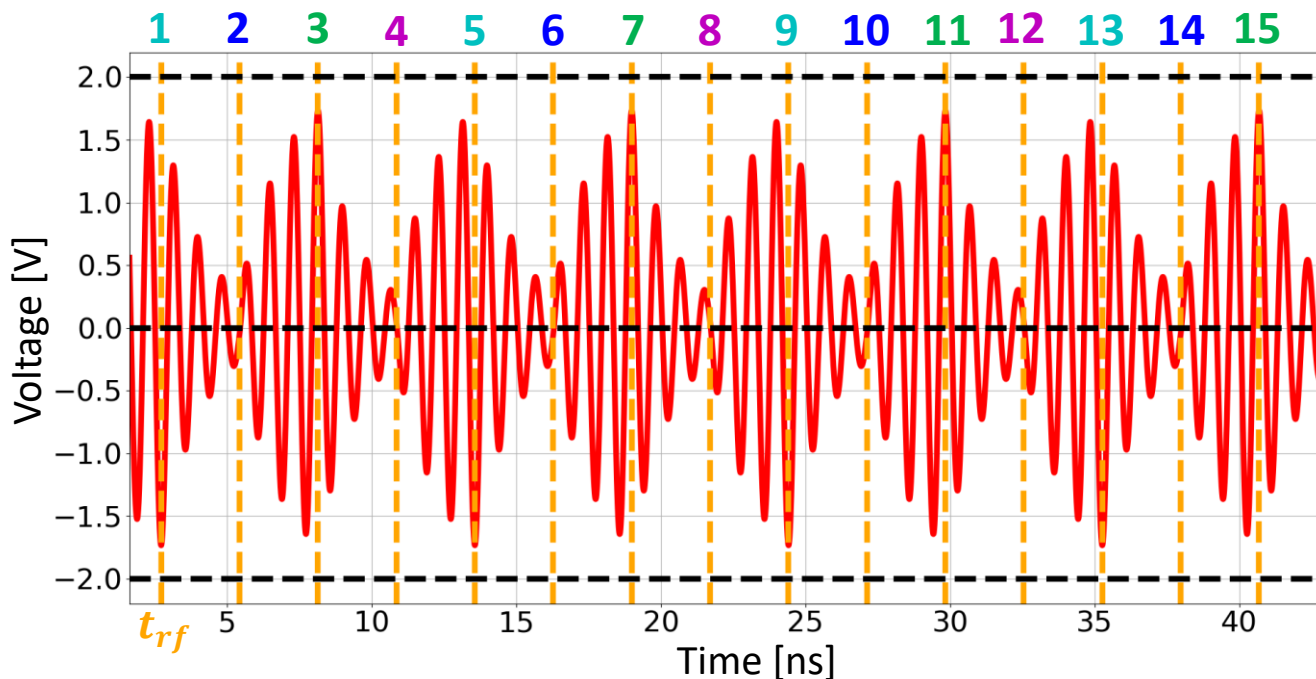
$$\begin{pmatrix} V_{0,3} \\ \dot{V}_{0,3} \end{pmatrix} = p(t_{rf}, V_{FBkick,3}, V_{0,2}, \dot{V}_{0,2}) \quad V(t_3) = p(t_3, V_{FBkick,4}, V_{0,3}, \dot{V}_{0,3}) \Big|_{1^\circ} \quad t_3 = \frac{\Delta\varphi_3 - \Delta\varphi_{SR}}{\omega_{rf}} \quad V(t_4) = p(t_4, V_{FBkick,4}, V_{0,3}, \dot{V}_{0,3}) \Big|_{1^\circ} \quad t_4 = t_{rf} + \frac{\Delta\varphi_4 - \Delta\varphi_{SR}}{\omega_{rf}}$$

Another example: residual voltage and kicker efficiency (1/3)

□ Let's suppose that

- 120 bunches in DAFNE perform coupled-bunch motion with $\mu = 30$;
- the phase-shift between consecutive bunches is $\Delta\phi_{30} = \pi/2$;
- the oscillation-amplitudes $\widehat{\Delta\varphi}$ and $\widehat{\delta}$ are the same for all the bunches
 - at turn n , the bunches 1, 5, 9, ... have coordinates $(0, \widehat{\delta})$, the bunches 2, 6, 10, ... have coordinates $(\varphi_{SR} + \widehat{\Delta\varphi}, 0)$ etc.;
 - the feedback ideal-corrections are $V_{FBkick,(1,5,\dots)} = -2 \text{ V}$,
 $V_{FBkick,(2,6,\dots)} = 0 \text{ V}$, $V_{FBkick,(3,7,\dots)} = 2 \text{ V}$, $V_{FBkick,(4,8,\dots)} = 0 \text{ V}$.

Kicker voltage at turn n ($\mu = 30$)

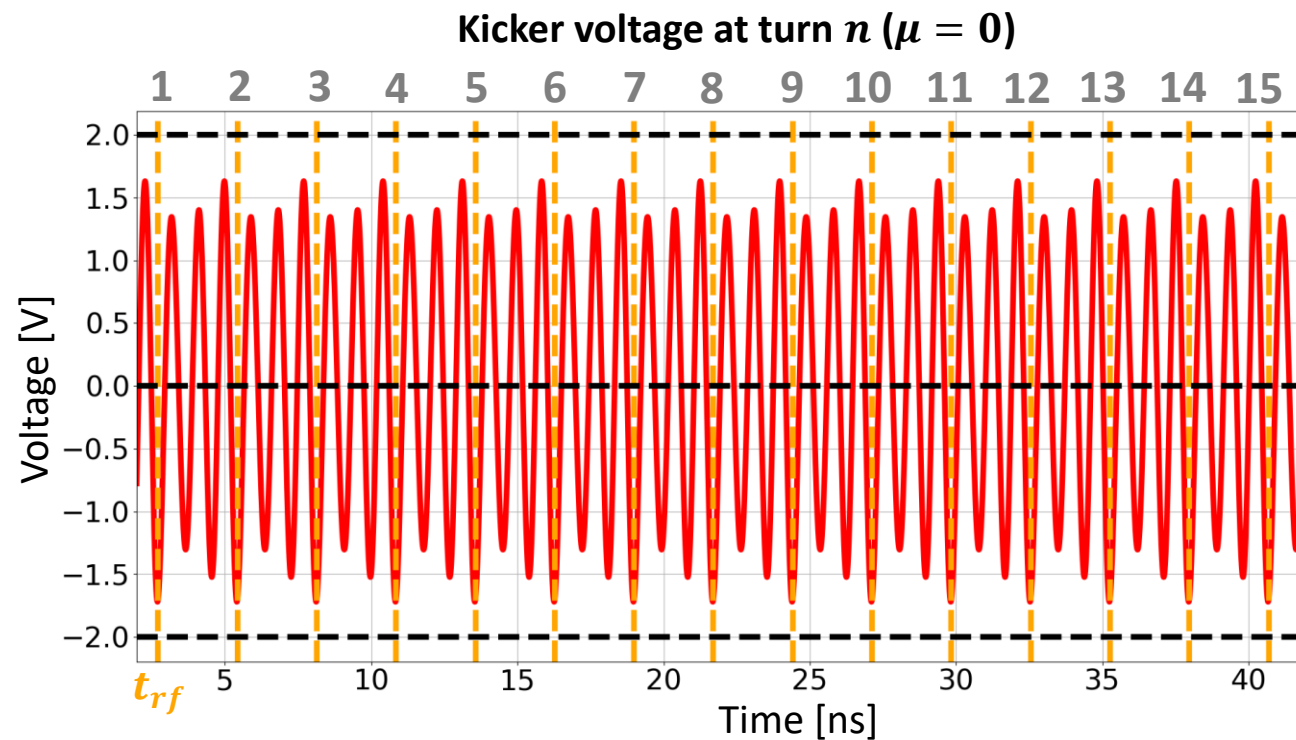
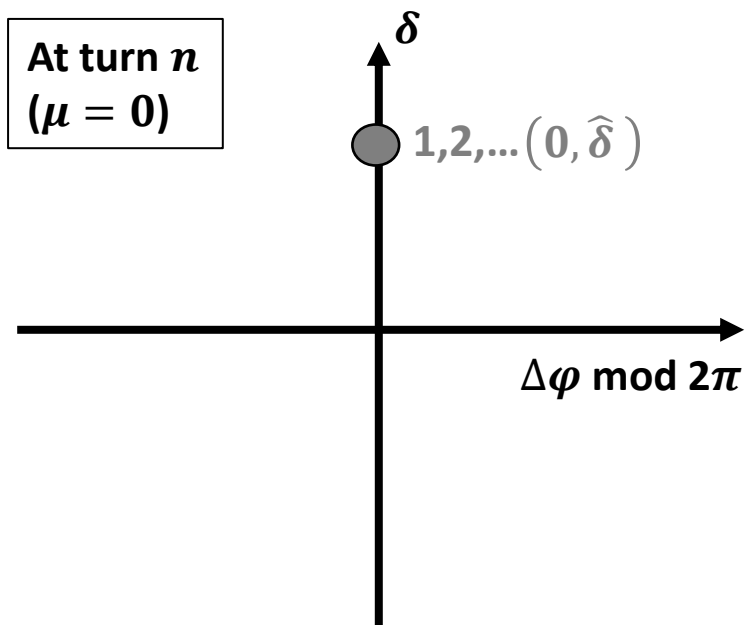


- We assume that $\widehat{\Delta\varphi}$ and $\widehat{\delta}$ are small so that each bunch k sees essentially the corresponding $V(kt_{rf})$.
- The bunches 1, 5, ... see -1.733 V instead of -2 V.
 - Error 14.3%.
 - The bunches 2, 6, ... see -0.05 V instead of 0 V.
 - Error 0.05 V.
 - The bunches 3, 7, ... see 1.733 V instead of 2 V.
 - Error 14.3%.
 - The bunches 4, 8, ... see 0.05 V instead of 0 V.
 - Error 0.05 V.

Another example: residual voltage and kicker efficiency (2/3)

□ Let's now suppose that

- the 120 bunches perform coupled-bunch oscillations with $\mu = 0$ ($\Delta\phi_0 = 0$) and that at turn n the coordinates of all bunches are $(0, \hat{\delta})$;
- the feedback ideal-corrections are all $V_{FBkick,k} = -2$ V.



□ We assume again that $\widehat{\Delta\varphi}$ and $\hat{\delta}$ are small so that each bunch k sees the corresponding $V(kt_{rf})$.

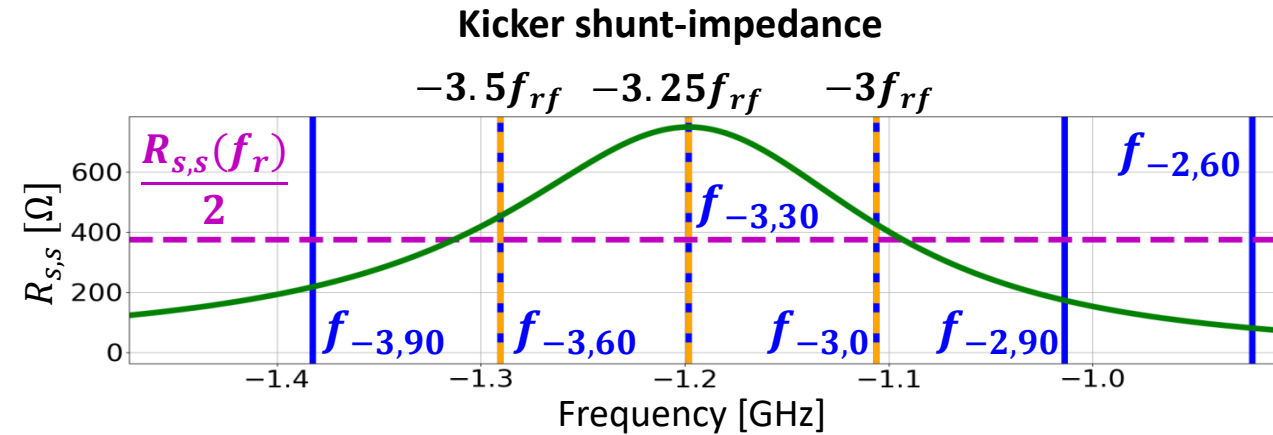
- All the bunches see -1.70 V instead of -2 V.
 - Error 16.2% (instead of 14.3% obtained for $\mu = 30$).

□ This example indicates that the kicker is more efficient (smaller differences between ideal and actual kicks) when $\mu = 30$. Why?

Another example: residual voltage and kicker efficiency (3/3)

□ **First explanation (frequency domain):** the resonant frequency of the kicker is $3.25f_{rf}$, therefore the shunt-impedance (kicker-efficiency) has its maximum at $3.25f_{rf}$.

- As already seen, if we consider negative frequencies, $-3.25f_{rf}$ corresponds to $\mu = 30$, so we expect a better kicker-efficiency for $\mu = 30$.
- $R_{s,s}$ decreases as the distance from the resonant frequency increases, so we expect a worse kicker-efficiency for $\mu = 0$.



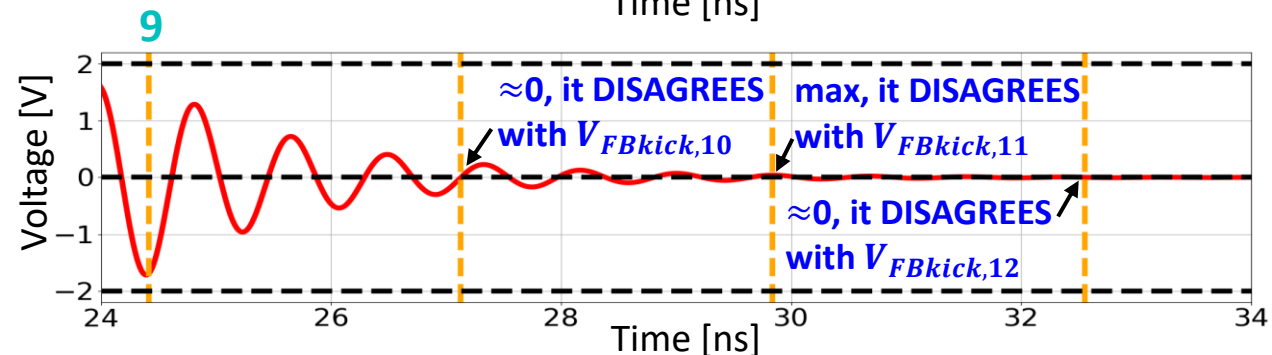
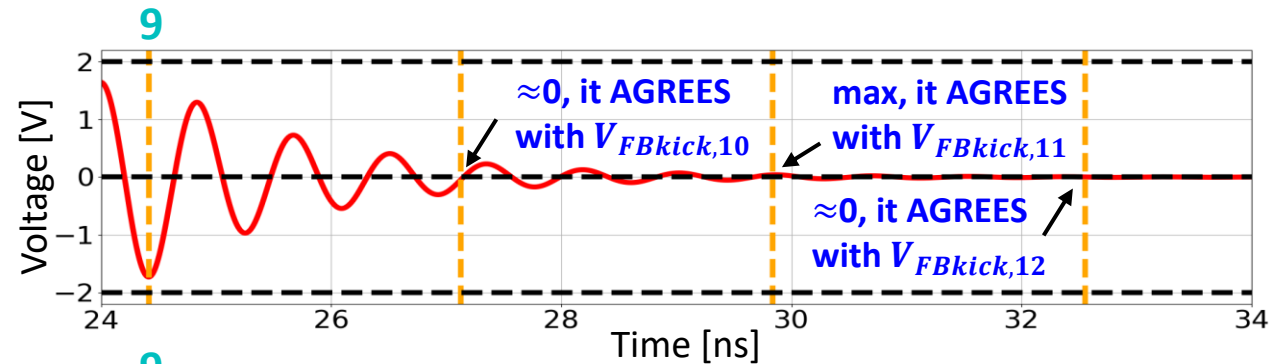
□ **Second explanation (time domain):** let's suppose that $f(t) \equiv 0$ after the bunch 9 traverses the kicker, so that we can examine the evolution of the residual voltage as a function of time.

$$V_{res}(t) = e^{-\Gamma t} \left\{ \left[\cos(\omega_n t) + \frac{\Gamma}{\omega_n} \sin(\omega_n t) \right] V_0 + \frac{\sin(\omega_n t)}{\omega_n} \dot{V}_0 \right\}$$

$$\approx V_0 e^{-\Gamma t} \cos(\omega_r t)$$

- V_{res} is zero when the bunches 10 and 12 cross the kicker, whereas V_{res} is a local maximum when the bunch 11 arrives.
 - $\mu = 30$: agreements with $V_{FBkick,(10,12)}=0$, $V_{FBkick,11}=2$.
 - $\mu = 0$: disagreements with $V_{FBkick,(10,11,12)} = -2$.

Residual voltage after the bunch 9 transit, $\mu=30$ (top), $\mu=0$ (bottom)



Equations of motion in the code: RF+SR+HOM+FB+BBZ

□ Including the actual corrections given by the kicker, the equations of motion become

$$\Delta\varphi_k^{(n+1)} = \Delta\varphi_k^{(n)} + 2\pi h \alpha_0 \delta_k^{(n)}$$

$$\delta_k^{(n+1)} = \delta_k^{(n)} - \frac{U_0}{E_0} (1 + 2\delta_k^{(n)}) + \frac{eV_{FB,k}^{(n+1)}}{E_0} + \frac{e\hat{V}_{rf} \cos \Delta\varphi_k^{(n+1)}}{E_0} + \frac{e}{E_0} \sum_{j=1}^{N_{HOM}} [V_{k,j,RES}^{(n+1)} + V_{k,j,IND}] + \frac{eV_{kicker,k}^{(n+1)}}{E_0} + \frac{eV_{bbZ,k}}{E_0}$$

- where $V_{FB,k}^{(n+1)}$ is the actual voltage provided by the kicker to the bunch k at turn $(n + 1)$. As we saw, $V_{FB,k}^{(n+1)}$ depend on
- the ideal voltage-correction $V_{FBkicker,k}^{(n)}$ evaluated at turn n ;
 - the kicker parameters ω_r , Q and $R_{S,S}$;
 - the frequency ω_e and phase φ_e of the kicker-generator;
 - the arrival time of the bunch k at turn $n + 1$, or $\Delta\varphi_k^{(n+1)}$.

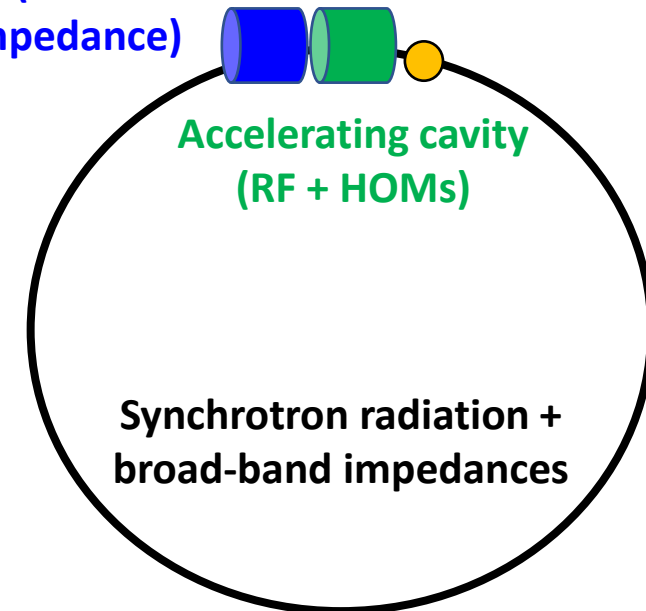
□ The effects of broad-band impedances which don't couple consecutive bunches can be simply included in the energy equation of motion as instantaneous voltages $V_{bbZ,k}$.

- Usually these impedances (e.g. resistive wall) are due to non-resonant devices and are spread all along the ring.
- $V_{bbZ,k}$ depend on the bunch charge $Q_{b,k}$.
- If all the charges are equal, then V_{bbZ} is constant for all bunches and all turns.

Kicker (correction
+ impedance)

Accelerating cavity
(RF + HOMs)

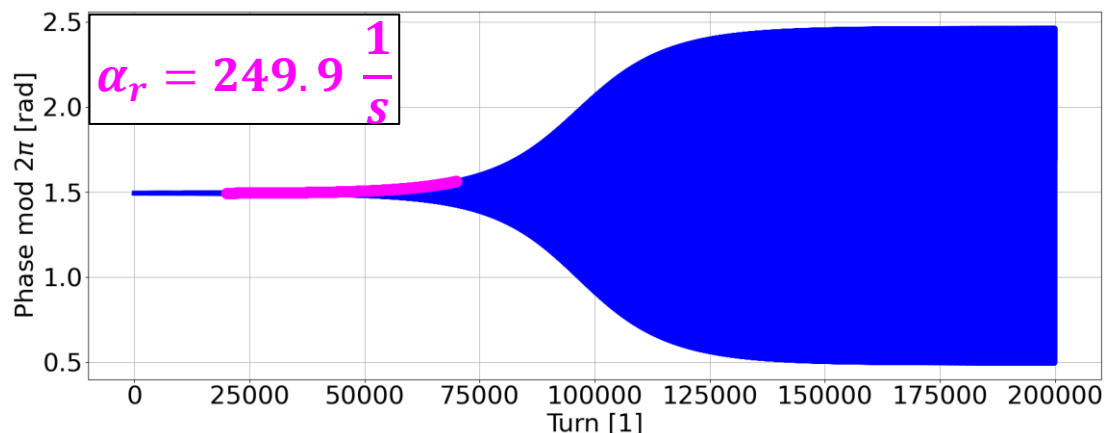
Synchrotron radiation +
broad-band impedances



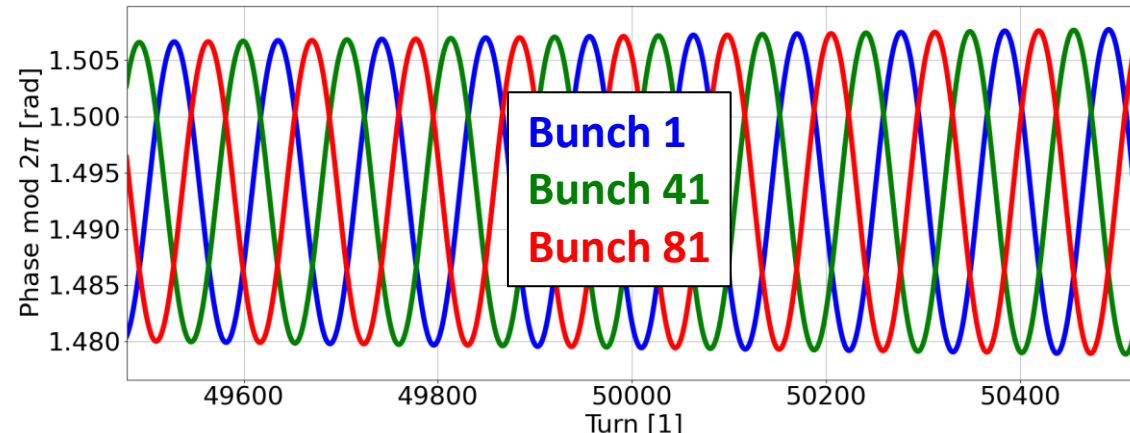
Example 1: coupled-bunch instability damped by the kicker (1/2)

- We assume the DAFNE parameters $U_0 = 8.88$ keV, $E_0 = 510$ MeV, $\hat{V}_{rf} = 130$ kV and $\alpha_0 = 0.018$.
- Moreover we assume that
 - three equally-spaced bunches with $I_b = 15$ mA, $\sigma_z = 10$ mm circulate in the machine.
 - At turn 0 the bunches are displaced by 0.25 mrad with respect to $\Delta\varphi_{HOM}$ (equal for all the bunches due to symmetry).
 - an HOM excites the coupled-bunch mode $\mu = 1$, $\Delta\varphi_1 = 2\pi/3$.
 - $R_s = 4000 \Omega$, $Q = 40000$;
 - An instability is obtained if $f_r = (3l - 2)f_0 + f_{s0}$, $l > 1$. We choose $l = 100$, therefore $f_r = 915.5$ MHz.
- We first simulate the three bunches without the feedback correction for 200000 turns. The kicker impedance is added to the HOM.
 - The oscillation-amplitudes are essentially the same for the three bunches.
 - The grow-rate computed analytically is 247.4 1/s which is in very good agreement with the one computed numerically.
 - As expected, the phase changes by 120° for consecutive bunches.

Phase evolution of bunch 1 and grow-rate from the exponential fit



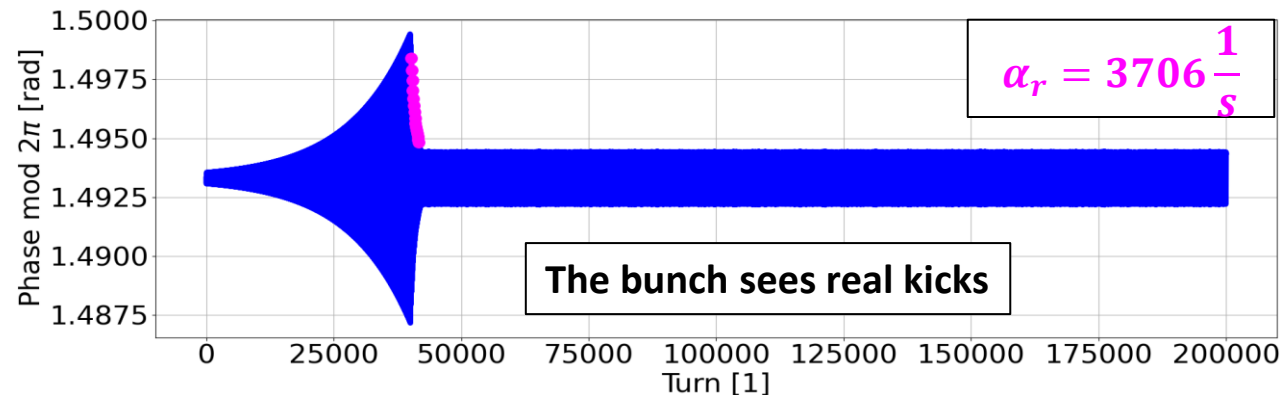
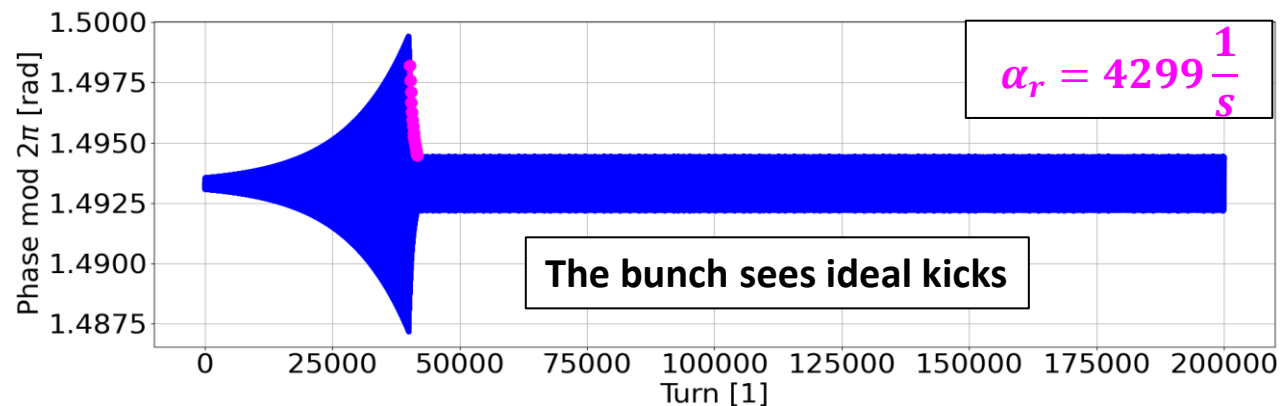
Zoom on the phase evolutions of the three bunches



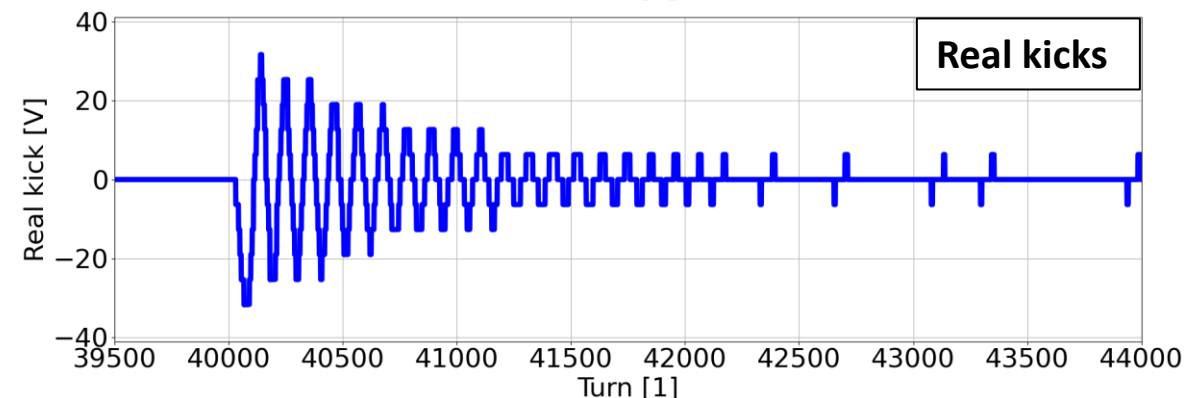
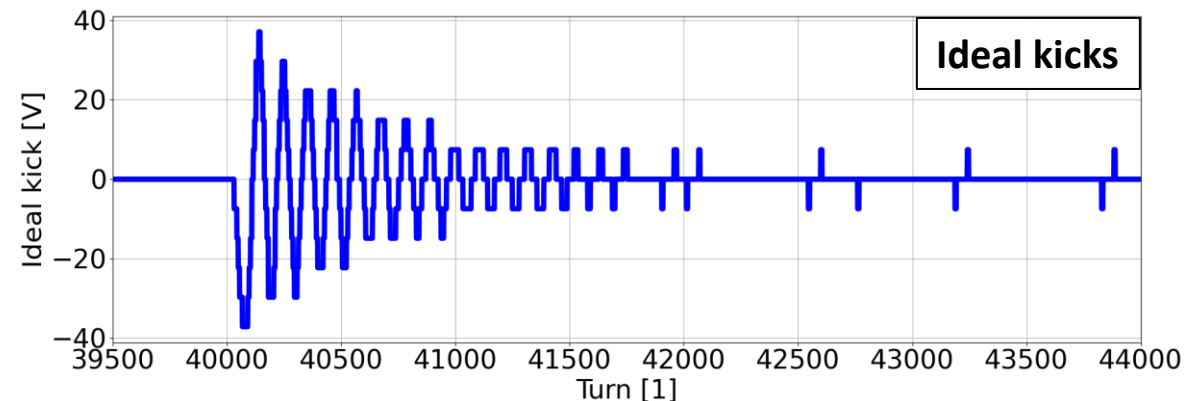
Example 1: coupled-bunch instability damped by the kicker (2/2)

- We then include the voltage corrections of the kicker, first assuming that the bunches see the ideal kicks $V_{FBkick,k}$.
 - The feedback acts only from turn 40000 onwards and produces essentially the same damping behaviour for the three bunches.
 - $N_{tap} = 16, d_{DSF} = 6$. The total feedback gain isn't too high, so that enough phase oscillations can be used to perform a proper fit.
 - The analytical damping rate of the feedback is 4536 1/s.
 - The total analytical damping rate is $(4536-247) 1/s = 4289 1/s$, which is in very good agreement with the numerical one.
- As expected, the damping rate decreases when the bunches see the real voltage-corrections, which in general are lower than the ideal ones.

Phase evolution of bunch 1 and grow-rate from the exponential fit.



Voltage kicks for the bunch 1.



Example 2: coupled-bunch instability damped by the feedback (1/2)

- As a second example we use operational/expected parameters for a DAFNE typical run.
 - Bunch current, length and peak RF voltage are taken from 2014 measurements.

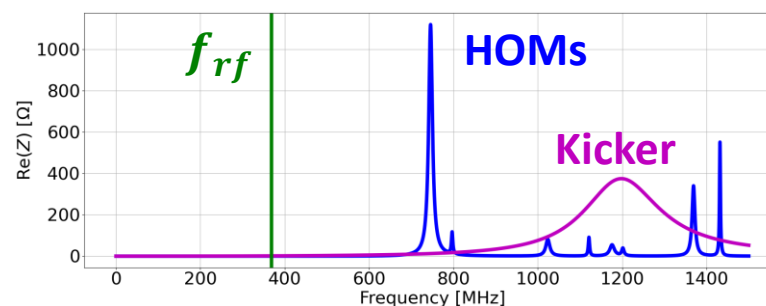
Main beam and machine parameters

Parameters	Values
Harmonic number h	120
Ring circumference C_r	97.587 m
Mom. compaction factor α_0	0.018
Nominal energy E_0	510 MeV
Revolution frequency f_0	3.07 MHz
RF frequency f_{rf}	368.65 MHz
Synchr. radiation energy loss U_0	8.88 keV
Peak RF voltage V_{rf}	130 kV
Zero-amplitude synchr. freq. f_{s0}	28.72 kHz
Beam filling pattern	105 contiguous bunches
RMS bunch length σ_z	19 mm
Bunch current I_b	19.5 mA

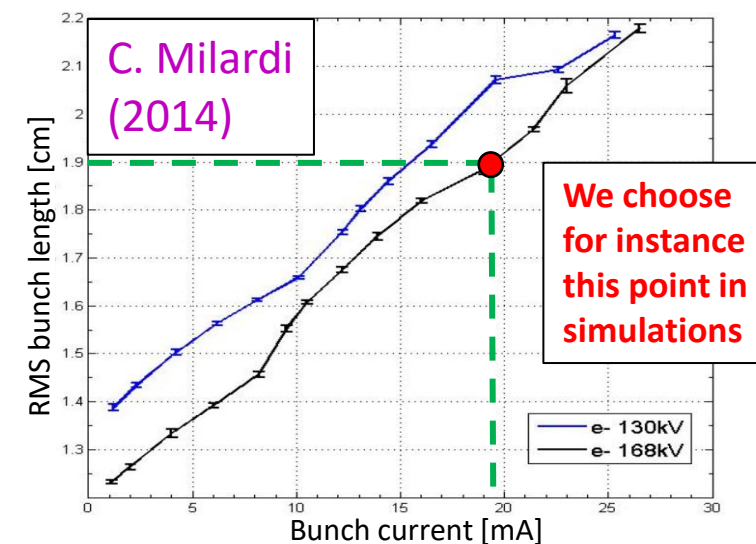
Some important feedback parameters

Parameters	Values
ADC number of bits $n_{bit,ADC}$	8
Max. ADC voltage $V_{max,ADC}$	200 mV
Number of taps N_{tap}	16
Down sampling factor d_{DSF}	6
Kicker resonant frequency f_r	$3.25f_{rf}$
Kicker quality factor Q	5.45
Kicker shunt impedance $R_{s,s}(f_r)$	750 Ω
Max. kicker voltage $V_{MAXkick}$	950 V

Beam-coupling impedances (HOMs + kicker)



Measurements of bunch length vs intensity

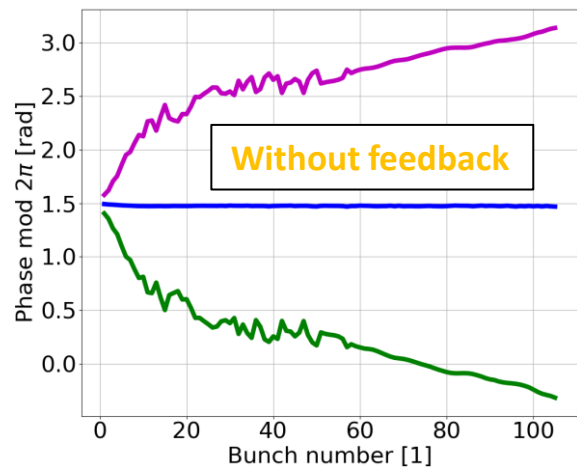


Parameters of waveguide-damped HOMs

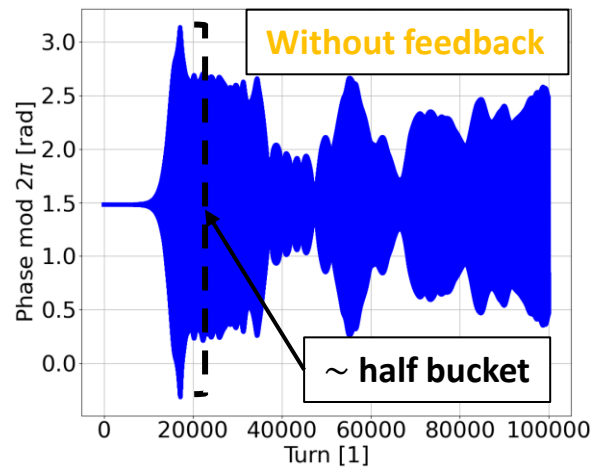
	f_r [MHz]	R_s [Ω]	Q
1	746	1120	70
2	797	105	210
3	1024	81	90
4	1121	90	300
5	1176	54	90
6	1201	36	180
7	1369	340	170
8	1432	550	550

Example 2: coupled-bunch instability damped by the feedback (2/2)

Min, mean and max bunch phase along 100000 turns

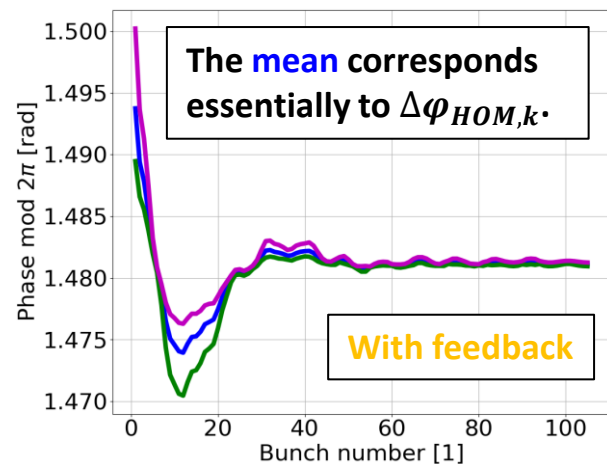


Phase evolution for the bunch 105

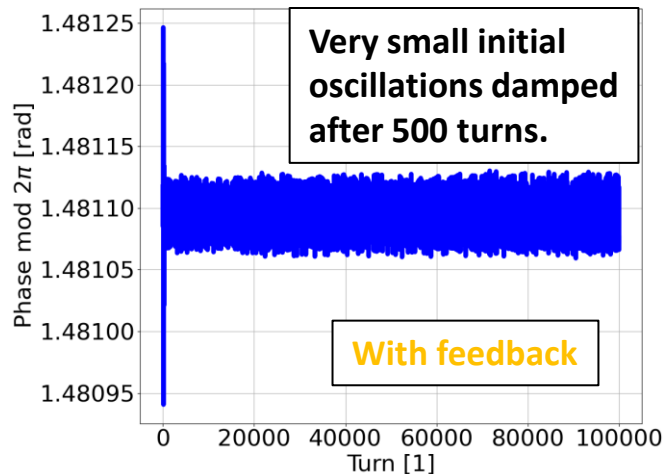


- 100000 turns are simulated, the maximum running time is just 16 minutes.
- The simulation outcomes depend on the bunches initial conditions.
 - Here the bunches start in $(\Delta\varphi_{HOM,k}, 0)$, so very small initial displacements due to non-perfect matching routine.
- Without feedback all the bunches are unstable and the maximum oscillation amplitude is essentially an increasing function of the bunch number.
 - The oscillation amplitude of the most unstable bunch (105) is half bucket at turn 17000, then non-linearities damp the growth.
- With feedback the oscillations are damped for all the bunches.
 - The feedback responds differently with different bunches.

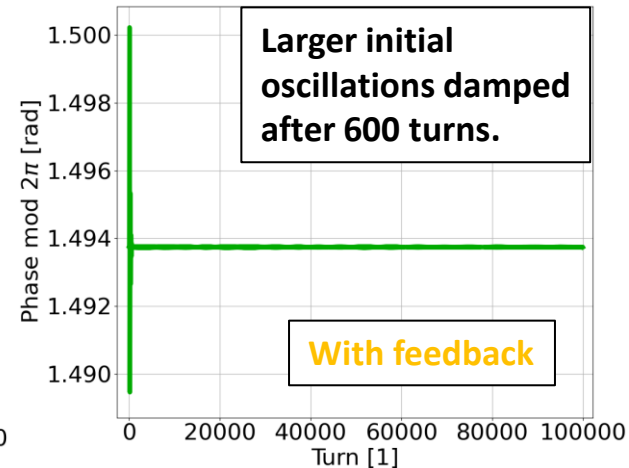
Min, mean and max bunch phase along 100000 turns



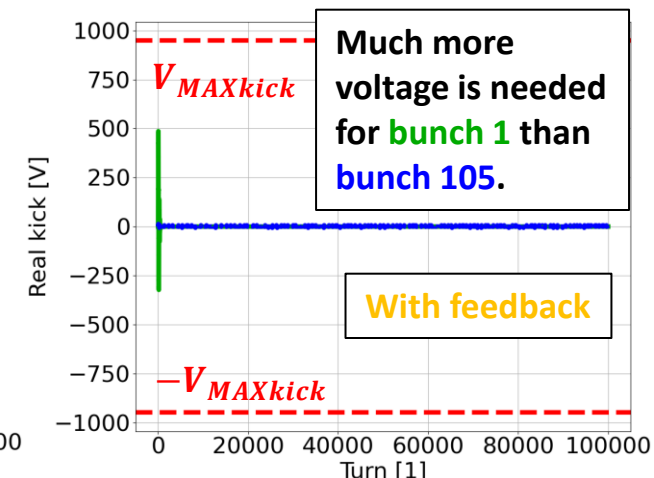
Phase evolution for the bunch 105



Phase evolution for the bunch 1



Kicker voltage evolution for the bunches 1 and 105



Contents

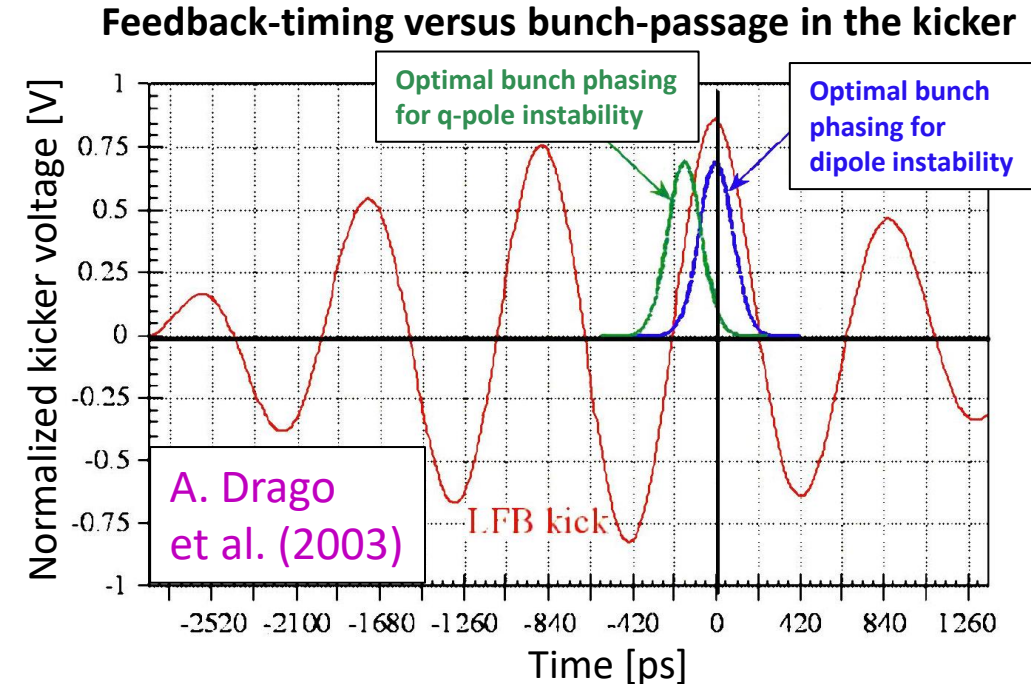
- ❑ Introduction.
- ❑ Single-particle longitudinal beam-dynamics with synchrotron radiation.
 - Equations of motion, synchrotron radiation, small-amplitude synchrotron oscillations, ...
- ❑ Longitudinal beam-dynamics with synchrotron radiation and Higher Order Modes (HOMs).
 - HOM induced voltage, synchronous phase shift, HOM initial conditions, coupled-bunch instabilities, ...
- ❑ Longitudinal beam-dynamics with synchrotron radiation, HOMs and bunch-by-bunch feedback.
 - Models of the feedback components, growth and damping-rates, cavity-kicker, ideal and real corrections, ...
- ❑ Conclusions and suggested next steps.
- ❑ Appendices.
 - Execution of the new-Python and old-Fortran codes, structure of the code, exponential fits in Python, ...
- ❑ References.

Conclusions

- ❑ The new Python code is ready to be used for longitudinal beam-dynamics simulations of the DAFNE accelerator.
 - The current version is able to simulate coupled-bunch instabilities and the effects of the bunch-by-bunch feedback.
 - Some important improvements to the code can still be done (see next slide).
- ❑ This presentation covered in detail all the features of the code.
 - The theoretical principles required to fully understand the code were explained in depth.
 - Numerous examples with plots and animations were provided to demonstrate the code capabilities.
- ❑ Several benchmarks between simulations and analytical formulas were performed to prove the code reliability.
 - In particular we found good agreements concerning grow-rates of coupled-bunch instabilities and feedback damping-rates.
- ❑ Some additional functionalities were added to the new code, for instance
 - Computation of the synchronous phases taking into account the beam-induced voltages. This allows for instance
 - the matching of the beam with respect to the induced voltages;
 - the feedback compensation of the synchronous-phase shifts due to induced-voltages.
 - Inclusion of the cavity-kicker beam-coupling impedance in simulation.
- ❑ Some new studies were performed, for example
 - Accurate models of the signal manipulations performed by the feedback-system (pickup, comb generator, mixer, ...).
 - In particular, measurements of the comb-generator transfer-function were needed to properly model the bursts generation.
 - Optimized design of the FPGA sinusoidal filter and determination of the optimal down-sampling-factor.
- ❑ Preliminary simulations of DAFNE operational scenarios were performed confirming the importance of the feedback for beam stability.

Suggested next steps

- ❑ The work presented here isn't definitive, in particular the following next steps can be done.
- ❑ Implementation in the Python code of the RF feedback for the compensation of beam-loading in the accelerating cavity.
 - This feedback is required to reduce the significant beam-coupling impedance of the fundamental mode.
 - This feedback is already implemented in the Fortran code and its effects have already been studied in simulation in the past.
 - Simulations without this feedback assume that the beam-loading is perfectly compensated.
- ❑ Benchmarks between simulations and beam measurements taken during the next 2021 DAFNE run.
 - This would confirm that the models and assumptions used in the code are accurate enough.
- ❑ Extension of the code to represent each bunch with millions of macroparticles so that more realistic simulations can be performed.
 - The effects of arbitrary beam-coupling impedances could be studied.
 - Other types of instabilities, already observed in measurements, could be seen also in simulation, for instance
 - Microwave: it's caused by short-range wakefields with wavelengths much shorter than the bunch length. It leads to bunch-lengthening and beam-quality degradation.
 - Longitudinal quadrupole (q-pole): it's probably caused by the broadband machine-impedance and can be cured delaying the kicker correction signal with respect to the bunch passage.
 - However multi-bunch simulations with 105 bunches are cumbersome.
 - The code must be optimized and parallelized following for instance the example of the CERN BLonD code.



Contents

- ❑ Introduction.
- ❑ Single-particle longitudinal beam-dynamics with synchrotron radiation.
 - Equations of motion, synchrotron radiation, small-amplitude synchrotron oscillations, ...
- ❑ Longitudinal beam-dynamics with synchrotron radiation and Higher Order Modes (HOMs).
 - HOM induced voltage, synchronous phase shift, HOM initial conditions, coupled-bunch instabilities, ...
- ❑ Longitudinal beam-dynamics with synchrotron radiation, HOMs and bunch-by-bunch feedback.
 - Models of the feedback components, growth and damping-rates, cavity-kicker, ideal and real corrections, ...
- ❑ Conclusions and suggested next steps.
- ❑ Appendices.
 - Execution of the new-Python and old-Fortran codes, structure of the code, exponential fits in Python, ...
- ❑ References.

Computation of the decay rate of an oscillating function (1/3)

- ❑ Python is used to evaluate the grow-rate of an oscillating increasing or decreasing function
 - The first used routine `scipy.signal.find_peaks` is able to find all the local maxima of a given signal.
 - The second used routine `scipy.optimize.curve_fit` is able to fit the local maxima with an exponential function.

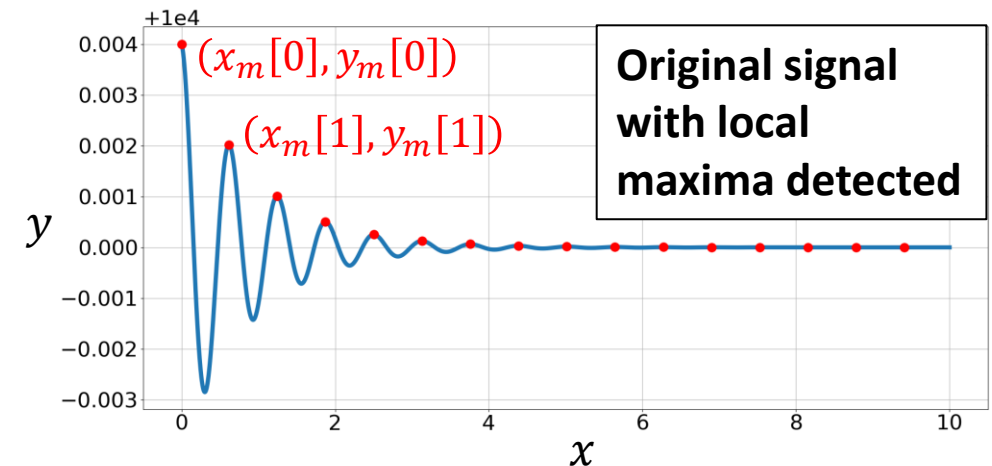
- ❑ **Example:** our original signal $y(x)$ is made of samples from

$$Y(x) = 0.004e^{-1.1x} \cos(10x) + 10000 \quad x \in [0,10]$$

- The envelope traversing the local maxima of $Y(x)$ has equation

$$L(x) = Ae^{Bx} + C = 0.004e^{-1.1x} + 10000$$

- ❑ We assume that $Y(x)$ and $L(x)$ aren't known. **The goal is to find the decay rate of the signal**, i.e. the value $B = -1.1$.



- ❑ **The first step is to find the local maxima of $y(x)$ with the `find_peaks` routine.** The output arrays are x_m and y_m (length N).
 - A check has to be done on $(x[0], y[0])$ which can belong to the envelope or not depending on the specific case.
 - If $y[0] > y[1]$ and $y[0] > y_m[1]$, then $(x[0], y[0])$ belongs to the envelope (as in our example).
- ❑ **The second step is to fit the points $(x_m[i], y_m[i])$ with the `curve_fit` routine, aiming at finding A , B and C of $L(x)$.**
 - The exponential function to be used for the fit is

$$M(x) = ae^{bx} + c$$

- where a , b and c are the three parameters to be determined.

Computation of the decay rate of an oscillating function (2/3)

□ The `curve_fit` routine needs as input the initial guesses for a , b and c , which we call a_0 , b_0 and c_0 .

➤ If these guesses are too far from A , B and C , then the routine provides unacceptable results.

➤ **First method to find a_0 , b_0 and c_0 :**

- $c_0 = \langle y \rangle$, where $\langle y \rangle$ is the mean of the y array. Indeed, for large x , $L(x) \approx C$ and also $L(x) \approx \langle y \rangle$.
- a_0 and b_0 are easily found solving the system

$$\begin{cases} y_m[0] = a_0 e^{b_0 x_m[0]} + c_0 \\ y_m[1] = a_0 e^{b_0 x_m[1]} + c_0 \end{cases} \quad \Rightarrow \quad b_0 = \frac{\ln \frac{y_m[0] - c_0}{y_m[1] - c_0}}{x_m[0] - x_m[1]} \quad a_0 = (y_m[0] - c_0) e^{-b_0 x_m[0]}$$

➤ **Second method to find a_0 , b_0 and c_0 (from Jacquelin J. "Regressions et equations integrals", 2014):**

- More general method which doesn't need the y array but only x_m and y_m .

$$S_1 = 0, k = 2, \dots, N$$

$$1) \quad S_k = S_{k-1} + \frac{1}{2} (y_m[k-1] + y_m[k-2]) (x_m[k-1] - x_m[k-2])$$

$$2) \quad D = \begin{pmatrix} \sum_{k=1}^N (x_m[k-1] - x_m[0])^2 & \sum_{k=1}^N (x_m[k-1] - x_m[0]) S_k \\ \sum_{k=1}^N (x_m[k-1] - x_m[0]) S_k & \sum_{k=1}^N S_k^2 \end{pmatrix}^{-1}$$

$$3) \quad b_0 = D[1,0] \sum_{k=1}^N (y_m[k-1] - y_m[0]) (x_m[k-1] - x_m[0]) + D[1,1] \sum_{k=1}^N (y_m[k-1] - y_m[0]) S_k$$

$$4) \quad \begin{cases} y_m[0] = a_0 e^{b_0 x_m[0]} + c_0 \\ y_m[1] = a_0 e^{b_0 x_m[1]} + c_0 \end{cases} \quad \Rightarrow \quad \begin{aligned} a_0 &= \frac{y_m[0] - y_m[1]}{e^{b_0(x_m[0]-x_m[1])}} \\ c_0 &= y_m[0] - a_0 e^{b_0 x_m[0]} \end{aligned}$$

Computation of the decay rate of an oscillating function (3/3)

□ Aiming at finding $A = 0.004$, $B = -1.1$, $C = 10000$, the `curve_fit` routine provides as results

➤ **1st method:** $a_0 = 3.996 \cdot 10^{-3}$, $b_0 = -1.111$, $c_0 = 1.000 \cdot 10^4$ ➡ $a = 3.998 \cdot 10^{-3}$, $b = -1.106$, $c = 1.000 \cdot 10^4$

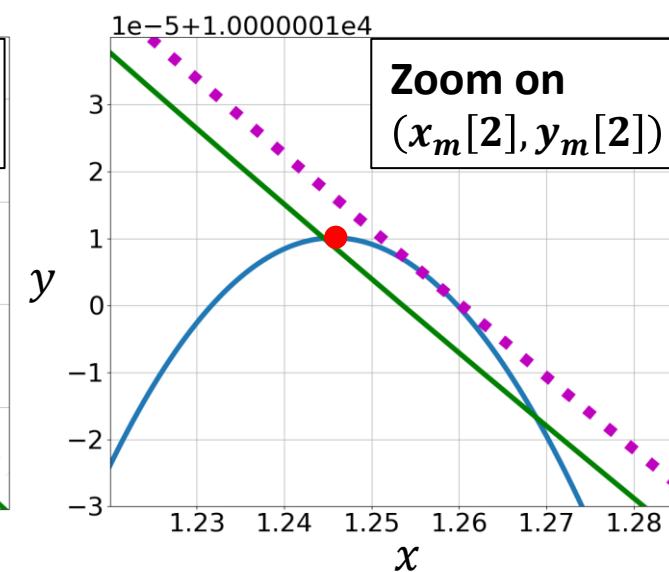
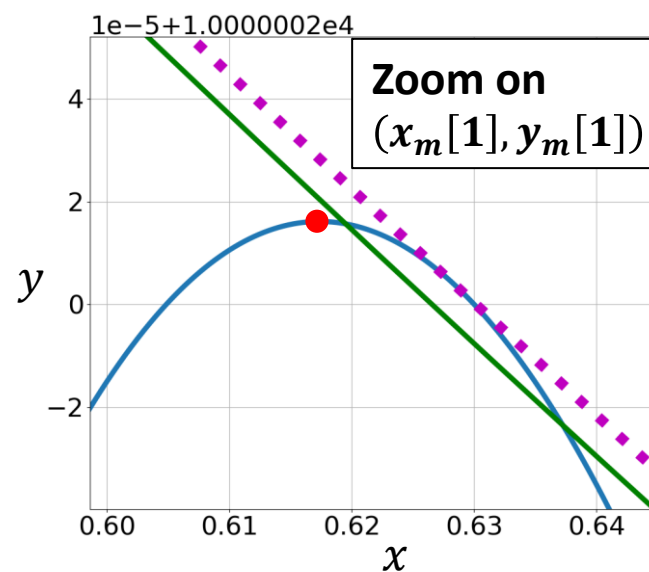
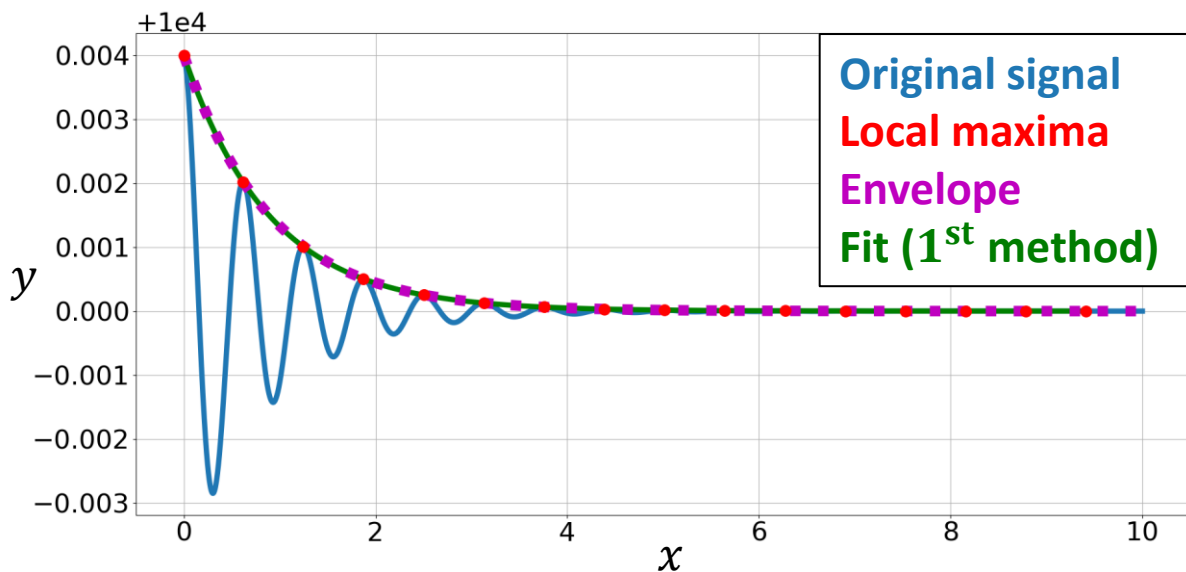
➤ **2nd method:** $a_0 = 1.105 \cdot 10^{-3}$, $b_0 = -0.949$, $c_0 = 1.000 \cdot 10^4$ ➡ $a = 3.998 \cdot 10^{-3}$, $b = -1.102$, $c = 1.000 \cdot 10^4$

□ Both methods provide initial guesses relatively close to A , B and C .

➤ This allows the `curve_fit` routine to work properly and provide results very close to A , B and C .

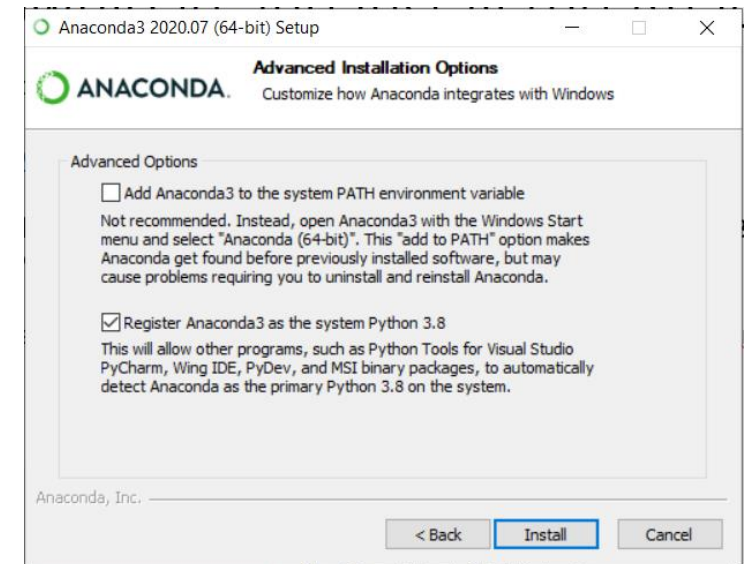
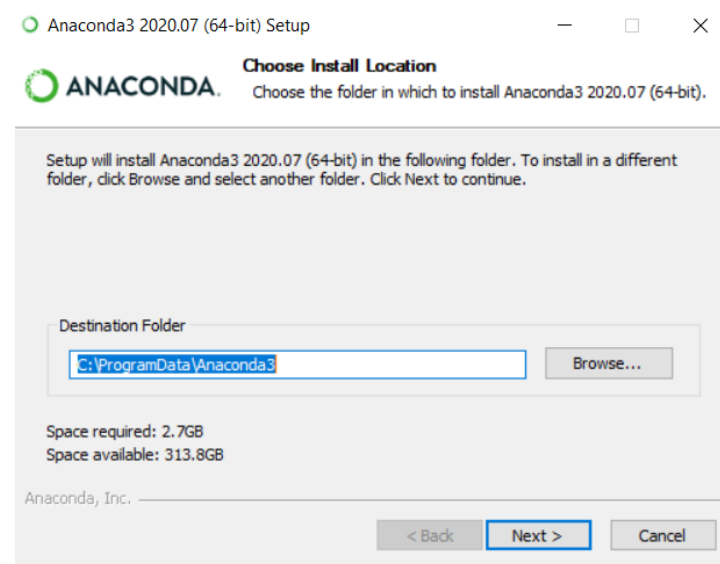
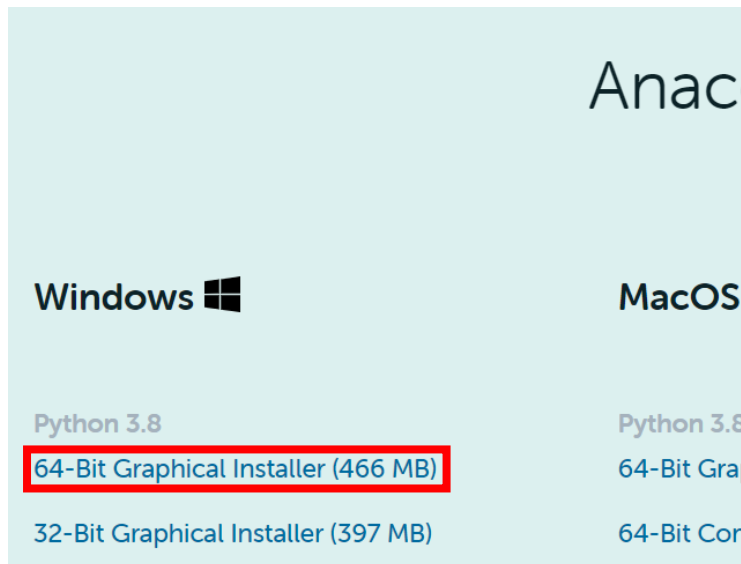
□ Note that the envelope $L(x)$ doesn't cross the local maxima but it crosses points at the right of them.

➤ The fit, which tends to be close to the local maxima, is below the envelope. This explains why a is slightly smaller than A .



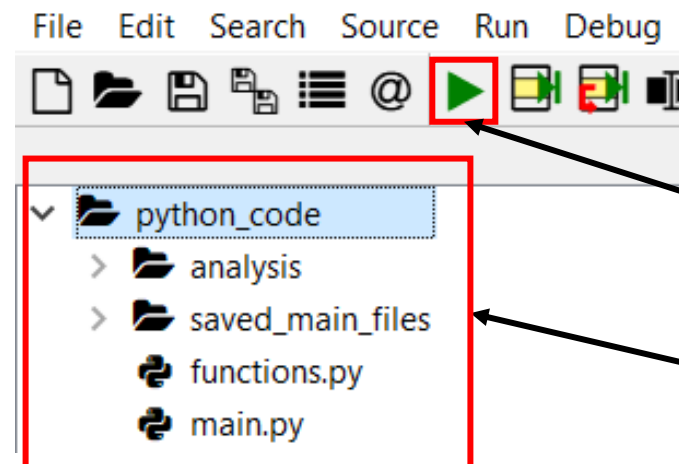
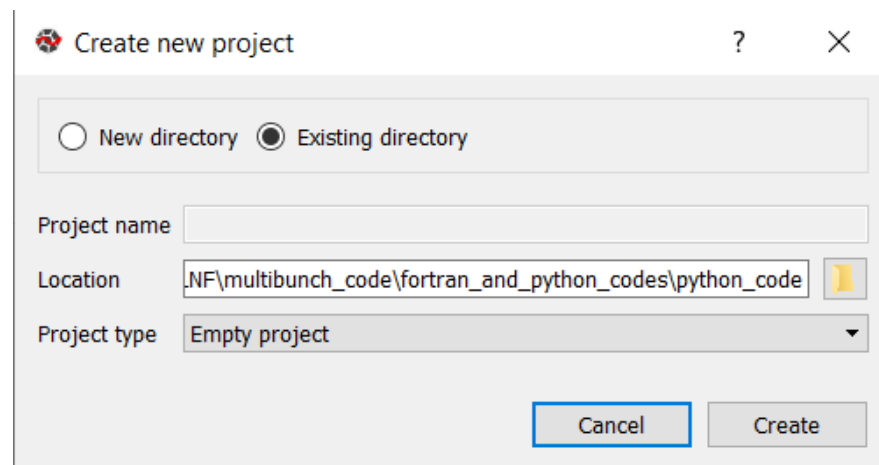
Python code: download and installation of the Anaconda distribution

- ❑ The open-source Anaconda Python distribution with its Spyder editor can be used. The following instructions are for Windows 10, 64 bit.
- ❑ Go to <https://www.anaconda.com/products/individual>.
- ❑ In the 'Anaconda Installers' section, in the 'Windows' column, click on '64-Bit Graphical Installer' and download the executable of around 500 MB.
- ❑ During the installation procedure
 - Select the 'Destination Folder', e.g. 'ProgramData\Anaconda3'.
 - In 'Advanced Options', mark only 'Register Anaconda...' and click Install.



Python code: creation of a new Spyder project and import

- ❑ After the Anaconda installation, the Spyder editor is available.
- ❑ Search for Spyder in your PC typing 'Spyder (Anaconda 3)' into the search box.
 - When found, you can also pin it to the Taskbar with a right click for an easier access.
- ❑ Open Spyder and go to 'Projects -> New Project...'.
 - Mark 'Existing directory'.
 - Click on the folder icon in the field 'Location' and select the 'python_code' folder.
 - The 'python_code' folder can be anywhere.
 - Leave 'Empty project' in the 'Project type' field and click on Create.
- ❑ All the files of the Python code are now accessible inside Spyder from the Management panel on the left.
 - In general Python files can be easily run clicking on the green-triangle icon.



Button to run
Python files

Management panel

Python code: structure

❑ The folder 'analysis' contains several Python files useful to perform analyses and computations.

- Example of file: signal manipulations from the longitudinal pick-up to the mixer.
- Each file can be run independently of the others.
- All these files are like 'add-ons' with respect to the main code: they aren't essential to launch simulations with the main code and they don't affect the main code.

❑ The folder 'saved_main_files' contains main-files which the user saved in order to be able to relaunch the corresponding simulations later on.

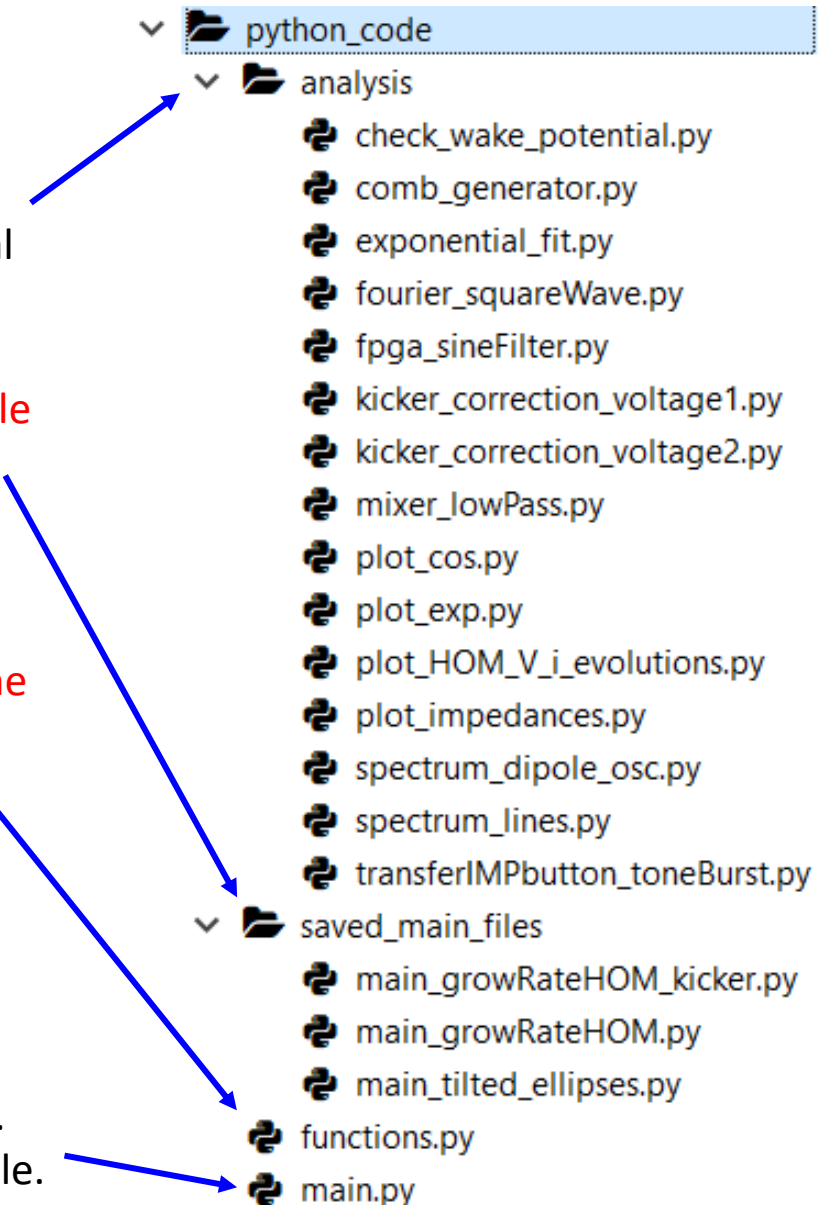
- Example of saved main-file: simulation of a certain coupled-bunch instability for three equally-spaced bunches in DAFNE.

❑ The file 'functions.py' contains several essential routines which are called and used in the main files and also in the files contained in the 'analysis' folder.

- Examples of functions: generation of beam matched with collective effects, computation of kicker voltage-corrections and of voltages due to the HOMs.
- All these functions aren't supposed to be run directly.

❑ The file 'main.py' is the main-file which should be run to perform a simulation.

- Once a simulation is well set up, the user can decide to copy this file into the 'saved_main_files' folder and rename the copied file with a more significant name.
- The input-parameters for the simulation should be specified directly in this main-file.
- This main-file directly provides all the simulation outputs.



Python code: example of input-parameters in the main file

□ Essentially four types of input-parameters must be set in the main file:

- **Machine parameters:** harmonic number, circumference, momentum compaction, nominal energy, peak RF voltage, ...
- **Beam properties:** filling scheme, bunch charge and standard-deviation, initial displacements with respect to the synchronous phases.
- **Impedance parameters:** boolean variables to include HOMs and kicker impedances in simulation, parameters of the HOMs, possibility to match with collective effects either the entire beam or all the bunches except one for injection-transient studies, ...
- **Bunch-by-bunch feedback parameters:** boolean variable to turn the feedback on, how many turns to wait for the feedback action, different gains, computation of optimal filter coefficients, possibility to apply the ideal or the real voltage-corrections to the bunches, ...

```

### Beam properties
configuration_beam = 2 # filled_buckets contains the indices of
if configuration_beam == 1: # 30 equally-spaced bunches minus the
    filled_buckets = np.arange(1,h,4)
    filled_buckets = np.delete(filled_buckets, [1])
elif configuration_beam == 2: # typical DAFNE filling pattern (1,31,62)
    filled_buckets = np.arange(1,106)
elif configuration_beam == 3: # 30 equally-spaced bunches (1,5,9,13,17,21,25,29)
    filled_buckets = np.arange(1,h,4)
elif configuration_beam == 4:
    filled_buckets = np.arange(1,h,4)
    filled_buckets = np.insert(filled_buckets, [1,30], [2,120])
elif configuration_beam == 5:
    filled_buckets = np.arange(1,h,4)
    filled_buckets = np.insert(filled_buckets, [1,30], [2,120])
    filled_buckets = np.delete(filled_buckets, [0])
elif configuration_beam == 6: # one bunch (1)
    filled_buckets = np.arange(1,2)
elif configuration_beam == 7: # 4 equally-spaced bunches (1,31,62,93)
    filled_buckets = np.arange(1,h,30)
current_per_bunch = 15e-3 # [A] current per bunch
sigma_z = 18.8e-3 # [m] std of the Gaussian profile, needed only
positions_PhaseShifts_wrt_phiS = np.array([1]) # which bunches to
PhaseShifts_wrt_phiS = np.array([0]) # [rad] phase shifts for the
positions_deltaShifts_wrt_0 = np.array([]) # which bunches to de
deltaShifts_wrt_0 = np.array([]) # [1] delta shifts for these bu

```

```

### Machine
h = 120 # [1] Ha
Cring = 97.587 #
alpha = 0.018 #
E0 = 510e6 # [e
U0 = 8.88e3 # [
# se
V_max = 1.3e5 #
n_turn = 10000 #

```

```

### Impedance parameters
HOM_induced_voltage = True
include_kicker_impedance = True
if HOM_induced_voltage:
    table_modes = np.array([[ 745.7, 16, 24000, 70], #
                             [ 796.8, 0.5, 40000, 210],
                             [1023.6, 0.9, 28000, 90],
                             [1121.1, 0.3, 12000, 300],
                             [1175.9, 0.6, 5000, 90],
                             [1201.5, 0.2, 9000, 180],
                             [1369.0, 2.0, 5000, 170],
                             [1431.7, 1.0, 4000, 550]])
HOM_initially_unloaded = False # if False, it comput
overwrite_phiSR_with_phiHOM = True # if True, the in
bunch_to_neglect_in_matching = [] # Leave [] if you
number_iterations = 100 # number of iterations for t
# Parameters for the evaluation of the analytical HO
compute_grow_rate_HOM = True # Boolean to evaluate o
mu = 0
lmax = 100
index_bunch = 0
qmax = 10000
l1 = -66
overwrite_fsn_with_fs0 = False

```

```

### Feedback with cavity-kick
feedback = False # boolean fo
ntfb = 1 # number of turns af
zb = 0.43 # [Ohm] abs of butt
gp = 1 # [1] attenuation-leve
gc = 0.25 # [1] attenuation-l
ga = 2e2 # [1] gain of the an
ga2 = 1 # [1] gain of the amp
gm = 0.5 # [1] mixer convers
gl = 6 # [1] harmonic of the
dphcou = 0 # [rad] initial co
pccoup = 0 # [%] coupling fac
dphlo = 0 # [rad] phase error
compensate_dphHOM = False # b
percnoi = 0 # [%] noise coeff
vmaxadc = 0.2 # [V] maximum t
nbitdac = 8 # number of bits
downsampling = 'auto' # optio
if downsampling == 'auto':
    nc = 16 # number of taps
if downsampling == 'manual':
    nc = 16 # number of taps
    dsf = 6 # down sampling j
    phi_2 = 0 # phase offset
gdsp = 0.1 # FIR gain in the
gdac = 0.5 # DAC gain
nbitdac = 8 # number of bits
kicker_bandwidth = 220e6 # [F
fres_fRF = 3.25 # [1] kicker
kicker_max_Rss = 750 # [Ohm]
max_ampl_power = 600 # [W] ma
kickextRF = 3.25 # [1] kicker
kicker_Rss = 750 # [Ohm] kick
phi_e = 0 # [rad] kicker-gene
true_kick = False # boolean t

```

Fortran code: download of Code Blocks

- ❑ The open-source Code Blocks can be used as editor. The following instructions are for Windows 10, 64 bit.
- ❑ Go to <http://www.codeblocks.org/>, click on 'Downloads', then on 'Download the binary release'.



- ❑ We need a version which contains the compiler MinGW, i.e. 'codeblocks-20.03mingw-setup.exe'.

- ❑ Click on FossHUB and download the 'Code Blocks Windows 64 bit (including compiler)' version.



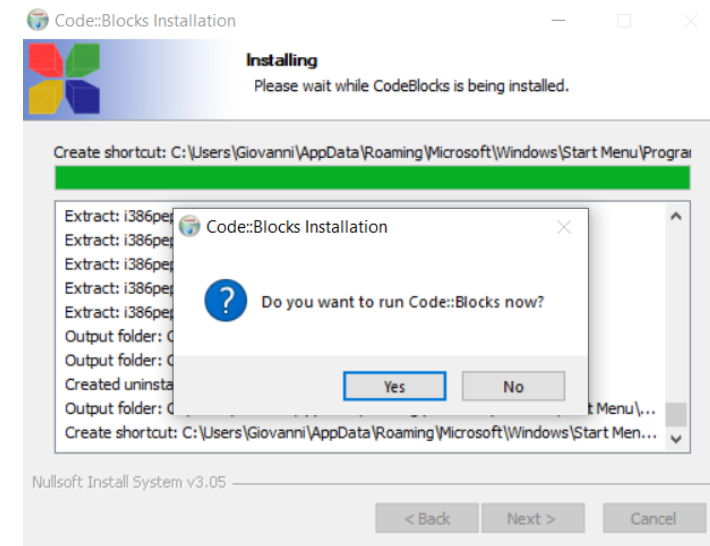
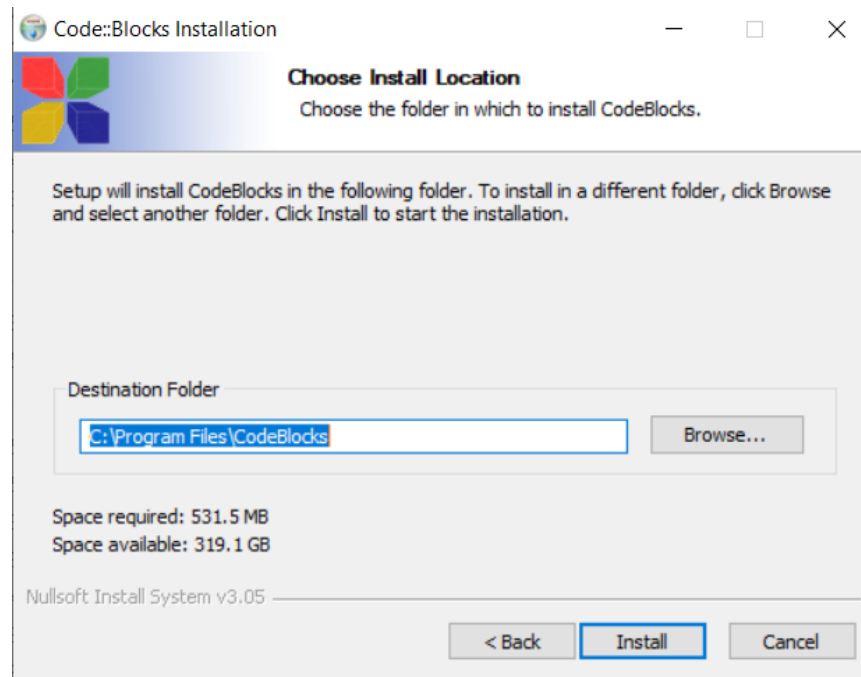
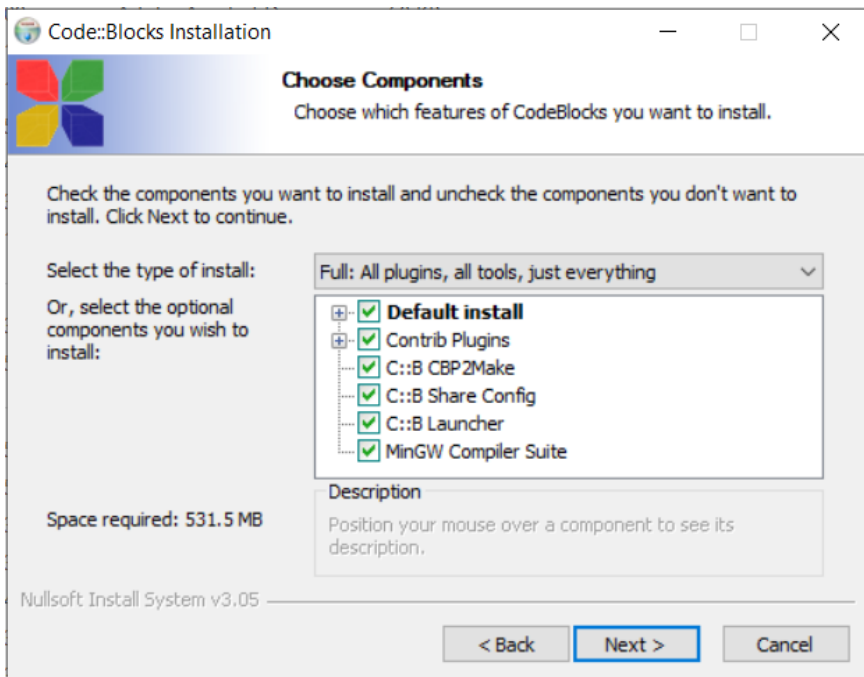
Windows XP / Vista / 7 / 8.x / 10:

DOWNLOAD
Code Blocks Windows 64 bit (including compiler)

File	Date	Download from
codeblocks-20.03-setup.exe	29 Mar 2020	FossHUB or Sourceforge.net
codeblocks-20.03-setup-nonadmin.exe	29 Mar 2020	FossHUB or Sourceforge.net
codeblocks-20.03-nosetup.zip	29 Mar 2020	FossHUB or Sourceforge.net
codeblocks-20.03mingw-setup.exe	29 Mar 2020	FossHUB or Sourceforge.net
codeblocks-20.03mingw-nosetup.zip	29 Mar 2020	FossHUB or Sourceforge.net
codeblocks-20.03-32bit-setup.exe	02 Apr 2020	FossHUB or Sourceforge.net
codeblocks-20.03-32bit-setup-nonadmin.exe	02 Apr 2020	FossHUB or Sourceforge.net
codeblocks-20.03-32bit-nosetup.zip	02 Apr 2020	FossHUB or Sourceforge.net
codeblocks-20.03mingw-32bit-setup.exe	02 Apr 2020	FossHUB or Sourceforge.net
codeblocks-20.03mingw-32bit-nosetup.zip	02 Apr 2020	FossHUB or Sourceforge.net

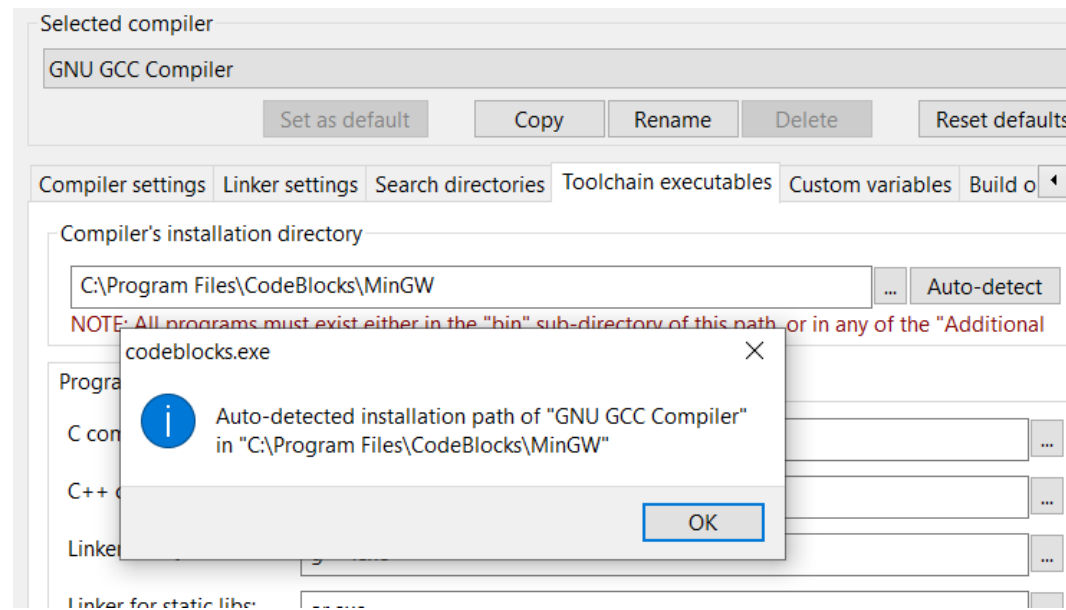
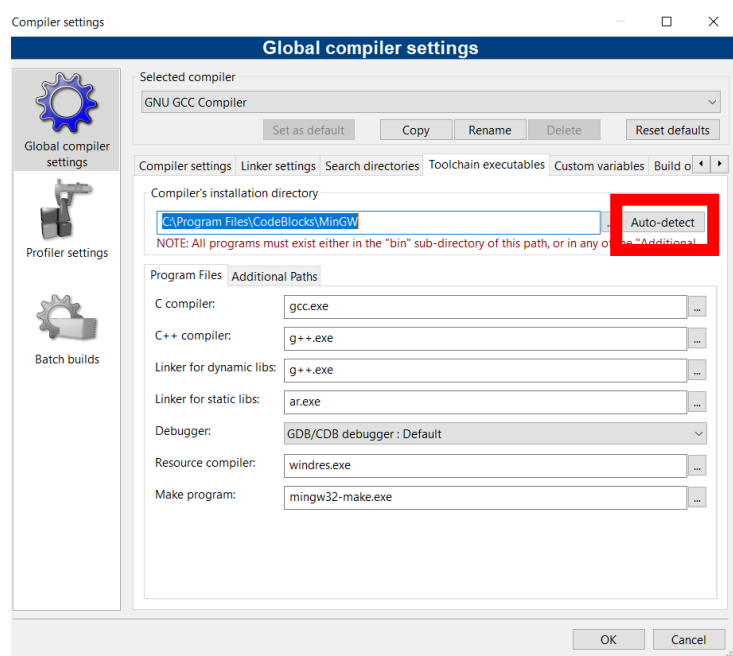
Fortran code: installation of Code Blocks

- ❑ Now we need to install Code Blocks. Click on the downloaded executable of around 150 MB.
- ❑ If possible, install all the components (Full).
- ❑ Choose the destination folder (Program Files is OK)
- ❑ Open Code Blocks at the end of the installation.



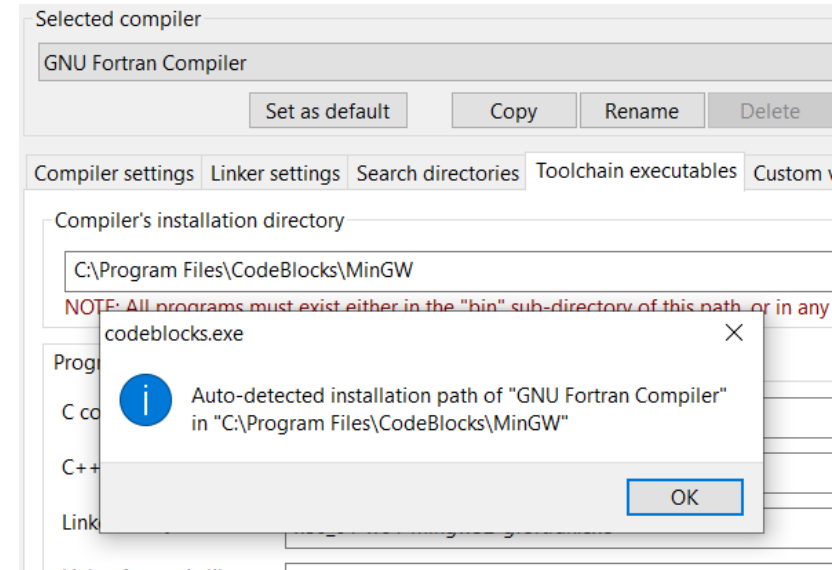
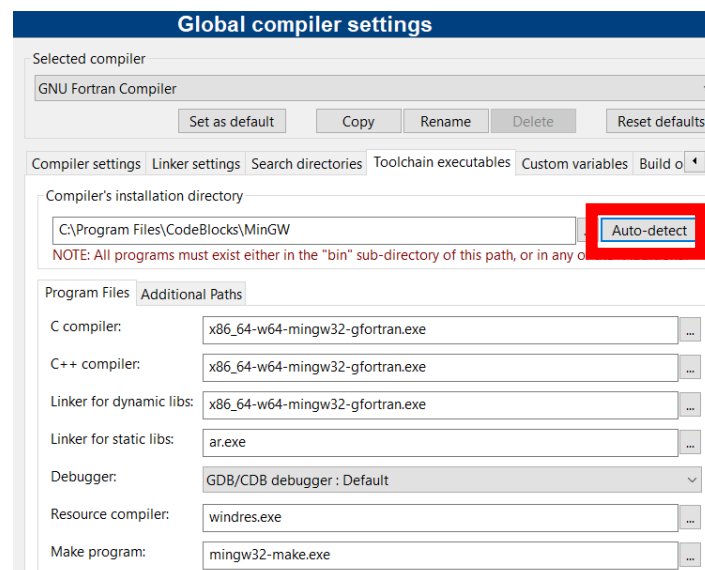
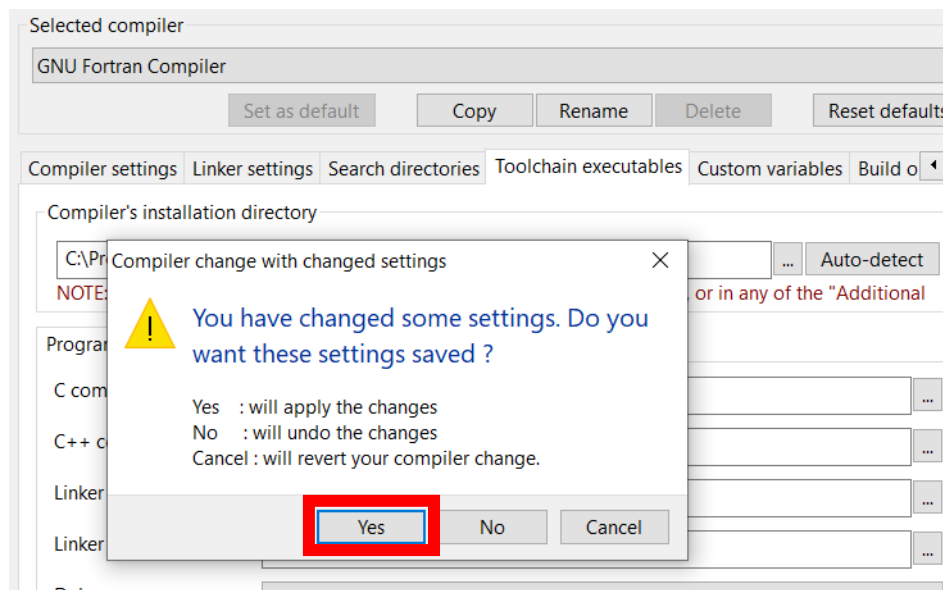
Fortran code: setting of the GNU GCC compiler

- ❑ Inside Code Blocks, go to 'Settings -> Compiler...'
- ❑ Choose 'GNU GCC Compiler' in 'Selected compiler'.
- ❑ Go to 'Toolchain executables'.
- ❑ In 'Compiler's installation directory', type the path of the 'MinGW' subfolder present in the Code Blocks installation directory.
- ❑ Click on 'Auto-detect'. A window appears reporting that the 'GNU GCC Compiler' has been found. Click OK.



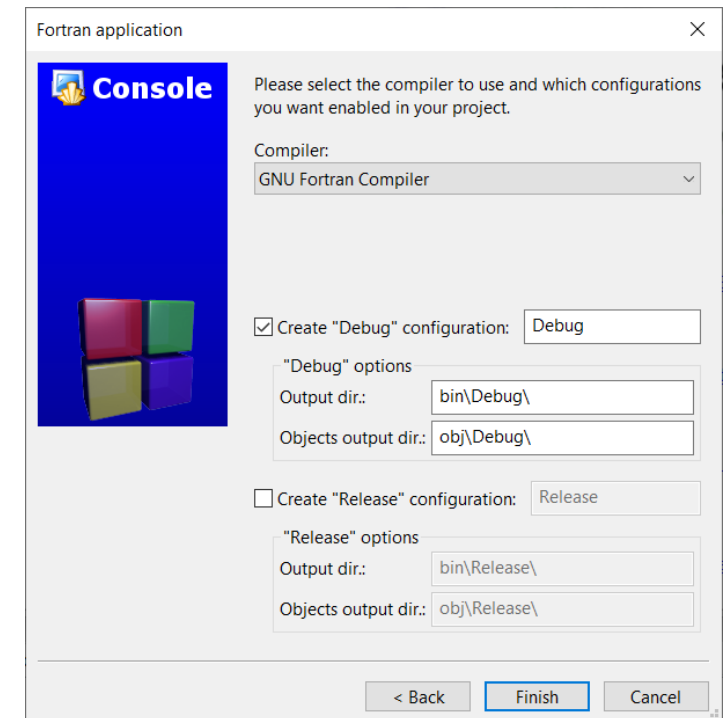
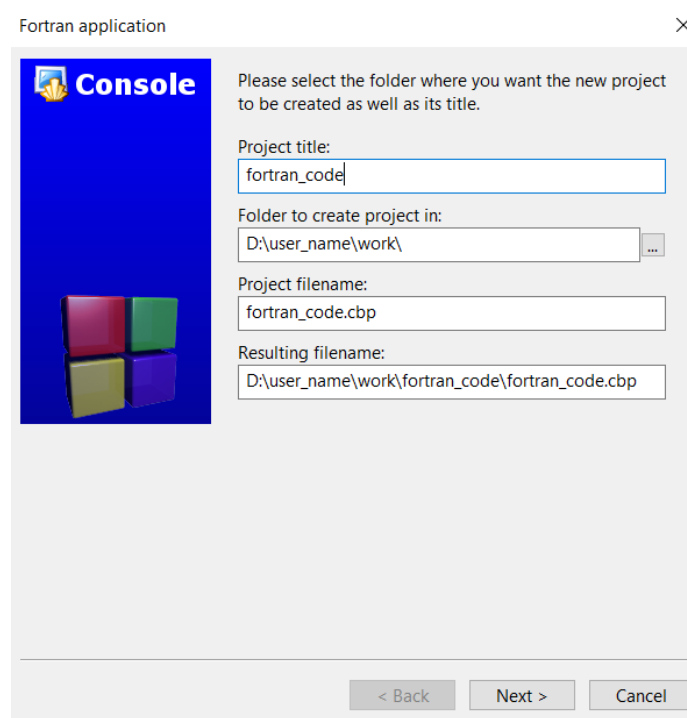
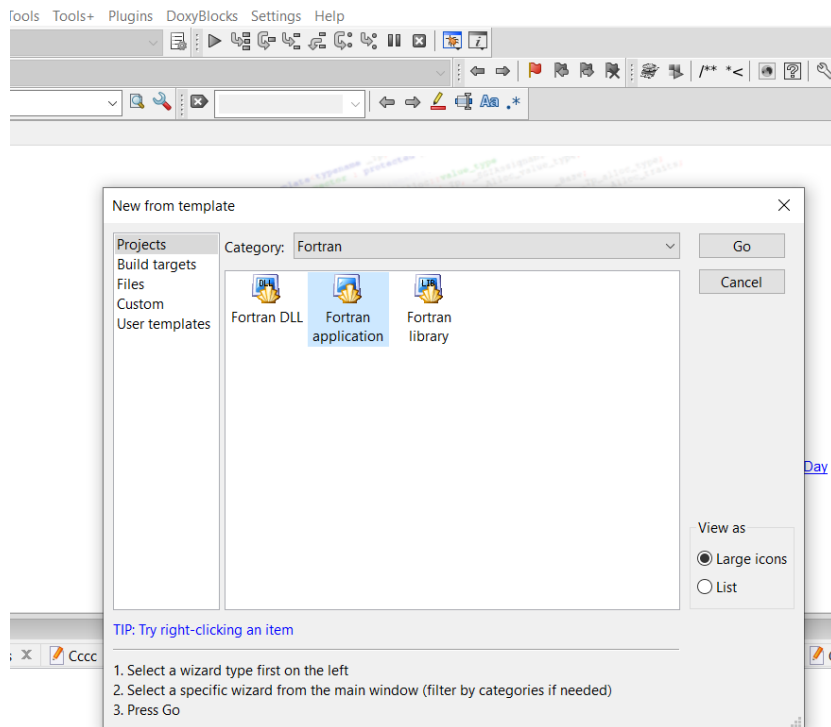
Fortran code: setting of the GNU Fortran compiler

- ❑ Choose 'GNU Fortran Compiler' in 'Selected compiler'.
- ❑ Save the applied changes when asked.
- ❑ Go to 'Toolchain executables'.
- ❑ In 'Compiler's installation directory', type the path of the 'MinGW' subfolder present in the Code Blocks installation directory.
- ❑ Click on 'Auto-detect'. A window appears reporting that the 'GNU Fortran Compiler' has been found. Click OK and again OK.



Fortran code: creation of a new project

- ❑ Inside Code Blocks, go to 'File -> New -> Project...'
- ❑ In 'Category' select Fortran and click on Fortran application.
- ❑ In the 'Fortran application' window,
 - choose the name of the project in 'Project title', e.g. 'fortran_code'.
 - choose the folder where to store the project and click Next.
 - In 'Compiler' select 'GNU Fortran Compiler' and mark 'Create "Debug" configuration'. Click on Finish.

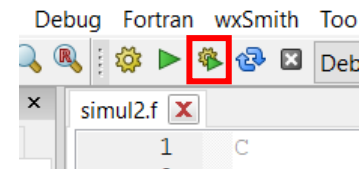
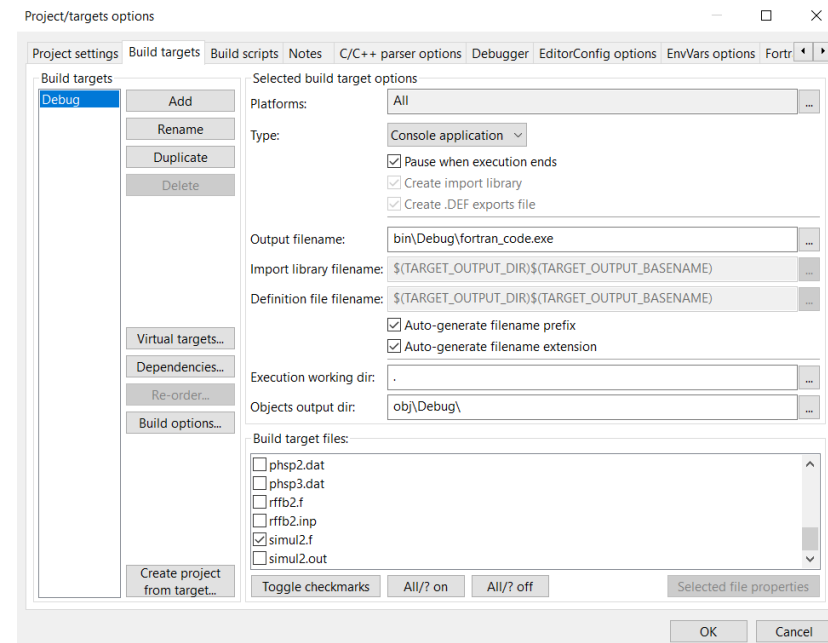
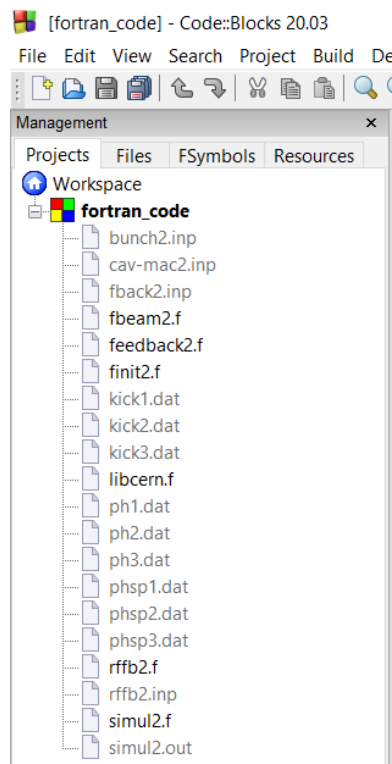


Fortran code: import, build-targets and simulation run

- Copy all the files from the folder 'fortran_code_original' into the folder 'fortran_code' just created.
 - Delete the file main.f90 from the folder 'fortran_code'.
- Inside Code Blocks, in the Management panel -> Projects,
 - Right click on main.f90 and 'Remove file from project'.
 - Right click on 'fortran_code' and 'Add files recursively...'
 - Select the folder 'fortran_code'.
 - Select all the files and click OK.
- Inside Code Blocks, in the Management panel -> Projects,
 - Right click on 'fortran_code' and 'Properties...'
 - Go to the tab 'Build targets'.
 - In the 'Build target files' part, select only 'simul2.f'.
 - Click OK.
- Open 'simul2.f' from the Workspace in the Management panel and click on the icon 'Build and run'.

Name	Date modified	Type	Size
bunch2.inp	11/01/2000 11:10	INP File	7 KB
cav-mac2.inp	11/01/2000 11:10	INP File	2 KB
fback2.inp	30/03/2010 14:12	INP File	2 KB
fbeam2.f	11/01/2000 11:10	F File	2 KB
feedback2.f	30/03/2010 13:57	F File	2 KB
finit2.f	11/01/2000 11:10	F File	2 KB
fortran_code.cbp	11/09/2020 10:31	project file	1 KB
kick1.dat	31/03/2010 13:14	DAT File	219 KB
kick2.dat	31/03/2010 13:14	DAT File	211 KB
kick3.dat	31/03/2010 13:14	DAT File	221 KB
libcern.f	18/01/2000 18:43	F File	7 KB
ph1.dat	31/03/2010 13:14	DAT File	185 KB
ph2.dat	31/03/2010 13:14	DAT File	185 KB
ph3.dat	31/03/2010 13:14	DAT File	185 KB
phsp1.dat	31/03/2010 13:14	DAT File	224 KB
phsp2.dat	31/03/2010 13:14	DAT File	224 KB
phsp3.dat	31/03/2010 13:14	DAT File	224 KB
rffb2.f	11/01/2000 11:10	F File	2 KB
rffb2.inp	11/01/2000 11:10	INP File	1 KB
simul2.f	30/03/2010 14:08	F File	39 KB
simul2.out	31/03/2010 13:14	OUT File	28 KB

'fortran_code' folder



Contents

- ❑ Introduction.
- ❑ Single-particle longitudinal beam-dynamics with synchrotron radiation.
 - Equations of motion, synchrotron radiation, small-amplitude synchrotron oscillations, ...
- ❑ Longitudinal beam-dynamics with synchrotron radiation and Higher Order Modes (HOMs).
 - HOM induced voltage, synchronous phase shift, HOM initial conditions, coupled-bunch instabilities, ...
- ❑ Longitudinal beam-dynamics with synchrotron radiation, HOMs and bunch-by-bunch feedback.
 - Models of the feedback components, growth and damping-rates, cavity-kicker, ideal and real corrections, ...
- ❑ Conclusions and suggested next steps.
- ❑ Appendices.
 - Execution of the new-Python and old-Fortran codes, structure of the code, exponential fits in Python, ...
- ❑ **References.**

References (1/2)

- Analog Devices, “Mixers and modulators”, MT-080 Tutorial, 2008.
- Analog Devices, “Multiplier application guide”, 1978.
- S. Bartalucci et al., “Analysis of methods for controlling multibunch instabilities in DAΦNE”, Particle Accelerators, 1995.
- M. Bassetti et al., “A time domain simulation code of the longitudinal multibunch instabilities”, DAΦNE technical note G-19, 1993.
- M. Bassetti et al., “DAΦNE longitudinal feedback”, LNF-92-033-PG, 1992.
- R. Boni et al., “A waveguide overloaded cavity as longitudinal kicker for the DAΦNE bunch-by-bunch feedback system”, Particle Accelerators, 1996.
- D. Briggs et al., “Computer modelling of bunch-by-bunch feedback for the SLAC B-factory design”, SLAC-PUB-5466, 1991.
- D. Briggs et al., “Prompt bunch-by-bunch synchrotron oscillation detection via a fast phase measurement”, SLAC-PUB-5525, 1991.
- A. Drago, “Diagnostica e misure 2 (anelli)”, corso per la formazione di operatori e conduttori di macchine acceleratrici, 2007.
- A. Drago, “Longitudinal feedback systems at the lepton collider DAFNE”, Joint ARIES Workshop on Electron and Hadron Synchrotrons, 2018.
- A. Drago et al., “Longitudinal quadrupole instability and control in the Frascati DAΦNE electron ring”, Phys. Rev. STAB, 2003.
- P. Forck, P. Kowina, and D. Liakin, “Beam position monitors”, Synchrotron Radiation News, 2008.
- J. D. Fox et al., “Feedback implementation options and issues for B factory accelerators”, SLAC-PUB-5932, 1992.
- J. D. Fox et al., “Stripline transversal filter techniques for sub-picosecond bunch timing measurements”, SLAC-PUB-12631, 2007.
- G. Franzini et al., “Feedback layout at DAΦNE”, DAFNE Machine Development Meeting, 2020.
- A. Gallo et al., “An overdamped cavity for the DAΦNE longitudinal feedback”, DAΦNE technical note RF-17, 1995.
- A. Gallo, M. Migliorati and L. Palumbo, “Efficiency of the broadband RF cavity longitudinal kicker in DAΦNE”, NIM, 1998.
- A. Gallo, F. Marcellini and M. Migliorati, “Implementation of the fast RF feedback on the DAΦNE beam ...”, DAΦNE technical note RF-14, 1994.
- A. Gallo et al., “Simulations of the bunch-by-bunch feedback operation with a broadband RF cavity ...”, DAΦNE technical note G-31, 1995.
- General Radio Company, “The frequency spectrum of a tone burst”, engineering department instrument notes, 1965.
- A. Ghigo et al., “Kickers and power amplifiers for the DAΦNE bunch-by-bunch longitudinal feedback system”, LNF-96-033-PQ, 1996.
- H. Hindi et al., “Down sampled signal processing for a B factory bunch-by-bunch feedback system”, SLAC-PUB-5772, 1992.
- J. Jacquelin, “Regressions et equations integrales”, engineering department note, 2014.
- E. Jensen, “RF cavity design”, CERN Yellow Report CERN-2014-009, 2014.

References (2/2)

- S. Khan, “Collective phenomena in synchrotron radiation sources”, Springer, 2006.
- I. S. Ko, Y. Kim and J. Y. Huang, “Status of longitudinal feedback system for the PLS storage ring”, PAC, 1999.
- A. Latina, “Introduction to transverse beam dynamics”, JUAS, 2016.
- F. Marcellini, M. Serio and M. Zobov, “DAΦNE broad-band button electrodes”, DAΦNE technical note CD-6, 1996.
- M. Migliorati and L. Palumbo, “Multibunch and multiparticle simulation code with an alternative approach ...”, Phys. Rev. STAB, 2015.
- M. Migliorati, “Past collective effects studies for DAFNE”, CERN ICE meeting, 2012.
- M. Migliorati, “Effetti collettivi nella dinamica dei fasci in una macchina acceleratrice circolare con applicazioni ...”, PhD thesis, 1996.
- M. K. Park et al., “Longitudinal feedback control system for the PLS”, EPAC, 2000.
- S. Prabhakar, “New diagnostics and cures for coupled-bunch instabilities”, SLAC-Report-554, 2001.
- C. Sanelli and M. Preger, “The DAΦNE main ring magnet prototypes”, EPAC, 1996.
- H. Schmickler, “Multi-bunch feedback systems”, CAS, 2015.
- D. Teytelman, “Architectures and algorithms for control and diagnostics of coupled-bunch instabilities ...”, SLAC-Report-633, 2003.
- D. Teytelman et al., “Design and testing of Gproto bunch-by-bunch signal processor”, EPAC, 2006.
- D. Teytelman, “FBE-368L longitudinal RF signal processor”, technical user manual, 2012.
- D. Teytelman, “iGp-120F signal processor”, technical user manual, 2008.
- D. Teytelman and J. Fox, “Set-up of PEP-II longitudinal feedback systems for even/odd bunch spacings”, SLAC-PUB-9217, 2002.
- K. A. Thompson, “Simulation of longitudinal coupled-bunch instabilities”, Asymmetric B-Factor Collider note, 1991.
- R. P. Walker, “Radiation damping”, CAS, 1994.
- L. Wu-Bin et al., “A waveguide overloaded cavity kicker for the HLS II longitudinal feedback system”, Chinese Physics C, 2014.
- A. Young, J. Fox and D. Teytelman, “VXI Based Multibunch Detector and QPSK Modulator for the PEP-II/ALS/DAFNE ...”, SLAC-PUB-7485, 1997.
- M. Zobov et al., “Collective effects and impedance study for the DAΦNE Φ-factory”, LNF-95/041, 1995.